ZooKeys 1097: 1–46 (2022)
doi: 10.3897/zookeys.1097.83916
https://zookeys.pensoft.net

RESEARCH ARTICLE

A peer-reviewed open-access journal
ZooKeys
Launched to accelerate biodiversity research

A review of the cavernicolous Trichopolydesmidae (Diplopoda, Polydesmida) from the Carpathian-Balkan arch and the Rhodope Mountains, with descriptions of two new genera and three new species

Dragan Antić[1,2], Boyan Vagalinski[3], Pavel Stoev[4,5], Nesrine Akkari[6]

1 *University of Belgrade–Faculty of Biology, Institute of Zoology, Studentski trg 16, 11000 Belgrade, Serbia* **2** *Serbian Biospeleological Society, Trg Dositeja Obradovića 2, 21000 Novi Sad, Serbia* **3** *Institute of Biodiversity and Ecosystem Research at the Bulgarian Academy of Sciences, 2 Yurii Gagarin Street, 1113, Sofia, Bulgaria* **4** *National Museum of Natural History, Bulgarian Academy of Sciences, Tsar Osvoboditel Blvd. 1, Sofia 1000, Bulgaria* **5** *Pensoft Publishers, Sofia, Bulgaria* **6** *3rd Zoological Department, Natural History Museum Vienna, Burgring 7, 1010 Vienna, Austria*

Corresponding author: Dragan Antić (dragan.antic@bio.bg.ac.rs)

Academic editor: Didier Vanden Spiegel | Received 16 March 2022 | Accepted 31 March 2022 | Published 19 April 2022

http://zoobank.org/66F17436-DF36-4FFD-B2D3-021F14D40D62

Citation: Antić D, Vagalinski B, Stoev P, Akkari N (2022) A review of the cavernicolous Trichopolydesmidae (Diplopoda, Polydesmida) from the Carpathian-Balkan arch and the Rhodope Mountains, with descriptions of two new genera and three new species. ZooKeys 1097: 1–46. https://doi.org/10.3897/zookeys.1097.83916

Abstract

All cavernicolous species of the millipede family Trichopolydesmidae from the Carpathian-Balkan arch and the Rhodope Mountains have been reviewed. At present the family has been shown to comprise five or six genera with eight or nine species. Two new genera have been described, viz., *Balkanodesminus* **gen. nov.**, with two new species: *B. dentatoides* **sp. nov.** and *B. serbicus* **sp. nov.**, from Bulgaria and Serbia, respectively, and the monospecific *Rhodopodesmus* **gen. nov.**, with *R. niveus* **sp. nov.**, from Bulgaria. Two new combinations and one new status have been proposed: *Balkanodesminus bulgaricus* (Strasser, 1962) **comb. nov.** ex *Bacillidesmus bulgaricus* Strasser, 1962 and *Balkanodesminus dentatus* (Strasser, 1966a) **comb. nov.**, **stat. nov.** ex *Bacillidesmus bulgaricus dentatus* Strasser, 1966a. All genera and species are diagnosed with the inclusion of the most relevant remarks for each of them. Old museum types are checked for *Bacillidesmus filiformis* (Latzel, 1884) with lectotype designation, as well as for *Trichopolydesmus eremitis* Verhoeff, 1898. An identification key to all six genera and a distribution map for the eight species are provided, as well as brief remarks and general considerations on the family Trichopolydesmidae.

Keywords

Balkan Peninsula, Bulgaria, caves, millipedes, new combination, new status, Serbia, taxonomy

Copyright *Dragan Antić et al.* This is an open access article distributed under the terms of the Creative Commons Attribution License (CC BY 4.0), which permits unrestricted use, distribution, and reproduction in any medium, provided the original author and source are credited.

Introduction

The type species of the family Trichopolydesmidae, *Trichopolydesmus eremitis* Verhoeff, 1898 was described based on a single male collected in a cave near Băile Herculane in Romania. Given the limited general knowledge on the millipedes of that time, Verhoeff (1898) stated that the genus *Trichopolydesmus* Verhoeff, 1898 could in some respects be related to the genus *Strongylosoma* Brandt, 1833 (today in Paradoxosomatidae). At the same time, based on Latzel's (1884) specimens of the species *Brachydesmus filiformis* Latzel, 1884, Attems (1898) erected a new genus, *Bacillidesmus* Attems, 1898, which is today considered to be closely related to *Trichopolydesmus*. For these two genera, Verhoeff (1910) created two monospecific subfamilies within the family Polydesmidae, viz., Trichopolydesminae and Bacillidesminae. Brölemann (1916), to a certain extent, accepted Verhoeff's (1910) higher taxonomic ranking of the aforementioned taxon, but considered it as the tribe Trichopolydesmini, to which he assigned several other European and North African genera (mostly from the Mediterranean region). Later on, Attems (1926, 1940) considered *Trichopolydesmus* and *Bacillidesmus* as members of the family Vanhoeffeniidae, an opinion with which Vehoeff (1941b) largely disagreed, considering Vanhoeffeniidae unacceptably heterogeneous. In that same paper he (Verhoeff 1941b) put the genus *Trichopolydesmus*, together with some South American taxa, in its own family, Trichopolydesmidae, not taking into consideration Brölemann's (1916) earlier classification of the tribe Trichopolydesmini. In the same work, Verhoeff (1941b) erected the monospecific family Bacillidesmidae for the genus *Bacillidesmus*. As for the family Vanhoeffeniidae, Jeekel (1956) argued that its type genus *Vanhoeffenia* Attems, 1908 (see Attems 1908) is rather a member of the family Sphaerotrichopodidae, thus suppressing the family Vanhoeffeniidae. This act was apparently missed by some authors (e.g., Ceuca 1958 and Schubart 1960) who continued using the name Vanhoeffeniidae. Some years later, Jeekel (1965) synonymized Sphaerotrichopodidae and Vanhoeffeniidae under Dalodesmidae.

In the second half of the 20th century, the status and the composition of Trichopolydesmidae remained debatable. Ribaut (1955) followed Brölemann's (1916) vision and included *Galliocookia* Ribaut, 1955 in the tribe Trichopolydesmini. Tabacaru (1975, 1980) treated the family Trichopolydesmidae in Verhoeff's (1941b) sense, with some South American taxa, but focused only on European taxa, and besides *Trichopolydesmus*, he added some other taxa, including *Bacillidesmus*. Hoffman (1980) restricted the family to only a few European genera. This concept was more or less followed by Mauriès (1984) who put in the family several European genera sensu Tabacaru (1975, 1980) and Hoffman (1980), one North African genus sensu Brölemann (1916), as well as several other European genera. Thus, considering Trichopolydesmidae to comprise taxa with chiefly Mediterranean distributions. Golovatch (2011) followed Mauriès' (1984) classification and additionally assigned to it the genus *Caucasodesmus* Golovatch, 1985 from the Caucasus and the Crimean Peninsula.

As far as the higher classification is concerned, Hoffman (1980) recognized the superfamily Trichopolydesmoidea within the suborder Polydesmidea. According

to the same author, this superfamily includes all taxa that once belonged to the family Vanhoeffeniidae. He (Hoffman 1980) classified them into four families, viz., Trichopolydesmidae, Macrosternodesmidae, Nearctodesmidae and Fuhrmannodesmidae. In addition to these four families, Golovatch (2011) added the small Mediterranean family Mastigonodesmidae, simultaneously sharing Hofmann's (1980) view that the Fuhrmannodesmidae is a very heterogeneous family and that its members need to be divided into several natural groups. Two years later, Golovatch et al. (2013) further included in the group the family Opisotretidae, which had earlier been classified in the superfamily Polydesmoidea (sensu Hoffman 1980) or in its own superfamily Opisotretoidea (sensu Simonsen 1990). Interestingly, in the same year, Golovatch (2013) synonymized the families Mastigonodesmidae, Macrosternodesmidae, Nearctodesmidae, and Fuhrmannodesmidae with the family Trichopolydesmidae, leaving the Trichopolydesmoidea with only two families, viz., Trichopolydesmidae and Opisotretidae. In this way, Trichopolydesmidae became a large and obviously very heterogeneous group of millipedes. This view of the family Trichopolydesmidae was not well accepted by other authors, primarily due to the lack of a good diagnosis of this group (Antić et al. 2014; Tabacaru and Giurginca 2016). Tabacaru and Giurginca (2016) largely disagreed with such a classification of Trichopolydesmidae and restricted it to the European taxa only (12 genera), with the family's distribution spanning from the Iberian Peninsula, through the Alps, the Balkans, the Aegean region, the Crimean Peninsula all the way to the North Caucasus. A disagreement with Golovatch's (2013) classification was also expressed by Shear and Reddell (2017). These authors excluded the families Macrosternodesmidae and Nearctodesmidae from Trichopolydesmidae, leaving Macrosternodesmidae as a separate family with two subfamilies, Macrosternodesminae and Nearctodesminae, simultaneously synonymizing the superfamily Trichopolydesmoidea under Polydesmoidea. Finally, Golovatch et al. (2018, 2022), obviously accepted this act by Shear and Reddell (2017), but still treated Trichopolydesmidae in a broader sense, including Fuhrmannodesmidae and Mastigonodesmidae therein, with > 220 species in approximately 100 genera.

In the present paper, we review the cavernicolous members of the millipede family Trichopolydesmidae in the Carpathian-Balkan arch and the Rhodope Mountains (stretched between Bulgaria and Greece) and demonstrate that its fauna contains five or six genera with eight or nine species, including two genera and three species described here as new.

Material and methods

Preservation, dissecting, imaging, map

Specimens preserved in 70% ethanol were examined with a Nikon SMZ 745T and a Zeiss Stemi 2000-C binocular stereo microscopes (IZB), a Nikon SMZ25 stereo

microscope (NHMW), or a Carl Zeiss Discovery V8 stereo microscope (Institute of Biodiversity and Ecosystem Research). The gonopods and legs were dissected and mounted in glycerin for temporary microscope preparations and observed with a Carl Zeiss Axioscope 40 microscope (IZB). The gonopod and legs of *Bacillidesmus filiformis* type specimens, as well as habitus and gonopod of *Trichopolydesmus eremitis* holotype were photographed with a DS-Ri-2 camera mounted on a Nikon Eclipse Ni microscope using NIS-Elements Microscope Imaging Software with an Extended Depth of Focus (EDF) patch (NHMW). Photograph of *T. eremitis* male deposited in VMNH were taken with a Canon 9D camera with a 65 mm Canon MP-E macro lens (Canon, Tokyo, Japan) mounted on a Stackshot vertical rail system (Cognisys, Michigan, USA) and focus stacked in Helicon Focus Pro 7 (HeliconSoft, Kharkiv, Ukraine) (VMNH). Drawings of gonopods were executed using a computer monitor and pictures made with a Canon PowerShot A80 digital camera connected to an Axioscope 40 microscope (IZB) or with a DS-Ri-2 camera mounted on a Nikon Eclipse Ni microscope (NHMW). Pictures of specimens were taken using a Nikon DS-Ri-2 camera mounted on a Nikon SMZ25 stereo microscope using NIS-Elements Microscope Imaging Software with an Extended Depth of Focus (EDF) patch (NHMW). For Scanning electron microscopy (SEM) the specimens were: (1) cleaned in an ultrasonic bath (50–60 Hz) for 5 to 10 seconds (maximum), (2) dehydrated in an ascending alcohol series (70%, 80%, 90%, 96% EtOH, 2 × 10–15 min each) and acetone; (3) air dried. Specimens were mounted on aluminum stubs equipped with a sticky aluminum tape, coated with platinum (Leica EM SCD500) and studied with a JEOL JSM 6610-LV at an accelerating voltage of 15 kV or with a JEOL JSM-6460-LV (NHMW). Pictures of live animals were taken with an Olympus Stylus Tough TG-6 (Fig. 2A), Canon PowerShot SX530 HS (Fig. 10A) and a Canon EOS 700D (Fig. 14A) digital camera.

The distribution map was created using Google Earth Pro (ver. 7.3.3.7786) and Adobe Photoshop CS6. The final images were processed with Adobe Photoshop CS6.

Gonopod terminology

The description of the basic parts of the gonopods of the new taxa followed Golovatch and VandenSpiegel (2015) with some modifications. The two basic parts of the gonopod are the coxa (cx) with a mesal cannula (ca), and the telopodite. The telopodite is composed of prefemorite (pf) and acropodite (a). The prefemorite is transverse to the main axis of the animal's body, setose, and makes a nearly right angle with the acropodite. The acropodite is longitudinally divided into two branches, the mesal, solenomeral branch (sb), and the lateral solenophore (sph). Mesally on the prefemorite there is a seminal fossa (sf), from which the seminal groove (sg) starts and runs along the mesal side of the acropodite all the way to the bifurcation point, then passes onto the solenomeral branch and ends with a small opening on the solenomere (s). Detailed and minute structures of the gonopods are explained directly in the figure captions and/or in the text. For more details on the terminology of the Polydesmoidea gonopods, see Shear and Marek (2021).

Museum and collection acronyms

IZB	Institute of Zoology, University of Belgrade – Faculty of Biology, Belgrade, Serbia;
NHMW	Naturhistorisches Museum Wien, Vienna, Austria;
NMNHS	National Museum of Natural History, Bulgarian Academy of Sciences, Sofia, Bulgaria;
VMNH	Virginia Museum of Natural History, Martinsville, Virginia, USA;
ZMB	Museum für Naturkunde Berlin, Germany;
ZSM	Zoologische Staatssammlung München, Munich, Germany.

Results

Class Diplopoda de Blainville in Gervais, 1844
Order Polydesmida Pocock, 1887
Family Trichopolydesmidae Verhoeff, 1910

Taxa from the Carpathians

Genus *Bacillidesmus* Attems, 1898

Type species. *Brachydesmus filiformis* Latzel, 1884, by monotypy.

Diagnosis. The monospecific *Bacillidesmus* seems to be the only European Trichopolydesmidae characterized by four regular rows of relatively long trichoid setae on rings 4–18 (Fig. 1A).

In addition, the diagnosis can be amended with the following combination of characters (see also Remarks): small species (4–4.5 mm), 19 body rings (including telson), sensilla basiconica completely enclosed inside the pit of antennomere 6, hypoproct with only two long distal setae, paraprocts with only 2+2 long setae, anterior legs in male with ventral denticles on prefemora, femora, postfemora, tibiae and tarsi (Fig. 1E, F), gonopod telopodite deeply divided into two branches, solenomere (s) and solenophore (sph) situated one below the other, solenomere long and simple, with a lamella, but without additional processes (Figs 1G, 17A–C).

Bacillidesmus filiformis (Latzel, 1884)

Figs 1, 17A–C

Brachydesmus filiformis Latzel, 1884: 128, 129.
Bacillidesmus filiformis—Attems 1898: 481, figs 97, 98; Attems 1940: 170, fig. 244; Strasser 1962: 443, 444; Strasser 1966a: 341–343; Kime and Enghoff 2011: 72.

Diagnosis. As for the monospecific genus.

Material examined. ***Lectotype*** ♂ (NHWM MY3754), designated herewith, "SO Ungarn", leg. Latzel, don. Latzel 1919. One microslide with only one gonopod. Body in two pieces in ethanol: head with rings 1–6 and rings 8–19; second gonopod, antennae and ring 7 missing.

Paralectotype. 1 ♀ (NHWM MY10266), whole body in ethanol, same data as for lectotype.

Distribution. Unknown.

Remarks. In the original description, Latzel (1884) stated that he analyzed one pair (1 ♂, 1 ♀) that he had collected personally in "südöstlichen Ungarn" (= southeastern part of the Kingdom of Hungary). Later, Strasser (1962) assumed that the species came from "present-day Yugoslavia north of the Danube". This refers to today's Vojvodina, northern Serbia. However, the southeastern part of the Kingdom of Hungary included both Banat Mountains and Southern Carpathians (= Transylvanian Alps) in present-day Romania. Bearing in mind that this area is already inhabited by three trichopolydesmid genera, it seems more plausible that *Bacillidesmus filiformis* could have originated from present-day Romania, rather than northern Serbia which is characterized mainly by agricultural fields. It also remains unknown if this species is cavernicolous or epigean.

This taxon was originally described as *Brachydesmus filiformis* Latzel, 1884. Attems (1898) analyzed both Latzel's specimens of *filiformis*, and based on numerous differences with the genus *Brachydesmus* Heller, 1858, he correctly established a new genus, *Bacillidesmus*. At the same time, Attems (1898) gave the first gonopod drawing of this taxon (Fig. 17A). Later, in his famous "Polydesmoidea III", Attems (1940) provided a new drawing of the *filiformis* gonopod (Fig. 17B), which is slightly different from his 1898 drawing. After studying Attems' microslide with only one gonopod in poor condition (Figs 1G, 17C) we can confirm that it coincides a bit more with his schematic drawing from 1940. Unfortunately, the second gonopod, as well as ring 7 and both antennae of the lectotype, are most likely lost. It remains unclear whether Attems could have used the now-lost gonopod for the first drawing, or in both cases he used this one, which is still present today, but over time there have been partial changes in its position on the microslide or a partial deformation. Given that Attems (1898) also made a drawing of the antenna, which is missing today, it is very possible that there was another microslide with the second gonopod and antenna/antennae, which we failed to find. However, based on Attems' (1898, 1940) drawings and the newly examined type material of the gonopod, some conclusions could be drawn here.

The genus *Bacillidesmus* had remained monospecific until Strasser (1962) provisionally included therein a new taxon from Bulgaria, based on a single female. Just a few years later, and this time with males in the hands, Strasser (1966a) confirmed that two more taxa belonged to the genus *Bacillidesmus*, viz., *B. bulgaricus bulgaricus* Strasser, 1962 and *B. bulgaricus dentatus* Strasser, 1966a. However, after a detailed examination of the type material of *Bacillidesmus filiformis*, as well as material of *B. bulgaricus bulgaricus* and *B. bulgaricus dentatus*, and two related new species from Serbia and Bulgaria, we believe that *Bacillidesmus* should include only *filiformis*, while the remaining aforementioned taxa should be assigned to a new genus, *Balkanodesminus* gen. nov., which we describe below. The new genus differs significantly from *Bacillidesmus* both

Figure 1. *Bacillidesmus filiformis* (Latzel, 1884), type material **A** paralectotype ♀ (NHMW MY10266), habitus, lateral view **B** lectotype ♂ (NHMW MY3754) body rings 8–19, dorsal view **C** lectotype ♂ (NHMW MY3754) head and body rings 1–6, dorsal view **D** paralectotype ♀ (NHMW MY10266) left leg 4, posterior view **E** lectotype ♂ (NHMW MY3754) right leg 4, anterior view **F** lectotype ♂ (NHMW MY3754) right leg 10, posterior view **G** lectotype ♂ (NHMW MY3754) gonopod, mesal or lateral view. Abbreviations: **s** solenomere, **sph** solenophore. Scale bars: 0.5 mm (**A–C**), 0.1 mm (**D–F**), 0.05 mm (**G**).

in somatic and gonopodal characters. The most striking difference in the gonopod structure is that in *Bacillidesmus filiformis* the solenomeral branch is simple, without a distal solenomeral process, while in *bulgaricus bulgaricus*, *bulgaricus dentatus* and the two new species it is transversely bifid. In addition, these two genera differ significantly in several somatic traits: *Bacillidesmus* has regular rows of metatergal setae, mainly four, whereas *Balkanodesminus* gen. nov. shows 4–8 irregular rows; sensilla basiconica on antennomere 6: completely enclosed inside the pit in *Bacillidesmus*, vs. partially exposed outside the pit in *Balkanodesminus* gen. nov.; setae on paraprocts: 2+2 long setae in *Bacillidesmus*, vs. 2+2 long and ca. 10+10 shorter ones in *Balkanodesminus* gen. nov.; setae on hypoproct: 1+1 long distal setae in *Bacillidesmus*, vs. densely setose, including two long distal setae in *Balkanodesminus* gen. nov.; femora of all male legs swollen in *Bacillidesmus*, vs. only femora of legs 1–3 swollen in *Balkanodesminus* gen. nov.; anterior male legs in *Bacillidesmus* with ventral denticles, vs. denticles absent in *Balkanodesminus* gen. nov. These diferences are sound enough to propose a new genus for the taxa described by Strasser (*B. bulgaricus bulgaricus*, *B. bulgaricus dentatus*) and the two newly described species. Moreover, *Bacillidesmus filiformis* seems to show more affinity to some of the Carpathian genera (which is another proof that this genus could be from the Carpathians, see under *Banatodesmus* and *Trichopolydesmus*), while *Balkanodesminus* gen. nov., from the Balkan Mountains, shares many similarities with *Rhodopodesmus* gen. nov. (see below).

Genus *Banatodesmus* Tabacaru, 1980

Type species. *Trichopolydesmus* (*Banatodesmus*) *jeanneli* Tabacaru, 1980, by monotypy.

Diagnosis. Different from other European Trichopolydesmidae by the presence of an enlarged, oval, paddle-like solenomere (s in Fig. 4), with an additional, small, claw-like, distal solenomeral process (dsp in Fig. 4).

In addition, the diagnosis can be amended with the following combination of characters: medium-sized species (7–7.5 mm), 20 body rings (including telson), rings with 4–6 irregular rows of long trichoid metatergal setae, sensilla basiconica completely enclosed inside the pit of antennomere 6, hypoproct with only two long distal setae, paraprocts with only 2+2 long setae, gonopod acropodite divided into two branches, solenophore (sph in Fig. 4) with three processes, of which the longest is S-shaped (broken off in the SEM image).

Banatodesmus jeanneli (Tabacaru, 1980)

Figs 2–4, 17D, 18

Trichopolydesmus (*Banatodesmus*) *jeanneli* Tabacaru, 1980: 156, figs 1–3.
Trichopolydesmus jeanneli—Ceuca 1992: 416.
Trichopolydesmus (*Banatodesmus*) *jeanneli*—Giurginca 2021: 86, fig. 52 (*Banatodesmus* obviously mistakenly listed as a subgenus, see below).

Banatodesmus jeanneli—Tabacaru 1996: 68, fig. 1A; Tabacaru et al. 2003: 133; Tabacaru and Giurginca 2016: 101, fig. 14C, D; Kime and Enghoff 2011: 72, 262.

Diagnosis. As for the monospecific genus.

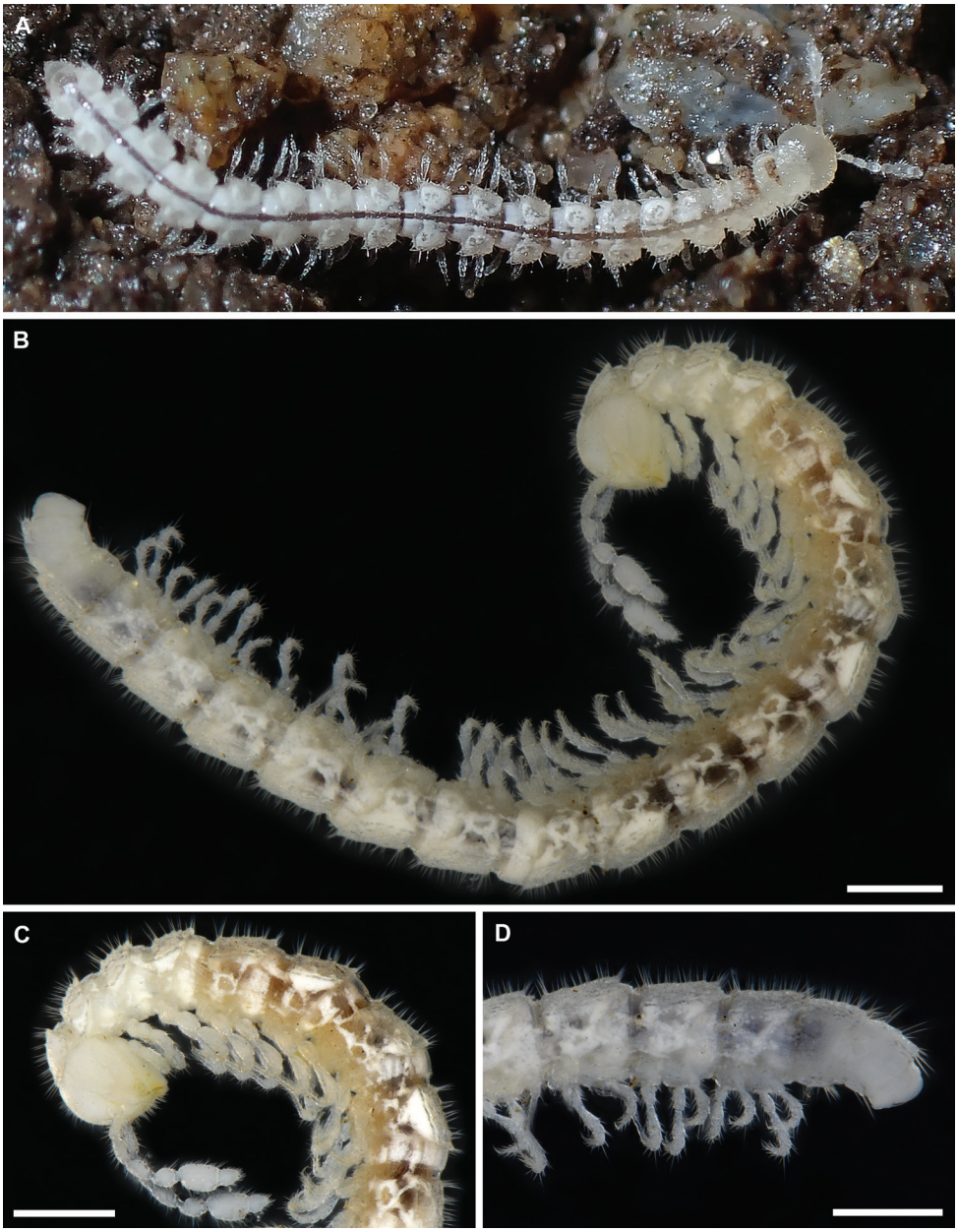

Figure 2. *Banatodesmus jeanneli* (Tabacaru, 1980), ♂(♂) from Peştera Haiducească de la Moldova Nouă Cave, Romania, habitus **A** in situ, dorsal view (photo D. Antić) **B** lateral view (IZB) **C** anterior part of body, lateral view (IZB) **D** posterior part of body, lateral view (IZB). Scale bars: 0.5 mm.

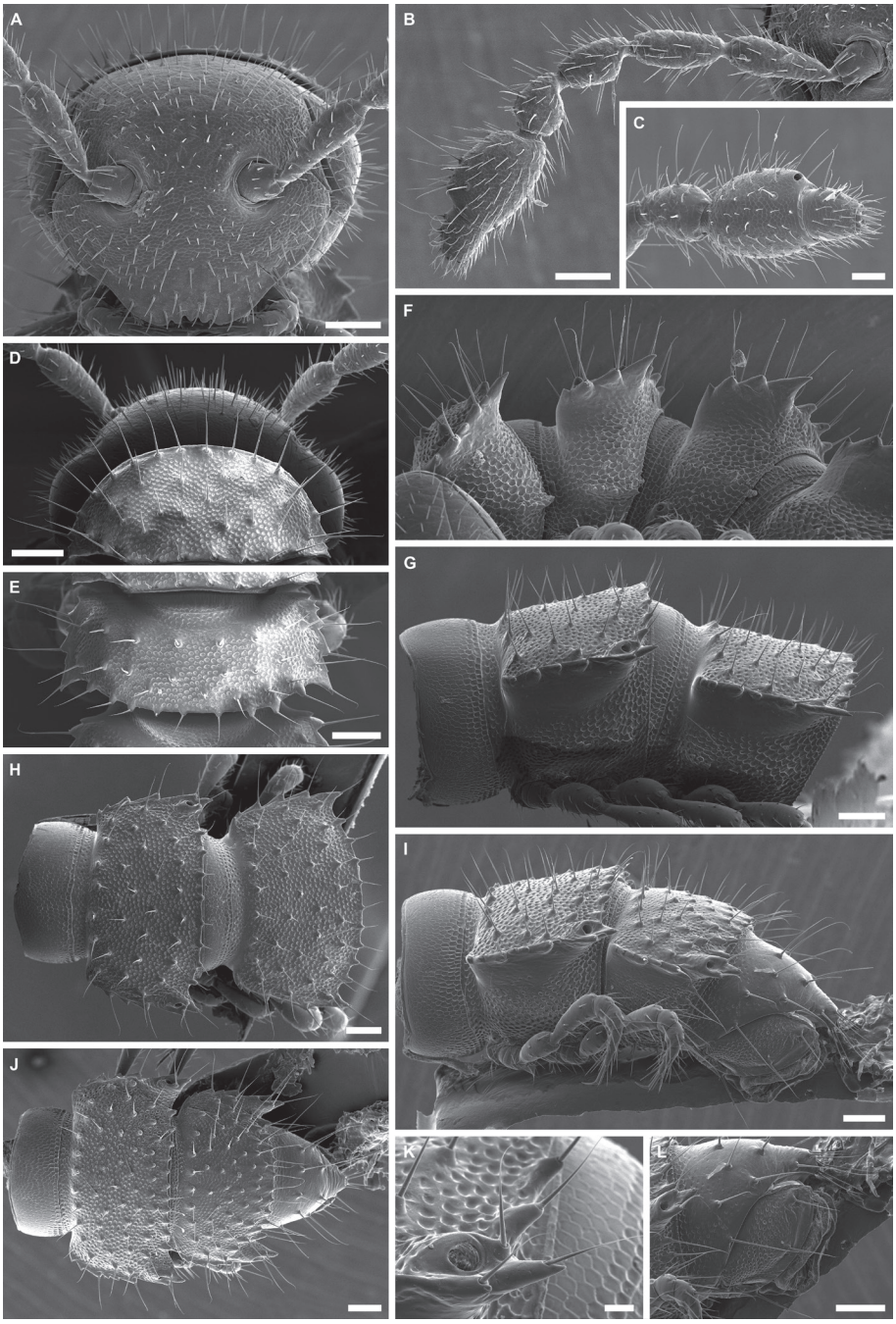

Figure 3. *Banatodesmus jeanneli* (Tabacaru, 1980), ♂ from Peştera Haiducească de la Moldova Nouă Cave, Romania, habitus (NHMW MY10257) **A** head, anterior view **B** right antenna, anterior view **C** distal antennomeres of left antenna, anterior view **D** head and collum, dorsal view **E** body ring 2, dorsal view **F** body rings 2–5, ventro-lateral view **G** body rings 10 and 11, lateral view **H** body rings 10 and 11, dorsal view **I** body rings 18–20, lateral view **J** body rings 18–20, dorsal view **K** left ozopore 10, lateral view **L** telson, lateral view. Scale bars: 0.1 mm (**A, B, D–J, L**), 0.05 mm (**C**), 0.02 mm (**K**).

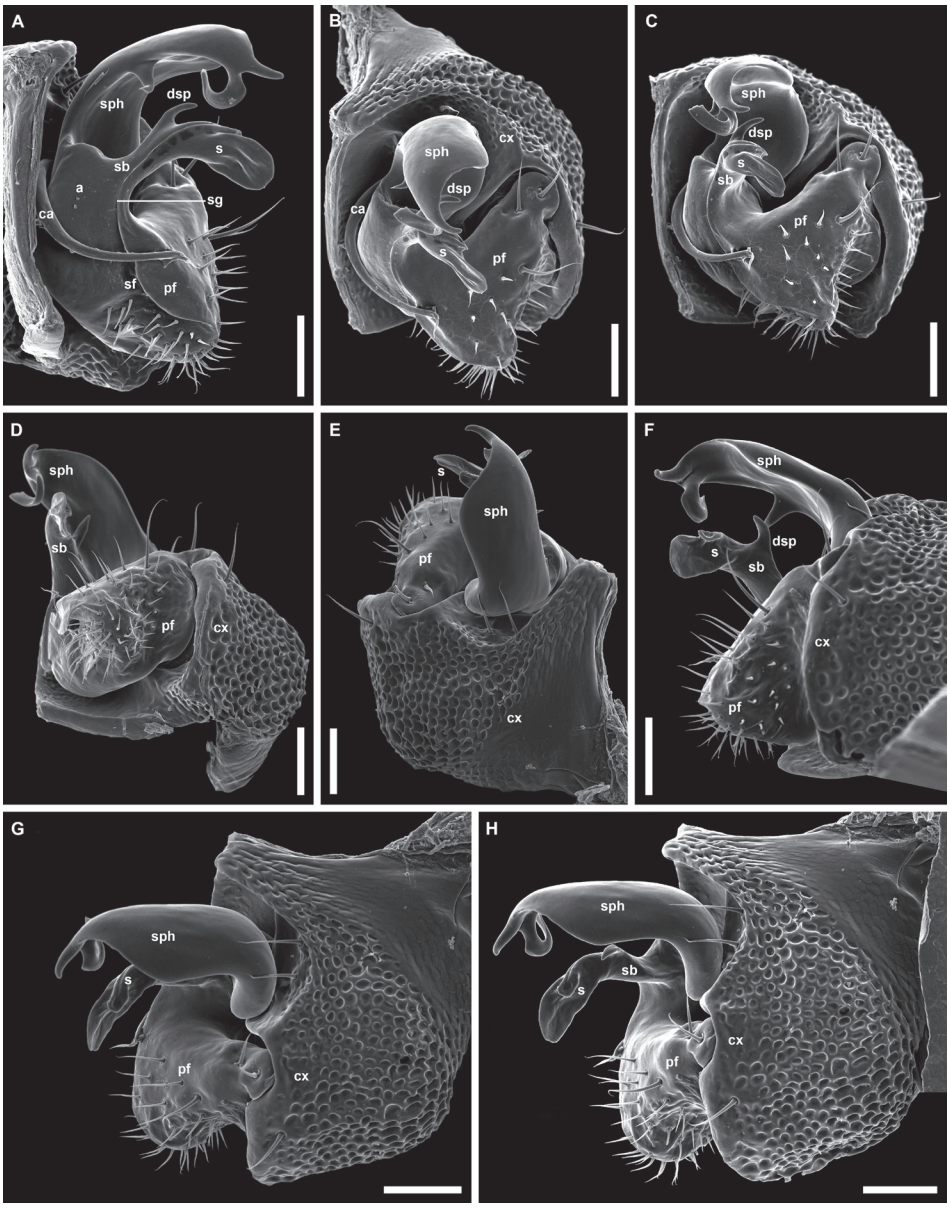

Figure 4. *Banatodesmus jeanneli* (Tabacaru, 1980), ♂ from Peştera Haiducească de la Moldova Nouă Cave, Romania, left gonopod (NHMW MY10257) **A** mesal view **B** antero-distal view **C** distal view **D** posterior view **E** anterior view **F** lateral view **G, H** antero-lateral views. Abbreviations: **a** acropodite, **ca** cannula, **cx** coxa, **dsp** distal solenomeral process, **pf** prefemorite, **s** solenomere, **sb** solenomeral branch, **sf** seminal fossa, **sg** seminal groove, **sph** solenophore. Tip of "S" shaped process of **sph** broken. Scale bars: 0.05 mm.

Material examined. 1 ♂, 1 ♀ (IZB), Romania, Banat, Moldova Noua, Peştera Haiducească de la Moldova Nouă Cave (= Gaura Turceasca, Grota Haiducilor), 44.7314, 21.7394, 28.X.2021, leg. D. Antić & D. Stojanović, 1 ♂ (used for SEM, NHMW MY10257), same data as for the previous material.

Distribution. This species has been described and is still known only from two caves in the Banat Mountains in Romania, Peştera Haiducească de la Moldova Nouă and Peştera de la Lacul Dracului caves (Fig. 18).

Remarks. Originally, *Banatodesmus* was described as a subgenus of *Trichopolydesmus* Verhoeff, 1898 (Tabacaru 1980). Later, Mauriès (1984) reasonably considered it as a separate genus, this being generally accepted today. Recently, in his book on Romanian millipedes, Giurginca (2021) referred to it as "*Trichopolydesmus* (*Banatodesmus*) *jeanneli*". This was apparently a mistake, since in the rest of the text *Banatodesmus* was clearly treated as a genus.

The sample examined here is the first record of this taxon since its original description. Two males and one female were discovered at one of the two type localities, Peştera Haiducească de la Moldova Nouă Cave. It is interesting that all three specimens were collected not far from the entrance to the cave, within one square meter, near a small stream that flows through the cave. The female was found under a piece of rotten wood, while both males were taken from under two deeply embedded stones.

Although Tabacaru (1980) provided an excellent description and very fine drawings (Fig. 17D) of this taxon, the recently found specimens gave us the opportunity to document this taxon with photographs and SEM images of the habitus and gonopods (Figs 2–4).

As mentioned above, *Bacillidesmus filiformis* seems to show some habitual and gonopodal similarities with *Banatodesmus*. Both taxa share sensilla basiconica of antennomere 6 completely enclosed in the pit, paraprocts with only two long setae each, and hypoproct with only two long distal setae. In addition, the solenomeral branch and the solenophore are oriented mostly antero-posteriorly rather than meso-laterally to each other.

Genus *Napocodesmus* Ceuca, 1974

Type species. *Napocodesmus endogeus* Ceuca, 1974, by monotypy.

Diagnosis. This is the only European genus of Trichopolydesmidae that is characterized by hook-shaped posterolateral cones on metaterga, see Ceuca (1974) and Tabacaru (1975).

Napocodesmus florentzae Tabacaru, 1975

Figs 17E, F, 18

Napocodesmus florentzae Tabacaru, 1975: 73, figs 1–6.

Napocodesmus florentzae—Ceuca 1992: 416; Tabacaru et al. 2003: 133; Tabacaru and Giurginca 2016: 100, fig. 13; Kime and Enghoff 2011: 72, 265; Giurginca 2021: 88, fig. 54.

Diagnosis. Cannot be compared to *N. endogeus* since its description was based on females only (see under Remarks).

Besides the hook-shaped posterolateral cones on the metaterga, this species differs from other European Trichopolydesmidae by the simplified gonopods with the acropodite divided in its distal third into two branches, a slender and claw-like solenophore and a wide and flattened, sublamelliform solenomere, both branches being parallel and oriented completely meso-laterally to each other (Fig. 17E, F).

In addition, the diagnosis can be amended with the following combination of characters: small species (3.4 mm), 19 body rings (including telson), sensilla basiconica on antennomere 6 partially exposed outside the pit, hypoproct with more than two long distal setae, paraprocts with more than 2+2 long setae, metaterga with 4–7 irregular rows of trichoid setae.

Distribution. This species is known only from its type locality, Peştera cu Două Uşi Cave, Suşița Verde Valley, Vâlcan Mountains, Gorj County, Romania (Fig. 18).

Remarks. Tabacaru (1975) stated that he had collected a male and a female, but that the female was lost during a breeding experiment. The excellent description and drawings (Fig. 17E, F) he gave were based on only one male, which, if it still exists, should be treated as the holotype by monotypy.

The type species of this genus, *N. endogeus*, was described based on nine females found in the soil near the Biology Department at the University of Cluj in Romania (Ceuca 1974). Akkari and Enghoff (2011) cited this species from deep soil in an orchard in Moldova. Before that, Golovatch and Kime (2009) stated that this species is very common and abundant in Moldova's apple orchards, but probably accidentally under the name *N. florentzae*, instead of *N. endogeus*.

Napocodesmus florentzae shares some similarities in its habitus with *Balkanodesminus* gen. nov. and *Rhodopodesmus* gen. nov., viz., small size, 19 body rings, 4–7 rows of irregular trichoid setae (4–8 in two last-mentioned genera), sensilla basiconica on antennomere 6 partially exposed outside the pit, and hypoproct and paraprocts with more than two long setae.

Genus *Trichopolydesmus* Verhoeff, 1898

Type species. *Trichopolydesmus eremitis* Verhoeff, 1898, by monotypy.

Diagnosis. Differs from other European Trichopolydesmidae by the gonopod acropodite divided into three branches, where solenomere is thin, long and acuminate, and devoid of additional process.

In addition, the diagnosis can be amended with the following combination of characters: medium-sized species (8.5 mm), 20 body rings (including telson), sensilla basiconica on antennomere 6 partially exposed outside the pit, paraprocts and hypoproct densely setose (Fig. 5F, G), metaterga with 4–6 irregular rows of long trichoid setae, podomeres of anterior legs in males with denticles on their ventral side, tarsi with rare sphaerotrichomes (Fig. 5H, I).

***Trichopolydesmus eremitis* Verhoeff, 1898**
Figs 5, 17G, H, 18

Trichopolydesmus eremitis Verhoeff 1898: 363, figs 6–8.
Trichopolydesmus eremitis—Attems 1899: 429; Attems 1940: 168, fig. 240; Verhoeff 1941a: 186, figs 15, 16; Verhoeff 1941b: 44, figs 47, 48; Ceuca 1958: 340, figs 7–9; Ceuca 1992: 416; Tabacaru et al. 2003: 133; Tabacaru and Giurginca 2016: 100, fig. 14A, B; Kime and Enghoff 2011: 72, 266; Giurginca 2021: 89, fig. 55.

Diagnosis. As for the monospecific genus.

Material examined. ***Holotype*** ♂ (by monotypy, two microslides: ZSM-A20033529 and ZMB 13160), Herkulesbad (Băile Herculane, Romania), leg. K. Verhoeff. ZSM-A20033529 (Fig. 5A): head in several pieces, only first three antennomeres of one antenna, collum, rings 3–5, 8–10, 12, 13–14, 15–20. ZMB 13160 (Fig. 5B): gonopods, one leg pair (7?).

Additional material. 1 ♂ (VMNH110683), body in two pieces in alcohol (Fig. 5C), ring 7 and gonopods missing. For more details see below.

Distribution. Known from several caves in the southern part of the Carpathians in Romania: Peştera Hoţilor de la Băile Herculane (type locality), Peştera nr. 40 de la Ineleţ, Peştera Cicioara, Peştera Cornetul Vârcanilor, Peştera Cloşani, Peştera Vacilor de la Cloşani and Peştera din Poiana Lazului (= Peştera lui Mihai Arjoc, = Peştera din Piatra Mică) (Verhoeff 1898; Ceuca 1958; Tabacaru et al. 2003) (Fig. 18).

Remarks. Verhoeff (1898) described this taxon from a single male he collected in the Hoţilor Cave in Băile Herculane. As he himself stated, several subsequent attempts to collect additional specimens in this cave were unsuccessful. Tabacaru (1980) stated that numerous searches in this cave failed too. One of us (DA) visited this cave in 2014 but also failed to find this species. In 2021, a small group of myriapodologists, including two of us (DA and BV) were not successful either. From Hoţilor Cave, only the male type specimen originally described by Verhoeff (1898) is known.

Sixty years after its original description, Ceuca (1958) examined more than 20 specimens of *T. eremitis* from three other caves and gave new and more detailed drawings of the gonopods (Fig. 17G, H), as well as some notes on female habitus.

Hoffman (1980) wrote that he had received a male from Traian Ceuca, whose photograph is included in this paper (Fig. 5C). Unfortunately, colleague Jackson Means informed us that there is no original label with this individual, but that on the jar, marked with MIR02733, it is written: "Trichopolydesmidae: *Trichopolydesmus eremitus* Verhoeff TOPOTYPES !! Hungary". This was probably an accidental mistake during the subsequent labeling. The male sent by Ceuca to Hoffman comes from one of the three caves in Romania listed in Ceuca's (1958) paper. Considering the number of collected males from those three caves, we can only guess that this male comes from the Cloşani cave.

Figure 5. *Trichopolydesmus eremitis* Verhoeff, 1898 **A, D–F, I** holotype ♂ (ZSM-A20033529) **B, H, J, K** holotype ♂ (ZMB 13160) **C** ♂ (VMNH110683) **A** microslide with habitus parts **B** microslide with gonopods and one lag pair **C** habitus, lateral view **D** collum, dorsal view **E** body rings 13 and 14, dorsal view **F** hypoproct, ventral view **G** telson, ventral view **H** leg ?7 **I** left legs 10 and 11 **J, K** ?left gonopod, distomesal and distoanterolateral views, respectively. Scale bars: 0.5 mm (**C**), 0.1 mm (**D–K**).

Similarly to *Bacillidesmus filiformis*, this species also has ventral denticles on podomeres of male anterior legs (Fig. 5H, I). However, some other habitual characteristics are similar to *Napocodesmus*, *Balkanodesminus* gen. nov. and *Rhodopodesmus* gen. nov., viz., sensilla basiconica on antennomere 6 partially exposed outside the pit, while hypoproct and paraprocts are with more than two long setae (Fig. 5F, G). Legs and antennomeres (as well as antennae in general) in this species are somewhat longer (slender) than in other representatives from the Carpathian-Balkan arch and the Rhodope Mountains, thus it seems to be the most strongly adapted to cave life among them.

Taxa from the Balkan (Stara Planina) Mountain range

(Besides Stara Planina Mountain, this range includes the Predbalkan in Bulgaria, as well as numerous mountains in eastern Serbia)

Genus *Balkanodesminus* gen. nov.

http://zoobank.org/B53F3D76-3549-4DD0-96BC-8BD848613381

Type species. *Bacillidesmus bulgaricus* Strasser, 1962, by present designation.

Diagnosis. Differs from all European Trichopolydesmidae by the presence of a characteristic acropodite of the gonopods divided into two parallel and mostly meso-laterally oriented branches, where solenomeral branch is transversely bipartite, consisting of slender solenomere and well-developed distal solenomeral process. The most similar genus is *Rhodopodesmus* gen. nov., but it differs from *Balkanodesminus* gen. nov. and all other European Trichopolydesmidae by the presence of trifid solenomeral branch (for more details see under *Rhodopodesmus* gen. nov.).

In addition, the diagnosis can be amended with the following combination of characters: small size (3.7–5.2 mm), 19 body rings (including telson), sensilla basiconica on antennomere 6 partially exposed outside the pit, hypoproct with more than two long distal setae, paraprocts with more than 2+2 long setae, metaterga with 4–8 irregular rows of trichoid setae.

Name. The new genus is named after the Balkan Mountains, its type locality, in combination with the suffix *-desminus*, as a diminutive of *-desmus*, the common suffix in Polydesmida, referring to the small size of its species, in contrast to confamiliar Dinaric *Balkanodesmus* Antić & Reip, in Antić et al. 2014, the largest Balkan trichopolydesmid. The name is a masculine noun.

Included species.

Balkanodesminus bulgaricus (Strasser, 1962) gen. nov., comb. nov. ex *Bacillidesmus*
Balkanodesminus dentatus (Strasser, 1966a) gen. nov., comb. nov., stat. nov. ex *Bacillidesmus*
Balkanodesminus dentatoides gen. nov. et sp. nov.
Balkanodesminus serbicus gen. nov. et sp. nov.

Balkanodesminus bulgaricus* (Strasser, 1962) gen. nov., comb. nov. ex *Bacillidesmus
Figs 6, 17I, 18

Bacillidesmus? bulgaricus Strasser, 1962: 443, figs 7–10.
Bacillidesmus bulgaricus bulgaricus—Strasser 1966a: 341, figs 13–15; Strasser 1973: 419; Stoev 2004: 149; Stoev 2007: 384; Beron 2015: 80, 410; Bachvarova et al. 2017: 521.
Bacillidesmus bulgaricus—Ceuca 1992, 416; Kime and Enghoff 2011: 71, 262.

Diagnosis. Differs from *Balkanodesminus dentatoides* gen. nov. et sp. nov. and *B. dentatus* gen. nov., comb. nov., stat. nov. by the presence of longer (vs. shorter) metatergal setae and their smaller (vs. greater) number of rows, as well as by the presence of more simplified gonopods, with uniramous (vs. biramous) distal solenomeral process, and smaller and smooth (vs. larger and denticulated) lamella of solenophore. From *B. serbicus* gen. nov. et sp. nov., with which it shares similar habitus and similar gonopods, it differs by the presence of larger (vs. smaller) lamella of solenophore, slender, almost straight (vs. more robust and sigmoid) distal projection of solenophore, distal projection without (vs. with) basal lobe and slenderer (vs. stouter) solenomere and distal solenomeral process, where the solenomere exceeds the distal solenomeral process by ½ (vs. ¼) of its length.

Material examined. 2 ♂♂, 6 ♀♀ (NMNHS-10813), Bulgaria, Vratsa District, Chiren, Ponora Cave, clay, 27.I.1998, leg. B. Petrov & T. Ivanova.

Distribution. This species shows a somewhat scattered distribution (see Fig. 18). It is present in caves starting from Vidin Municipality, through Chuprene and Chiprovtsi municipalities all the way to Vratsa municipality. These are Varkan Cave, Vidin Municipality (Strasser 1973), Desni suhi pech Cave, Chuprene Municipality (Strasser 1973), Mishin kamik Cave (type locality) and Vreloto v seloto Cave, both Chiprovtsi Municipality (Strasser 1962, 1966a), as well as Mladenovata peshtera Cave and Ponora Cave, Vratsa Municipality (Strasser 1966a; Stoev 2004).

Remarks. Strasser (1962) described this species based on a poorly preserved female that he placed with uncertainty in the genus *Bacillidesmus*. He emphasized a very important difference in sensilla basiconica on 6th antennomere being partially exposed in *bulgaricus*, while they are completely enclosed in their pit in *filiformis*.

Four years later, when males became available, Strasser (1966a) confirmed that *bulgaricus* belonged to the genus *Bacillidesmus*, based on some similarities in gonopod structures, and identified two subspecies, viz., *B. bulgaricus bulgaricus* and *B. bulgaricus dentatus*. Subsequently, both subspecies were recognized as such by Stoev (2004, 2007), Beron (2015) and Bachvarova et al. (2017). On the other hand, Ceuca (1992), and Kime and Enghoff (2011) considered *dentatus* as a separate species, *B. dentatus*. Here, we treat both taxa as separate species (see below).

Based on the distribution of the genus *Balkanodesminus* gen. nov., and the scattered distribution of *B. bulgaricus* gen. nov., comb. nov., we are not excluding the possibility that not all records of *bulgaricus* are in fact of that species. Illustrations of gonopods are known only from the two easternmost populations, from the Mladenovata peshtera Cave (Strasser 1966a) and Ponora Cave (present study).

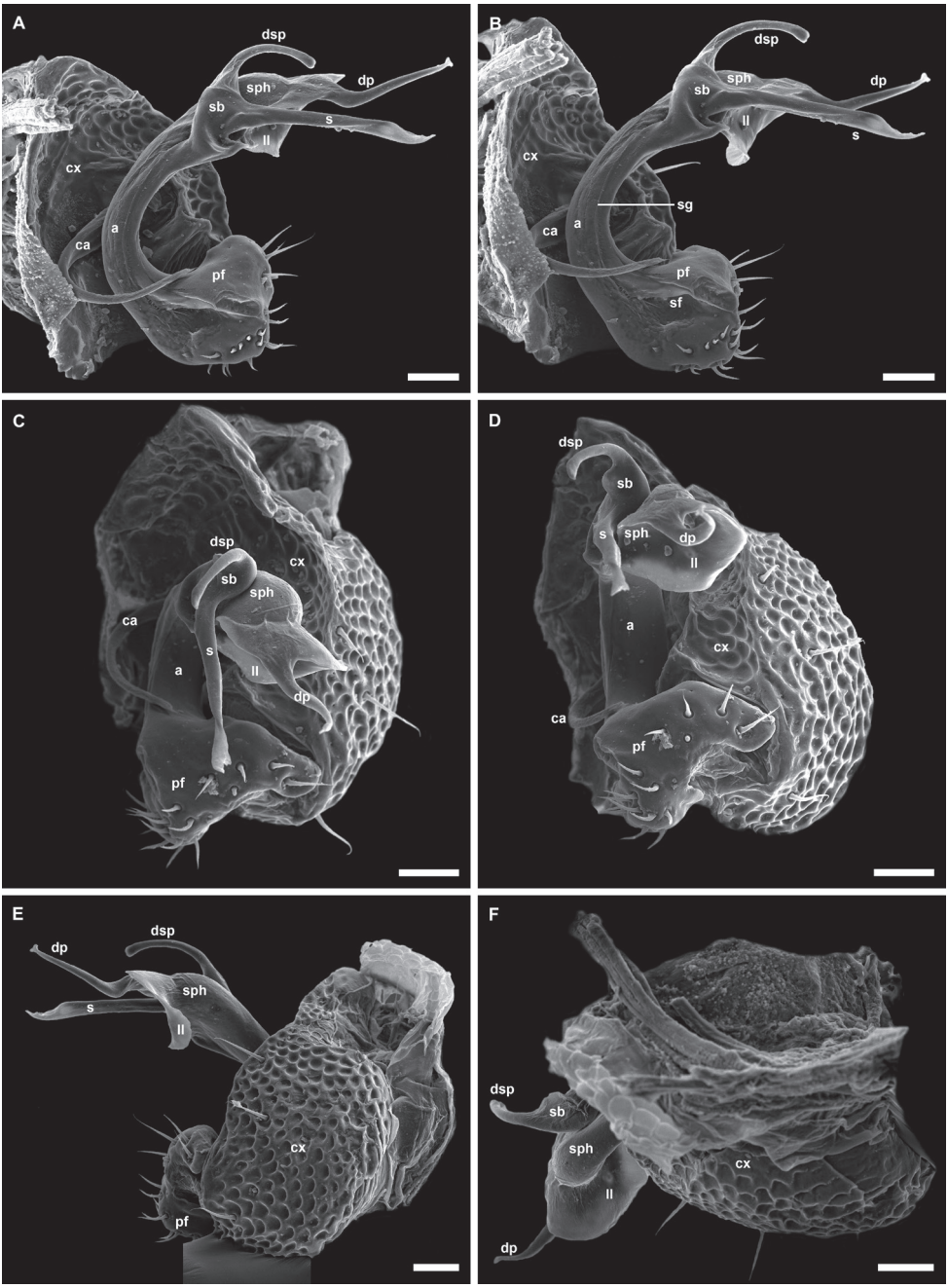

Figure 6. *Balkanodesminus bulgaricus* (Strasser, 1962) gen. nov., comb. nov., ♂ from Ponora Cave, Bulgaria, left gonopod (NMNHS-10813) **A, B** mesal views **C** antero-distal view **D** distal view **E** lateral view **F** anterior view. Abbreviations: **a** acropodite, **ca** cannula, **cx** coxa, **dp** distal projection of solenophore, **dsp** distal solenomeral process, **ll** lamella of solenophore, **pf** prefemorite, **s** solenomere, **sb** solenomeral branch, **sf** seminal fossa, **sg** seminal groove, **sph** solenophore. Scale bars: 0.02 mm.

***Balkanodesminus dentatus* (Strasser, 1966a) gen. nov., comb. nov., stat. nov.**
Figs 17L, 18

Bacillidesmus bulgaricus dentatus Strasser, 1966a: 341, figs 16, 17.
Bacillidesmus bulgaricus dentatus in part.—Stoev 2007: 384; Beron 2015: 80, 411; Bachvarova et al. 2017: 521.
Bacillidesmus dentatus in part.—Ceuca 1992: 416; Kime and Enghoff 2011: 71, 262.
not *Bacillidesmus bulgaricus dentatus*—Stoev 2004: 149.

Diagnosis. Differs from *Balkanodesminus bulgaricus* gen. nov., comb. nov. and *B. serbicus* gen. nov. et sp. nov. by the presence of shorter (vs. longer) metatergal setae and their greater (vs. smaller) number of rows, as well as by the presence of more complicated (vs. more simplified) gonopods, with biramous (vs. uniramous) distal solenomeral process and larger and denticulated (vs. smaller and smooth) lamella of solenophore. From *B. dentatoides* gen. nov. et sp. nov., with which it shares similar habitus and similar gonopods, it differs by the presence of more robust (vs. slenderer) solenomere, by short process (vs. triangular tooth) on distal solenomeral process, and by the presence (vs. absence) of additional short subdistal process at distal projection of solenophore. In addition, lateral lamella and basal lobe less developed than in *B. dentatoides* gen. nov. et sp. nov.

Material examined. 1 ♀, 1 juv. (NMNHS-10814), Bulgaria, Vratsa District, Byala Slatina Municipality, Drashan, Drashanskata peshtera Cave (type locality), 22.IX.1992, leg. P. Beron.

Distribution. So far, this species is known only from its type locality, Drashanskata peshtera Cave (Fig. 18).

Remarks. Originally described as a subspecies, *Bacillidesmus bulgaricus dentatus*. Strasser (1966a) pointed out significant differences in the structure of the gonopod between *bulgaricus* and *dentatus*, as well as differences in body size. However, he did not notice the differences in the length and arrangement of metatergal setae between the two taxa. The descriptions of the two new species below, one of which is similar to *bulgaricus* in body size, habitus and gonopods, and the other one to *dentatus*, clearly indicate the presence of two groups of species within this genus.

As mentioned above, Ceuca (1992), and Kime and Enghoff (2011) treated this taxon as a separate species, *Bacillidesmus dentatus*, without, however, any formal taxonomic act. For the sake of stability of nomenclature here we formally raise this taxon to the species level and transfer it to the newly established genus as *Balkanodesminus dentatus* gen. nov., comb. nov., stat. nov.

***Balkanodesminus dentatoides* gen. nov. et sp. nov.**
http://zoobank.org/BEF9EB03-1DC8-4C13-BE0F-DE8A2AD0C257
Figs 7–9, 17M, N, 18

Bacillidesmus bulgaricus dentatus—Stoev 2004: 149.

Bacillidesmus bulgaricus dentatus in part.—Stoev 2007: 384; Beron 2015: 80, 411; Bachvarova et al. 2017: 521; Kime and Enghoff 2011: 71, 262.

Diagnosis. Differs from *Balkanodesminus bulgaricus* gen. nov., comb. nov. and *B. serbicus* gen. nov. et sp. nov. by the presence of shorter (vs. longer) metatergal setae and their greater (vs. smaller) number of rows, as well as by the presence of more complicated (vs. more simplified) gonopods, with biramous (vs. uniramous) distal solenomeral process and larger and denticulated (vs. smaller and smooth) lamella of solenophore. From *B. dentatus* gen. nov., comb. nov., stat. nov., with which it shares similar habitus and similar gonopods, it differs by the presence of slenderer (vs. more robust) solenomere, by small triangular tooth (vs. short process) on distal solenomeral process, and by the absence (vs. presence) of additional short subdistal process at distal projection of solenophore. In addition, lateral lamella and basal lobe more robust than in *B. dentatus* gen. nov., comb. nov., stat. nov.

Name. The species name is a combination of the name *dentatus* and the Ancient Greek suffix *-oides*, referring to the species' particularly strong resemblance to *Balkanodesminus dentatus* gen. nov., comb. nov., stat. nov. Adjective.

Material examined. ***Holotype*** ♂ (NMNHS-10815), Bulgaria, Lovech District, Yablanitsa Municipality, Brestnitsa, Saeva dupka Cave, clay, 13.X.1997, leg. B. Petrov & P. Stoev.

Paratypes. 2 ♂♂ (NMNHS-10816, 10817), 1 ♀, (NMNHS-10818), same data as for holotype; 1 ♂ (used for SEM, NHMW MY10258) same data as for holotype.

Additional material. 1 ♂ (right gonopod used for SEM, NHMW MY10267), 2 ♂♂ (NMNHS-10819, 10820), 2 ♀♀ (NMNHS-10821, 10822), Lovech District, village of Sopot, Sopotska peshtera Cave, 8.V.2004, leg. P. Beron.

Description. ***Number of body rings and measurements*:** Body with 19 rings (including telson) in adults, moniliform. Holotype male 3.8 mm long, width of midbody pro- and metazonae 0.25 mm and 0.30 mm, respectively. Paratype males 3.4–3.9 mm long, width of midbody pro- and metazonae 0.23–0.25 mm and 0.29–0.31 mm, respectively. Paratype female 4.3 mm long, width of midbody pro- and metazona 0.30 and 0.35 mm, respectively.

***Coloration*:** Entirely pallid, slightly translucent (Fig. 7).

***Head*:** Broader than collum, setose (Fig. 7B); epicranial suture poorly developed; isthmus between antennae ≈ 1.3 × broader than diameter of antennal socket. Labrum with three labral teeth, and with 3+3 labral and five supralabral setae (Fig. 8B). Gnathochilarium without peculiarities. Antennae rather short, clavate (Figs 7B, 8C, D). Antennomere length 6 > 2 = 3 = 4 > 5 > 7 = 1. Antennae 0.6 mm long in the holotype male; length/breadth ratios of antennomeres 1–7: 1 (1), 2 (2), 3 (2), 4 (2), 5 (1), 6 (1) and 7 (1). Antennomere 6 with four sensilla trichodea and with strongly developed disto-dorsal pit with numerous long sensilla basiconica partially exposed outside the pit (Fig. 8D). Antennomere 7 with one sensillum trichodeum and a small bulge with three sensilla basiconica spiniformia (Fig. 8C, D). Four apical cones (Fig. 8D).

***Collum*:** Semi-circular, with one or two lateral incisions and ≈ 7 irregular rows of medium sized and trichoid setae.

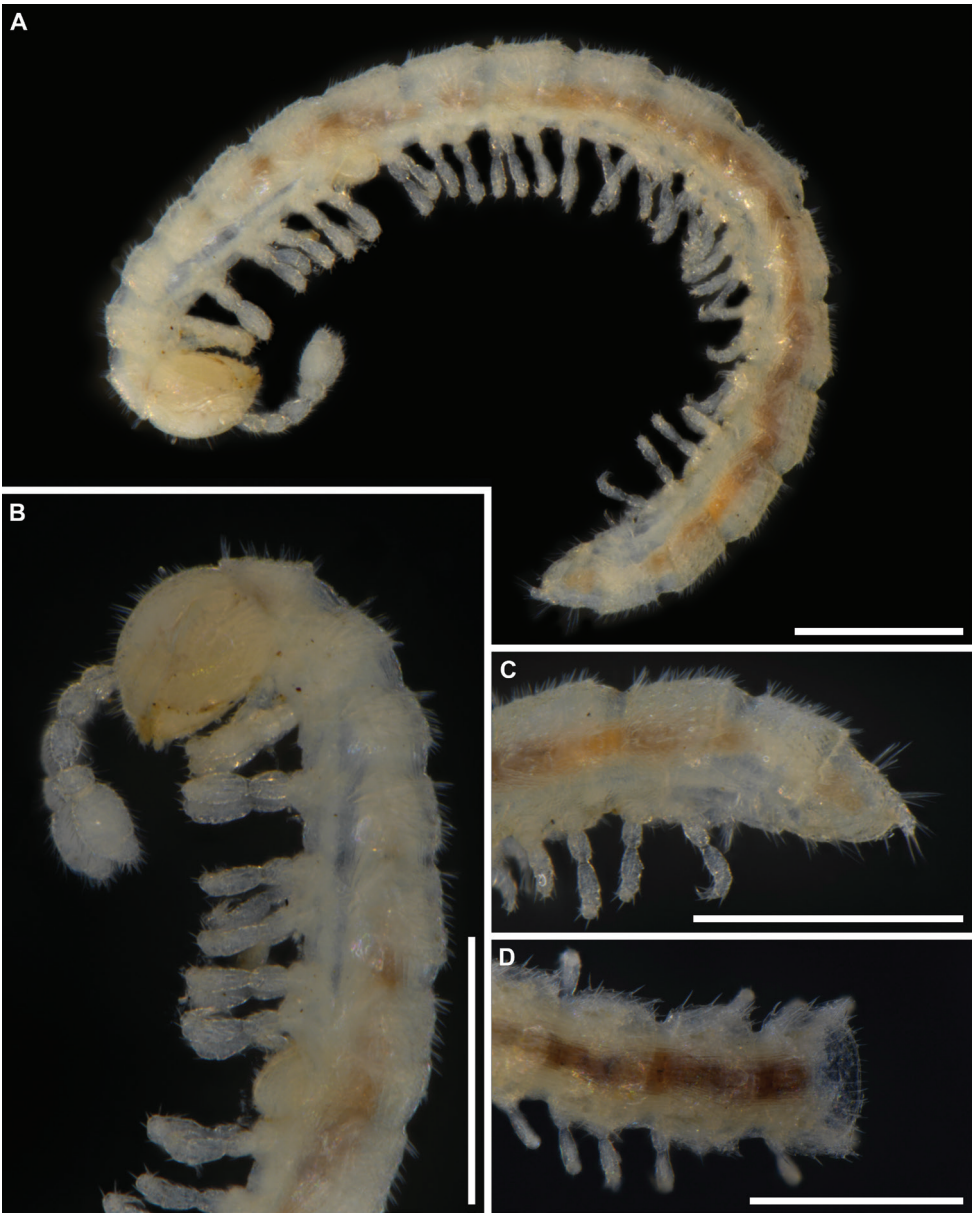

Figure 7. *Balkanodesminus dentatoides* gen. nov. et sp. nov., holotype ♂ (**A–C**, NMNHS-10815) and paratype ♂ (**D**, NHMW MY10258), habitus **A** lateral view **B** anterior part of body, lateral view **C** posterior part of body, lateral view **D** midbody rings, dorsal view. Scale bars: 0.5 mm.

***Body rings*:** Tegument shining, texture alveolate, reticulate and scaly. Rings densely setose. Setae rather short and trichoid, originating from small tubercules (Figs 7, 8A, E–G, I). Posteriormost tubercules mostly with a small thorn. Rings 2–4 with ≈ 4 rows of setae (Fig. 8A). Rings 5–18 with ≈ 6–8 irregular rows of setae (Fig. 8E–G, I).

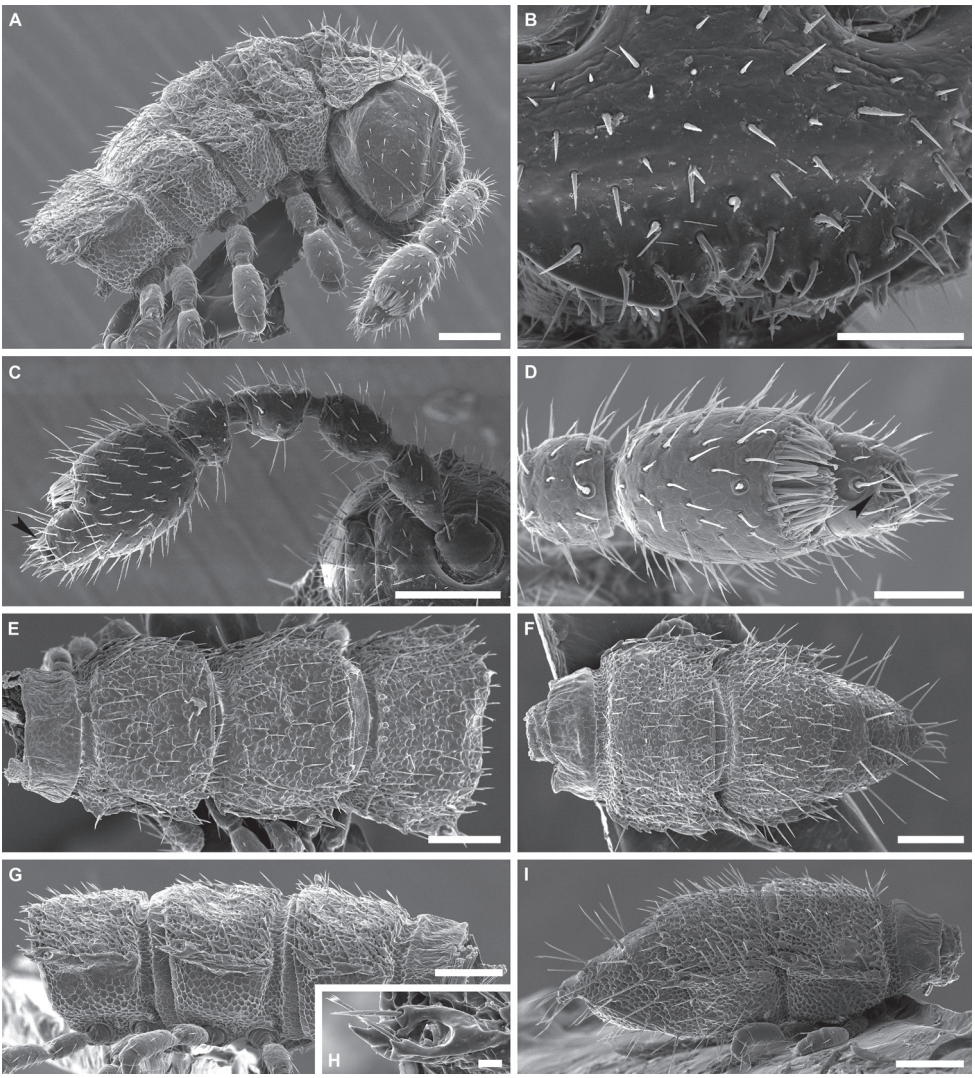

Figure 8. *Balkanodesminus dentatoides* gen. nov. et sp. nov., paratype ♂ habitus (NHMW MY10258) **A** anterior part of body, lateral view **B** labrum, anterior view **C** right antenna, anterior view (arrow indicates small bulge with sensilla basiconica spiniformia) **D** distal antennomeres of right antenna, dorsal view (arrow indicates small bulge with sensilla basiconica spiniformia) **E, F** body rings 8–10, lateral and dorsal views, respectively **G** right ozopore 10, lateral view **H, I** body rings 17–19, dorsal and lateral views, respectively. Scale bars: 0.1 mm (**A, C, E, F, H, I**), 0.05 mm (**B, D**), 0.01 mm (**G**).

Paraterga serrated, with 5–7 teeth (Figs 7D, 8E–G, I). Pore formula normal: 5, 7, 9, 10, 12, 13, 15–18. Poriferous metazonae with an enlarged postero-lateral cone bearing an ozopore and three medium-sized setae (Fig. 8H). Epiproct blunt, directed slightly ventrad (Figs 7C, 8F, I). Paraprocts semi-spherical, each with two long setae originating from small tubercules and ≈ 10 shorter setae without tubercules (Fig. 8I).

Hypoproct trapeziform with 2 long distal setae and numerous shorter setae throughout (Fig. 7C). Sterna unmodified, poorly setose. Pleurosternal carinae absent, only a few small teeth sometimes present on rings 2 and 3 (Fig. 8A). Gonopod aperture large, subsemi-circular.

***Walking legs*:** Legs 1–3 in males with swollen femur; coxa 2 with a short mesal apophysis (cf. Strasser 1966a: 341, fig. 13). No other peculiarities.

Gonopods (Figs 9, 17M, N): Coxa (cx) large, semi-circular in ventral and lateral views, with differentiated gonocoel mesally; lateral part swollen, alveolate, with three long setae near mesal ridge. Cannula (ca) long, C-shaped. Telopodite relatively long compared to coxa, consisting of a transverse, setose prefemorite (pf) and a somewhat C-shaped (in lateral and mesal views) acropodite (a) longitudinally divided in the distal half into two branches, solenomeral branch (sb) and solenophore (sph). Solenomeral branch positioned mesally, with a narrow "neck", then abruptly expands and transversely divides into two processes, solenomere (s) and distal solenomeral process (dsp). Extended part of solenomeral branch with spiculiform outgrowths. Solenomere (s) very long, slender, subdistally with a small bifurcation. Distal solenomeral process (dsp) extends in the same direction as solenomere and is half as long as solenomere; bifurcated=with small additional mesal tooth (t). Solenophore (sph) longer and more robust than solenomeral branch, characterized by a robust, lateral, ear-shaped lamella (ll) and a distal projection (dp). Lateral lamella (ll) begins at bifurcation of solenomeral branch and solenophore, surrounding laterally solenophore up to beginning of distal ending; lateral margins of lamella denticulated. Distal projection (dp) with strongly developed, basal lamellar lobe (bl), with mesal thickening (mt) and with relativelly short and acuminate process (ap). Seminal groove (sg) starts from seminal fossa (sf) mesally on prefemorite, extends along mesal side of acropodite up to bifurcation of solenomeral branch and solenophore, then passes on lateral side of solenomeral branch, further on solenomere, ending distally.

Habitat. Saeva dupka Cave is a show cave which is now heavily impacted by electrification and continuous touristic flow. The cave has naturally formed 400 meters of corridors and halls. The samples from the cave were taken in 1997, under stones in clay, when the cave was temporarily closed for visitors due to the change of its governance during the democratic changes in Bulgaria. After more than 20 years of active exploration of the cave, new material needs to be collected to assess whether the species was influenced by the human activities. Saeva dupka Cave is inhabited by numerous and diverse invertebrate taxa, but the only troglobiont currently on record is the local endemic *Bulgariella tranteevi* Z. Karaman, 1958 (Coleoptera, Leiodidae) (Beron 2015).

Distribution. So far known only from two caves in Lovech District (Fig. 18).

Remarks. Based on material from Saeva dupka Cave, Stoev (2004) already noticed that there were certain differences in the structure of gonopods of that sample and *Bacillidesmus dentatus*, and he did not exclude the possibility that it belonged to a new taxon. However, he still treated this as *Bacillidesmus bulgaricus dentatus*. After reviewing the material that was available to him, as well as based on the newly studied material, we describe it above as a new species.

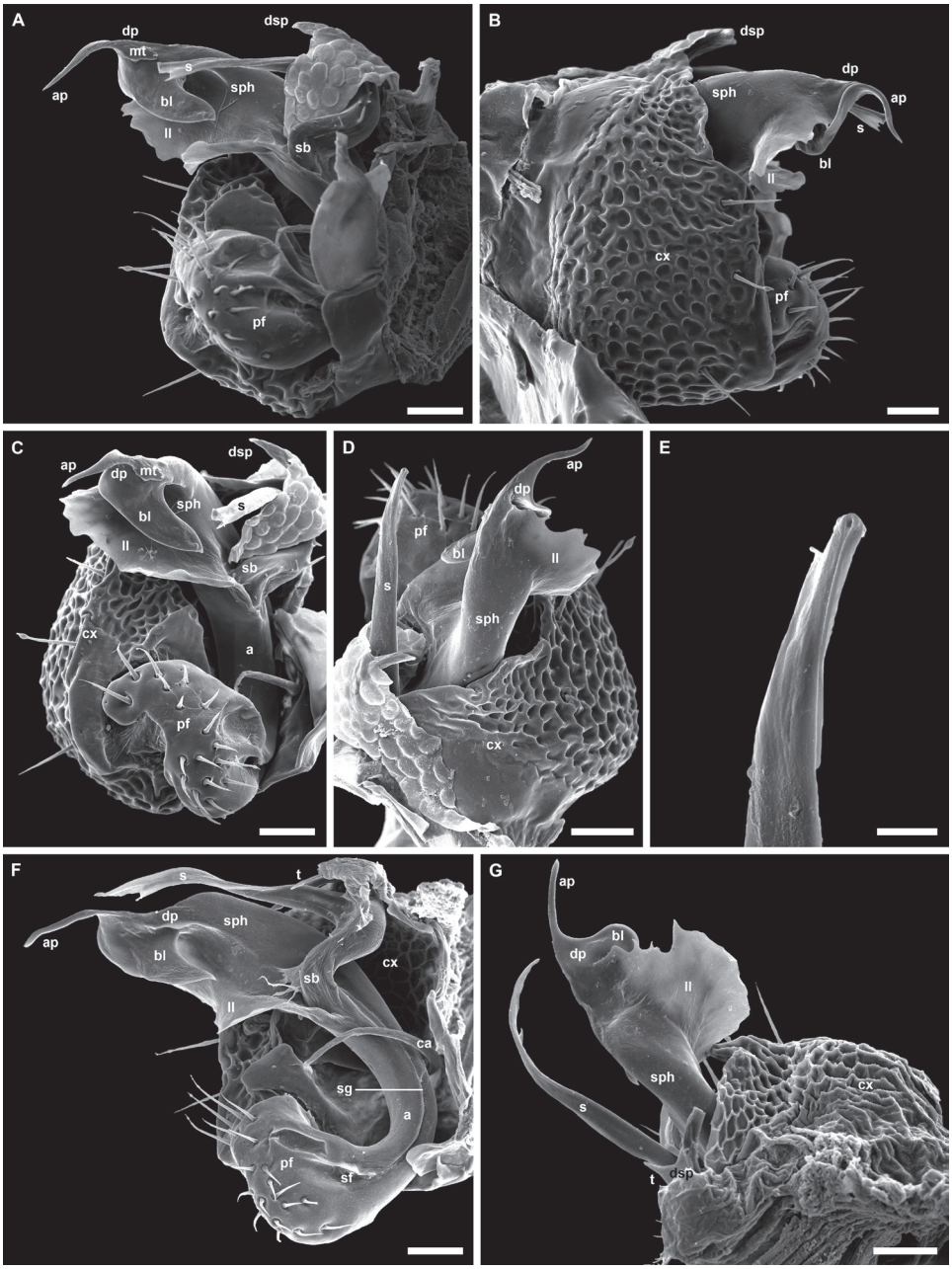

Figure 9. *Balkanodesminus dentatoides* gen. nov. et sp. nov., right gonopods **A–E** paratype ♂ (NHMW MY10258) **A** mesal view **B** lateral view **C** meso-distal view **D** antero-distal view **E** tip of solenomere, distal view **F, G** ♂ from Sopotska peshtera Cave (NHMW MY10267), mesal and antero-disto-lateral views, respectively. Abbreviations: **a** acropodite, **ap** acuminate process of solenophore, **bl** basal lamellar lobe of solenophore, **ca** cannula, **cx** coxa, **dp** distal projection of solenophore, **dsp** distal solenomeral process, **ll** lamella of solenophore, **mt** mesal thickening of solenophore, **pf** prefemorite, **s** solenomere, **sb** solenomeral branch, **sf** seminal fossa, **sg** seminal groove, **sph** solenophore, **t** mesal tooth of distal solenomeral process. Scale bars: 0.02 mm (**A–D, F, G**), 0.005 mm (**E**).

***Balkanodesminus serbicus* gen. nov. et sp. nov.**
http://zoobank.org/2684D82A-21C8-4235-8B2C-39886C7440B1
Figs 10–13, 17J, 18

Diagnosis. Differs from *Balkanodesminus dentatoides* gen. nov. et sp. nov. and *B. dentatus* gen. nov., comb. nov. by the presence of longer (vs. shorter) metatergal setae and their smaller (vs. greater) number of rows, as well as by the presence of more simplified gonopods, with uniramous (vs. biramous) distal solenomeral process and smaller and smooth (vs. larger and denticulated) lamella of solenophore. From *B. bulgaricus* gen. nov., comb. nov., with which it shares similar habitus and similar gonopods, it differs by the presence of smaller (vs. larger) lamella of solenophore, more robust and sigmoid (vs. slender, almost straight) distal projection of solenophore, distal projection with (vs. without) basal lobe, and more robust (vs. slenderer) solenomere, exceeding the distal solenomeral process by ¼ (vs. ½) of its length.

Name. The specific name is an adjective derived from the type locality.

Material examined. ***Holotype*** ♂ (NHMW MY10262), Serbia, Niš, Mt. Kalafat, village of Cerje, Cerjanska Cave (= Provalija Cave), 29.X.2017, leg. D. Antić.

Paratypes. 1 ♂ (NHMW MY10263), 1 ♀ (used for SEM, NHMW MY10264), 1 ♀, 7 juveniles (NHMW MY10265), same data as for holotype.

Description. ***Number of body rings and measurements*:** Body with 19 rings (including telson) in adults, moniliform (Fig. 10). Holotype male and paratype male 4.8 mm and 4.7 mm long, respectively; width of midbody pro- and metazonae 0.30 mm and 0.45 mm, respectively. Paratype females 5.0 mm and 5.2 mm long, width of midbody pro- and metazonae 0.35 mm and 0.50 mm, respectively.

***Coloration*:** Entirely pallid, slightly translucent (Fig. 10).

***Head*:** Broader than collum, setose; epicranial suture poorly developed; isthmus between antennae ≈ 1.7 × broader than diameter of antennal socket (Fig. 11A, B). Labrum with three labral teeth, and with 3+3 labral and five supralabral setae (Fig. 11A). Gnathochilarium without peculiarities. Antennae rather short, clavate (Fig. 11). Antennomere length 6 > 2 = 3 = 4 > 5 > 7 = 1. Antennae 0.7 mm long in the holotype male; length/breadth ratios of antennomeres 1–7: 1 (1), 2 (2), 3 (2), 4 (2), 5 (1), 6 (1.5) and 7 (1). Antennomere 6 with four sensilla trichoidea and with strongly developed disto-dorsal pit with numerous long sensilla basiconica partially exposed outside the pit (Fig. 11E, F). Antennomere 7 with one sensillum trichodeum and a small bulge with three sensilla basiconica spiniformia (Fig. 11E). Four apical cones (Fig. 11C).

***Collum*:** Semi-circular, with one or two lateral incisions and ≈ 5 irregular rows of relatively long and trichoid setae.

***Body rings*:** Tegument shining, texture alveolate, reticulate and scaly. Setae relatively long and trichoid, originating from small tubercules (Figs 10B, 12). Posteriormost tubercules mostly with a small thorn (Fig. 12A, E). Rings 2–4 with three mostly regular rows of setae, one anterior and two posterior (Fig. 10B). Rings 5–18 with ≈ 4–6 irregular rows of setae (Figs 10B, 12). Paraterga serrated, with four or five teeth (Fig. 12A, D, E). Pore formula normal: 5, 7, 9, 10, 12, 13, 15–18. Poriferous metazonae with an enlarged postero-lateral cone bearing an ozopore and three medium-sized setae (Fig. 12C). Epiproct blunt,

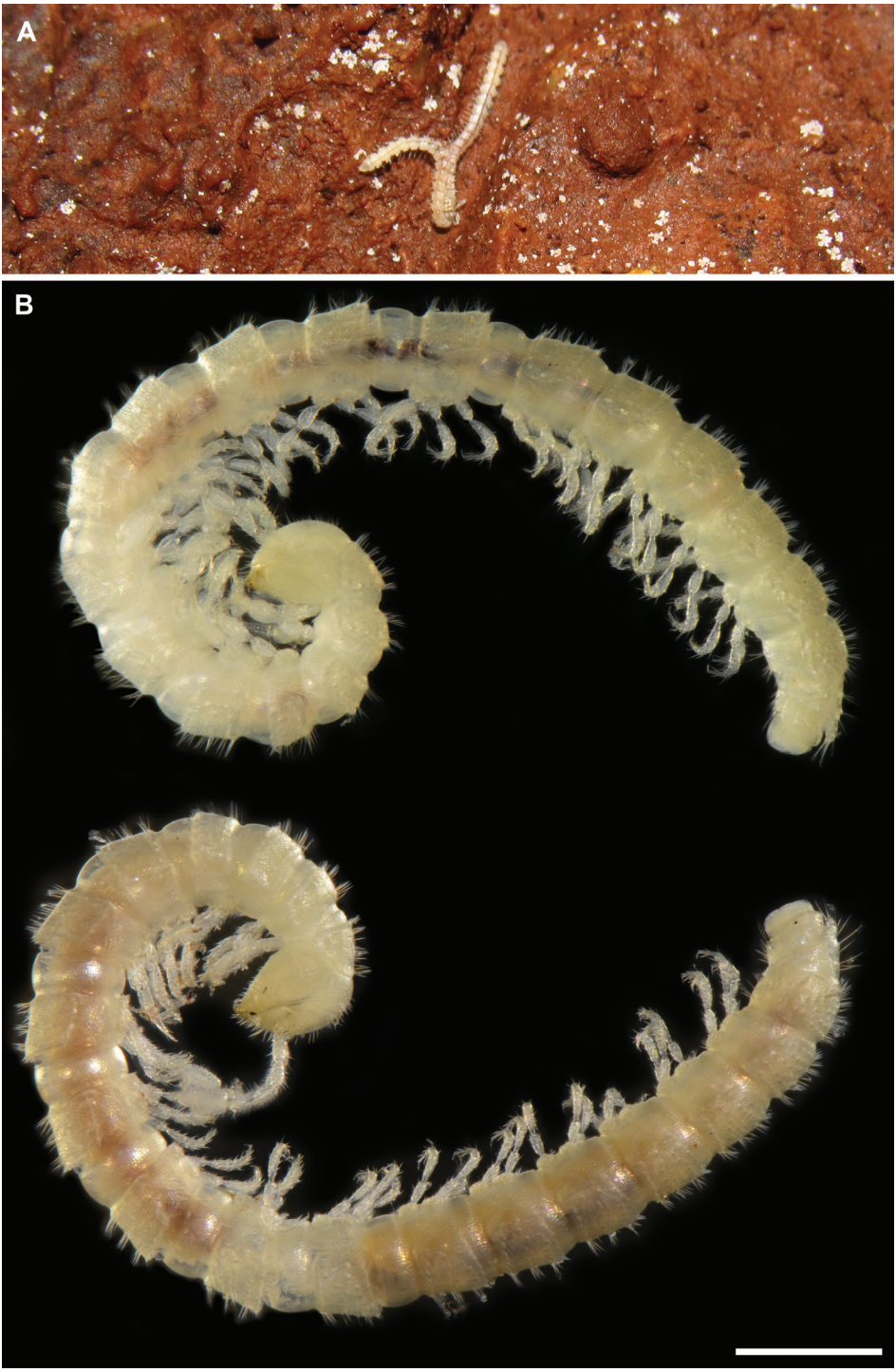

Figure 10. *Balkanodesminus serbicus* gen. nov. et sp. nov., habitus (NHMW) **A** mating in situ (photo D. Antić) **B** holotype ♂ (NHMW MY10262) and paratype ♀ (NHMW MY10265), respectively, lateral views. Scale bar: 0.5 mm.

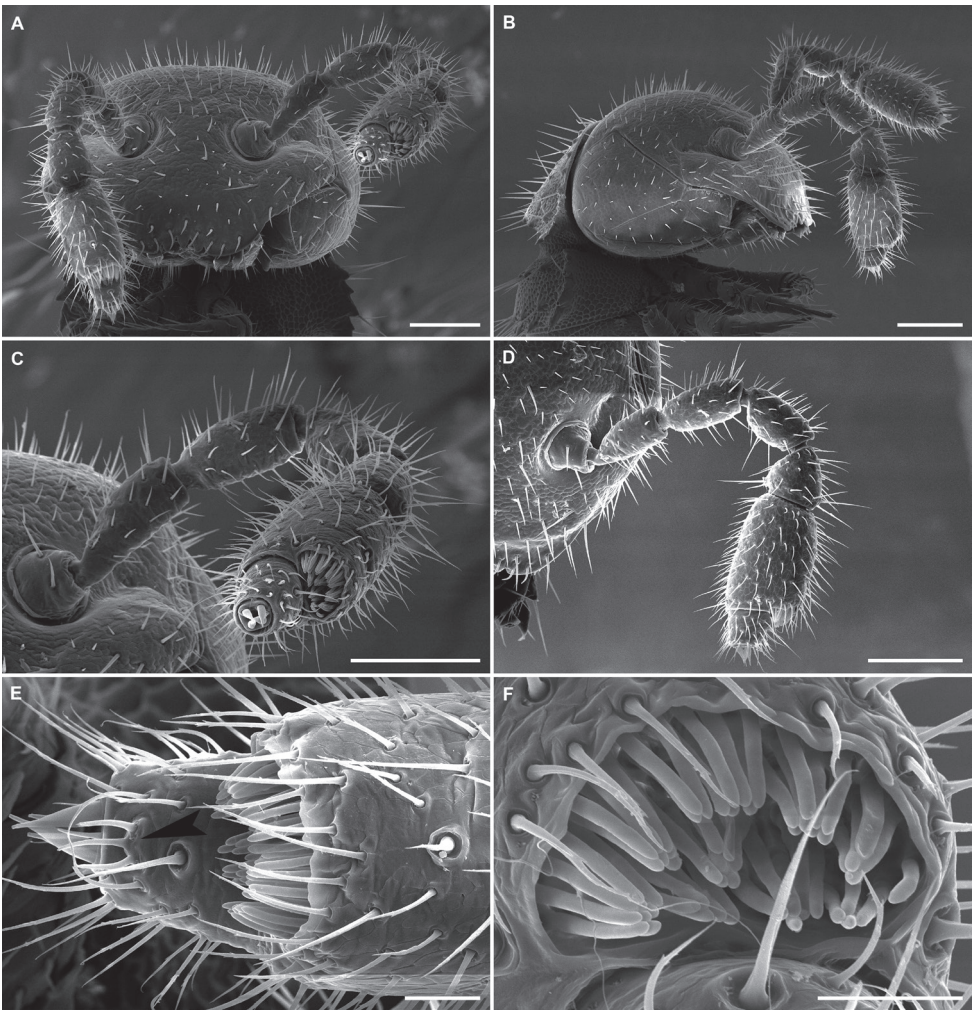

Figure 11. *Balkanodesminus serbicus* gen. nov. et sp. nov., paratype ♀ habitus (NHMW MY 10264) **A** head, anterior view **B** head and collum, lateral view **C, D** left antenna, semi-anterior and anterior views, respectively **E** right antennomeres 6 and 7, dorsal view (arrow indicates small bulge with sensilla basiconica spiniformia) **F** sensilla basiconica of left antennomere 6, disto-dorsal view. Scale bars: 0.1 mm (**A–D**), 0.02 mm (**E, F**).

directed slightly ventrad (Fig. 12G, H). Paraprocts semi-spherical, each with 2 long setae originating from small tubercules and ≈ 10 shorter setae without tubercules (Fig. 12H). Hypoproct trapeziform, with two long distal setae and numerous shorter setae throughout (Fig. 12H). Sterna unmodified, poorly setose. Pleurosternal carinae absent, only a few small teeth sometimes present on rings 2 and 3. Gonopod's aperture large, subsemi-circular.

***Walking legs*:** Legs 1–3 in males with swollen femur; coxa 2 with a short mesal apophysis (cf. Strasser 1966a: 341, fig. 13). No other peculiarities.

Gonopods (Figs 13, 17J): Coxa (cx) large, semi-circular in ventral and lateral views, with differentiated gonocoel mesally; lateral part swollen, alveolate, with three long setae near mesal ridge. Cannula (ca) long, C-shaped. Telopodite long compared to coxa,

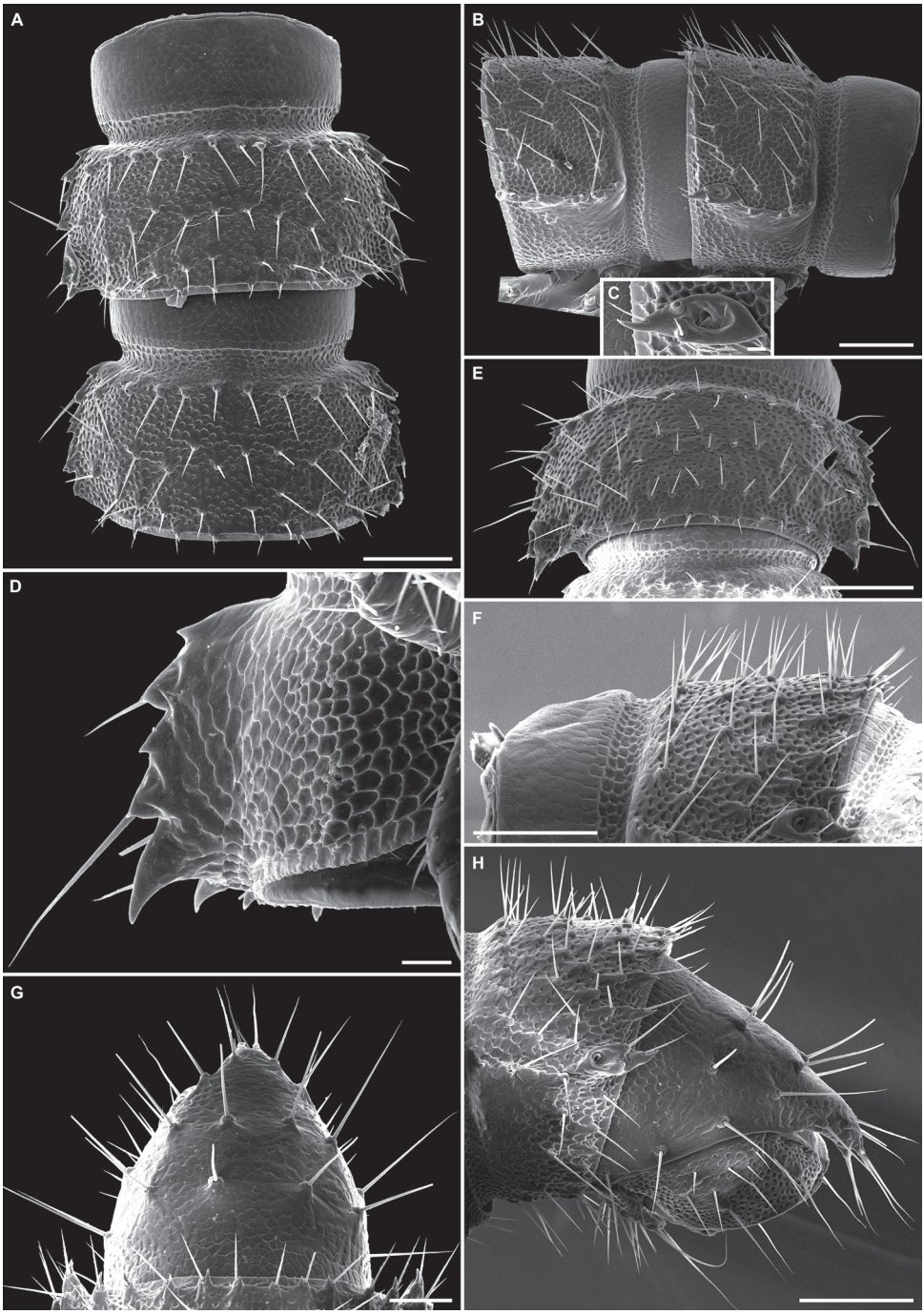

Figure 12. *Balkanodesminus serbicus* gen. nov. et sp. nov., paratype ♀ habitus (NHMW MY10264) **A, B** mid-body rings 10 and 11, dorsal and lateral views respectively **C** right ozopore 10, lateral view **D** right half of body ring 4, ventral view **E, F** body ring 17, dorsal and lateral views, respectively **G** telson, dorsal view **H** body ring 18 and telson, lateral view. Scale bars: 0.1 mm (**A, B, E, F, H**), 0.05 mm (**G**), 0.02 mm (**D**), 0.01 mm (**C**).

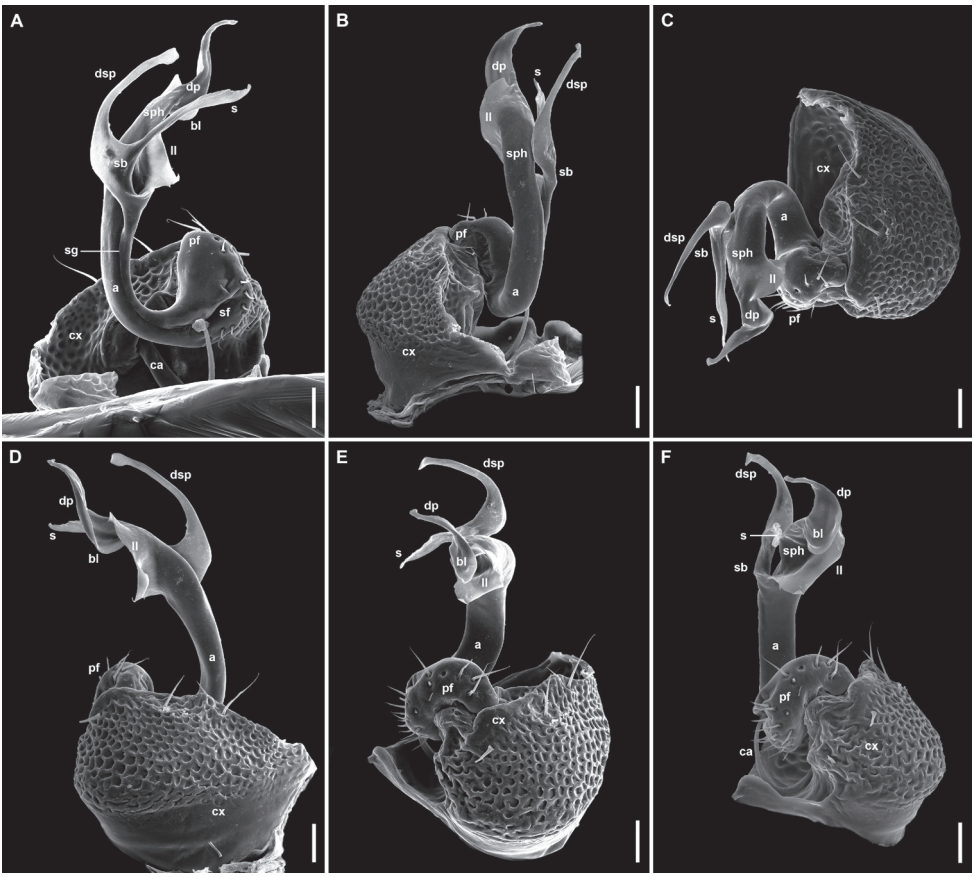

Figure 13. *Balkanodesminus serbicus* gen. nov. et sp. nov., paratype ♂ left gonopod (NHMW MY10263) **A** mesal view **B** anterior view **C** distal view **D** lateral view **E** postro-lateral view **F** posterior view. Abbreviations: **a** acropodite, **bl** basal lamellar lobe of solenophore, **ca** cannula, **cx** coxa, **dp** distal projection of solenophore, **dsp** distal solenomeral process, **ll** lamella of solenophore, **pf** prefemorite, **s** solenomere, **sb** solenomeral branch, **sf** seminal fossa, **sg** seminal groove, **sph** solenophore. Scale bars: 0.02 mm.

consisting of a transverse, setose prefemorite (pf) and a somewhat C-shaped (in lateral and mesal views) acropodite (a) longitudinally divided in its distal half into two branches, solenomeral branch (sb) and solenophore (sph). Solenomeral branch positioned mesally, with a narrow base, then abruptly expands and transversely divides into two processes, solenomere (s) and distal solenomeral process (dsp). Solenomere (s) long, slender, distally expanded (in lateral and mesal views), forming U-shaped rift with distal solenomeral process. Distal solenomeral process (dsp) extends in the same direction as solenomere, ¾ the length of solenomere; ending with a small expansion (in lateral and mesal views). Solenophore (sph) longer and more robust than solenomeral branch, characterized by a lateral, ear-shaped lamella (ll) and a distal projection (dp). Lateral lamella (ll) begins at bifurcation of solenomeral branch and solenophore, surrounding laterally solenophore

up to beginning of distal projection; lateral margins of lamella smooth. Distal projection (dp) sigmoid (in lateral and mesal views), with well-developed, basal lamellar lobe (bl). Seminal groove (sg) starts from seminal fossa (sf) mesally on prefemorite, extends along mesal side of acropodite up to bifurcation of solenomeral branch and solenophore, then passes on lateral side of solenomeral branch, further on solenomere, ending subdistally.

Habitat. With its 6131 m of explored channels, the Cerjanska Cave represents one of the longest and most significant fluviokarst underground systems in Serbia. This is a relatively simple speleological object, consisting of one main river channel in two levels with a length of 4903 m, as well as several side channels with a total length of 1228 m (Nešić 2016). Numerous arthropod taxa have been registered in the cave, from epigean, guanophiles, trogloxenes, and troglophiles to troglobionts (Pavićević et al. 2016). The troglobionts include the endemic Balkan harvestman *Paranemastoma bureschi* (Roewer, 1926), the millipede *Dazbogosoma naissi* Makarov & Ćurčić in Makarov et al. 2012, and the carabid beetle *Duvalius rtanjensis provalijae* Pavićević, Zatezalo & Popović, 2016, the latter two endemics of Cerjanska Cave.

Despite many years of speleological and biospeleological research in the Cerjanska Cave, the new taxon was not registered until the first Biospeleological Expedition of the Serbian Biospeleological Society, organized at the end of October 2017. All 11 specimens were found in a small area, in the initial part of the cave. One male, one female and seven juveniles were found on the left side of the river, on a small branch of a tree lying on the wet sand. Another male and female were found just on the opposite side of the river, on the wall, in copulation (Fig. 10A).

Distribution. So far, known only from its type locality, the Cerjanska Cave, Serbia (Fig. 18).

Remarks. This is the first representative of the family Trichopolydesmidae in Serbia.

Taxa from the Rhodope Mountains

Genus *Rhodopodesmus* gen. nov.

http://zoobank.org/1D609274-0185-4A6E-85CF-D32654CBFEF9

Type species. *Rhodopodesmus niveus* gen. nov. et sp. nov., by monotypy.

Diagnosis. Differs from all European Trichopolydesmidae by the presence of characteristic acropodite of the gonopods divided into two branches that are parallel and completely meso-laterally oriented to each other, with solenomeral branch transversely tripartite, where the proximal-most branch is the shortest, while solenomere and distal solenomeral process are longer and of the same length. The most similar genus is *Balkanodesminus* gen. nov., but it differs from *Rhodopodesmus* gen. nov., by the presence of bifid solenomeral branch (for more details on gonopod differences see below under Remarks).

In addition, the diagnosis can be amended with the following combination of characters: small size (4.3–5.4 mm), 19 body rings (including telson), sensilla basiconica on antennomere 6 partially exposed outside the pit, hypoproct with more than two long distal setae, paraprocts with more than 2+2 long setae, metaterga with 4–8 irregular rows of medium-sized trichoid setae.

Name. The new genus is named after the Rhodope Mountains, its type locality, in combination with *–desmus*, the common suffix in Polydesmida. The name is a masculine noun.

***Rhodopodesmus niveus* gen. nov. et sp. nov.**
http://zoobank.org/CC18A689-89BD-4197-922D-9CB3D8B3EA77
Figs 14–16, 17K, 18

Bacillidesmus sp. nov.—Vagalinski and Stoev 2011: 135.
Bacillidesmus sp. [nov.]—Beron 2015: 80.

Diagnosis. As for the monospecific genus.

Name. The specific name is a Latin adjective; *niveus* refers to the snow-white body color of the living specimens. Furthermore, the name of the type locality, cave Snezhanka, in Bulgarian means Snow White, the heroine from the fairy tale of the Brothers Grimm.

Material examined. ***Holotype*** ♂ (NMNHS-10823), Bulgaria, Pazardzhik District, Peshtera Municipality, Peshtera, Snezhanka Cave, N 42.00222, E 24.27764, 26.X.2020, leg. D. Antić & B. Vagalinski.

Paratypes. 3 ♀♀ (one used for SEM, NMNHS-10824–10826), same data as for holotype; 1 ♀ (used for SEM, NHMW MY10259) same data as for holotype.

Additional material. 1 ♂ (fragments, one gonopod available, NMNHS-10827), 1 ♀ (fragments, NMNHS-10828), both fragments, 1 whole juvenile (NMNHS-10829), same cave but 18.IX.2005, leg. P. Beron.

Description. ***Number of body rings and measurements*:** Body with 19 rings (including telson) in adults, moniliform (Fig. 14). Holotype male 5.3 mm long, width of midbody pro- and metazonae 0.35 mm and 0.50 mm, respectively. Paratype females 4.3–5.4 mm long, width of midbody pro- and metazonae 0.35–0.40 mm and 0.45–0.60 mm, respectively.

***Coloration*:** Living animals snow white (Fig. 14A), slightly translucent. Yellowish in alcohol (Fig. 14B–E).

***Head*:** Broader than collum, setose; epicranial suture poorly developed; isthmus between antennae ≈ 1.7 × broader than diameter of antennal socket (Fig. 15A, D). Labrum with three labral teeth, and with 3+3 labral and five supralabral setae (Fig.15A). Gnathochilarium without peculiarities. Antennae rather short, clavate (Figs 14A, C, 15B, C). Antennomere length 6 > 2 = 3 = 4 > 5 > 7 = 1. Antennae 0.8 mm long in holotype male; length/breadth ratios of antennomeres 1–7: 1 (1), 2 (2), 3 (2), 4 (2), 5 (1), 6 (1.5) and 7 (1). Antennomere 6 with four sensilla trichodea and with strongly developed disto-dorsal pit with numerous long sensilla basiconica partially exposed outside the pit (Fig. 15C). Antennomere 7 with one sensillum trichoideum and a small bulge with three sensilla basiconica spiniformia (Fig. 15B, C). Four apical cones (Fig. 15C).

***Collum*:** Semi-circular, with one or two lateral incisions and ≈ 6 irregular rows of medium sized and trichoid setae (Fig. 15D, F).

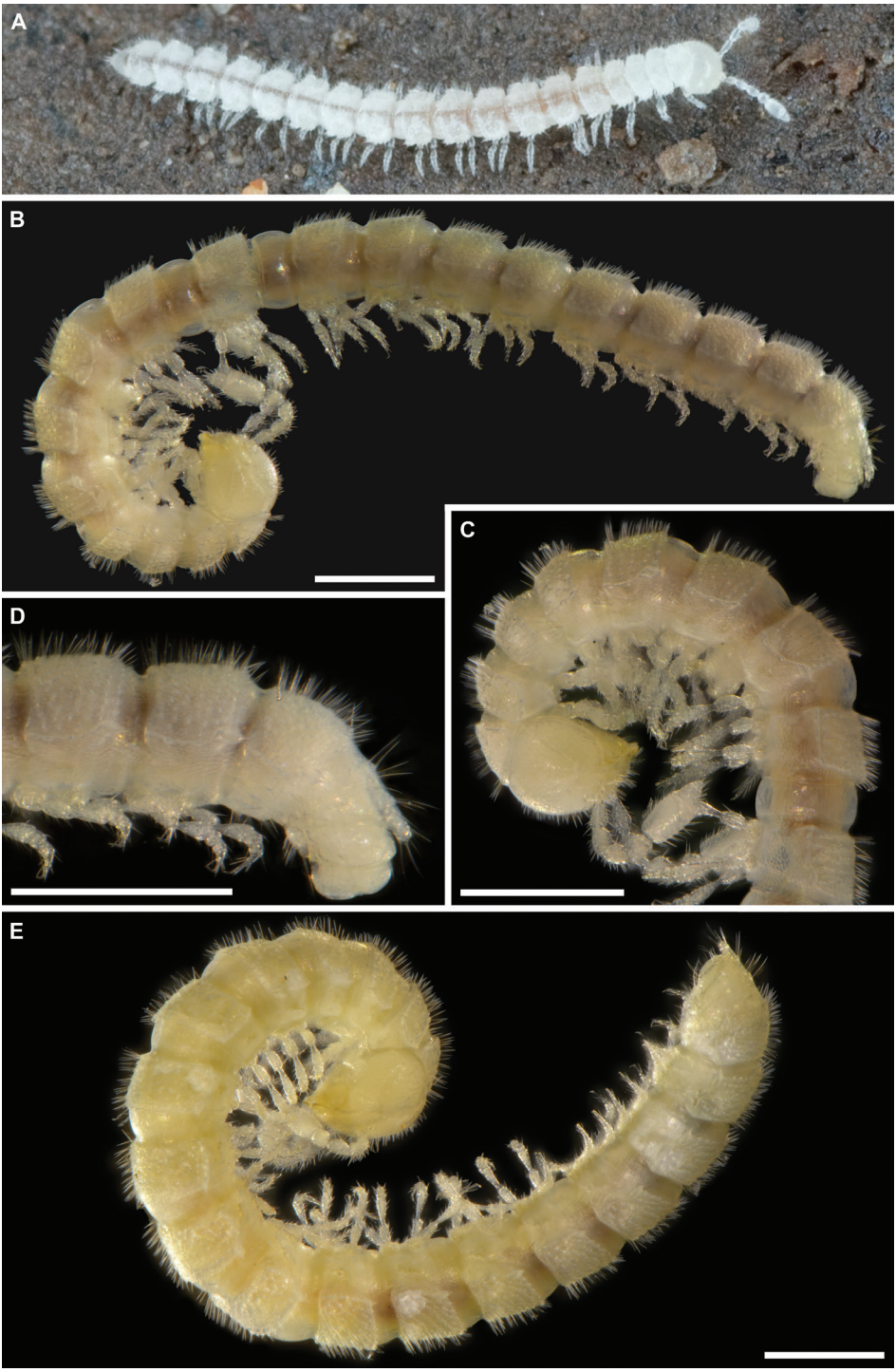

Figure 14. *Rhodopodesmus niveus* gen. nov. et sp. nov., holotype ♂ (**A–D**, NMNHS-10823) and paratype ♀ (**E**, NHMW MY10259) habitus **A** in situ, dorsal view (photo H. Reip) **B** lateral view **C** anterior part of body, lateral view **D** posterior part of body, lateral view **E** lateral view. Scale bars: 0.5 mm.

***Body rings*:** Tegument shining, texture alveolate, reticulate and scaly. Rings densely setose (Fig. 14B–E). Setae medium sized and trichoid, originating from small tubercules (Fig. 15D–F, H–J). Posteriormost tubercules mostly with a small thorn (Fig. 15E). Rings 2–4 with ≈ 4 rows of setae (Fig. 15D, F). Rings 5–18 with ≈ 6–8 irregular rows of setae (Fig. 15D–F, H–J). Paraterga serrated, with 5–7 teeth (Fig. 15E, H). Pore formula normal: 5, 7, 9, 10, 12, 13, 15–18. Poriferous metazonae with enlarged posterolateral cone bearing an ozopore and three medium-sized setae (Fig. 15G). Epiproct triangular in dorsal view, directed slightly caudoventrad (Fig. 15H, I). Paraprocts semi-spherical, each with two long setae originating from small tubercules and ≈ 10 shorter setae without tubercules (Fig. 15I). Hypoproct trapeziform, with two long distal setae and numerous shorter setae throughout (Fig. 15I). Sterna unmodified, poorly setose. Pleurosternal carinae absent, only a few small teeth present on rings 2 and 3 (Fig. 15F). Gonopod aperture large, subsemi-circular.

***Walking legs*:** Legs 1–3 in males with swollen femur, especially femur 2; coxa 2 with a short mesal apophysis (cf. Strasser 1966a: 341, fig. 13). No other peculiarities.

Gonopods (Figs 16, 17K): Coxa (cx) large, semi-circular in ventral view, with deep gonocoel mesally; anterior third much lower than rest of coxa, shield-like, thus lateral, swollen and alveolate part rectangular in lateral view; with ≈ 15 setae. Cannula (ca) long, C-shaped. Telopodite long compared to coxa, consisting of a transverse, setose prefemorite (pf) and more or less C-shaped (in lateral and mesal views) acropodite (a) longitudinally divided in distal half into two branches, solenomeral branch (sb) and solenophore (sph). Solenomeral branch positioned mesally, transversely divided into three processes, besides solenomere (s) and distal solenomeral process (dsp), there is an additional, proximal solenomeral process (psp), more or less spatulate and forming C-shaped rift with solenomere. Both solenomere (s) and distal solenomeral process (dsp) long, slender, of same length, forming acute angle at bifurcation. Solenophore (sph) longer than solenomeral branch, characterized by a lateral lamella (ll) and a distal projection (dp). Lateral lamella (ll) with triangular lobe. Distal projection (dp) long, thin and twisted. Seminal groove (sg) starts from seminal fossa (sf) mesally on prefemorite, extends along mesal side of acropodite up to bifurcation of solenomeral branch and solenophore, then passes on lateral side of solenomeral branch, further proximally on solenomere, ending distally.

Habitat. Snezhanka Cave consists of a single gallery forming six distinct halls with total length of 348 m. The entrance is located at 865 m a.s.l. The cave is rich in diverse sinter formations and sinter ponds. It was established as a natural monument in 1961, and has served as show cave since 1968 (Petrov and Stoev 2007). Most of the cave's invertebrate fauna known at present includes either trogloxenes or troglophiles (Beron 2015), with the exception of the local endemic *Paralovricia beroni* Giachino, Guéorguiev & Vailati, 2011 (Coleoptera, Carabidae), which is considered a probable hypogean, although not typical troglobitic species (Giachino et al. 2011). Another myriapod known from this cave is *Lithobius lakatnicensis* Verhoeff, 1926.

All five recently collected specimens of *Rhodopodesmus niveus* gen. nov. et sp. nov. by D.A. and B.V. were found in the middle part of the cave at two spots, and all were in rotten wood.

Distribution. So far, known only from its type locality, the Snezhanka Cave, Bulgaria (see also under Remarks) (Fig. 18).

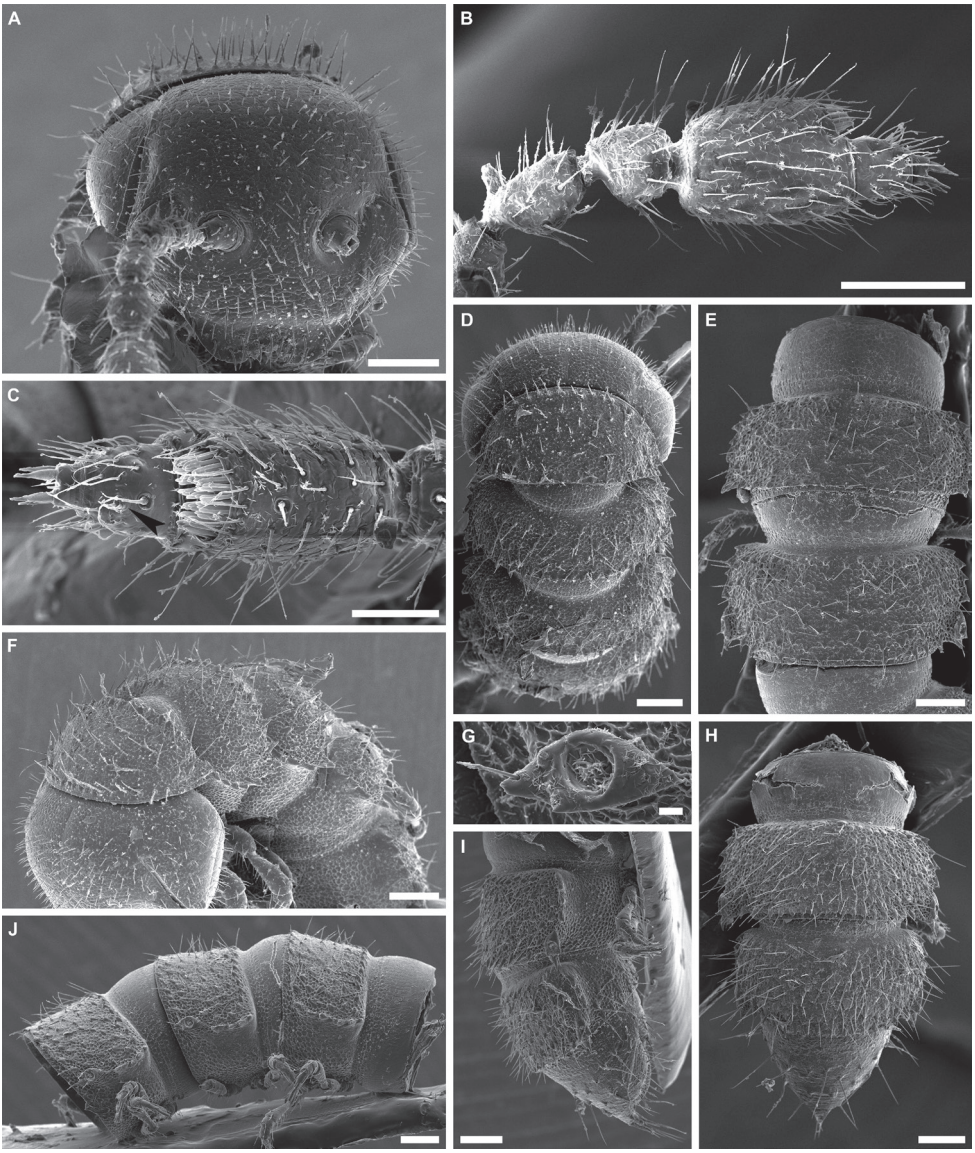

Figure 15. *Rhodopodesmus niveus* gen. nov. et sp. nov., paratype ♀ habitus (NHMW MY10259) **A** head, anterior view **B** right antenna, lateral view **C** tip of right antenna, dorsal view (arrow indicates small bulge with sensilla basiconica spiniformia) **D** anterior part of body, dorsal view **E** body rings 8 and 9, dorsal view **F** anterior part of body, dorso-lateral view **G** right ozopore 9, lateral view **H, I** body rings 17–19, dorsal and lateral views, respectively **J** body rings 8–10. Scale bars: 0.1 mm (**A, B, D–F, H–J**), 0.05 mm (**C**), 0.02 mm (**G**).

Remarks. As mentioned above, it seems that the most similar genus to *Rhodopodsemus* gen. nov. is *Balkanodesminus* gen. nov., which makes sense due to their distributions. These two genera share not only similarities in certain habitus features but also in the gonopods. Both include small-bodied species with 19 rings in adults, with sensilla basiconica on antennomere 6 partially exposed outside the pit, hypoproct with more than two long

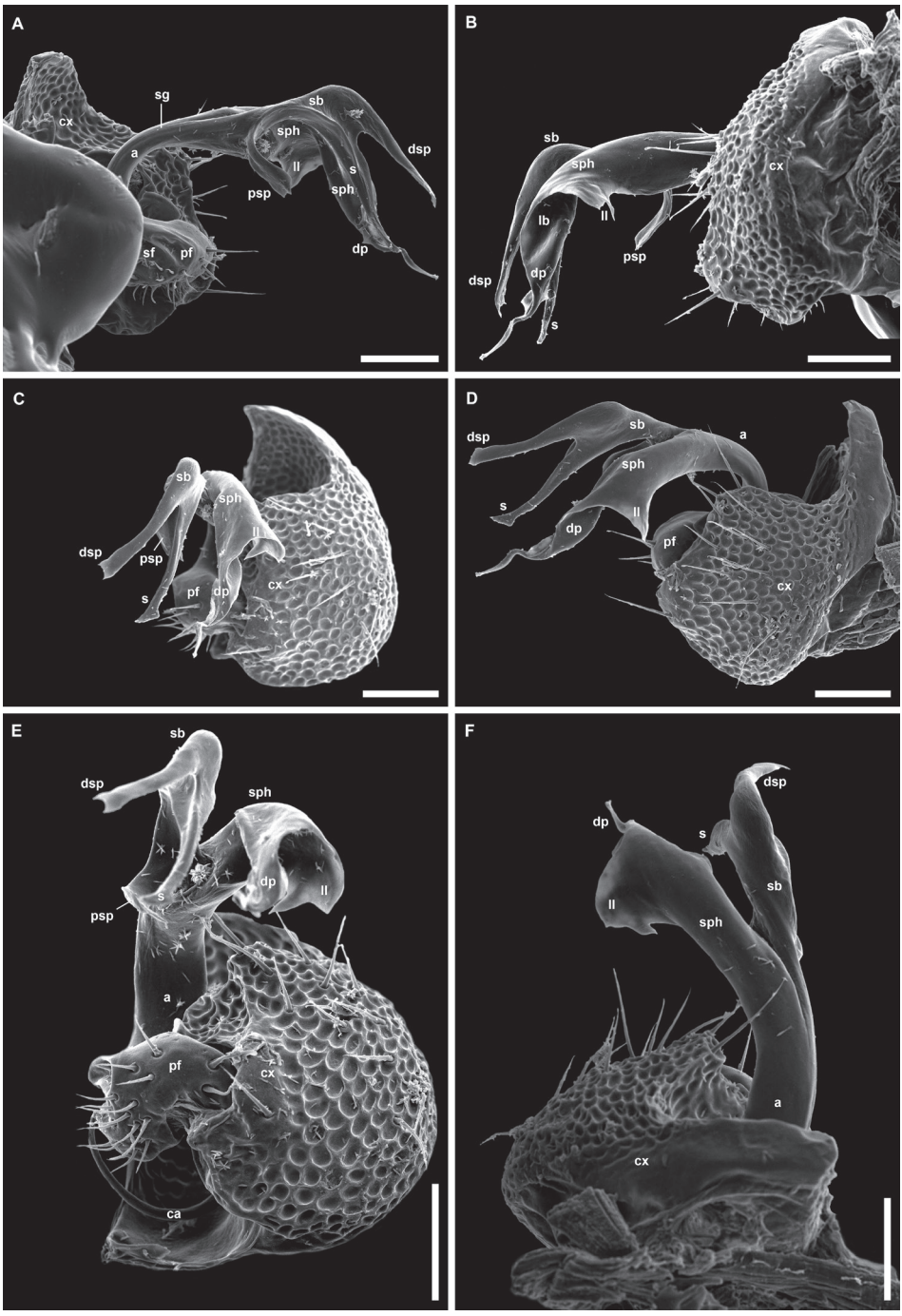

Figure 16. *Rhodopodesmus niveus* gen. nov. et sp. nov., holotype ♂ left gonopod (NMNHS-10823) **A** mesal view **B** lateral view **C** disto-lateral view **D** antero-lateral view **E** postero-distal view **F** anterior view. Abbreviations: **a** acropodite, **ca** cannula, **cx** coxa, **dp** distal projection of solenophore, **dsp** distal solenomeral process, **ll** lamella of solenophore, **pf** prefemorite, **psp** proximal solenomeral process, **s** solenomere, **sb** solenomeral branch, **sf** seminal fossa, **sg** seminal groove, **sph** solenophore. Scale bars: 0.05 mm.

distal setae and paraprocts with more than 2+2 long setae. The conformation of the gonopods is very similar, where the acropodite is longitudinally divided into two branches, with the solenomeral branch transversely divided into long and relatively slender solenomere and well-developed distal process in both genera. Based on this, both genera differ from other European Trichopolydesmidae. However, in *Rhodopodesmus* gen. nov. the solenomeral branch is trifid, where in addition to solenomere and distal process, in the base of this branch there is another, proximal process, which is more or less spatulate. These two genera also differ in some details of the gonopod coxa. *Rhodopodesmus* gen. nov. has a very deep gonocoel, i.e., the anterior third of the coxa is much lower than the rest it, in the form of a shield, so that the rest of the coxa has a more or less rectangular shape laterally, while in *Balkanodesminus* gen. nov. it is semi-circular. Also, the coxa in *Rhodopodesmus* gen. nov. has circa 15 setae, while the same in species of *Balkanodesminus* gen. nov. bears only 3.

It is worth mentioning that specimens of *Rhodopodesmus* gen. nov. were found in two more caves in the Rhodopes, viz., one female in Dupkata (= Dupcheto) Cave near Rakitovo and one male and one female in Skoka Cave near Ribnovo. Unfortunately, the material from Skoka Cave (including one male) could not be relocated in NMNHS for this study, and we still do not know whether it is *R. niveus* gen. nov. et sp. nov. or a new species. The female from Dupkata Cave probably belongs to *R. niveus* gen. nov. et sp. nov. considering its proximity to the type locality of this species. Both localities are mapped (Fig. 18, yellow squares), and already noted under *Bacillidesmus* sp. nov. by Vagalinski and Stoev (2011).

Key to the cavernicolous genera of Trichopolydesmidae from the Carpathian-Balkan arch and the Rhodope Mountains (including *Bacillidesmus*)

1 Adults with 20 body rings (including telson) **2**
– Adults with 19 body rings (including telson) **3**
2 Acropodite of the gonopods trifid, with slender solenomere..... ..... ***Trichopolydesmus*** **(Fig. 17G, H)**
– Acropodite of the gonopods bifid, with enlarged, oval, paddle-like solenomere ..... ***Banatodesmus*** **(Fig. 17D)**
3 Sensilla basiconica completely enclosed inside the pit of antennomere 6..... ..... ***Bacillidesmus*** **(Fig. 17A–C)**
– Sensilla basiconica partially exposed outside the pit of antennomere 6..... **4**
4 Posterior cones of metaterga hook-shaped. Solenomeral branch of acropodite simple, only with solenomere.....***Napocodesmus*** **(Fig. 17E, F)**
– Posterior cones of metaterga not hook-shaped. Solenomeral branch of acropodite transversely bifid or trifid **5**
5 Gonopod coxa with ≈ 15 setae. Solenomeral branch of acropodite transversely trifid.....***Rhodopodesmus*** **gen. nov. (Fig. 17K)**
– Gonopodal coxa with three setae. Solenomeral branch of acropodite transversely bifid..... ***Balkanodesminus*** **gen. nov. (Fig. 17I, J, L–N)**

To distinguish easily all six genera and nine species see Fig. 17.

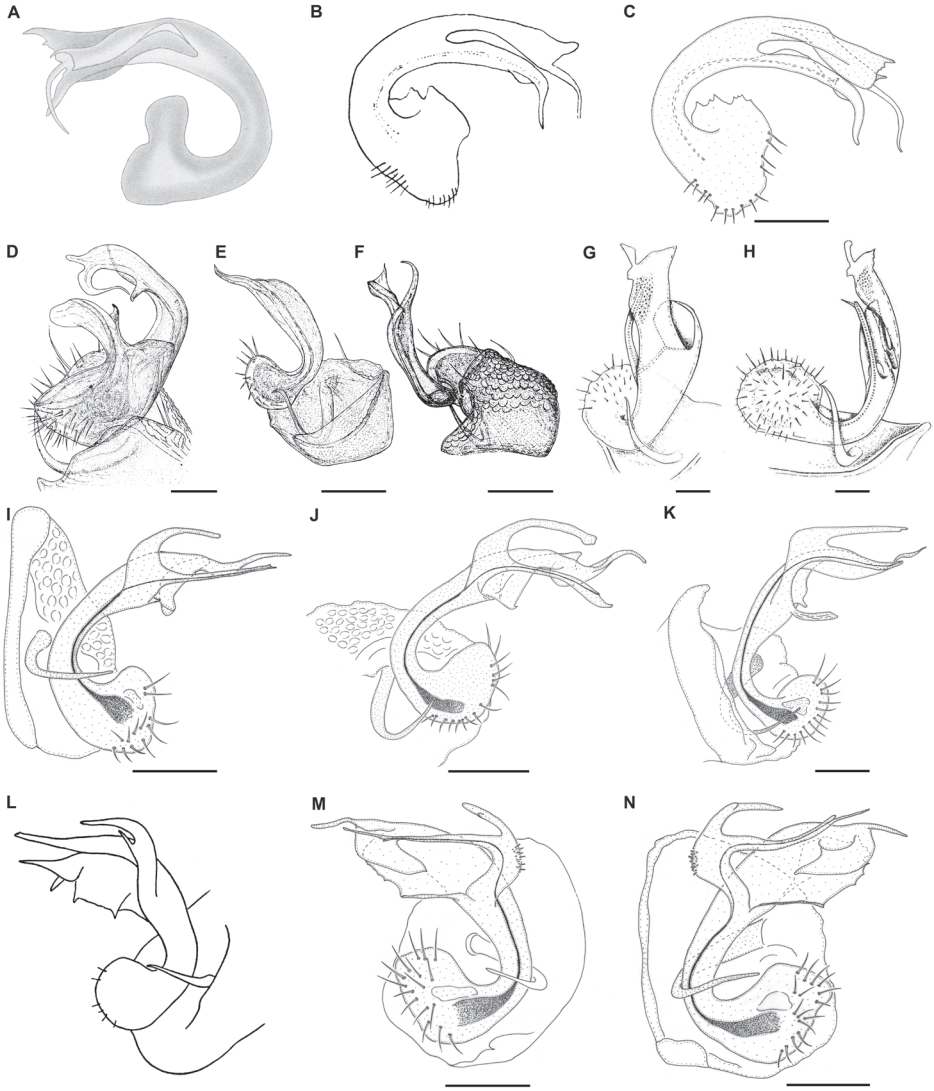

Figure 17. Gonopods of cavernicolous Trichopolydesmidae from the Carpathian-Balkan arch and Rhodopes **A–C** *Bacillidesmus filiformis* (Latzel, 1884) lectotype ♂ (NHWM MY3754) **A** after Attems (1898) **B** ?left gonopod, ?mesal view, after Attems (1940) **C** ?left gonopod, ?mesal view, present study **D** *Banatodesmus jeanneli* (Tabacaru, 1980) syntype ♂, right gonopod, mesal view, after Tabacaru (1980) **E, F** *Napocodesmus florentzae* Tabacaru, 1975 holotype ♂, right gonopod, mesal and anterior views, respectively, after Tabacaru (1975) **G, H** *Trichopolydesmus eremitis* Verhoeff, 1898 ♂ from Cloşani cave, right gonopod, antero-mesal and mesal views, respectively, after Ceuca (1958) **I** *Balkanodesminus bulgaricus* (Strasser, 1962) gen. nov., comb. nov. ♂ from Ponora Cave (NMNHS-10813), left gonopod, mesal view **J** *Balkanodesminus serbicus* gen. nov. et sp. nov. paratype ♂ (NHMW MY10263), left gonopod, mesal view **K** *Rhodopodesmus niveus* gen. nov. et sp. nov. holotype ♂ (NMNHS-10823), left gonopod, mesal view **L** *Balkanodesminus dentatus* (Strasser, 1966a) gen. nov., comb. nov., stat. nov. syntype ♂, right gonopod, mesal view, after Strasser (1966a) **M** *Balkanodesminus dentatoides* gen. nov. et sp. nov. paratype ♂ (NHMW MY10258), right gonopod, mesal view **N** *Balkanodesminus dentatoides* gen. nov. et sp. nov. ♂ from Sopotska Cave (NHMW MY10267), left gonopod, mesal view. Scale bars: 0.05 mm.

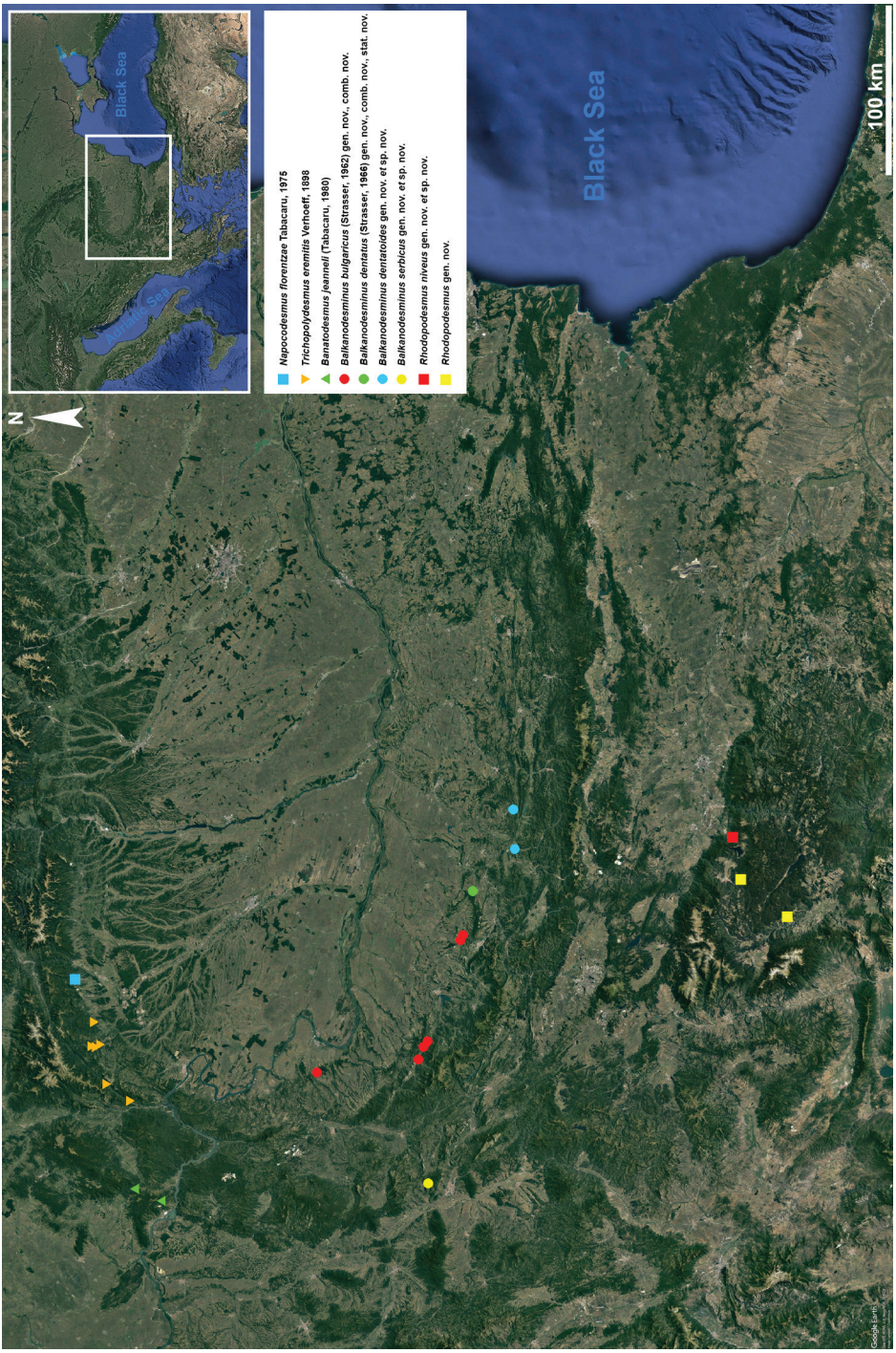

Figure 18. Distribution of cavernicolous Trichopolydesmidae from the Carpathian-Balkan arch and the Rhodope Mountains.

Additional material examined

Cottodesmus crissolensis Verhoeff, 1936

Material examined. ***Syntype*** ♀ (NHMW MY3760), Italy, Kottische Alpen [Cottian Alps], Monte Viso, oberhalb [above] Crissolo, 1300–1500 m a.s.l., 2–3.10.1932, leg. K. Verhoeff, don. Verhoeff 01.VII.1940.

Haplocookia enghoffi Akkari & Mauriès, 2018

Material examined. ***Paratype*** ♂ (NHMW MY9367), Tunisia, Cap Bon peninsula, Nabeul district, Jebel Abderrahman, 28.XI.2004, leg. N. Akkari.

Heterocookia tunisiaca Ceuca, 1967

Material examined. 1 ♂ (NHMW MY9992), Tunisia, Ariana Governorate, El Ghazela, garden, under stones, 24.XI.2003, leg. N. Akkari.

Discussion

The family Trichopolydesmidae, as accepted today (see Golovatch et al. 2018, 2022), includes ≈ 100 genera and > 220 species, which are mostly distributed in the Northern Hemisphere. Unfortunately, the family cannot be clearly defined and diagnosed, as it includes a wide range of taxa that differ significantly not only in appearance, but also in gonopod conformation. However, according to Tabacaru and Giurginca (2016), this family is composed of exclusively European genera: *Trichopolydesmus* (monospecific), *Bacillidesmus* (monospecific), *Cottodesmus* Verhoeff, 1936 (2 species), *Galliocookia* Ribaut, 1955 (4 species), *Verhoeffodesmus* Strasser, 1959 (monospecific), *Occitanocookia* Mauriès, 1980 (monospecific), *Caucasodesmus* (5 species), *Napocodesmus* (2 species), *Banatodesmus* (monospecific), *Balkanodesmus* Antić & Reip in Antić et al. 2014 (monospecific), *Velebitodesmus* Antić & Reip in Antić et al. 2014 (monospecific), and *Solentanodesmus* Antić & Reip in Antić et al. 2014 (monospecific). The largest number of these genera, eight of them, viz., *Trichopolydesmus*, *Bacillidesmus*, *Verhoeffodesmus*, *Napocodesmus*, *Banatodesmus*, *Balkanodesmus*, *Velebitodesmus*, and *Solentanodesmus* are from the Balkans, and *Caucasodesmus* from the Caucasus and Crimea. With the addition of two new genera, *Balkanodesminus* gen. nov. and *Rhodopodesmus* gen. nov., they all seem to form a natural group characterized by the following combination of characters: metatergal setae always trichoid, in most cases on small tubercles arranged almost always in more than four irregular transverse rows, antennomere 5 without distodorsal sensilla basiconica, antennomere 6 always with sensilla basiconica in a distodorsal sensory pit, completely

or partially concealed inside, gonopod telopodite relatively long compared to gonopod coxa, basal part of prefemorite transverse to the body axis, acropodite uni-, bi- or triramous, always without seminal vesicle or pulvillus. Chiefly for the purpose of this discussion we will call this group "true" trichopolydesmids. The other three genera considered in Trichopolydesmidae sensu Tabacaru and Giurginca (2016), viz., *Cottodesmus*, *Galliocookia*, and *Occitanocookia*, also show some affinities with this group, but differ in a number of important characters. Both species of the genus *Cottodesmus* are characterized by bacilliform rather than trichoid setae on metaterga. Although Verhoeff (1936) described *C. crissolensis* Verhoeff, 1936 with trichoid setae, after examination of the female syntype, it becomes clear that the setae are bacilliform and arranged in four almost regular rows. Further, at least *C. crissolensis* is characterized by sensilla basiconica on both antennomeres 5 and 6, with no sensory pits in both cases. Similar to *Cottodesmus*, the genus *Occitanocookia* is characterized by sensilla basiconica on antennomeres 5 and 6, but with trichoid metatergal setae arranged in several irregular rows, as in the "true" trichopolydesmids. Furthermore, the latter genus shows gonopodal prefemorites that are set transverse to the body axis, and a somewhat curved acropodite, both characters observed in the "true" trichopolydesmids. The species *Galliocookia gracilis* Golovatch, 2011, found on Rhodes (very far from the remaining distribution area of the genus in France), possesses sensilla basiconica on antennomeres 5 and 6, while its other three congeners lack sensilla on antennomere 5, like in "true" trichopolydesmids. The generic assignment of the species described from Rhodes, Greece to *Galliocookia* is in our view questionable. In any case, the relatively small gonopodal coxa and prefemorite – which is almost coaxial with the acropodite – places the genus quite distant from the above-mentioned group.

In addition to these 14 genera of (autochthonous?) European Trihopolydesmidae, the recently established genus *Simplogonopus* Vagalinski, Golovatch, Akkari & Stoev, 2019, known from the Balkan mainland and Aegean islands, is classified in Trichopolydesmidae sensu Golovatch (2013) and Golovatch et al. (2018) (Vagalinski et al. 2019). This genus clearly belongs to Afrotropical trichopolydesmids, which are significantly different from the "true" trichopolydesmids from Europe in the presence of exclusively bacilliform metatergal setae distributed mainly in three regular transverse rows, distodorsal sensilla basiconica on antennomeres 5 and 6, but antennomere 6 without distodorsal pit and with relatively small gonopod telopodites, almost completely concealed by very large coxae. The genus *Simplogonopus* and all Afrotropical trichopolydesmids appear to form one natural group (cf. Golovatch et al. 2019, 2022) whose representatives were once assigned to the family Fuhrmannodesmidae.

Two more Mediterranean genera from North Africa are often attributed to the family Trichopolydesmidae as well, viz., *Heterocookia* Silvestri, 1898 and *Haplocookia* Brölemann, 1915 (Akkari and Mauriès 2018). However, these two genera differ from the "true" trichopolydesmids in the presence of three regular transverse rows of bacilliform metatergal setae, and in having both antennomeres 5 and 6 with a distodorsal group of sensilla basiconica, and in showing both gonocoxa and prefemorite rather small. These two latter taxa, as well as the above mentioned genus *Galliocookia*, have been attributed to the family Polydesmidae by Hoffman (1980). It is obvious that the current classification of Trichopoly-

desmidae is very chaotic and cannot be a ground for any phylogenetic approaches. Some authors believe that the family should be reduced to the European genera only, others assign to it also the North African genera or consider it in a broader sense, including many taxa once classified in the family Fuhrmannodesmidae (Golovatch 2013; Golovatch et al. 2018, 2022). The composition and the relationships of the taxa of Trichopolydesmidae could be resolved only after applying combined morphological and molecular phylogenetic methods. Until then, and relying on morphological characters hitherto applied to the classification of the group only, we tend to believe that Trichopolydesmidae should be restricted to the European genera sensu Tabacaru and Giurginca (2016), with the addition of the genera *Balkanodesminus* gen. nov. and *Rhodopodesmus* gen. nov. described above. The genera of what was previously considered as the family Fuhrmannodesmidae seem to form several natural groups (cf. Hoffman 1980; Golovatch 2011), while some other genera (*Heterocookia* and *Haplocookia*) might well be placed in Polydesmidae. Opinions on the classification of Trichopolydesmidae are highly subjective and, as emphasized earlier, only an integrative approach using molecular markers might clarify the picture in the future.

The Balkan Peninsula, including the southern Carpathians, is obviously a hotspot for the family Trichopolydesmidae, with as many as ten "true" trichopolydesmid genera known mostly from caves in the Balkans. All ten genera are characterized by four or more irregular rows of trichoid setae (except for *Bacillidesmus* with four regular rows), absence of sensilla basiconica on antennomere 5, presence of a distodorsal pit with sensilla basiconica on antennomere 6, as well as gonopods with a relatively transverse basal part of the prefemorite. The genus *Caucasodesmus*, known from caves in the north Caucasus and the Crimean Peninsula (see Golovatch 1985, 2011; Golovatch and VandenSpiegel 2015, 2017; Turbanov et al. 2018), also agrees with this combination of characters. The only exception is *C. inexpectatus* Golovatch, 1985, which has three rows of trichoid setae.

Two morphological clusters of Trichopolydesmidae could be recognized among the taxa inhabiting the Balkan Peninsula: the Dinaric and the Carpathian-Balkan-Rhodopean ones. All taxa described from the Dinarides are characterized by well-developed and denticulate pleurosternal carinae on rings 2–18 (see Antić et al. 2014), while taxa from the Carpathian-Balkanids and Rhodopes have only a few pleurosternal teeth on anterior rings (mainly on rings 2–4). Eight of ten Balkan genera are monospecific, including the genus *Verhoeffodesmus*, although Strasser (1959, 1966b) described two species (see Antić et al. 2014). Again, the Balkan Peninsula proves to be a prominent hotspot of millipede diversity in Europe. This primarily concerns the cave fauna, with trichopolydesmids being no exception. Better equipment and more manpower in the recent years have contributed to the discovery of interesting taxa, also from this group, primarily in the Dinarides, whence Antić et al. (2014) described three new monospecific genera. However, from the description of these three genera to date, about ten new taxa have been found in caves of the Dinarides, and these monospecific genera will be supplemented in the future (DA pers. obs.). It is worth mentioning that the fauna of the type locality of *B. serbicus* gen. nov. et sp. nov. has been investigated for years, but specimens of this taxon have been found only recently. This leaves no doubt that more trichopolydesmids will be revealed and described from the Balkans in the future.

Acknowledgements

We are grateful to all collectors who committed material for this study. DA and BV are thankful to Dalibor Stojanović (IZB), Hans Reip (Germany), and Karin Voigtländer (Germany) for their assistance during the field trips in Bulgaria and Romania and for the great time we had together. DA and NA are grateful to Wencke Wegner (NHMW) for the help during the SEM imaging and to Oliver Macek (NHMW) for his assistance with databasing and incorporating the new samples in the collection. DA thanks all members of the Serbian Biospeleological Society for the help during the first field trip of the Society in the caves of eastern Serbia. Our gratitude is extended to Jörg Spelda, Stefan Friedrich (ZSM), and Jason Dunlop and Anja Friederichs (ZMB) for providing information, photographs, and sending microslides of types on loan for us to study. Jackson Means (VMNH) kindly sent images and information on *T. eremitis* male from the collection under his care. We are very grateful to the reviewers, Sergei Golovatch (Russia) and William Shear (Virginia, U.S.A.), as well as the editor Didier Vanden Spiegel (Belgium), for helpful suggestions and corrections that have improved this paper.

This work was partially supported by the Serbian Ministry of Education, Science and Technological Development (Grant No. 451-03-9/2021-14/200178). Authorization no. 130 from 29 September 2021 was obtained by the Speleological Heritage Commission Romania for collecting cave millipedes on the territory of Romania.

References

Akkari N, Enghoff H (2011) On some surface structures of potential taxonomic importance in families of the suborders Polydesmidea and Dalodesmidea (Polydesmida, Diplopoda). ZooKeys 156: 1–24. https://doi.org/10.3897/zookeys.156.2134

Akkari N, Mauriès J-P (2018) A review of the family Trichopolydesmidae in North Africa with a description of a new species from Tunisia. ZooKeys 786: 117–128. https://doi.org/10.3897/zookeys.786.28270

Antić DŽ, Reip HS, Dražina T, Rađa T, Makarov SE (2014) Three new monotypic genera of Trichopolydesmidae from Croatia, Balkan Peninsula (Diplopoda, Polydesmida). Zootaxa 3884(2): 101–121. https://doi.org/10.11646/zootaxa.3884.2.1

Attems C (1898) System der Polydesmiden. I. Theil. Denkschriften der Akademie der Wissenschaften Wien, mathematisch-naturwissenschaftliche Klassen, 67: 221–482. http://biodiversitylibrary.org/page/27925127

Attems C (1899) System der Polydesmiden. II. Theil. Denkschriften der Akademie der Wissenschaften Wien, mathematisch-naturwissenschaftliche Klassen 68: 251–436. http://biodiversitylibrary.org/page/35890675

Attems C (1908) Die Myriopoden der Deutschen Südpolar-Expedition 1901–1903. D. Südpolar-Expedition 1901–19031: 415–433.

Attems C (1926) Myriapoda in Kükenthal & Krumbach. Handbuch der Zoologie, Berlin, Leipzig 4: 1–402.

Attems C (1940) Myriapoda 3. Polydesmoidea III. Fam. Polydesmidae, Vanhoeffeniidae, Cryptodesmidae, Oniscodesmidae, Sphaerotrichopidae, Periodontodesmidae, Rhachidesmidae, Macellolophidae, Pandirodesmidae. Das Tierreich 70: 1–577. https://doi.org/10.1515/9783111609645

Bachvarova D, Vagalinski B, Doichinov A, Stoev P (2017) New records of millipedes and centipedes from Bulgaria, with an annotated checklist of the Bulgarian myriapods. Zootaxa 4263(3): 507–526. https://doi.org/10.11646/zootaxa.4263.3.4

Beron P (2015) Cave Fauna of Bulgaria. East-West and National Museum of Natural History Publishers, 434 pp.

Brandt JF (1833) Tentaminum quorundam monographicorum Insecta Myriapoda Chilognathi Latreillii spectantium prodromus. Bulletin de la Societé Impériale des Naturalistes de Moscou 6: 194–209.

Brölemann HW (1915) Description d'un genre nouveau et d'une espèce nouvelle de Myriapodes d'Algérie. Bulletin de la Société d'histoire naturelle de l'Afrique du Nord 7(6): 88–94. https://doi.org/10.3406/bsef.1908.24297

Brölemann HW (1916) Essai de classification des Polydesmiens. Annales de la Société Entomologique de France 84: 523–608. https://doi.org/10.5962/bhl.part.24168

Ceuca T (1958) Contribuţii la cunoaşterea Diplopodelor din fauna R. P. Romîne. III. Diplopode cavernicole. Studii şi Cercetări de Biologie 2: 335–343.

Ceuca T (1967) Diplopodes de Tunisie (avec description d'une nouvelle espèce). Bulletin de l'Académie Polonaise des Sciences, Varsovie, Cl. 2, 15, 9: 551–554.

Ceuca T (1974) Noi contributii la cuonasterea diplopodelor din fauna României – New contributions to the knowledge of Diplopoda of the Roumanian Fauna. Studia Universitatis Babes-Bolyai. Seria Biologia 19: 91–97.

Ceuca T (1992) Quelques aspects sur la faunistique, l'écologie et la zoogeographie des diplopodes de la Région Balkanique. Bericht des naturwissenschaftlich-medizinischen Vereins in Innsbruck, Supplementum, 411–429.

Giachino PM, Guéorguiev B, Vailati D (2011) A new remarkable subterranean beetle of the Rhodopes: *Paralovricia* gen. n. *beroni* sp. n. belonging to Lovriciina new subtribe (Coleoptera, Carabidae, Trechinae, Bembidiini). ZooKeys 117: 59–72. https://doi.org/10.3897/zookeys.117.1612

Giurginca A (2021) Diplopoda of Romania. Editura Transversal, Targoviste, 258 pp.

Golovatch SI (1985) Two new genera of cave-dwelling millipedes (Diplopoda) with remarks on the milliped fauna of West Caucasian caves. International Journal of Speleology 14(1/4): 39–50. https://digitalcommons.usf.edu/cgi/viewcontent.cgi?article=1409&context=ijs

Golovatch SI (2011) The millipede genus *Caucasodesmus* Golovatch, 1985, with the description of a new species from the Crimea, Ukraine (Polydesmida, Diplopoda, Trichopolydesmidae). ZooKeys 93: 1–8. https://doi.org/10.3897/zookeys.93.1159

Golovatch SI (2013) A reclassification of the millipede superfamily Trichopolydesmoidea, with descriptions of two new species from the Aegean region (Diplopoda, Polydesmida). ZooKeys 340: 63–78. https://doi.org/10.3897/zookeys.340.6295

Golovatch SI, Kime RD (2009) Millipede (Diplopoda) distributions: A review. In: Xylander WER, Voigtländer K (Eds) Myriapoda and Onychophora of the world – Diversity, Biology

and Importance. Proceedings of the 14th International Congress of Myriapodology. 21–25 July 2008, Görlitz, Germany. Soil Organisms 81(3): 565–597.

Golovatch SI, VandenSpiegel D (2015) Two new species of the millipede genus *Caucasodesmus* Golovatch, 1985 from the Crimea, Russia (Diplopoda, Polydesmida, Trichopolydesmidae). Russian Entomological Journal 24(1): 1–6. https://doi.org/10.15298/rusentj.24.1.01

Golovatch S, Geoffroy J, Stoev P, Vanden Spiegel D (2013) Review of the millipede family Opisotretidae (Diplopoda, Polydesmida), with descriptions of new species. ZooKeys 302: 13–77. https://doi.org/10.3897/zookeys.302.5357

Golovatch SI, Turbanov IS, Vanden Spiegel D (2017) Contributions to the cave millipede fauna of the Crimean Peninsula (Diplopoda), with the description of a new species. Arthropoda Selecta 26(1): 103–111. https://doi.org/10.15298/arthsel.26.2.02

Golovatch SI, Nzoko Fiemapong AR, Tamesse JL, Mauriès J-P, VandenSpiegel D (2018) Trichopolydesmidae from Cameroon, 1: The genus *Hemisphaeroparia* Schubart, 1955. With a genus-level reclassification of Afrotropical genera of the family (Diplopoda, Polydesmida). ZooKeys 785: 49–98. https://doi.org/10.3897/zookeys.785.27422

Golovatch SI, Nzoko Fiemapong AR, Vanden Spiegel D (2019) Trichopolydesmidae from Cameroon, 2: A species-level reclassification of Afrotropical trichopolydesmids (Diplopoda, Polydesmida), with two new species and two new records from Cameroon, and two new species from the Nimba Mountains, Guinea. ZooKeys 891: 31–59. https://doi.org/10.3897/zookeys.891.46986

Golovatch SI, Gallo JS, Bichuette ME (2022) Two new species of the millipede family Trichopolydesmidae from Bahia state, northeastern Brazil, including a remarkable threatened troglobiont (Diplopoda, Polydesmida). Zootaxa 5115(3): 419–437. https://doi.org/10.11646/zootaxa.5115.3.7

Heller C (1858) Beiträge zur österreichischen Grotten-Fauna. Sitzungsberichte der Mathematisch-Naturwissenschaftlichen Classe der Kaiserlichen Akademie der Wissenschaften, Wien 26(1): 313–326.

Hoffman RL (1980) Classification of Diplopoda. Muséum d'Histoire naturelle, Genève, 1979, 238 pp.

Jeekel CAW (1956) Milliped miscellany – Part III. Beaufortia, Amsterdam 5(52): 73–99.

Jeekel CAW (1965) The identity of *Dalodesmus tectus* Cook, 1896, and the status of the family names Dalodesmidae Cook, 1896, Vanhoeffeniidae Attems, 1914, and Sphaerotrichopodidae Attems, 1914 (Diplopoda, Polydesmida). Entomologische Berichten 25: 236–239.

Karaman Z (1958) Über einige neue Coleopteren aus dem Balkan. Bulletin du Muséum d'histoire naturelle de Belgrade: Série B, Sciences biologiques 12: 221–229.

Kime RD, Enghoff H (2011) Atlas of European millipedes (Class Diplopoda). Vol. 1. Pensoft Publishers, Sofia-Moscow, 282 pp.

Latzel R (1884) Die Myriopoden der Österreichisch-ungarischen Monarchie. Zweite Hälfte. Die Symphylen, Pauropoden und Diplopoden. Alfred Hölder, Wien, 414 pp.

Makarov SE, Ćurčić BPM, Milinčić M, Pecelj MM, Antić DŽ, Mitić BM (2012) A new genus and species of the family Anthroleucosomatidae from Serbia (Myriapoda, Diplopoda, Chordeumatida). Archives of Biological Sciences 64(2): 793–798. https://doi.org/10.2298/ABS1202793M

Mauriès J-P (1980) Description d'une espèce nouvelle et d'un genre nouveau de Diplopodes polydesmides hypogés récoltés dans l'arrondissement de Béziers (Hérault). Bulletin de la Société d'Histoire Naturelle de Toulouse 116(3–4): 228–234.

Mauriès J-P (1984) Le genre *Galliocookia* Ribaut 1954. Deux espèces nouvelles des grottes de l'Ardèche et du Gard (Myriapoda, Diplopoda, Polydesmida). Bulletin de la Société d'histoire naturelle de Toulouse 119: 103–110.

Nešić D (2016) Provalija cave (Cerjanska cave), morphology and formation. In: Nešić D, Jović D (Eds) Natural monument Cerjanska Cave. Surroundings, Natural History, Protection. Institute for Nature Conservation in Niš, Niš, Serbia, 47–62.

Pavićević D, Zatezalo A, Popović M (2016) Biospeleological research of Cerjanska Cave and the northern part of Kalafat area. In: Nešić D, Jović D (Eds) Natural monument Cerjanska Cave. Surroundings, Natural History, Protection. Institute for Nature Conservation in Niš, Niš, Serbia, 90–99.

Petrov B, Stoev P (2007) The underground world of the mountain Rhodopes. UNDP, 'Rhodope project', 86 pp. [In Bulgarian]

Ribaut H (1955) Un nouveau genre et une nouvelle espece de Polydesmides des grottes du departement de l'Ardeche. Notes biospéologiques 9(2): 133–135.

Roewer C-F (1926) Opilioniden aus Höhlen des Balkan-Gebirges (Arachn.). Entomologische Mitteilungen 15: 299–302.

Schubart O (1960) Ein weiterer Beitrag zur Diplopoden-Fauna Marokkos. Bulletin de la Société des sciences naturelles du Maroc 40(3): 159–232.

Shear WA, Marek P (2021) Three new genera and eighteen new species of miniature polydesmid millipedes from the northwestern United States (Diplopoda, Polydesmida, Polydesmidae). Zootaxa 4975(1): 81–126. https://doi.org/10.11646/zootaxa.4975.1.3

Shear WA, Reddell JM (2017) Cave millipedes of the United States. XIV. Revalidation of the genus *Speorthus* Chamberlin, 1952 (Diplopoda, Polydesmida, Macrosternodesmidae), with a description of a new species from Texas and remarks on the families Polydesmidae and Macrosternodesmidae in North America. Insecta Mundi 0529: 1–13.

Silvestri F (1898) Contributo alla conosceza dei Diplopodi della fauna mediterranea. Annali del Museo civico di storia naturale di Genova, serie 2 18: 654–669. http://biodiversitylibrary.org/page/7785876

Simonsen Å (1990) Phylogeny and biogeography of the millipede order Polydesmida, with special emphasis on the suborder Polydesmidea. PhD thesis, Museum of Zoology, University of Bergen, 114 pp.

Stoev P (2004) New distributional records of millipedes from Bulgarian caves (Myriapoda: Diplopoda). Acta Zoologica Bulgarica 56(2): 145–154.

Stoev P (2007) Fauna and zoogeography of Myriapoda in Bulgaria. In: Fet V, Popov A (Eds) Monographiae Biologicae. Vol. 82. Biogeography and Ecology of Bulgaria. Springer, Dordrecht, 379–404. https://doi.org/10.1007/978-1-4020-5781-6_11

Strasser K (1959) *Verhoeffodesmus*, n. g., ein Höhlendiplopode aus Istrien (Polydesmoidea). Porocila 2: 99–106. [Acta carsologica]

Strasser K (1962) Diplopoden aus Bulgarien und Jugoslawien. Senckenbergiana Biologica 43(6): 437–470.

Strasser K (1966a) Über Diplopoden Bulgariens. Annales Zoologici 23(12): 325–385.

Strasser K (1966b) Neue Diplopoden aus Höhlen Jugoslawiens. Senckenbergiana Biologica 47(5): 379–398.

Strasser K (1973) Über Diplopoden Bulgariens, III. Annales Zoologici 30(15): 411–470.

Tabacaru I (1975) *Napocodesmus florentzae* n. sp. Travaux de l'Institut de Spéologie "Émile Racovitza" 14: 71–82.

Tabacaru I (1980) *Trichopolydesmus* (*Banatodesmus*) *jeanneli* n. sg., n. sp. Travaux de l'Institut de Spéologie "Émile Racovitza" 24: 155–161.

Tabacaru I, Giurginca A (2016) Identification key to the cavernicolous Diplopoda of Romania. Travaux de l'Institut de Spéologie "Émile Racovitza" 55(1): 81–117.

Tabacaru I, Giurginca A, Vanoaica L (2003) Cavernicolous Diplopoda of Romania. Travaux de l'Institut de Spéologie "Émile Racovitza" 41–42: 121–148.

Turbanov IS, Golovatch SI, VandenSpiegel D (2018) New interesting records of three cavernicolous millipede species from the Crimean Peninsula. Arthropoda Selecta 27(3): 201–209. https://doi.org/10.15298/arthsel.27.3.02

Vagalinski B, Stoev P (2011) An annotated checklist of the myriapods of the Western Rhodopes Mts (Bulgaria and Greece). In: Beron P (Ed.) Biodiversity of Bulgaria. 4. Biodiversity of Western Rhodopes (Bulgaria and Greece) II. Pensoft and National Museum of Natural History, Sofia, 129–143.

Vagalinski B, Golovatch SI, Akkari N, Stoev P (2019) *Simplogonopus rubellus* (Attems, 1902) gen. n., comb. n. (Diplopoda: Polydesmida: Trichopolydesmidae): Revealing the identity of an enigmatic eastern-mediterranean millipede. Acta Zoologica Bulgarica 71(3): 325–334. http://www.acta-zoologica-bulgarica.eu/downloads/acta-zoologica-bulgarica/2019/71-3-325-334.pdf

Verhoeff KW (1898) Beiträge zur Kenntniss paläarktischer Myriopoden. VII. Aufsatz: Ueber neue und wenig bekannte Polydesmiden aus Siebenbürgen, Rumänien und dem Banat. Archiv für Naturgeschichte 64(1): 363–372.

Verhoeff KW (1910) Über Diplopoden. 42. Aufsatz: Neue Polydesmiden aus Mitteleuropa und ihre Verwandten. Zoologischer Anzeiger 36(6–7): 132–145.

Verhoeff KW (1926) Zwei neue Höhlen-Myriopoden aus Bulgarien. Eine vorläufige Mitteilung. Zoologischer Anzeiger 65: 294–296.

Verhoeff KW (1936) Chilognathen aus Nordwestitalien und über einige andere mediterrane Diplopoden. 128. Diplopoden-Aufsatz. Zoologische Jahrbucher. Abteilung fur Systematik, Ökologie und Geographie der Tiere 68(4–5): 353–444.

Verhoeff KW (1941a) Höhlen-Diplopoden aus dem Trentino. Zeitschrift für Karst- und Höhlenkunde 1941(3–4): 179–189.

Verhoeff KW (1941b) Chilopoden und Diplopoden. In: Titschack E (Ed.) Beiträge zur Fauna Perus I. Hamburg 1(2): 5–80.

ZooKeys 1097: 47–63 (2022)
doi: 10.3897/zookeys.1097.81792
https://zookeys.pensoft.net

RESEARCH ARTICLE

A peer-reviewed open-access journal
ZooKeys
Launched to accelerate biodiversity research

A new millipede genus and species of the tribe Pachyiulini from the Caucasus (Diplopoda, Julida, Julidae)

Aleksandr P. Evsyukov[1], Boyan Vagalinski[2], Igor Y. Zabiyaka[3], Evgeniy V. Sadyrin[3]

1 *Don State Technical University, Department of Biology and General Pathology, Rostov-on-Don, Russia* **2** *Institute of Biodiversity and Ecosystem Research at the Bulgarian Academy of Sciences, Sofia, Bulgaria* **3** *Don State Technical University, Research and Education Center "Materials", Rostov-on-Don, Russia*

Corresponding author: Aleksandr P. Evsyukov (aevsukov@mail.ru)

Academic editor: Pavel Stoev | Received 7 February 2022 | Accepted 4 March 2022 | Published 19 April 2022

http://zoobank.org/18F467AF-6AC6-4412-9794-5A004A671F5B

Citation: Evsyukov AP, Vagalinski B, Zabiyaka IY, Sadyrin EV (2022) A new millipede genus and species of the tribe Pachyiulini from the Caucasus (Diplopoda, Julida, Julidae). ZooKeys 1097: 47–63. https://doi.org/10.3897/zookeys.1097.81792

Abstract

A new genus and species of the millipede tribe Pachyiulini, *Bellatoiulus golovatchi* **gen. et sp. nov.**, is described from the Lesser Caucasus, Azerbaijan. Cybertypes of the new species are created from the physical holotype male and from a paratype female. The distribution and ecological features of the new species, and the position of the new genus within Pachyiulini are discussed.

Keywords

Azerbaijan, *Bellatoiulus golovatchi*, cybertype, taxonomy

Introduction

The tribe Pachyiulini, also referred as the subfamily Pachyiulinae, is a monophyletic trans-Palaearctic group (Enghoff et al. 2013), but most of its diversity is restricted to the Mediterranean Region. It includes 15–20 genera (Antić et al. 2018), or 16–22 gen-

Copyright *Aleksandr P. Evsyukov et al.* This is an open access article distributed under the terms of the Creative Commons Attribution License (CC BY 4.0), which permits unrestricted use, distribution, and reproduction in any medium, provided the original author and source are credited.

era or subgenera (Vagalinski 2020). According to Hoffman (1980), the tribe includes both the largest and the smallest members of Julidae.

In the Caucasus *sensu lato*, the tribe is represented by three genera: *Pachyiulus* Berlese, 1883, *Amblyiulus* Silvestri, 1896, and *Syrioiulus* Verhoeff, 1914 (Evsyukov 2016; Evsyukov et al. 2021). While the largest julid millipedes belong to the former genus, the latter two genera include julids of mostly moderate size. No minute Pachyiulini or "micropachyiulinines", like for example the genera *Geopachyiulus* Verhoeff, 1899, *Micropachyiulus* Verhoeff, 1899, or *Hylopachyiulus* Attems, 1904, have hitherto been known from the Caucasus.

Here we describe a new genus for a tiny new species of this tribe from the Azerbaijani part of the Lesser Caucasus and create cybertypes of the new species from the physical male holotype and a female paratype. Until now cybertypes have not been very common in millipede taxonomy and are known only for two species (Akkari et al. 2015; Rosenmejer et al. 2021).

Materials and methods

The specimens were stored in 70% ethanol. All material has been shared between the collections of the Zoological Museum of the Moscow State University, Russia (**ZMUM**), the National Museum of Natural History, Sofia, Bulgaria (**NMNHS**), and the Natural History Museum of Denmark, Copenhagen, Denmark (**NHMD**) (formerly ZMUC–Zoological Museum, University of Copenhagen). Some body parts of males (antennae, gonopods, legs, etc.) and females (vulvae and leg pairs 2) were dissected and mounted in glycerol on temporary microscopic slides or prepared for scanning electron microscopy (SEM). Photographs were taken using a Zeiss StereoDiscovery V.20 microscope and processed with Zeiss ZEN software (Don State Technical University, Rostov-on-Don, Russia). Line drawings were executed using microphotographs taken with a ProgRes C7 digital camera connected to a Zeiss Axio Imager 2 microscope (Institute of Biodiversity and Ecosystem Research, Sofia, Bulgaria), which were then displayed on a laptop screen and copied on tracing paper.

Scanning electron micrographs were taken with a Zeiss CrossBeam 340 (Don State Technical University, Rostov-on-Don, Russia). For SEM micrographs, the gonopods, legs etc. were dehydrated in alcohol (96 and 100%) and acetone, glued to aluminium SEM-stubs and air dried.

Creation of cybertypes was carried out using a Zeiss Xradia Versa 520 X-ray computed micro-tomography unit (Don State Technical University, Rostov-on-Don, Russia). X-ray projections acquisition parameters were as follows: X-ray tube voltage 60 kV, power 4.5 V, magnification objective 0.4×, sample rotation 360°, exposure time 4 s, X-ray tube filter LE6. For each scan 2001 projections in total were obtained. The source-object-detector distances were adjusted according to the sample sizes to give the desired field view for each sample. Thus, the voxel sizes were 4.7 and 5.8 μm

for the male holotype and the female paratype, respectively. For each scanning, the tube with the sample was placed at the closest possible distance to the X-ray source. The 2048 × 2048-pixel CCD camera was kept at –59 °C and the acquisition was performed with camera binning factor = 2, which resulted in up to 1024 × 1024-pixel sized projection images. The X-ray source filter was selected based on the observed transmittance values according to the recommendations of the Xradia Versa 520 User's Guide A003030 Rev. B. The exposure time was selected to maintain count (intensity) values >5000 with the selected source parameters and filter. The option for Dynamic Ring Removal, which enables small random motions of the sample during acquisition, was enabled for all projections. During each tomography procedure, 10 reference (air) X-ray images were acquired with equal time intervals between them. Average of these references was applied to each projection. An up to one-hour warm-up scan was performed with the same source parameters before each acquisition. X-ray projections were reconstructed using XRMReconstructor 12.0.8086.19558 software with manually adjusted center shift values, σ = 0.5 Gaussian blur filter and BH = 0.05 standard beam hardening correction.

The reconstructed tomographic images were exported as 16-bit DICOM image stacks (without compression and retaining the original voxel values) for volume rendering in VGStudio MAX 3.5 software (Volume Graphics GmbH, Heidelberg, Germany). The DICOM files were rendered using *Volume renderer (Phong)*. The *Draw* instrument was used to highlight individual structures, and after initial highlighting the region of interest was modified using *Smoothing* tool.

For contrasting before micro-CT examination samples were soaked in 100% alcohol for 2 h and then transferred to a 1% iodine alcohol solution for 48 h (Metscher 2009). For stabilisation of the samples during scanning, they were mounted in plastic tubes (1 ml syringe) in 0.3% aqueous agarose (Metscher 2011). Cybertypes were created from the physical male holotype and a female paratype (Faulwetter et al. 2013). All 3D images and metadata of the physical types are deposited at https://morphobank.org (O'Leary and Kaufman 2012), project number 4180. After examination all material was returned to 70% alcohol.

The distribution map was created using Google Earth Pro 7.3.4.

All images were processed in Adobe Photoshop CS6.

Descriptive abbreviations and symbols

BRF body ring formula. Indicates the number of podous (including collum and the gonopod-bearing segment/ring) and apodous segments/rings in an individual. This formula is **p+a+T**, where **p** is the number of podous body rings, **a** is the number of apodous body rings, and **T** represents the telson (Enghoff et al. 1993). Only adults have been analysed in the present study.

H vertical body diameter measured at a mid-body ring

L body length measured at the ozopore level

Taxonomic part

Class Diplopoda Blainville-Gervais, 1844
Order Julida Leach, 1814
Family Julidae Leach, 1814

Genus *Bellatoiulus* gen. nov.
http://zoobank.org/E87D3EDE-5038-439A-A904-7E0F87BB4546

Type species. *Bellatoiulus golovatchi* gen. et sp. nov., by present designation.

Diagnosis. A genus of the julid tribe Pachyiulini, distinguished from all contribal genera by the unique presence of a lateral process on the opisthomere, as well as by the following combination of gonopodal and external somatic characters: promere with mesal ridge distally extending in a strong process, caudal face without apical denticles/ridges; opisthomere without anterior and caudal lamellae or these being vestigial, mesomeral process well-differentiated, crest-like, solenomere with a deep and narrow apical fovea; ommatidia absent, mandibular stipites in males not expanded, vertigial and metazonal setae present, pre-anal ring with an epiproct.

Name. Derived from the Latin *bellator* meaning "soldier", "warrior", after the remarkably "armed" appearance of the gonopods including the club-like mesal and lateral processes of the promere and the opisthomere, respectively, and the apically serrated mesomeral process; plus *Julus*, the type genus of the family Julidae. Masculine.

***Bellatoiulus golovatchi* gen. et sp. nov.**
http://zoobank.org/A8A39314-2E0B-4E99-A65A-EBB595D16EF2

Material examined. ***Holotype*:** ♂ (unbroken) (ZMUM): Azerbaijan, Drmbon [Heyvalı] ca 30 km WSW of Mardakert [Ağdərə], 800–850 m a.s.l., *Quercus*, *Carpinus*, *Acer*, etc. forest, litter, 1–2.VI.1987, S. Golovatch & K. Eskov leg. ***Paratypes*:** 1 ♂ (in 3 pieces, with dissected gonopods, leg-pair 2, a mid-body and an end-body leg) , 1 ♀ (in 2 pieces, right vulva dissected) (NMNHS), 1 ♂ (in 2 pieces, with dissected leg-pair 2 and a mid-body leg), 1 ♀ (unbroken) (NHMD), 6 ♂♂ (4 unbroken, 2 in 2 pieces, with dissected gonopods, head, antenna, leg-pairs 1, 2, 3, 8 and a mid-body leg), 42 ♀♀ (30 unbroken, 11 broken in two or more pieces, 1 with dissected vulvae and leg-pair 2), 21 juv. (ZMUM), same collecting data as for holotype.

Non-type material: 7 ♂♂, 12 ♀♀, 2 juv. (ZMUM), Azerbaijan, Nadirkhanly [Nadirxanlı] ca 12 km NE of Kelbajar [Kəlbəcər], 1200 m a.s.l., *Fraxinus* & *Juglans* stand, litter, 1.VI.1987, S. Golovatch & K. Eskov leg.; 2 ♂♂ (1 ♂ in 2 pieces, with dissected gonopods), 10 ♀♀, 8 juv. (ZMUM), Azerbaijan, ca 15 km WSW of Mardakert [Ağdərə], 1100 m a.s.l., *Quercus*, *Fagus*, *Acer*, etc. forest, litter, 2.VI.1987, S. Golovatch & K. Eskov leg.

Cybertypes: http://morphobank.org/permalink/?P4180. Created from the physical ♂ holotype and a ♀ paratype.

Name. The new species honours our friend and colleague, Prof. Sergei Golovatch (Moscow, Russia), an outstanding myriapodologist and one of the collectors of the material used for the present species description.

Description. Measurements: holotype with BRF 45+2+T, L = 12 mm, H = 0.6 mm; paratype and non-type ♂♂ with BRF 40–46+1–3+T, L = 10–12 mm, H = 0.5–0.6 mm; paratype and non-type ♀♀ with BRF 37–51+1–4+T, L = 9.5–14 mm, H = 0.5–0.7 mm.

Colouration (Fig. 1): completely pallid, gut and defence glands partly visible by transparency (alcohol-fixed material).

Head (Figs 2A, 1, 5, 8): ommatidia absent. 2 vertigial, 4 (usually) or 5 (rarely) supralabral and 8–14 labral setae. Antennae (Fig. 2B) 1.4–1.7 times as long as head in males, and 1.3–1.4 times in females; antennomeres 2 and 5 subequal in length, somewhat longer than 3 and 4, and much longer than 6; 5 ca 1.6 times as long as broad and ca 1.5 times as broad as 2; the four apical cones relatively small; distal margins of antennomeres 5 and 6 dorsolaterally with several bacilliform sensilla basiconica, those on antennomere 5 of similar size to the apical cones, those on antennomere 6 somewhat finer. Mandibular stipites in males not expanded. Labrum tridentate. Gnathochilarium without peculiarities; proximal part of stipites non-setose, distally with three setae usual for the family, stipital palps normally developed, each bearing a group of extremely small apical sensilla; promentum small, rhomboid, separating lamellae linguales in roughly their proximal third, the latter each bearing three or four setae in a longitudinal row.

Trunk and legs: collum mostly smooth, with only two or three faint longitudinal grooves just next to posterolateral corner. Body rings (Figs 1, 2F, G, 5, 8) slightly to moderately vaulted. Prozonae generally smooth, with sparse, very short and fine, irregular striae. Metazonae with sparse, shallow longitudinal striations, most striae not

Figure 1. Habitus of *Bellatoiulus golovatchi* gen. et sp. nov. **A** male paratype **B** female paratype (both ZMUM). Scale bars: 1.0 mm.

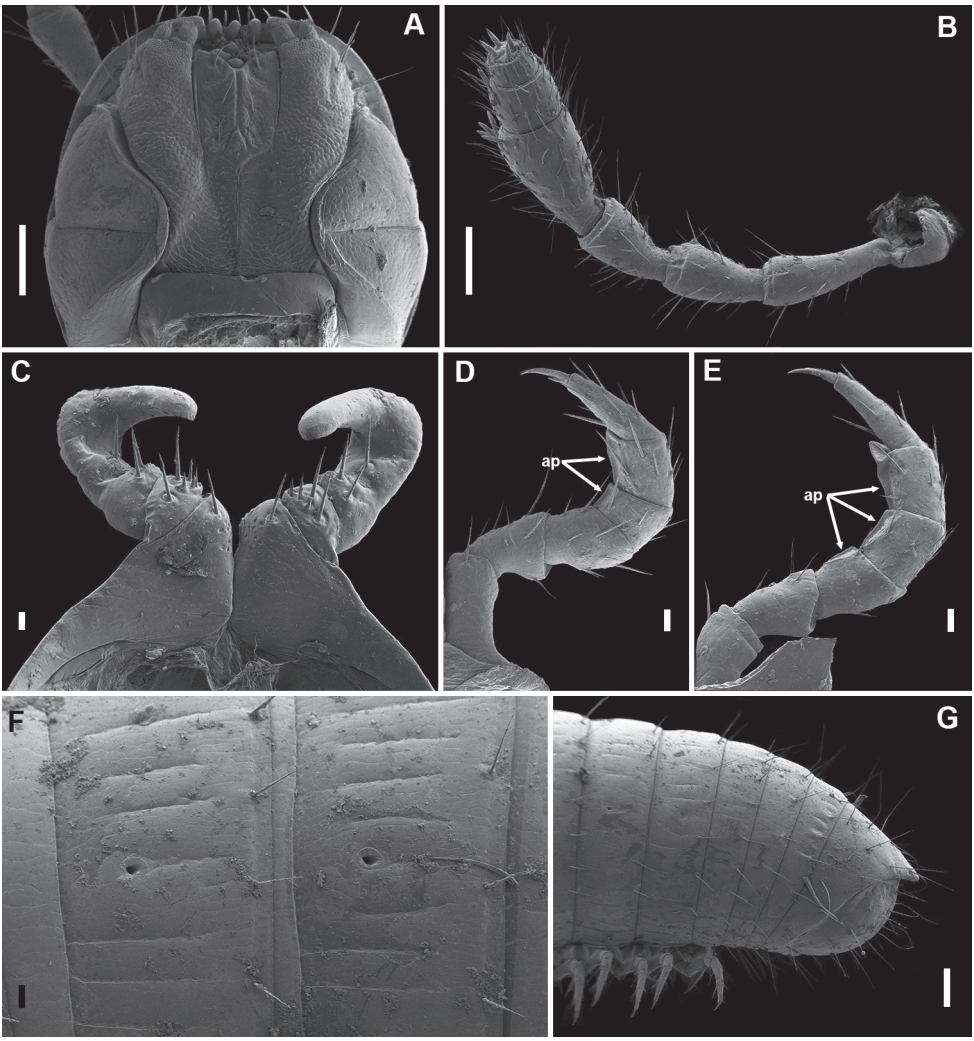

Figure 2. *Bellatoiulus golovatchi* gen. et sp. nov., male paratype (ZMUM). **A** head, ventral view **B** right antenna, lateral view **C** leg pair 1, frontal view **D** right leg 2, frontal view **E** left leg 3, caudal view **F** ozopores in midbody rings, lateral view **G** posterior part of body, lateral view. Abbreviation: **ap** adhesive pads. Scale bars: 0.1 mm (**A, B, G**); 0.01 mm (**C**); 0.02 mm (**D, E, F**).

crossing entire length of metazona; hind margins with a rather dense whorl of erect to somewhat slanting setae, these being 0.12–0.2 times as long as H in males, and 0.1–0.17 times in females. Ozopores (Fig. 2F) small, placed behind pro-metazonal suture at ca 1/3–2/5 of metazonal length measured from front to back. Walking legs (Figs 2D, E, 7A) of moderate length: mid-body legs (Fig. 2E) 0.8–0.9 times as long as H in males and 0.7–0.8 times in females. Tarsus of mid-body legs 1.5–1.7 times as long as tibia and ca 3.5 times as long as apical claw. Legs 2 in males with accessory claw, legs 3 and following pairs without; female legs altogether without accessory claw.

Telson (Fig. 2G): Pre-anal ring sparsely covered with long setae. Epiproct short and stout (considerably surpassed by the longest paraproctal setae), straight to slightly bent ventrad, roof-like, ending bluntly without distinct hyaline tip. Hypoproct small, rounded, not protruding behind hind margins of paraprocts in both sexes; ventral surface with a pair of median setae. Paraprocts sparsely to moderately setose, with a row of shorter setae along each paraproct's caudal margin.

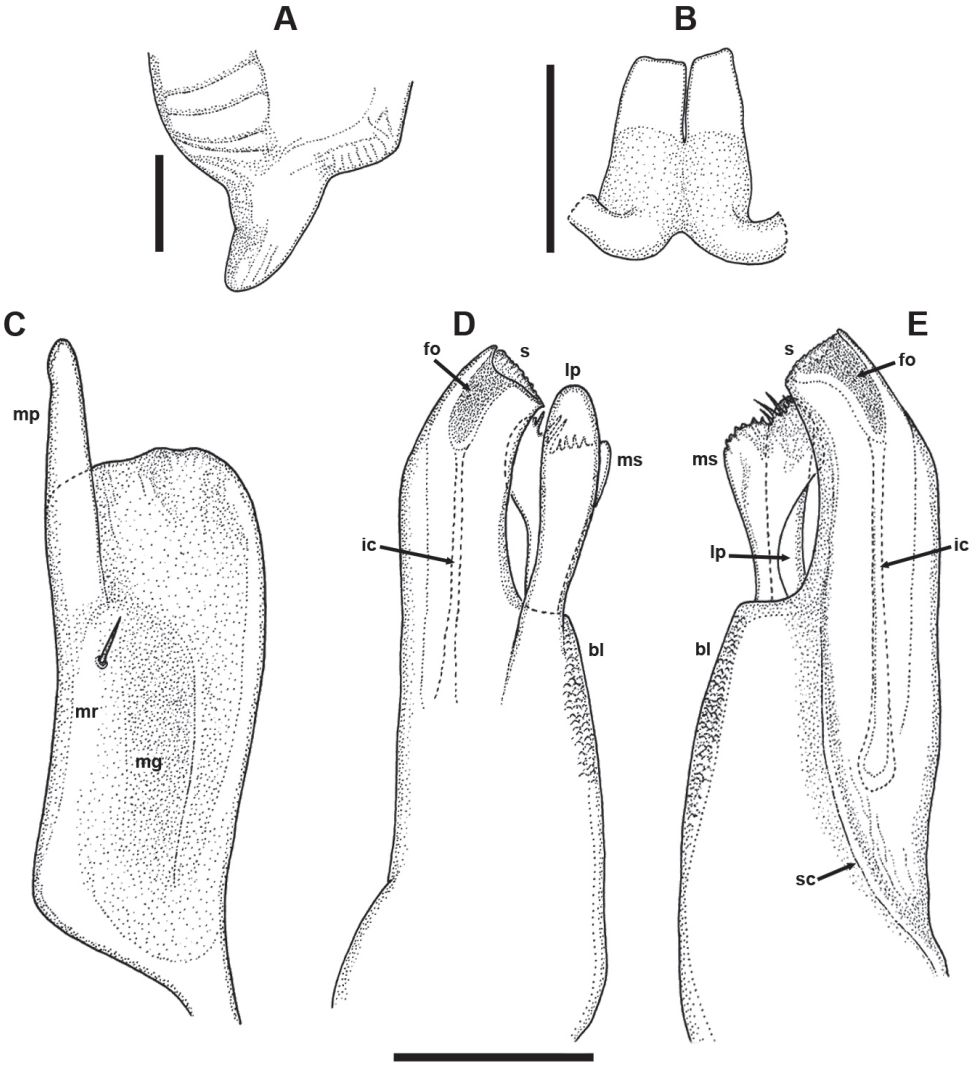

Figure 3. *Bellatoiulus golovatchi* gen. et sp. nov., male paratype (NMNHS). **A** right ventral edge of pleurotergum 7, ventro-lateral view **B** penis, caudal view **C** left promere, caudal view **D** left opisthomere, lateral, slightly caudal view **E** left opisthomere, mesal view. Abbreviations: **bl** basofrontal lobe **fo** fovea **lp** lateral process **mg** median grove **mp** mesal process **mr** mesal ridge **ms** mesomeral process **ic** (supposed) inner canal **s** solenomere, **sc** sperm canal. Scale bars: 0.1 mm.

Male sexual characters: leg-pair 1 (Fig. 2C) 3-segmented, typical hooks oriented fronto-mesad; tibial outgrowth slender, tarsal remnant absent. Leg-pair 2 (Fig. 2D) slightly thicker than following pairs, ventrally with crested adhesive pads (**ap**), one each on postfemur and tibia; next several pairs (Fig. 2E) with a small femoral pad in addition; the pads gradually diminishing towards end-body, completely disappearing in legs of the last third. Pleurotergum 7 (Fig. 3A) ventrally forming well-pronounced, shovel-like lobes originating from the border zone between pro- and metazona, protruding ventrad behind gonopods, not concealing them from lateral view. Penis (Fig. 3B) very small, non-sclerotised, set deeply above coxae 2, with a short basal part and rather slender, flattened, completely transparent apical lobes.

Gonopods (Figs 3C–E, 4, 6, and **g** in Fig. 5C, D): *in situ* protruding from gonopodal sinus with their apical parts. Promere (Fig. 3C, and **p** in Figs 4A–C, 6B–

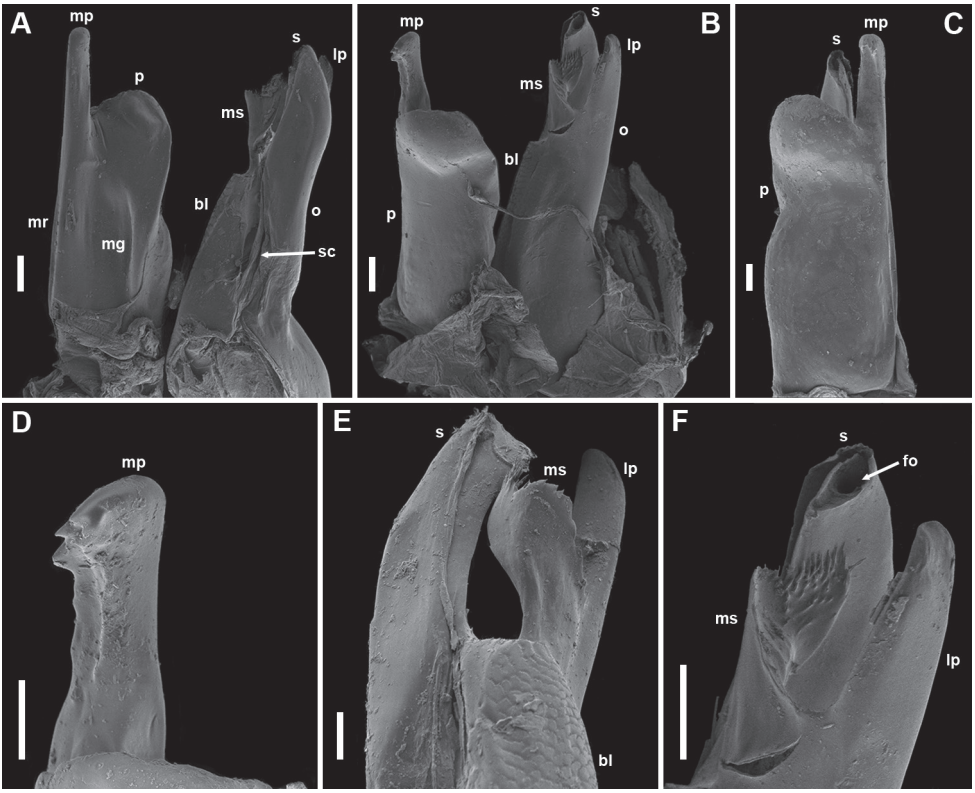

Figure 4. *Bellatoiulus golovatchi* gen. et sp. nov., male paratype (ZMUM). **A** left gonopods, mesal view (promere strongly turned mesad) **B** right gonopods, fronto-lateral view **C** left gonopods, frontal view **D** mesal process of right promere, fronto-lateral view **E** end of left opisthomere, meso-frontal view **F** end of right opisthomere, fronto-lateral view. Abbreviations: **bl** basofrontal lobe **fo** apical fovea **lp** lateral process **mg** median groove **mp** mesal process **mr** mesal ridge **ms** mesomeral process **o** opisthomere **p** promere **s** solenomere **sc** sperm canal. Scale bars: 0.03 mm (**A, B, F**); 0.02 mm (**C, D, E**).

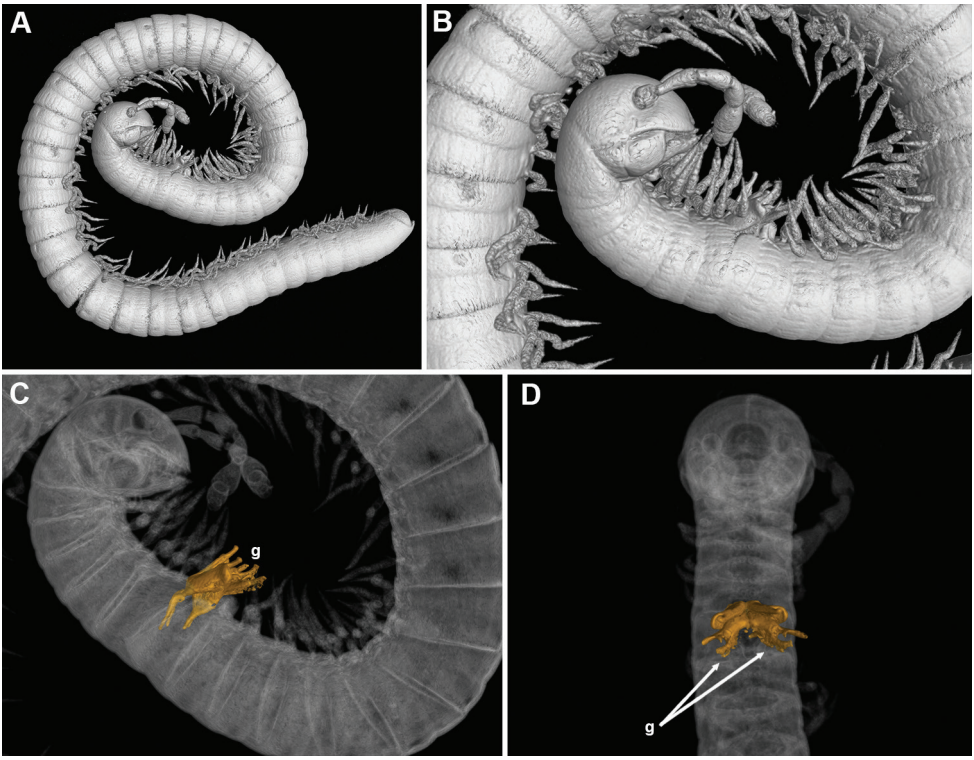

Figure 5. *Bellatoiulus golovatchi* gen. et sp. nov., male cybertype. **A** habitus, lateral view **B** anterior half of body, lateral view **C** anterior half of body with highlighted gonopods, lateral view **D** anterior body part with highlighted gonopods, ventral view. Abbreviation: **g** gonopods. Images not to scale.

E) rather stout, roughly quadrangular, insignificantly widening distally, with slightly concave mesal margin and gently sigmoid lateral margin, connected in a flat to broadly rounded apical margin; caudal face with a broad median groove (**mg**), and a broad, not too strongly pronounced mesal ridge (**mr**) bearing one or two short setae at mid-height, distally extending in a long and straight mesal process (Fig. 4D, and **mp** in Figs 3C, 4A–C, 6), with a somewhat clavate apex bearing several blunt teeth on its frontal side. Opisthomere (Figs 3D, E, 4E, F, and **o** in Figs 4A, B, 6A, C–E) relatively slender, reaching nearly level to mesal process of promere; frontal face with a broad, massive, microsquamous, basofrontal lobe (**bl**); mesomeral process (**ms**) originating just distally to the lobe, being strongly flattened, somewhat twisted around its axis, distally widening, apically bearing a group of minute seti- or spiniform filaments; a well-developed club or ping-pong paddle-like lateral process (**lp**) with smooth surface, almost reaching level to solenomere; solenomere (**s**) tubular, reaching higher than mesomeral process, distally somewhat bent latero-frontad, with a deep and narrow apical fovea (**fo**), and an (presumably) inner canal (**ic**) running vertically right basally

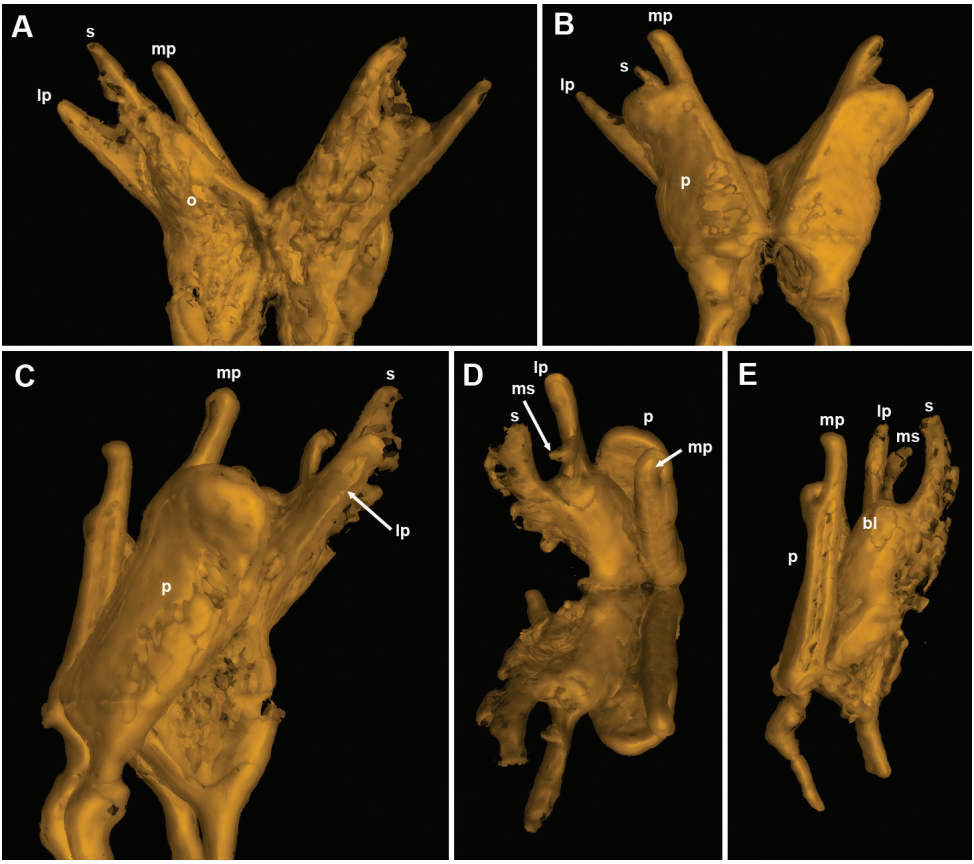

Figure 6. *Bellatoiulus golovatchi* gen. et sp. nov., male cybertype. **A** gonopods, caudal view **B** gonopods, frontal view **C** gonopods, lateral view **D** gonopods, ventral view **E** left gonopod, mesal view. Abbreviations: **bl** basofrontal lobe **lp** lateral process **mp** mesal process **ms** mesomeral process **o** opisthomere **p** promere **s** solenomere. Images not to scale.

to fovea, mesal side with a sperm canal (**sc**), distally somewhat deviating frontad, caudal lamella absent.

Female sexual characters: leg-pairs 1 (Fig. 7A) and 2 only slightly thicker than following legs. Vulva (Figs 7B–D, 9, and **v** in Fig. 8C, D) stout, roughly cylindrical, slightly compressed on sides; bursa (**bu**) mostly symmetric, median cleft (**mc**) positioned on top within a rather deep and narrow median field (**mf**); operculum (**op**) higher than bursa, ending with two very long, tapering, hyaline protrusions (**hp**); a row of four or five setae on each bursal valve and a group of several setae distally on each side of the operculum; bursal side sclerites non-setose. Receptaculum seminis composed of two nearly straight tubes: a shorter and somewhat thinner posterior one (**pt**), and an anterior one (**at**), slightly widening at bottom.

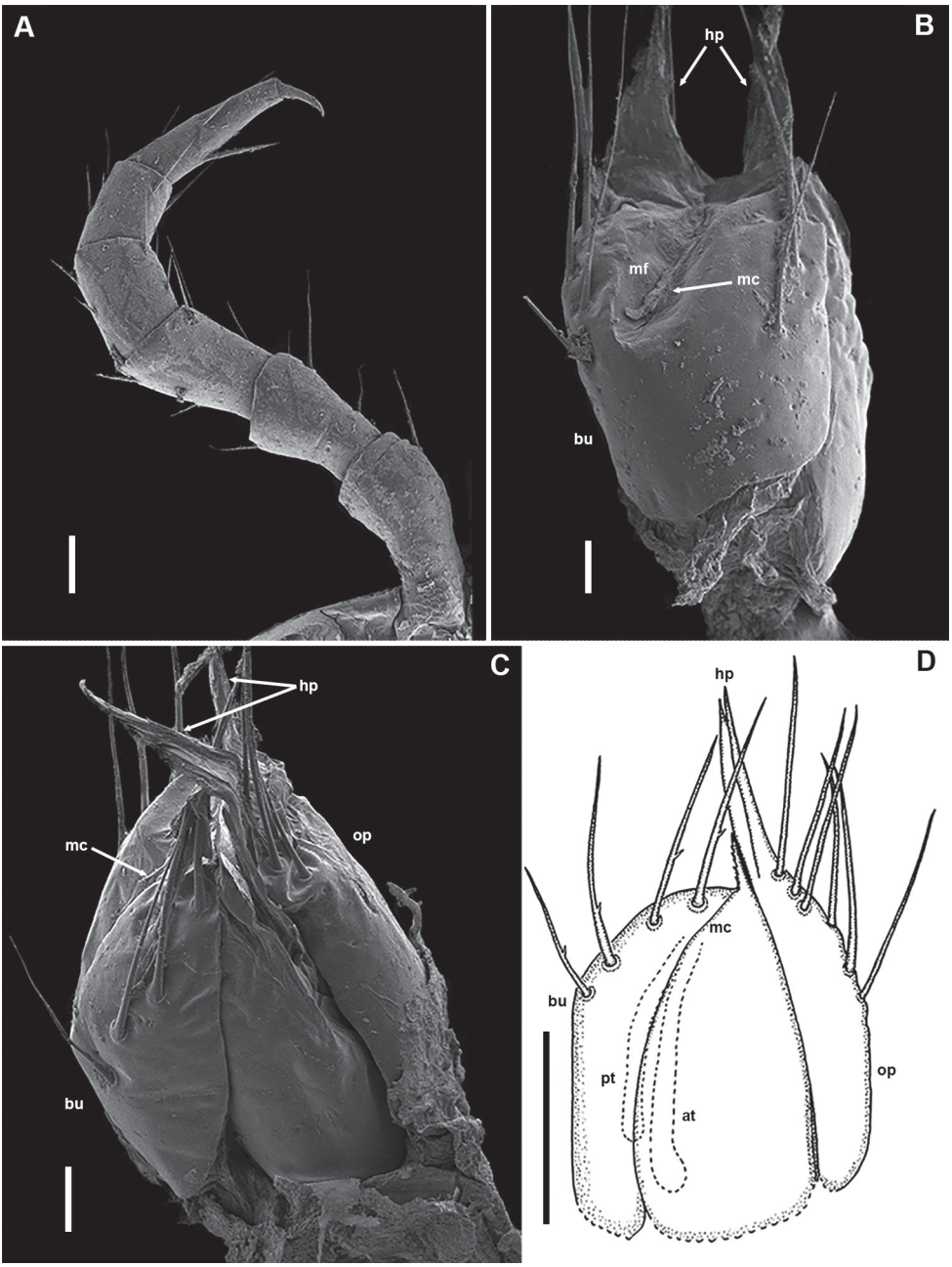

Figure 7. *Bellatoiulus golovatchi* gen. et sp. nov., female paratypes (ZMUM) **A–C** and NMNHS **D**). **A** right leg 2, caudal view **B** left vulva, caudal view **C** right vulva, fronto-mesal, slightly apical view **D** right vulva, fronto-mesal view. Abbreviations: **at** anterior tube **bu** bursa **hp** hyaline protrusions **mc** median cleft **mf** median field **op** operculum **pt** posterior tube. Scale bars: 0.03 mm (**A**); 0.02 mm (**B, C**); 0.1 mm (**D**).

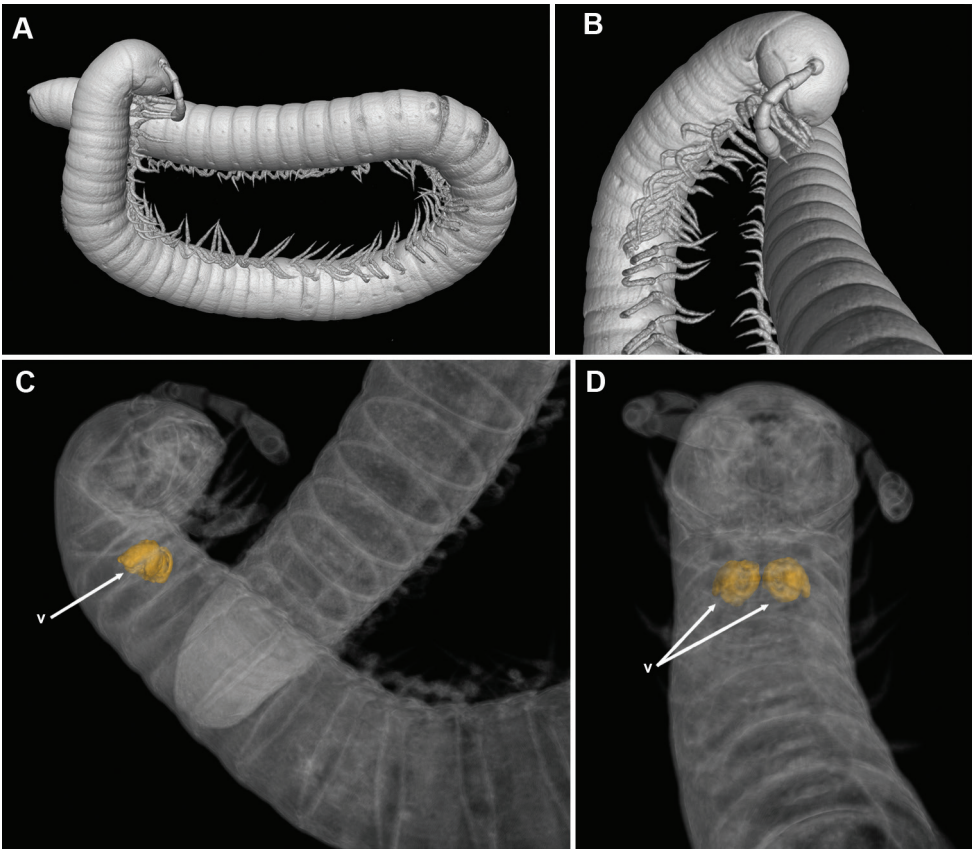

Figure 8. *Bellatoiulus golovatchi* gen. et sp. nov., female cybertype. **A** habitus, lateral view **B** anterior and posterior body parts, ventrolateral and dorso-lateral views, respectively **C** anterior and posterior body parts with highlighted vulvae, lateral views **D** anterior body part with highlighted vulvae, ventral view. Abbreviation: **v** vulvae. Images not to scale.

Discussion

Notes on the position of the genus *Bellatoiulus* gen. nov. within Pachyiulinae/Pachyiulini

Bellatoiulus golovatchi gen. et sp. nov. exhibits a highly distinctive genital (both gonopodal and vulval) morphology, making it hardly comparable to any other genus of Julidae. However, its affiliation to the tribe Pachyiulini seems unquestionable, mainly because of the following male sexual characters: promere without flagellum and with a mesal ridge bearing one or two setae; opisthomere with a well-developed, but not freely articulated, mesomeral process, and with an apical fovea; penis completely non-sclerotised, with relatively long, parallel, apical lobes, without differentiated membranous tubes (corresponding to the "pachyiuline penis type", as defined by Enghoff (1996)).

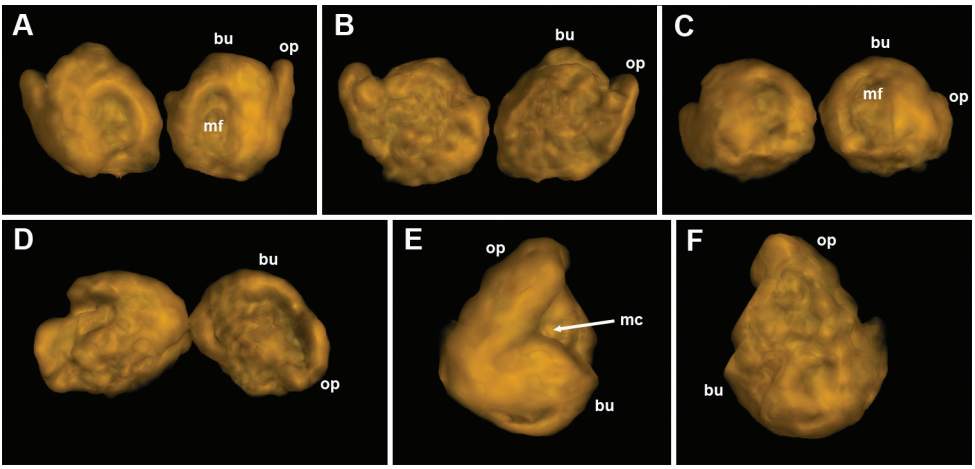

Figure 9. *Bellatoiulus golovatchi* gen. et sp. nov., female cybertype. **A** vulvae, caudal view **B** vulvae, frontal view **C** vulvae, ventral view **D** vulvae, dorsal view **E** right vulva, lateral view **D** right vulva, mesal view. Abbreviations: **bu** bursa **mc** median cleft **mf** median field **op** operculum. Images not to scale.

The classification of the Pachyiulini is still problematic in terms of both delimitations between genera, and the recognition of natural groups of genera based on synapomorphies. One of the few attempts of a subdivision of the tribe is that of Mauriès (1982), where all genera are divided into three groups depending on the presence/absence of an apical fovea and a flagelloid process on the solenomere. Each of these groups is divided into subgroups based on the presence/absence of a mesomeral process and of some external characteristics, such as vertigial setae, modified male mandibles, etc. The genus *Bellatoiulus* gen. nov. falls into the second group, which is characterized by a well-developed fovea and the absence of a flagelloid process. In addition to the genera *Mesoiulus* Berlese, 1886 (although in fact the type species, *M. paradoxus* Berlese, 1886, lacks a true fovea, as revealed by Enghoff (1992)) and *Cypriopachyiulus* Strasser, 1967, which was recognised by Mauriès (1982), the genera *Parapachyiulus* Golovatch, 1979, *Dangaraiulus* Golovatch, 1979, Caucasian species of *Amblyiulus* Silvestri, 1896, and perhaps *Syrioiulus* Verhoeff, 1914 (the fovea in many of its species is rather shallow, saddle-like) also belong to this group (Golovatch 1979, 2018; Antić et al. 2018; Evsyukov et al. 2021). *Bellatoiulus golovatchi* gen. et sp. nov. combines plesiomorphic and apomorphic characters according to Mauriès (1982). A plesiomorphic character is the presence of a mesomeral process (shared with all of the above-listed genera). However, other characters are apomorphic. Such are the unmodified male mandibles found in certain species of *Amblyiulus*, *Mesoiulus*, and *Syrioiulus* and the absence of ocelli, as in *Mesoiulus* and in some species of *Amblyiulus* and *Syrioiulus*. Absence of vertigial setae also brings the genus *Bellatoiulus* gen. nov. close to some species of *Amblyiulus*, *Syrioiulus*, *Parapachyiulus*, and *Mesoiulus*.

The new genus differs substantially from other tiny pachyiulinine genera (H of males ca 0.5 mm), such as the Carpathian–Balkan *Hylopachyiulus* Attems, 1904, *Geopachyiulus*

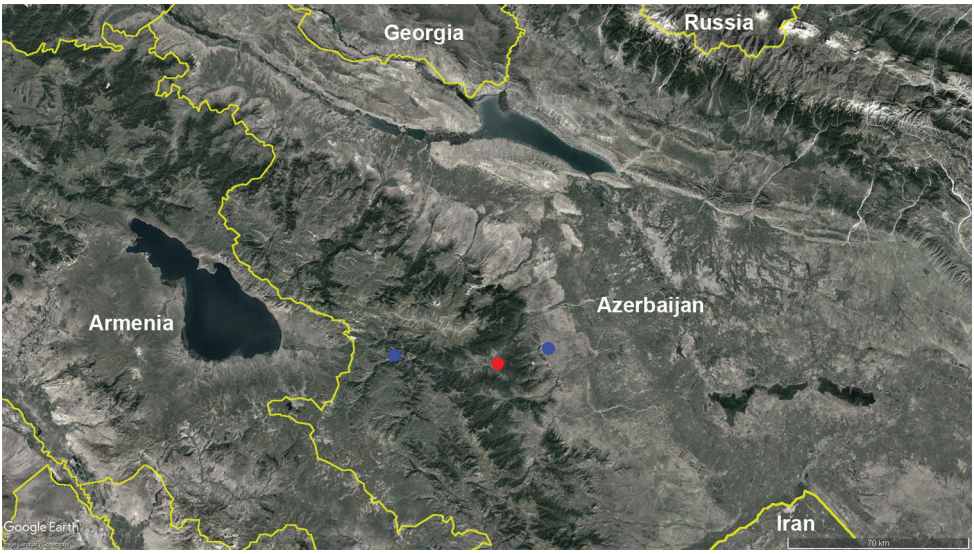

Figure 10. Distribution of *Bellatoiulus golovatchi* gen. et sp. nov. Red circle: type locality; blue circles: records of addition material.

Verhoeff, 1899, and *Micropachyiulus* Verhoeff, 1899. Apart from the unique lateral process, the opisthomere of *Bellatoiulus* gen. nov., unlike that in the aforementioned genera, has a fovea and lacks caudal lamella, the latter being well-developed in all three of them. The mesomeral process is well-differentiated in *Bellatoiulus* gen. nov. and *Geopachyiulus*, in contrast to *Micropachyiulus* and *Hylopachyiulus*, in which it is either poorly developed or mostly fused to the solenomere. Thus, there must be at least two groups of Pachyiulini genera that miniaturised independently of each other.

Notes on the distribution and ecology

Apparently, *Bellatoiulus golovatchi* gen. et sp. nov. is endemic to the eastern part of the Lesser Caucasus within Azerbaijan (Fig. 10), where it inhabits deciduous forests. However, future surveys may show that the species is also present in the adjacent territories of Armenia and Iran. According to the botanical biogeographic regionalisation of Menitsky (1991), the geographic distribution of the new species falls within the Murguz-Murovdag district of Eastern Transcaucasia.

Despite the absence of ommatidia and body pigmentation, *B. golovatchi* gen. et sp. nov. can hardly be regarded as an endogean or pedobiont, let alone a subterranean or hypogean form. Judging from both the present habitat information on the new species and personal observations on other blind (or with a strongly reduced number of ommatidia) and pale pachyiulinines, for example, species of *Apfelbeckiella* Verhoeff, 1901 or *Micropachyiulus* Verhoeff, 1899, *B. golovatchi* gen. et sp. nov. must be an inhabitant of the upper-most soil layer, immediately below the leaf litter. It could be thus assigned to the main life-form of Diplopoda–that of the stratobionts (Golovatch 1987), or alternatively to the

hemiedaphic fauna (see e.g., Deltshev et al. 2011). By all means, the minute size and pale colouration combined with little or no surface activity and often patchy distribution within a confined geographic area make the "micropachyiulini" one of the least explored julids. Another study on a group of such genera distributed in the Balkans, the Southern Carpathians, and the Caucasus is currently in preparation (Vagalinski et al. in prep.).

Acknowledgements

We are most grateful to S.I. Golovatch and K.Y. Eskov (both Moscow, Russia), the collectors who provided us their material for study. The present study was supported by RFBR, project number 20-54-18008, and BNSF, project number KP-06-Russia/6-11.12.2020. X-ray and SEM study were conducted using the equipment of Research and Education Center "Materials" at Don State Technical University. We are most thankful to Sergei Golovatch (Moscow, Russia), Henrik Enghoff (Copenhagen, Denmark) and Dragan Antić (Belgrade, Serbia), the reviewers, for their very helpful corrections and suggestions that have considerably improved our paper. Pavel Stoev (Sofia, Bulgaria) very helpfully served as the managing editor.

References

Akkari N, Enghoff H, Metscher B (2015) A new dimension in documenting new species: High-detail imaging for myriapod taxonomy and first 3D cybertype of a new millipede species (Diplopoda, Julida, Julidae). PLoS ONE 10(8): e0135243. https://doi.org/10.1371/journal.pone.0135243

Antić DŽ, Rađa T, Akkari N (2018) Revision of the genus *Hylopachyiulus* Attems, 1904, with a description of a new species from Croatia (Diplopoda, Julida, Julidae). Zootaxa 4531(2): 225–241. https://doi.org/10.11646/zootaxa.4531.2.4

Attems C (1904) Neue palaearktische Myriopoden nebsts Beiträgen zur Kenntnis einiger alten Arten. Archiv für Naturgeschichte 70(1): 179–196.

Berlese A (1883) Acari, Myriopoda et Scorpiones hucusque in Italia reperta. Acari, Miriapodi e Scorpioni Italiani. Fascicolo VI. Acari, Myriapoda et Scorpiones huscque in Italia reperta 6. Padova, 1–192. https://doi.org/10.5962/bhl.title.69269

Deltshev C, Lazarov S, Naumova M, Stoev P (2011) A survey of spiders (Araneae) inhabiting the euedaphic soil stratum and the superficial underground compartment in Bulgaria. Arachnologische Mitteilungen 40: 33–46. https://doi.org/10.5431/aramit4005

Enghoff H (1992) *Dolichoiulus*–A mostly Macaronesian multitude of millipedes. With the description of a related new genus from Tenerife, Canary Islands (Diplopoda, Julida, Julidae). Entomologica Scandinavica (Supplement 40): 1–158. https://doi.org/10.1163/187631292X00010

Enghoff H (1996) The penis as a phylogenetic character in the millipede family Julidae. In: Geoffroy JJ, Mauriès J-P, Nguyen Duy-Jacquemin M (Eds) Acta Myriapodologica. Mémoires du Museum National d'Histoire Naturelle 169: 313–326.

Enghoff H, Dohle W, Blower JG (1993) Anamorphosis in millipedes (Diplopoda)–The present state of knowledge with some developmental and phylogenetic considerations. Biological Journal of the Linnean Society. Linnean Society of London 109(2): 103–234. https://doi.org/10.1111/j.1096-3642.1993.tb00305.x

Enghoff H, Petersen G, Seberg O (2013) The aberrant millipede genus *Pteridoiulus* and its position in a revised molecular phylogeny of the family Julidae (Diplopoda: Julida). Invertebrate Systematics 27(5): 515–529. https://doi.org/10.1071/IS13016

Evsyukov AP (2016) The millipede *Pachyiulus krivolutskyi* Golovatch, 1977, the easternmost species of the eastern Mediterranean genus *Pachyiulus* Berlese, 1883, endemic to the western Caucasus (Diplopoda: Julida: Julidae). Russian Entomological Journal 25(4): 299–306. https://doi.org/10.15298/rusentj.25.3.12

Evsyukov AP, Golovatch SI, Antić DŽ (2021) The millipede genera *Amblyiulus* Silvestri, 1896 and *Syrioiulus* Verhoeff, 1914 in the Caucasus, with notes on their distributions (Diplopoda, Julida, Julidae). ZooKeys 1048: 109–143. https://doi.org/10.3897/zookeys.1048.68454

Faulwetter S, Vasileiadou A, Kouratoras M, Dailianis T, Arvanitidis C (2013) Micro-computed tomography: Introducing new dimensions to taxonomy. ZooKeys 263: 1–45. https://doi.org/10.3897/zookeys.263.4261

Golovatch SI (1979) The composition and zoogeographic relationship of the diplopod fauna of Middle Asia. Part 2. Zoologicheskii zhurnal 58(9): 1313 -1325. [in Russian, a summary in English]

Golovatch SI (1987) On life forms in millipedes (Diplopoda). In: Striganova BR (Ed.) Soil fauna and soil fertility. Proceeding of the 9th International Colloquium on Soil Zoology, Nauka, Moscow, 210–213.

Golovatch SI (2018) The millipede subfamily Pachyiulinae in Israel, with the description of a new species (Diplopoda, Julida, Julidae). Zoologicheskii zhurnal 97(7): 791–805. https://doi.org/10.1134/S0044513418070073

Hoffman RL (1980) Classification of the Diplopoda. Muséum d'Histoire naturelle, Genève, 237 pp.

Mauriès J-P (1982) *Dolichoiulus tongiorgii* (Strasser), Diplopode halophile nouveau pour la faune de France. Remarques sur la classification des Pachyiulini (Myriapoda, Diplopoda, Iulida). Bulletin du Muséum National d'Histoire Naturelle, Série 4 4(3–4): 433–444.

Menitsky YL (1991) The project, "A synopsis of the Caucasian flora". A map of the floristic districts. Botanicheskii Zhurnal 76(11): 1513–1521 [in Russian]. http://arch.botjournal.ru/?t=issues&id=19911111&rid=pdf_0005139

Metscher BD (2009) MicroCT for comparative morphology: Simple staining methods allow high-contrast 3D imaging of diverse non-mineralized animal tissues. BMC Physiology 9(1): e11. https://doi.org/10.1186/1472-6793-9-11

Metscher BD (2011) X-ray microtomographic imaging of intact vertebrate embryos. Cold Spring Harbor Protocols 2011(12): 1462–1471. https://doi.org/10.1101/pdb.prot067033

O'Leary MA, Kaufman SG (2012) MorphoBank 3.0: Web application for morphological phylogenetics and taxonomy. http://www.morphobank.org

Rosenmejer T, Enghoff H, Mortiz L, Wesener T (2021) Integrative description of new Giant Pill-Millipedes from southern Thailand (Diplopoda, Sphaerotheriida, Zephroniidae). European Journal of Taxonomy 762: 108–132. https://doi.org/10.5852/ejt.2021.762.1457

Silvestri F (1896) I Diplopodi. Parte I. Sistematica. Annali del Museo Civico di Storia Naturale di Genova, Serie 2, 16: 121–254. http://biodiversitylibrary.org/page/7697911

Strasser K (1967) Über Diplopoden Griechenlands, einiger Ägäis-Inseln und Zyperns. Senckenbergiana Biologica 48(4): 269–293.

Vagalinski B (2020) A new species of *Syrioiulus* Verhoeff, 1914 from Iran, with remarks on the taxonomy of the genus (Diplopoda: Julida: Julidae). Revue Suisse de Zoologie 127(1): 83–94. https://doi.org/10.35929/RSZ.0008

Verhoeff KW (1899) Beiträge zur Kenntniss paläarktischer Myriopoden. IX. Aufsatz: Zur Systematik, Phylogenie und vergleichenden Morphologie der Juliden und über einige andere Diplopoden. Archiv für Naturgeschichte 65(1): 183–230.

Verhoeff KW (1914) Einige Chilognathen aus Palästina (Über Diplopoden 68. Aufsatz.). Verhandlungen der Zoologisch-botanischen Gesellschaft in Wien 64: 61–75.

Supplementary material 1

***Bellatoiulus golovatchi* gen. et sp. nov., male cybertype.**

Authors: Aleksandr P. Evsyukov, Boyan Vagalinski, Igor Y. Zabiyaka, Evgeniy V. Sadyrin

Data type: Video

Explanation note: Volume rendering of microCT image.

Copyright notice: This dataset is made available under the Open Database License (http://opendatacommons.org/licenses/odbl/1.0/). The Open Database License (ODbL) is a license agreement intended to allow users to freely share, modify, and use this Dataset while maintaining this same freedom for others, provided that the original source and author(s) are credited.

Link: https://doi.org/10.3897/zookeys.1097.81792.suppl1

Supplementary material 2

***Bellatoiulus golovatchi* gen. et sp. nov., female cybertype.**

Authors: Aleksandr P. Evsyukov, Boyan Vagalinski, Igor Y. Zabiyaka, Evgeniy V. Sadyrin

Data type: Video

Explanation note: Volume rendering of microCT image.

Copyright notice: This dataset is made available under the Open Database License (http://opendatacommons.org/licenses/odbl/1.0/). The Open Database License (ODbL) is a license agreement intended to allow users to freely share, modify, and use this Dataset while maintaining this same freedom for others, provided that the original source and author(s) are credited.

Link: https://doi.org/10.3897/zookeys.1097.81792.suppl2

ZooKeys 1097: 65–83 (2022)
doi: 10.3897/zookeys.1097.82527
https://zookeys.pensoft.net

RESEARCH ARTICLE

A peer-reviewed open-access journal
ZooKeys
Launched to accelerate biodiversity research

Two new species of cave-adapted pseudoscorpions (Pseudoscorpiones, Chthoniidae) from Yunnan, China

Yanmeng Hou[1], Zhizhong Gao[2], Feng Zhang[1]

1 *The Key Laboratory of Zoological Systematics and Application, Institute of Life Science and Green Development, Hebei University, Baoding, Hebei 071002, China* **2** *Department of Biology, Xinzhou Teachers University, Xinzhou 034000, Shanxi Province, China*

Corresponding authors: Zhizhong Gao (gaozhizhong1987@126.com), Feng Zhang (dudu06042001@163.com)

Academic editor: Jana Christophoryová | Received 20 February 2022 | Accepted 5 April 2022 | Published 20 April 2022

http://zoobank.org/6FC8EE30-904F-4E8D-9EF9-996F81F30693

Citation: Hou Y, Gao Z, Zhang F (2022) Two new species of cave-adapted pseudoscorpions (Pseudoscorpiones, Chthoniidae) from Yunnan, China. ZooKeys 1097: 65–83. https://doi.org/10.3897/zookeys.1097.82527

Abstract

Two new cave-adapted pseudoscorpion species belonging to the family Chthoniidae are described: *Tyrannochthonius pandus* **sp. nov.** from Biyu Cave (Yunnan: Luxi) and *Lagynochthonius laoxueyanensis* **sp. nov.** from Laoxueyan Cave (Yunnan: Yanshan). Both of them, collected from the dark zone of caves, are highly troglomorphic species.

Keywords

Karst biotope, *Lagynochthonius*, taxonomy, troglobionts, *Tyrannochthonius*

Introduction

China has the largest karst biotopes in the world, with the karst area reaching 3.44 million km^2, accounting for about one-third of the country's land area, and contains tens of thousands of karst caves, which are rich in animal resources (Zhao et al. 2015). Yunnan, located in southwest China, is one of the provinces with the most widely distributed karst landforms (11.09 × 10^4 km^2), especially in the eastern portion of Yunnan (Wang 2001). So far, at least 742 cave-dwelling species have been identified in China, and nearly 15% of them are from Yunnan (Latella 2019).

Copyright *Yanmeng Hou et al.* This is an open access article distributed under the terms of the Creative Commons Attribution License (CC BY 4.0), which permits unrestricted use, distribution, and reproduction in any medium, provided the original author and source are credited.

Subterranean-adapted pseudoscorpions are one of the representative groups of cave-dwelling arthropods. They are usually eyeless, have elongate appendages and can be easily found on cave walls or under rocks. To date, 33 cave-dwelling pseudoscorpion species, representing three families (Chthoniidae, Neobisiidae, Chernetidae), have been described from China. Among them, eight species are known from Yunnan (Schawaller 1995; Mahnert 2003, 2009; Mahnert and Li 2016; Gao et al. 2017; Li et al. 2017; Gao et al. 2018; Li et al. 2019; Feng et al. 2020; Gao et al. 2020; Zhang et al. 2020).

The genus *Tyrannochthonius* Chamberlin, 1929 contains 145 species, with at least 52 species occurring in caves, and is distributed in all continents except Antarctica (WPC 2022). This genus can be diagnosed as follows (see Material and methods for explanation of abbreviations): trichobothrium *sb* situated midway between *st* and *b*, or closer to *st*; trichobothria *ib* and *isb* situated close together in a median or sub-basal position on the dorsum of the chelal hand; chelal hand not distally constricted and the movable finger without a complex or strongly sclerotized apodeme at the base; fixed finger usually with one large, medial acuminate spine-like seta at its base, but can be reduced or absent in some cave-dwelling species; coxal spines generally long and present on coxae II only; epistome pointed, triangular or rounded, inconspicuous and usually with 2 closely-flanking setae at its base (Chamberlin 1962; Muchmore 1984, 1991; Muchmore and Chamberlin 1995; Edward and Harvey 2008). So far, nine species and one subspecies of this genus have been described from China, of which six are exclusively known from karst caves: *T. akaelus* Mahnert, 2009 from Sichuan, *T. ganshuanensis* Mahnert, 2009 from Sichuan and Hubei, *T. antridraconis* Mahnert, 2009 from Sichuan, *T. chixingi* Gao, Wynne & Zhang, 2018 from Guangxi, *T. harveyi* Gao, Zhang & Chen, 2020 and *T. zhai* Gao, Zhang & Chen, 2020 from Guizhou. All species are troglobites without eyes (Mahnert 2009; Gao et al. 2018; Gao et al. 2020; WPC 2022).

The genus *Lagynochthonius* Beier, 1951 was erected by Beier (1951) as a subgenus of *Tyrannochthonius*, but was later elevated to generic status by Chamberlin (1962). The genus is diagnosed by trichobothrium *sb* situated midway between *st* and *b*, or closer to *st*; trichobothria *ib* and *isb* situated close together in a median or sub-basal position on the dorsum of the chelal hand; coxal spines generally long and present on coxae II only; chelal hand distally constricted (or flask-shaped) and movable finger with complex or strongly sclerotized apodeme at its base and the modified tooth (*td*) of the fixed chelal finger displaced onto the dorso-antiaxial face (Chamberlin 1962; Harvey 1989; Muchmore 1991; Judson 2007; Edward and Harvey 2008). At present, this genus contains 55 species (seven species living in caves) distributed in Asia, Australia, Africa and America. Eight species of this genus have been described from China, of which only one is exclusively known from karst caves: *L. bailongtanensis* Li, Liu & Shi, 2019 from Yunnan (Li et al. 2019; WPC 2022).

Two new troglomorphic species of Chthoniidae have been recently found from the karst caves survey in Yunnan in 2021. These species are here described.

Materials and methods

The specimens examined for this study are preserved in 75% alcohol and deposited in the Museum of Hebei University (**MHBU**) (Baoding, China) and the Museum of Southwest University (**MSWU**) (Chongqing, China). Photographs, drawings and measurements were taken using a Leica M205A stereo-microscope equipped with a Leica DFC550 Camera and the Inkscape software (Ver. 1.0.2.0). Detailed examination was carried out with an Olympus BX53 general optical microscope. Images were edited and formatted using Adobe Photoshop 2022.

Terminology and measurements follow Chamberlin (1931) with some minor modifications to the terminology of trichobothria (Harvey 1992; Judson 2007) and chelicera (Judson 2007). The chela and chelal hand are measured in lateral view and others taken in dorsal view. All measurements are given in mm unless noted otherwise. Proportions and measurements of pedipalps and carapace correspond to length/width, those of legs to length/depth.

The following abbreviations are used in the text:

b basal trichobothrium;
sb sub-basal trichobothrium;
st sub-terminal trichobothrium;
t terminal trichobothrium trichobothrium;
ib interior basal trichobothrium;
isb interior sub-basal trichobothrium;
ist interior sub-terminal trichobothrium;
it interior terminal trichobothrium;
eb exterior basal trichobothrium;
esb exterior sub-basal trichobothrium;
est exterior sub-terminal trichobothrium;
et exterior terminal trichobothrium;
dx duplex trichobothria;
td modified tooth.

Taxonomy

Chthoniidae Daday, 1889

Tyrannochthonius Chamberlin, 1929

Type species. *Chthonius terribilis* With, 1906, by original designation.

Diagnosis. See Edward and Harvey (2008).

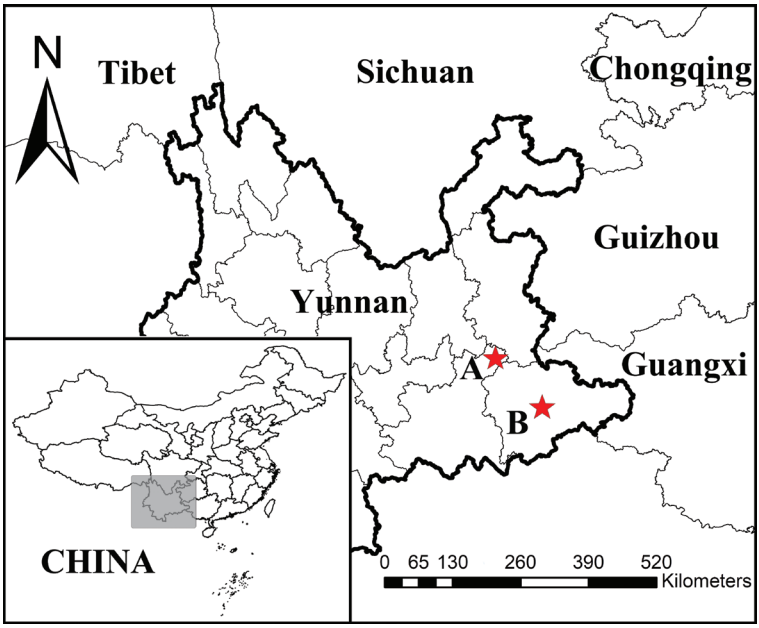

Figure 1. Study area, general cave locations, and type locality for each species, Yunnan Province, China **A** Biyu Cave, *Tyrannochthonius pandus* sp. nov. **B** Laoxueyan Cave, *Lagynochthonius laoxueyanensis* sp. nov.

***Tyrannochthonius pandus* sp. nov.**
http://zoobank.org/D9B22241-9699-41ED-936C-5169456BD61A
Chinese name. 弯指暴伪蝎
Figs 2–5

Type material. (Figs 1A, 6) ***Holotype***: China • ♂; Yunnan Province, Luxi County, Luyuandong Village, the Ancient Alu Cave National Park of China, Biyu Cave; 24°34.01'N, 103°45.16'E; 1722 m a.s.l.; 13 Oct. 2021; Zegang Feng, Yanmeng Hou, Lu Zhang and Liu Fu leg.; dark zone; Ps.-**MHBU**-HBUARA#2021-438-01. ***Paratype***: • 1♀; the same data as the holotype; Ps.-**MSWU**-HBUARA#2021-438-02.

Diagnosis. Moderately sized troglomorphic species with elongate appendages; carapace without eyes or eyespots; anterior margin of carapace gently serrate, epistome small, pointed, triangular, with 2 setae flanking base; posterior margin of carapace with 2 setae; tergites I–III with 2 setae; lacking chemosensory setae on dorsum of chelal hand; chelal fingers distinctly curved in dorsal view, with numerous large, gently curved, well-spaced teeth.

Etymology. The specific name is derived from the Latin word "*pandus*", meaning curved, refers to the curved chelal finger.

Description. Adult male (Figs 2, 3A, 4A–D, 5). ***Color***: generally pale yellow, chelicerae, pedipalps and tergites slightly darker, soft parts pale (Figs 2, 3A). ***Cephalothorax*** (Figs 4B, 5A): carapace 1.07 times longer than broad, gently narrowed

Figure 2. *Tyrannochthonius pandus* sp. nov., male habitus. Photographed when it crawled on stony natural habitat.

posteriorly, surface smooth; anterior margin slightly serrate; without any traces of eyes; epistome very pointed and small, triangular, with 2 setae flanking base; with 18 setae arranged s4s: 4: 4: 2: 2, most setae heavy, long and gently curved, anterolateral setae much shorter than others; without furrows but with 4 lyrifissures (Fig. 5A). Chaetotaxy of coxae: P 3, I 3, II 4, III 5, IV 5; manducatory process with two acuminate distal setae, anterior seta less than 1/2 length of medial seta; apex of coxa I with small, rounded anteromedial process; coxae II with 10 terminally indented coxal spines on each side, set as an oblique row, longer spines present in the middle of the row, becoming shorter distally and proximally and incised for about half their length (Fig. 5C); intercoxal tubercle absent; without sub-oral seta. ***Chelicera*** (Figs 4C, 5B): large, about as long as carapace, 2.44 times longer than broad; 5 setae on hand, all setae acuminate, ventrobasal seta shorter than others; movable finger with one medial seta. Cheliceral palm with moderate hispid granulation dorsally. Both fingers well provided with teeth, fixed finger with 11 teeth, distal one largest; movable finger with 8 retrorse continuous small teeth; galea completely vestigial (Fig. 5B). Rallum with 8 blades, the distal one longest and recumbent basally, with fine barbules and slightly set apart from the other blades, latter tightly grouped and with long pinnae, some of which are subdivided (Fig. 5D).

Figure 3. *Tyrannochthonius pandus* sp. nov. **A** holotype male, dorsal view **B** paratype female, dorsal view. Scale bars: 0.5 mm.

Pedipalp (Figs 4A, 5E–H): surface of palpal segments smooth; setae generally long and acuminate; femur 7.36, patella 2.55, chela 7.47, hand 2.80 times longer than deep; movable finger 1.71 times longer than hand and 0.64 times longer than chela, without large basal apodeme, only slightly sclerotized section present. Femur and dorsal hand without tactile setae but with 1 distal lyrifissure on patella (Fig. 5E). Fixed chelal finger and hand with 8 trichobothria, movable chelal finger with 4 trichobothria, *ib* and *isb* situated close together, submedially on dorsum of chelal hand; *eb*, *esb* and *ist* forming a straight oblique row at base of fixed chelal finger; *it* slightly distal to *est*, situated subdistally; *et* slightly near to tip of fixed finger, very close to chelal teeth; *dx* situated distal to *et*; *sb* situated closer to *st* than to *b*; *b* and *t* situated subdistally, *b* situated at same level as *est*; *t* situated distal to *est* (Fig. 5F). Microsetae (chemosensory setae) absent on hand and both chelal fingers. Sensilla absent. A tiny antiaxial lyrifissure present at base of fixed finger (slightly distal to *ist*). Both chelal fingers with a row of teeth, homodentate, spaced regularly along the margin, larger teeth present in the middle of the row, becoming smaller distally and proximally: fixed finger with 45 large, gently curved, well-spaced teeth, without intercalary teeth; movable finger with 44 small (slightly smaller than the teeth on fixed finger), retrorse, gently curved and well-spaced teeth (Fig. 5F). Chelal fingers distinctly curved in dorsal view (Fig. 5H). ***Opisthosoma*:** generally typical; pleural membrane finely granulate. Tergites and sternites undivided; setae uniseriate and acuminate. Tergal chaetotaxy I–XII: 2: 2: 2: 3: 4: 4: 4: 5: 5: 4: T2T: 0; tergites VIII and IX each with an unpaired median seta. Sternal chaetotaxy IV–XII: 10: 10: 9: 9: 9: 9: 8: 0: 2; sternites VI–IX with unpaired median seta. Anterior genital operculum with 10 setae, genital opening slit-like, with 15 marginal setae on each side (Fig. 4D). ***Legs*** (Fig. 5I, J): generally typical, long and slender. Femur of leg I 1.92 times longer than patella and with 1 lyrifissure at the base of femur; tarsus 2.50

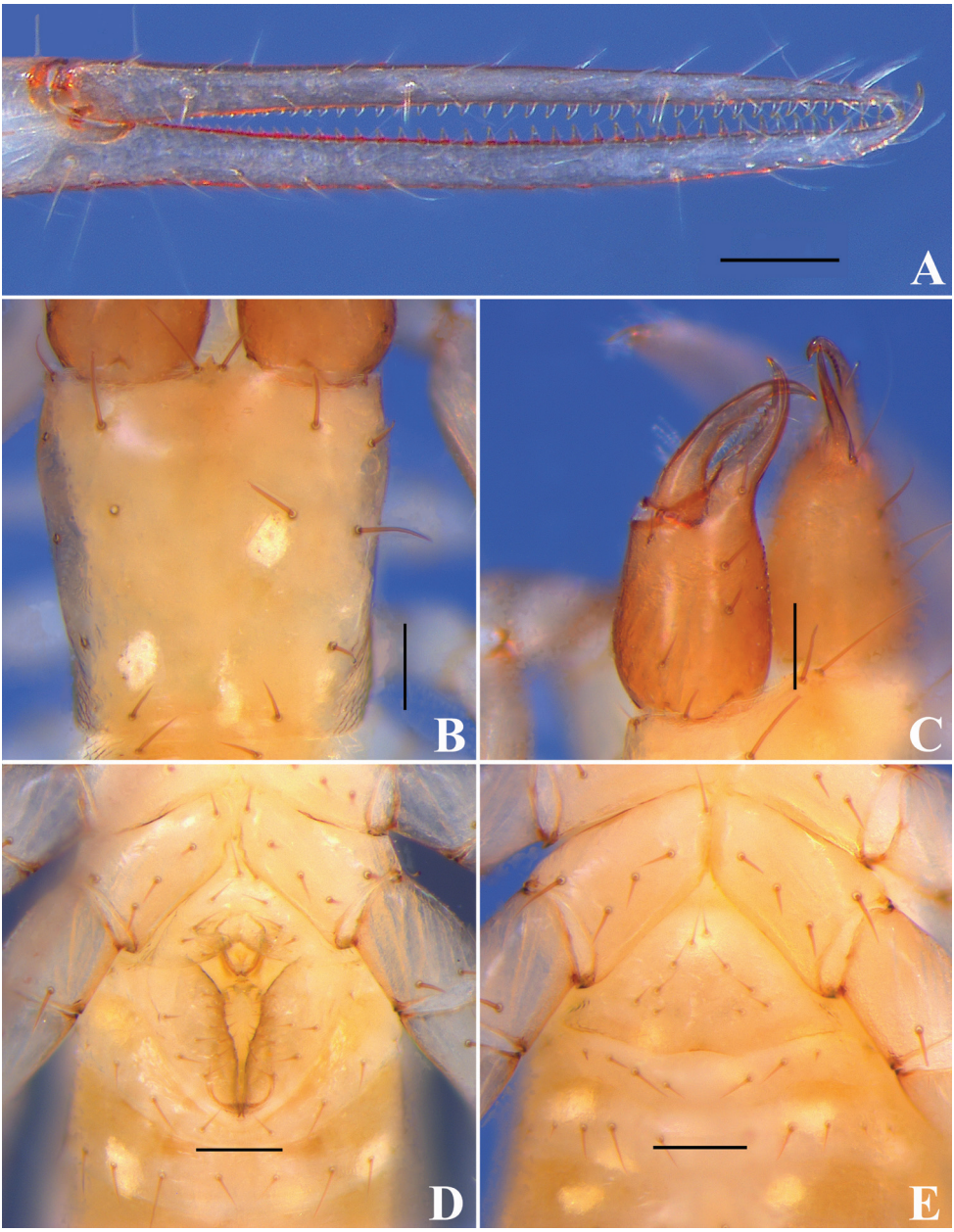

Figure 4. *Tyrannochthonius pandus* sp. nov., holotype male (**A–D**), paratype female (**E**) **A** chelal fingers (lateral view) **B** carapace (dorsal view) **C** left chelicera (dorsal view) **D** male genital area (ventral view) **E** female genital area (ventral view). Scale bars: 0.1 mm.

times longer than tibia. Femoropatella of leg IV 3.67 times longer than deep; tibia 6.29 times longer than deep; with basal tactile setae on both tarsal segments: basitarsus 4.00 times longer than deep (TS = 0.35), telotarsus 14.50 times longer than deep and 2.90

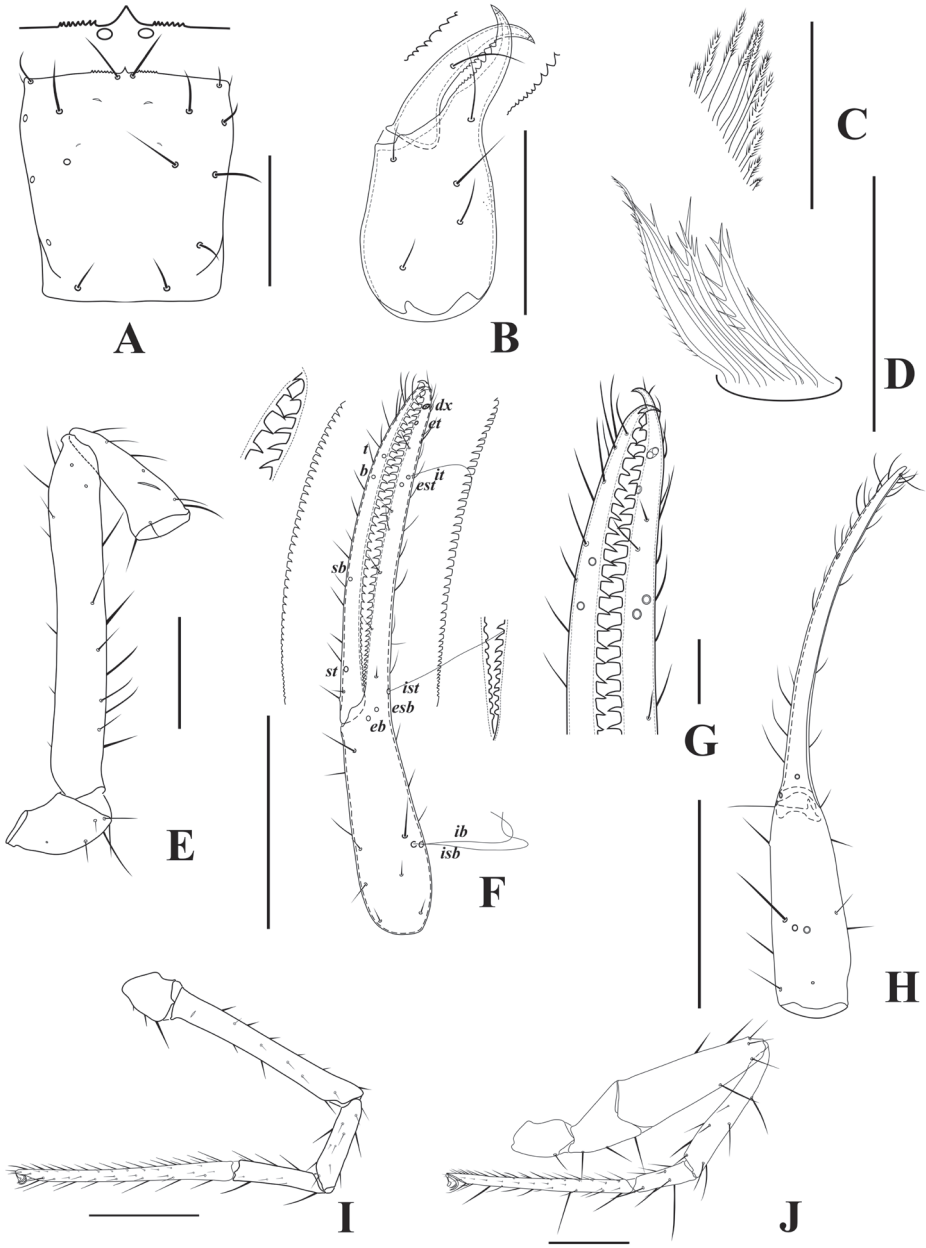

Figure 5. *Tyrannochthonius pandus* sp. nov., holotype male **A** carapace (dorsal view) with a detail of anterior margin **B** left chelicera (dorsal view) with details of teeth **C** coxal spines on coxae II (ventral view) **D** rallum **E** left pedipalp (minus chela, dorsal view) **F** left chela (lateral view) with details of teeth and with trichobothrial pattern (abbreviations explained in Material and methods) **G** finger tips of chela (lateral view) **H** left chela (dorsal view) **I** leg I (lateral view) **J** leg IV (lateral view). Scale bars: 0.25 mm (**A–B, E–F, H–J**); 0.10 mm (**C–D, G**).

times longer than basitarsus (TS = 0.33). Setae of leg I (trochanter to tibia) 3: 13: 12: 9, setae of leg IV (trochanter to basitarsus) 1: 3: 6: 9: 8. Arolium slightly shorter than the claws, not divided; claws simple. ***Dimensions of male holotype*** (length/width or, in the case of the legs, length/depth in mm; ratios in parentheses). Body length 1.41. Pedipalps: trochanter 0.18/0.13 (1.38), femur 0.81/0.11 (7.36), patella 0.28/0.11 (2.55), chela 1.12/0.15 (7.47), hand length 0.42/0.15 (2.80), movable finger length 0.72. Chelicera 0.44/0.18 (2.44), movable finger length 0.24. Carapace 0.45/0.42 (1.07). Leg I: trochanter 0.13/0.11 (1.18), femur 0.46/0.06 (7.67), patella 0.24/0.05 (4.80), tibia 0.20/0.04 (5.00), tarsus 0.50/0.04 (12.50). Leg IV: trochanter 0.20/0.11 (1.82), femoropatella 0.66/0.18 (3.67), tibia 0.44/0.07 (6.29), basitarsus 0.20/0.05 (4.00), telotarsus 0.58/0.04 (14.50).

Adult female (Figs 3B, 4E). Mostly same as males. Anterior genital operculum with 10 setae plus 7 setae on posterior margin. Body length 1.67. Pedipalps: trochanter 0.24/0.13 (1.85), femur 0.88/0.13 (6.77), patella 0.28/0.11 (2.55), chela 1.20/0.17 (7.06), hand length 0.49/0.17 (2.88), movable finger length 0.76. Chelicera 0.45/0.21 (2.14), movable finger length 0.23. Carapace 0.46/0.46 (1.00). Leg I: trochanter 0.14/0.11 (1.27), femur 0.50/0.06 (8.33), patella 0.26/0.06 (4.33), tibia 0.21/0.05 (4.20), tarsus 0.53/0.04 (13.25). Leg IV: trochanter 0.21/0.12 (1.75), femoropatella 0.70/0.19 (3.68), tibia 0.46/0.07 (6.57), basitarsus 0.21/0.06 (3.50), telotarsus 0.62/0.04 (15.50).

Remarks. Compared with the other six cave-dwelling species of the genus in China, *Tyrannochthonius pandus* sp. nov. is most similar to *T. ganshuanensis* in having only 2 setae on tergites I–III, the same chaetotaxy of carapace and triangular, a small epistome, but differs in the shape of teeth on chelal fingers (large, gently curved, well-spaced teeth, without intercalary teeth in *T. pandus*, but with pointed, well-spaced and intercalary teeth in *T. ganshuanensis*), the relative position of the trichobothria on the movable chelal finger (*sb* situated closer to *st* than to *b* in *T. pandus*, but *sb* situated closer to *b* in *T. ganshuanensis*). *Tyrannochthonius pandus* sp. nov. can be easily separated from *T. akaleus* by a smaller body size (1.67 vs. 2.10 mm in female), the teeth pattern on chelal fingers (intercalary teeth absent in *T. pandus*, but present in *T. akaleus*); from *T. harveyi* by the different setae number on the anterior and posterior margins of the carapace (*T. pandus* with 6 and 2 setae, respectively, but *T. harveyi* with 4 and 4 setae, respectively), the shape of the epistome (long and pointed in *T. pandus*, but rounded and inconspicuous in *T. harveyi*), the number of rallar blades (8 in *T. pandus*, but 6 in *T. harveyi*); and from *T. zhai*, *T. chixingi* and *T. antridraconis* by the number of setae on the anterior tergites (tergites I–III with 2 setae in *T. pandus*, but the other three with 4 setae). In addition, compared to the new species, *T. zhai* differs by the shorter body length (1.40 vs. 1.67 mm in female) and lacking an epistome; *T. chixingi* and *T. antridraconis* differs from the new species also by the presence of intercalary teeth on the fixed chelal finger (Mahnert 2009; Gao et al. 2018; Gao et al. 2020).

Distribution. This species is known only from the type locality, Biyu Cave (Figs 1A, 6). Biyu Cave is one of the tourist caves in the Ancient Alu Cave National Park of China, with the entrance located in the Jilong hillside. This beautiful cave is

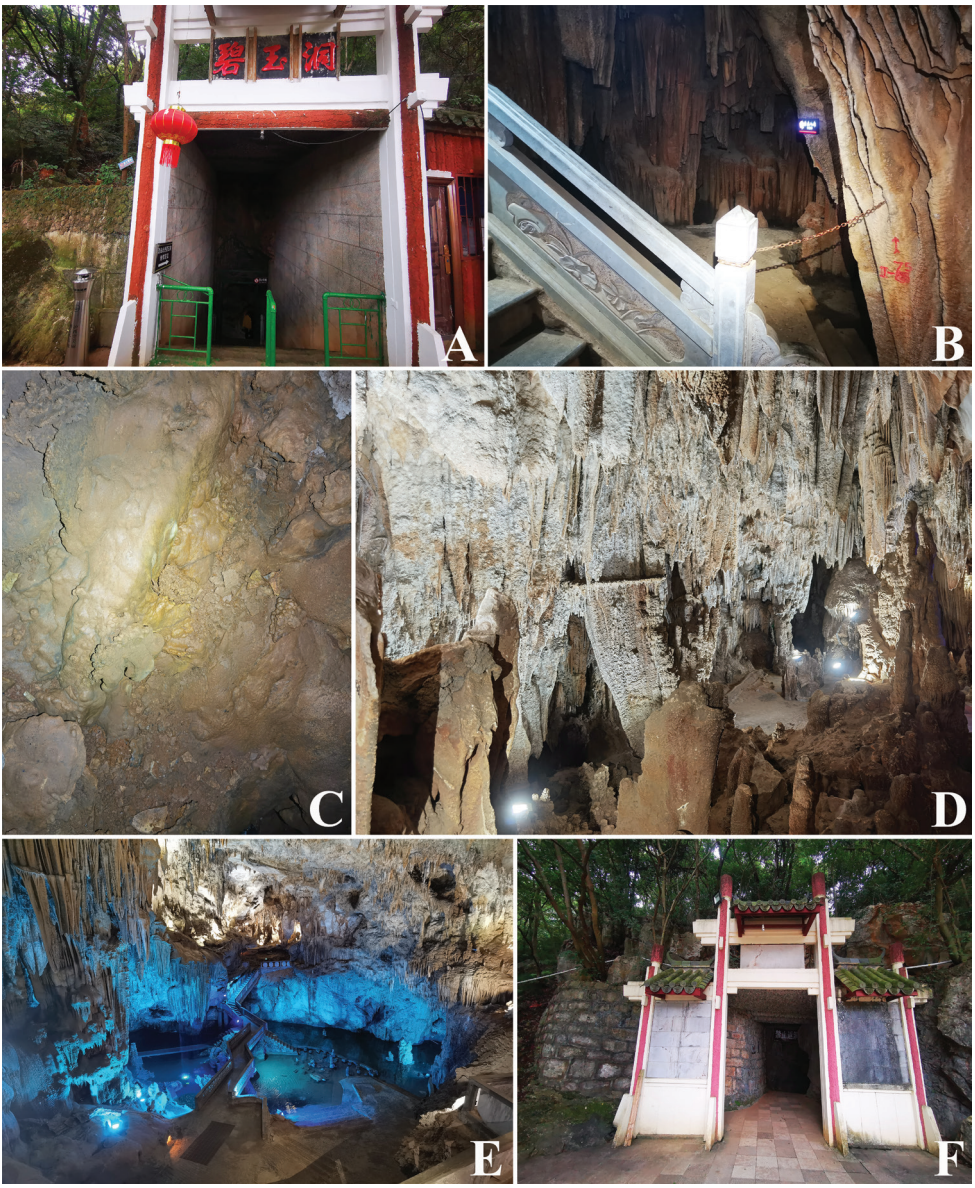

Figure 6. Biyu Cave, type locality of *Tyrannochthonius pandus* sp. nov. **A** entrance **B** access to an undeveloped area **C** area where *T. pandus* specimens were collected. **D, E** beautiful cave landscapes inside the cave **F** exit.

a valley type karst cave, with an internal height of 2 to 5 m and a width of 1 to 30 m. The cave has a latticed distribution. The stalactites in this cave are jasper colored, so it is called Biyu Cave (a quote from the cave's interior slogan). The specimens of this new species were collected from under a stone and on a stone wall in an undeveloped area

of the cave that is still in a natural condition. It is a small, dark, high humidity and low temperature space (temperature: 11 °C, humidity: 90%), which is suitable for the survival of the species.

Lagynochthonius Beier, 1951

Type species. *Chthonius johni* Redikorzev, 1922b, by original designation.

Diagnosis. See Judson (2007) and Edward and Harvey (2008).

Lagynochthonius laoxueyanensis sp. nov.

http://zoobank.org/4BD3052B-5217-4D93-B6FF-77DA99011228
Chinese name. 老穴岩拉伪蝎
Figs 7–10

Type material. (Figs 1B, 11) ***Holotype*:** China • ♂; Yunnan Province, Yanshan County, Zhela Township, Liuzhao Village, Laoxueyan Cave; 23°39.03'N, 104°35.74'E; 1665 m a.s.l.; 17 Oct. 2021; Zegang Feng, Yanmeng Hou, Lu Zhang and Liu Fu leg.; dark zone; Ps.-**MHBU**-HBUARA#2021-445-01. ***Paratypes*:** • 2♀; the same data as the holotype; Ps.-**MHBU**-HBUARA#2021-445-02, Ps.-**MSWU**-HBUARA#2021-445-03.

Diagnosis. Moderately sized troglomorphic species with elongate appendages; carapace without eyes or eyespots; anterior margin of carapace thin, finely denticulate, epistome pointed and small, triangular; posterior margin of carapace with two setae; tergites I–II with two setae. Pedipalps slender, femur 8.54 times longer than broad; chela 7.71 times longer than broad; chela fingers gently curved in dorsal view and fixed finger with a modified accessory tooth on dorso-antiaxial face (*td*).

Etymology. Latinized adjective derived from the name of the type locality, Laoxueyan Cave, Yunnan Province, China.

Description. Adult male (Figs 8A, 9A–D, 10). ***Color*:** generally pale yellow, chelicera, pedipalps and tergites slightly darker, soft parts pale (Fig. 8A). ***Cephalothorax*** (Figs 9B, 10A): carapace 1.02 times longer than broad, gently narrowed posteriorly, surface smooth, without furrows but with 1 small lyrifissure; anterior margin thin, finely denticulate; without any traces of eyes; epistome very pointed and small, triangular; with 18 setae arranged s4s: 4: 4: 2: 2, most setae heavy, long and gently curved, anterolateral setae much shorter than others (Fig. 10A). Chaetotaxy of coxae: P 3, I 3, II 4, III 5, IV 5; manducatory process with two acuminate distal setae, anterior seta less than 1/3 length of medial seta; apex of coxa I with small, rounded anteromedial process; coxae II with 9 terminally indented coxal spines on each side, set as an oblique row, longer spines present in the middle of the row, becoming shorter distally and proximally and incised for about half their length (Fig. 10C); intercoxal tubercle absent; without sub-oral seta. ***Chelicera*** (Figs 9C, 10B): large, about same length as carapace, 2.37 times longer than broad; 5 setae on hand, all setae acuminate,

Figure 7. *Lagynochthonius laoxueyanensis* sp. nov., female habitus. Photographed when it crawled on stony natural habitat.

ventrobasal seta shorter than others; movable finger with one medial seta. Cheliceral palm with moderate hispid granulation both ventral and dorsal side. Both fingers well provided with teeth, fixed finger with 12 teeth, distal one largest; movable finger with 10 retrorse continuous small teeth; galea weakly raised, keel-like (Fig. 10B). Rallum with 8 blades, the distal one longest and recumbent basally, with fine barbules and slightly set apart from the other blades, latter tightly grouped and with long pinnae, some of which are subdivided (Fig. 10D). ***Pedipalp*** (Figs 9A, 10E–G): surface of palpal segments smooth; chelal palm gradually constricted towards fingers; setae generally long and acuminate; femur 8.54, patella 2.73, chela 7.71, hand 3.10 times longer than broad; movable finger 1.45 times longer than hand and 0.58 times longer than chela, apodeme complex of movable finger strongly sclerotized. Femur and dorsal hand without tactile setae but with 1 lyrifissure distally at patella (Fig. 10E). Fixed chelal finger and hand with 8 trichobothria, movable chelal finger with 4 trichobothria, *ib* and *isb* situated close together, submedially on dorsum of chelal hand; *eb*, *esb* and *ist* forming a straight oblique row at base of fixed chelal finger; *it* slightly distal to *est*, situated subdistally; *et* slightly near to tip of fixed finger, very close to chelal teeth; *dx* situated

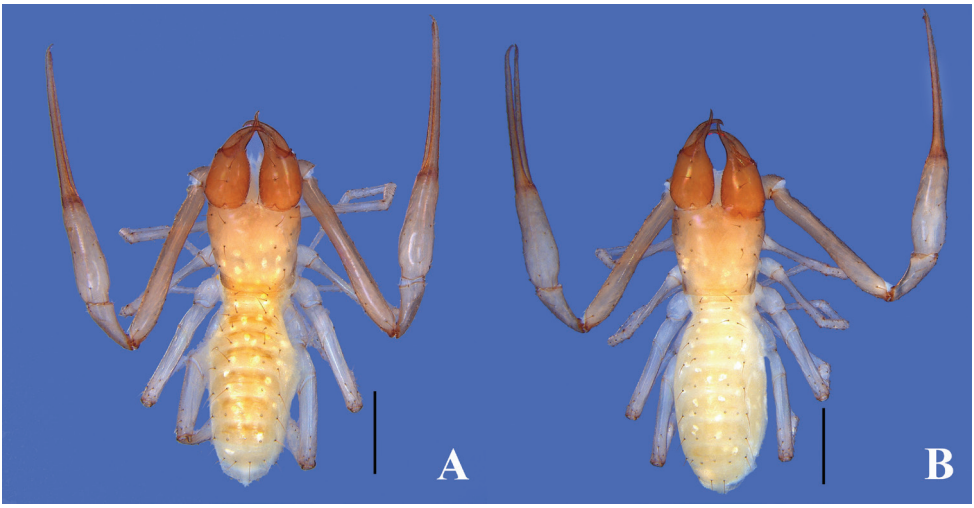

Figure 8. *Lagynochthonius laoxueyanensis* sp. nov. **A** holotype male, dorsal view **B** paratype female, dorsal view. Scale bars: 0.5 mm.

distal to *et*; *sb* situated closer to *st* than to *b*; *b* and *t* situated subdistally, *b* situated at same level as *est*; *t* situated distal to *est* and at same level as *it* (Fig. 10F). Microsetae (chemosensory setae) absent on hand and both chelal fingers. Sensilla absent but with 1 lyrifissure between *t* and *b*, *it* and *est*, respectively (Fig. 10G). Both chelal fingers with a row of teeth, homodentate, spaced regularly along the margin, larger teeth present in the middle of the row, becoming smaller distally and proximally: fixed finger with 24 large, erect, well-spaced teeth, without intercalary teeth; movable finger with 10 small (slightly smaller than the teeth on fixed finger), retrorse, serrated and well-spaced teeth; fixed finger also with a modified accessory tooth on dorso-antiaxial face (*td*) (Fig. 10F, G). Chelal fingers gently curved in dorsal view. ***Opisthosoma*:** generally typical; pleural membrane finely granulate. Tergites and sternites undivided; setae uniseriate and acuminate. Tergal chaetotaxy I–XII: 2: 2: 4: 4: 4: 4: 4: 5: 5: 4: T2T: 0; tergites VIII and IX each with an unpaired median seta. Sternal chaetotaxy IV–XII: 13: 11: 9: 9: 9: 9: 9: 0: 2; sternites IV–X with unpaired median seta. Anterior genital operculum with 9 setae, genital opening slit-like, with 15 marginal setae on each side (Fig. 9D). ***Legs*** (Fig. 10H, I): generally typical, long and slender. Fine granulation present on anterodorsal faces of trochanter IV and patella IV. Femur of leg I 1.88 times longer than patella and with 1 lyrifissure at the base of femur; tarsus 2.23 times longer than tibia. Femoropatella of leg IV 3.76 times longer than deep; tibia 6.33 times longer than deep; with tactile setae on both tarsal segments: basitarsus 3.57 times longer than deep, with basal tactile setae (TS = 0.24), telotarsus 12.80 times longer than deep and 2.56 times longer than basitarsus (TS = 0.41). Setae of leg I (trochanter to tibia) 3: 11: 11: 14, setae of leg IV (trochanter to basitarsus) 2: 3: 6: 14: 10. Arolium slightly shorter than the claws, not divided; claws simple. ***Dimensions of male holotype*** (length/width or, in the case of the legs, length/depth in mm; ratios in parentheses). Body

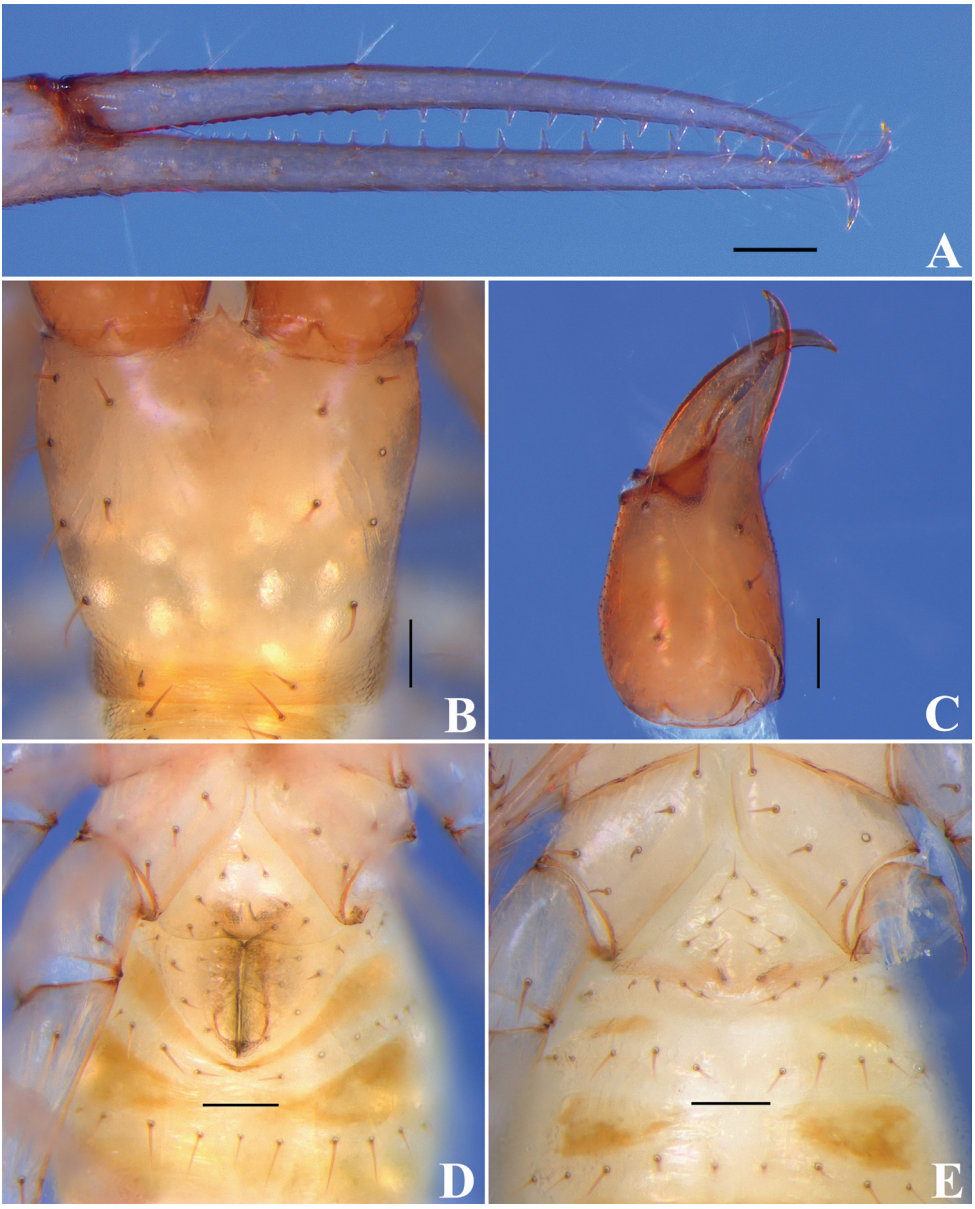

Figure 9. *Lagynochthonius laoxueyanensis* sp. nov., holotype male (**A–D**), paratype female (**E**) **A** chelal fingers (lateral view) **B** carapace (dorsal view) **C** left chelicera (dorsal view) **D** male genital area (ventral view) **E** female genital area (ventral view). Scale bars: 0.1 mm.

length 1.78. Pedipalps: trochanter 0.29/0.16 (1.81), femur 1.11/0.13 (8.54), patella 0.41/0.15 (2.73), chela 1.62/0.21 (7.71), hand length 0.65/0.21 (3.10), movable finger length 0.94. Chelicera 0.64/0.27 (2.37), movable finger length 0.34. Carapace 0.59/0.58 (1.02). Leg I: trochanter 0.17/0.11 (1.55), femur 0.60/0.07 (8.57), patella

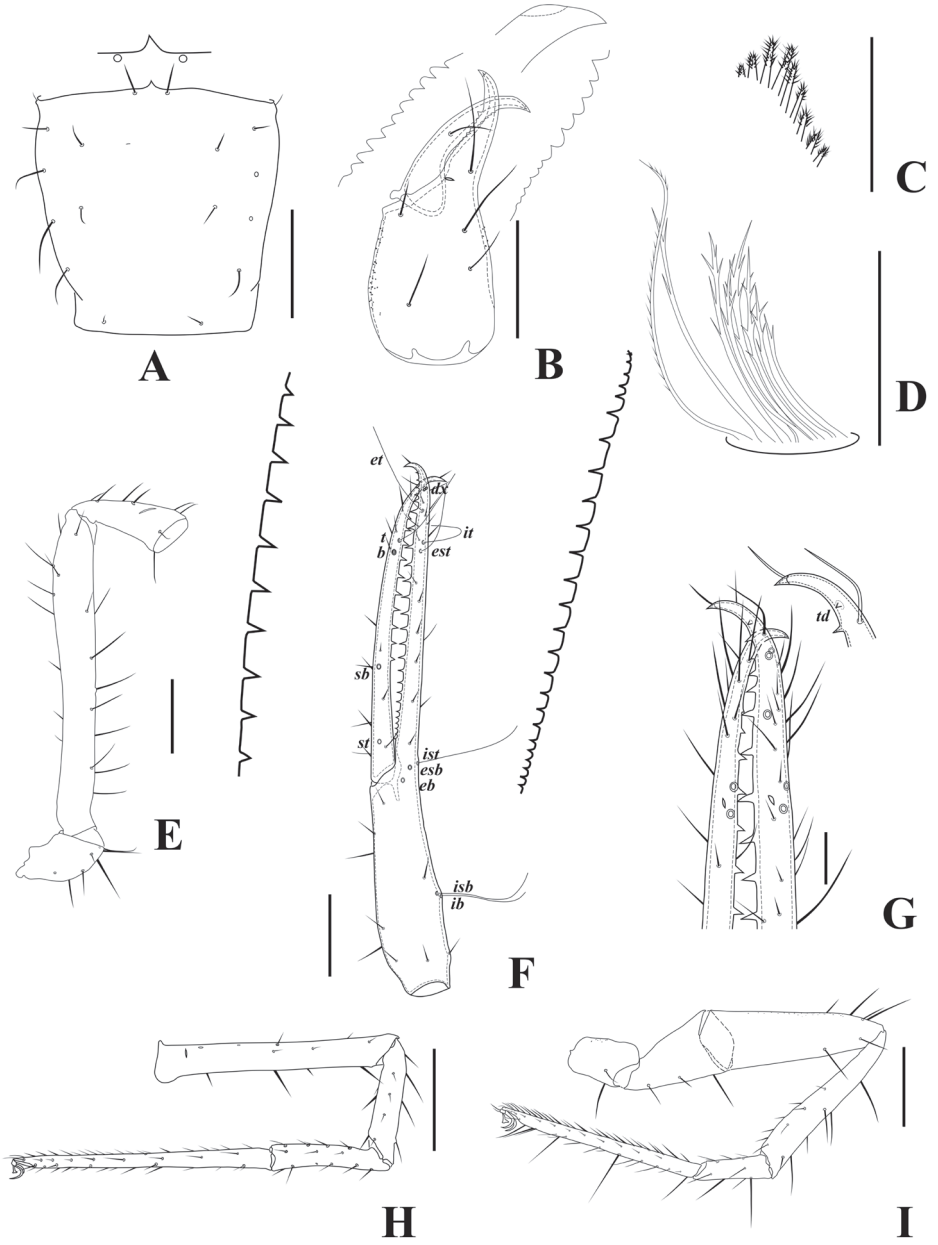

Figure 10. *Lagynochthonius laoxueyanensis* sp. nov., holotype male **A** carapace (dorsal view) with a detail of anterior margin **B** left chelicera (dorsal view) with details of teeth and tip of movable finger **C** coxal spines on coxae II (ventral view) **D** rallum **E** left pedipalp (minus chela, dorsal view) **F** left chela (lateral view) with details of teeth and with trichobothrial pattern (abbreviations explained in Material and methods) **G** finger tips of chela (lateral view) with detail of modified tooth **H** leg I without trochanter (lateral view) **I** leg IV (lateral view). Scale bars: 0.25 mm (**A, B, E, F, H, I**); 0.10 mm (**C, D, G**).

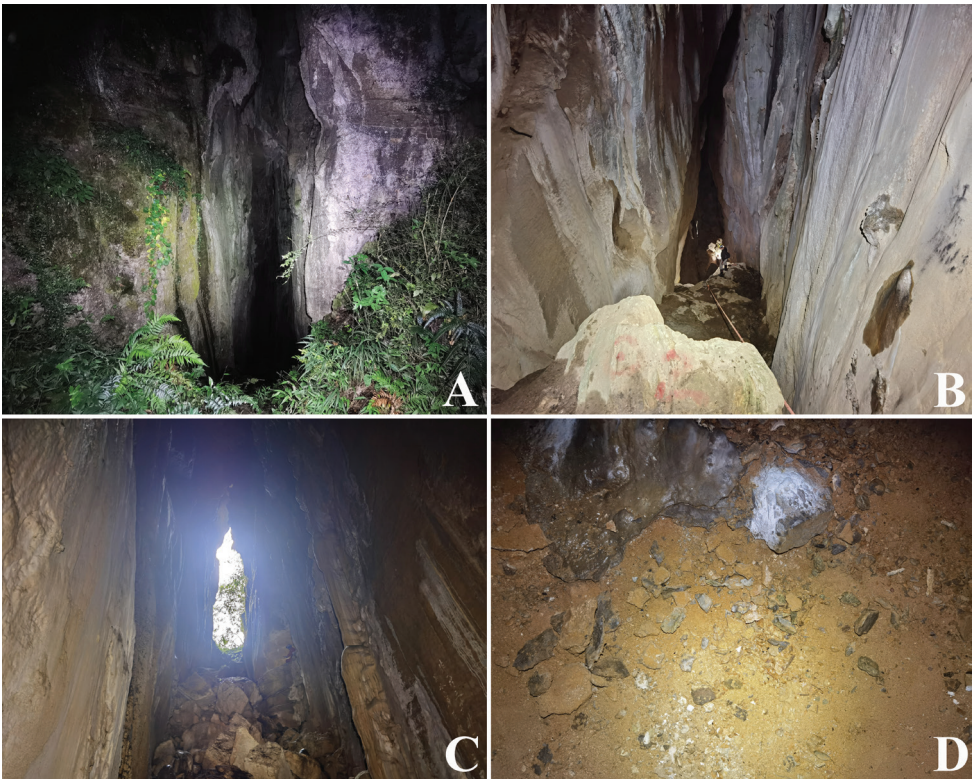

Figure 11. Laoxueyan Cave, type locality of *Lagynochthonius laoxueyanensis* sp. nov. **A** entrance **B** the only access to the deepest part of the cave **C** inside the cave entrance **D** area where *L. laoxueyanensis* specimens were collected.

0.32/0.07 (4.57), tibia 0.30/0.05 (6.00), tarsus 0.67/0.04 (16.75). Leg IV: trochanter 0.21/0.14 (1.50), femoropatella 0.79/0.21 (3.76), tibia 0.57/0.09 (6.33), basitarsus 0.25/0.07 (3.57), telotarsus 0.64/0.05 (12.80).

Adult females (Figs 7, 8B, 9E). Mostly same as males. Anterior genital operculum with 9 setae plus 10–12 setae on posterior margin. Body length 2.00–2.05. Pedipalps: trochanter 0.30–0.32/0.17–0.18 (1.76–1.78), femur 1.17/0.14–0.15 (7.80–8.36), patella 0.40–0.41/0.17 (2.35–2.41), chela 1.65–1.66/0.23–0.24 (6.88–7.22), hand length 0.66–0.70/0.23–0.24 (2.75–3.04), movable finger length 0.95–0.98. Chelicera 0.68–0.70/0.29–0.30 (2.33–2.34), movable finger length 0.36–0.37. Carapace 0.62/0.61 (1.02). Leg I: trochanter 0.18–0.20/0.13 (1.38–1.54), femur 0.61/0.07 (8.71), patella 0.32–0.33/0.07 (4.57–4.71), tibia 0.30/0.06 (5.00), tarsus 0.68–0.69/0.05 (13.60–13.80). Leg IV: trochanter 0.22–0.24/0.13–0.14 (1.69–1.71), femoropatella 0.81–0.82/0.21 (3.86–3.90), tibia 0.60–0.61/0.09–0.10 (6.10–6.67), basitarsus 0.26–0.27/0.06 (4.33–4.50), telotarsus 0.69/0.05 (13.80).

Remarks. Of all *Lagynochthonius* species found in hypogean environments around the world, only three species, *L. bailongtanensis* Li, Liu & Shi, 2019 (from China), *L. typhlus* Muchmore, 1991 (from Jamaica) and *L. curvidigitatus* Mahnert, 1997

(from Spain), have no eyes, and are all highly troglomorphic species. *Lagynochthonius laoxueyanensis* sp. nov. is most similar to *L. typhlus* in having only 2 setae on tergites I–II, but the latter has intercalary teeth on the chelal fingers and a smaller body size (1.28 vs. 2.00–2.05 mm in females). *Lagynochthonius laoxueyanensis* sp. nov. can be easily separated from *L. bailongtanensis* by its smaller body size (*L. laoxueyanensis* 1.78 mm in male, 2.00–2.05 mm in females; while *L. bailongtanensis* is 2.55–2.92 mm in males, 2.72–2.95 mm in females), the number of setae on the anterior tergites (tergites I–II with 2 setae in *L. laoxueyanensis*, but 4 in *L. bailongtanensis*), the shape of epistome (pointed and small in *L. laoxueyanensis*, but obtuse and inconspicuous in *L. bailongtanensis*) and the number of setae on the pedipalpal coxa (3 setae in *L. laoxueyanensis*, but 5 in *L. bailongtanensis*). *Lagynochthonius laoxueyanensis* sp. nov. can be easily separated from *L. curvidigitatus* by the presence of a pair of curved chelal fingers in the latter and the number of setae on tergites I–II (*L. laoxueyanensis* with 2 and 2 setae, respectively, but *L. curvidigitatus* with 3 and 4 setae, respectively) (Muchmore 1991; Mahnert 1997; Edward and Harvey 2008; Mahnert 2011; Li et al. 2019).

Distribution. This species is only known from the type locality, Laoxueyan Cave (Figs 1B, 11) which is located about 4 km southeast of Liuzhao Village (Yanshan County). The entrance of the cave is slit-shaped (18 m high and 4 m wide), and the total length of the cave is 88.5 m, and the vertical height of the cave is about 30 m. A descent access leads to the bottom of the cave. The bottom of the cave is a large space, covered with gravel, temperature around 13 °C, humidity over 90%. All of the specimens were collected from ground crevices near the end of the cave.

Acknowledgements

We thank the Ancient Alu Cave National Park of China staff for their support. We are grateful to Zegang Feng, Lu Zhang and Liu Fu for their assistance in the field, to Ms Angela Xuanyu Lin for revising the language, and to Dr. Jana Christophoryová and two reviewers, Dr. Mark S. Harvey and Dr. Katarína Krajčovičová, for their helpful suggestions that greatly improved this paper. This work was supported by the National Natural Science Foundation of China (No. 31872198), and the Natural Science Foundation of Hebei Province (No. C2021201030).

References

Beier M (1951) Die Pseudoscorpione Indochinas. Mémoires du Muséum National d'Histoire Naturelle, Paris, nouvelle série 1: 47–123.

Chamberlin JC (1931) The arachnid order Chelonethida. Stanford University Publications. Biological Sciences 7(1): 1–284.

Chamberlin JC (1962) New and little-known false scorpions, principally from caves, belonging to the families Chthoniidae and Neobisiidae (Arachnida, Chelonethida). Bulletin of the American Museum of Natural History 123: 303–352.

Edward KL, Harvey MS (2008) Short-range endemism in hypogean environments: the pseudoscorpion genera *Tyrannochthonius* and *Lagynochthonius* (Pseudoscorpiones: Chthoniidae) in the semiarid zone of Western Australia. Invertebrate Systematics 22(2): 259–293. https://doi.org/10.1071/IS07025

Feng ZG, Wynne JJ, Zhang F (2020) Cave-dwelling pseudoscorpions of China with descriptions of four new hypogean species of Parobisium (Pseudoscorpiones, Neobisiidae) from Guizhou Province. Subterranean Biology 34: 61–98. https://doi.org/10.3897/subtbiol.34.49586

Gao ZZ, Chen HM, Zhang F (2017) Description of two new cave-dwelling Bisetocreagris species (Pseudoscorpiones: Neobisiidae) from China. Turkish Journal of Zoology 41: 615–623. https://doi.org/10.3906/zoo-1602-39

Gao ZZ, Wynne JJ, Zhang F (2018) Two new species of cave-adapted pseudoscorpions (Pseudoscorpiones: Neobisiidae, Chthoniidae) from Guangxi, China. The Journal of Arachnology 46(2): 345–354. https://doi.org/10.1636/JoA-S-17-063.1

Gao ZZ, Zhang F, Chen HM (2020) Two new cave-dwelling species of *Tyrannochthonius* Chamberlin 1929 (Pseudoscorpiones: Chthoniidae) from the Guizhou karst, China. Zootaxa 4853(4): 572–580. https://doi.org/10.11646/zootaxa.4853.4.6

Harvey MS (1989) Two new cavernicolous chthoniids from Australia, with notes on the generic placement of the south-western Pacific species attributed to the genera *Paraliochthonius* Beier and Morikawia Chamberlin (Pseudoscorpionida: Chthoniidae). Bulletin - British Arachnological Society 8: 21–29.

Harvey MS (1992) The phylogeny and classification of the Pseudoscorpionida (Chelicerata: Arachnida). Invertebrate Taxonomy 6(6): 1373–1435. https://doi.org/10.1071/IT9921373

Judson MLI (2007) A new and endangered species of the pseudoscorpion genus *Lagynochthonius* from a cave in Vietnam, with notes on chelal morphology and the composition of the Tyrannochthoniini (Arachnida, Chelonethi, Chthoniidae). Zootaxa 1627(1): 53–68. https://doi.org/10.11646/zootaxa.1627.1.4

Latella L (2019) Biodiversity: China. In: White WB, Culver DC, Pipan T (Eds) Encyclopedia of Caves (3rd edn.). Academic Press, Amsterdam, 127–135. https://doi.org/10.1016/B978-0-12-814124-3.00016-9

Li YC, Shi AM, Liu H (2017) A new cave-dwelling species of Bisetocreagris Ćurčić (Arachnida, Pseudoscorpiones: Neobisiidae) from Yunnan Province, China. Entomologica Fennica 28(4): 212–218. https://doi.org/10.33338/ef.84688

Li YC, Liu H, Shi AM (2019) A new cave-dwelling species of *Lagynochthonius* (Arachnida: Pseudoscorpiones: Chthoniidae) from Yunnan Province, China. Zootaxa 4571(1): 28–34. https://doi.org/10.11646/zootaxa.4571.1.2

Mahnert V (1997) New species and records of pseudoscorpions (Arachnida, Pseudoscorpiones) from the Canary Islands. Revue Suisse de Zoologie 104: 559–585. https://doi.org/10.5962/bhl.part.80011

Mahnert V (2003) Four new species of pseudoscorpions (Arachnida, Pseudoscorpiones: Neobisiidae, Chernetidae) from caves in Yunnan Province, China. Revue Suisse de Zoologie 110: 739–748. https://doi.org/10.5962/bhl.part.80209

Mahnert V (2009) New species of pseudoscorpions (Arachnida, Pseudoscorpiones, Chthoniidae, Chernetidae) from caves in China. Revue Suisse de Zoologie 116(2): 185–201. https://doi.org/10.5962/bhl.part.79492

Mahnert V (2011) A nature's treasury: Pseudoscorpion diversity of the Canary Islands, with the description of nine new species (Pseudoscorpiones, Chthoniidae, Cheiridiidae) and new records. Revista Iberica de Aracnologia 19: 27–45.

Mahnert V, Li YC (2016) Cave-inhabiting Neobisiidae (Arachnida: Pseudoscorpiones) from China, with description of four new species of Bisetocreagris Ćurčić. Revue Suisse de Zoologie 123: 259–268.

Muchmore WB (1984) Pseudoscorpions from Florida and the Caribbean area. 13. New species of *Tyrannochthonius* and *Paraliochthonius* from the Bahamas, with discussion of the genera (Chthoniidae). The Florida Entomologist 67(1): 119–126. https://doi.org/10.2307/3494110

Muchmore WB (1991) Pseudoscorpions from Florida and the Caribbean area. 14. New species of *Tyrannochthonius* and *Lagynochthonius* from caves in Jamacia [sic], with discussion of the genera (Chthoniidae). The Florida Entomologist 74(1): 110–121. https://doi.org/10.2307/3495247

Muchmore WB, Chamberlin JC (1995) The genus *Tyrannochthonius* in the eastern United States (Pseudoscorpionida: Chthoniidae). Part 1. The historical taxa. Insecta Mundi 9: 249–257.

Schawaller W (1995) Review of the pseudoscorpion fauna of China (Arachnida: Pseudoscorpionida). Revue Suisse de Zoologie 102(4): 1045–1063. https://doi.org/10.5962/bhl.part.80489

Wang Y (2001) Analysis and Evaluation of Development and Utilization Conditions of Karst Water in Yunnan Province. Journal of Hydraulic Engineering 1: 49–52. [in Chinese]

WPC (2022) World Pseudoscorpiones Catalog. Natural History Museum Bern. https://wac.nmbe.ch/order/pseudoscorpiones/3 [Accessed on 20.03.2022]

Zhang C, Feng ZG, Zhang F (2020) Two new cave-dwelling pseudoscorpions (Pseudoscorpiones: Neobisiidae: Parobisium) from Yunnan, China. Zootaxa 4834(1): 107–120. https://doi.org/10.11646/zootaxa.4834.1.7

Zhao WJ, Zhang J, Xiu JF (2015) General situation of cave animals in China. Chinese Journal of Traditional Veterinary Science 11: 69–70. [in Chinese]

ZooKeys 1097: 85–101 (2022)
doi: 10.3897/zookeys.1097.80424
https://zookeys.pensoft.net

RESEARCH ARTICLE

A peer-reviewed open-access journal
ZooKeys
Launched to accelerate biodiversity research

Factors related to species richness, endemism, and conservation status of the herpetofauna (Amphibia and Reptilia) of Mexican states

Geoffrey R. Smith[1], Julio A. Lemos-Espinal[2]

1 *Department of Biology, Denison University, Granville, Ohio 43023, USA* **2** *Laboratorio de Ecología-UBIPRO, FES Iztacala UNAM, Avenida los Barrios 1, Los Reyes Iztacala, Tlalnepantla, edo. de México, 54090, Mexico*

Corresponding author: Julio A. Lemos-Espinal (lemos@unam.mx)

Academic editor: Uri García-Vázquez | Received 11 January 2022 | Accepted 25 March 2022 | Published 20 April 2022

http://zoobank.org/F5971CDD-537B-46FB-ACB6-5DBD7B8C788B

Citation: Smith GR, Lemos-Espinal JA (2022) Factors related to species richness, endemism, and conservation status of the herpetofauna (Amphibia and Reptilia) of Mexican states. ZooKeys 1097: 85–101. https://doi.org/10.3897/zookeys.1097.80424

Abstract

Mexico is a megadiverse country with high endemicity in its herpetofauna. We examine how species richness, proportion of state and country endemic species, and proportion of species in a category of conservation concern using listings in the International Union for Conservation of Nature (IUCN) Red List and the Secretaría del Medio Ambiente y Recursos Naturales (SEMARNAT) in 27 of 32 Mexican states are related to environmental and human demographic and socioeconomic variables. Amphibian and reptile species richness were positively related to latitude range and number of physiographic regions and negatively related to latitude. The proportion of state endemic amphibian species in a state was negatively related to latitude whereas no variables influenced the proportion in reptiles. The proportion of country endemics in a state was positively related to human population density and the number of physiographic regions and negatively related to per capita gross domestic product (GDP) and latitude range for amphibians; it was positively related to human population density and elevation range and negatively related to latitude range for reptiles. The proportion of amphibian species in an IUCN category of concern in a state was positively related to human population density and negatively related to latitude; for reptiles, it was negatively related to human population density. The proportion of SEMARNAT-listed species in a state was positively related to human population density for both amphibians and reptiles and negatively related to latitude range for amphibians. Our analyses found that larger macroecological patterns (e.g., latitudinal species gradient, heterogeneity-richness relationships) and human population density play important roles in determining the richness and conservation status of Mexican amphibians and reptiles.

Copyright *Geoffrey R. Smith & Julio A. Lemos-Espinal*. This is an open access article distributed under the terms of the Creative Commons Attribution License (CC BY 4.0), which permits unrestricted use, distribution, and reproduction in any medium, provided the original author and source are credited.

Keywords
amphibians, environmental factors, human demographic factors, IUCN status, reptiles, SEMARNAT listing, socioeconomic factors

Introduction

Much of Mexico consists of a transition zone (i.e., the Mexican Transition Zone) between the Nearctic and Neotropical zones (Villaseñor et al. 2020). As a consequence, Mexico has one of the highest levels of biodiversity of any country in the world (Morrone 2019), including amphibian and reptile richness (Wilson and Johnson 2010; Chen and Peng 2017). Mexico also has a high level of endemicity in its herpetofauna (Wilson and Johnson 2010; see also Murali et al. 2021).

Unfortunately, Mexico is not immune to global environmental decline. Indeed, Mexico is an area with high extinction debt and risk for amphibians and reptiles (Chen and Peng 2017). In addition, Mexico is one of the countries where the decline in the conservation status of amphibians is greatest (Rodrigues et al. 2014) and has a high proportion (ca 80%) of species of amphibians showing population declines (Becker and Loyola 2008). The biodiversity of Mexico is subject to a variety of pressures, such as climate change, land use change (including agriculture and livestock, mining, deforestation, and urbanization), invasive species, disease, exploitation, and pollution (Rodrigues et al. 2014; Lazcano et al. 2019; Ramírez-Bautista et al. 2020; González-Sánchez et al. 2021; Masés-García et al. 2021), which are the consequence of human demographic changes (e.g., population growth), socioeconomics, and governmental actions (Challenger et al. 2009; Sarukhán et al. 2015).

Human pressure on biodiversity has increased in the Neotropics (Geldmann et al. 2014). More specifically, mean annual temperatures in Mexico have increased around 0.2 °C from 1970–2000, with greater increases in northern Mexico than in southern Mexico (see also Pavia et al. 2009; Cuervo-Robayo et al. 2020). This climate change has driven changes in the vegetation and distribution of habitats, especially in the mountains of Mexico (Téllez-Valdés et al. 2006; Gómez-Mendoza and Arriaga 2007; Jiménez-García et al. 2021), and continued climate change is likely to result in the loss of suitable habitat in the future (Chacón-Prieto et al. 2021). Parts of Mexico are also undergoing rapid land use change through burning, human settlement, and conversion to agriculture, with extensive loss of forest, including in protected areas (Lorenzo et al. 2017; Hu et al. 2021). Habitat loss has impacted several species of terrestrial vertebrates in Mexico, especially endemic species in the Transvolcanic Mexican Belt, Mexican High Plateau, and the Humid Coastal Plains and Hills of the Gulf of Mexico, and the effects appear to be cumulative (i.e., not just recent habitat loss) (Mayani-Parás et al. 2021). The loss of habitat, and in particular forest habitats, has negatively affected the amphibians and reptiles of Mexico (Lara-Tufiño et al. 2019; Mayani-Parás et al. 2019), and a high proportion of endangered amphibians in Mexico are found in areas that have experienced transformation to agriculture or urbanization (Londoño-Murcia

and Sánchez-Cordero 2011) and these trends are likely to continue or increase in the future (Mendoza-Ponce et al. 2020).

Here we examine the distribution of amphibian and reptile species richness among 27 of 32 Mexican states. In particular, we examine relationships between species richness, proportion of state and country endemic species (i.e., the proportion of the species in a state that are state or country endemics), and proportion of a state's amphibian or reptile species in a category of conservation concern using the Interational Union for Conservation of Nature (IUCN) Red List (i.e., vulnerable, threatened, endangered, critically endangered, near extinction), and the proportion of a state's amphibian or reptile species listed in Secretaría del Medio Ambiente y Recursos Naturales (SEMARNAT) (2019) with environmental variables (state area, proportion of land protected, latitude, latitude range, elevation range, and number of physiographic regions) and human demographic and socioeconomic variables [human population, human population density, and per capita gross domestic product (GDP)].

Methods

We collected species lists for amphibians and reptiles of Mexican states from the available literature and updated these species lists using additional literature through November 2020 (see Suppl. material 1: Table S1 for sources used for base species lists and updates). We generally followed Frost (2020) and AmphibiaWeb (2020) for amphibian taxonomy and Uetz and Hošek (2019) for reptile species. We were able to compile updated species lists for 27 of the 32 Mexican federal entities (i.e., states), with the five remaining states lacking published updated species checklists (Suppl. material 2: Table S2). We include Mexico City (formerly known as Mexico, Distrito Federal) that comprises the urban area of Mexico City proper to the south and mountains and valleys with fragmented forests and grasslands to the north. For each species in our list, we obtained their global conservation status from the IUCN Red List version 2021-3 (https//:www.iucnredlist.org) and their Mexican conservation status from SEMARNAT (2019) (Suppl. material 2: Table S2). From these lists we gathered the following information for each state: species richness, proportion of state and country endemics, proportion of species in an IUCN category of concern (critically endangered, endangered, threatened, near threatened, and vulnerable), and the proportion of SEMARNAT-listed species under the categories of threatened and endangered for amphibians and reptiles separately (Table 1). For each state we collected data on human demographic and socioeconomic variables (human population, human population density, and per capita GDP) and geographic and climatic variables [state area, proportion of land protected, latitude (midpoint of state), latitude range (difference between minimum and maximum latitude), elevation range (difference between minimum and maximum elevations), and number of physiographic regions] (Table 2).

We used generalized linear models (Normal distribution, Identity link) for amphibians and reptiles separately to examine the relationships of the human demographic

Table 1. Amphibians and reptile species richness, proportion of species in a state that are state and country endemics, proportion of species that are in an IUCN category of concern, and the proportion of species that are SEMARNAT listed for Mexican states.

State	Amphibians					Reptiles				
	Species Richness	Prop. State Endemic	Prop. Country Endemic	Prop. IUCN	Prop. SEMARNAT	Species Richness	Prop. State Endemic	Prop. Country Endemic	Prop. IUCN	Prop. SEMARNAT
Aguascalientes	19	0	0.68	0.16	0.16	65	0	0.54	0.05	0.15
Baja California	17	0	0	0.29	0.06	103	0.23	0.32	0.21	0.23
Baja California Sur	3	0	0	0	0	84	0.44	0.57	0.13	0.32
Campeche	24	0	0.04	0	0	103	0	0.12	0.13	0.16
Chiapas	108	0.10	0.21	0.53	0.04	219	0.06	0.18	0.11	0.16
Chihuahua	37	0.03	0.35	0.11	0.03	140	0.01	0.33	0.06	0.15
Coahuila	24	0	0.25	0.17	0.04	117	0.06	0.30	0.15	0.22
Colima	39	0.03	0.68	0.13	0.08	117	0.04	0.66	0.11	0.18
Durango	36	0	0.6	0.11	0.03	119	0.02	0.45	0.05	0.18
Guerrero	78	0.32	0.76	0.45	0.11	181	0.15	0.68	0.08	0.16
Hidalgo	52	0.08	0.65	0.46	0.15	126	0.01	0.49	0.10	0.18
Jalisco	55	0.06	0.72	0.22	0.07	173	0.01	0.66	0.10	0.17
Mexico	49	0.08	0.77	0.42	0.21	99	0.01	0.71	0.08	0.17
Mexico City	18	0.11	0.83	0.5	0.39	45	0	0.76	0.04	0.22
Michoacán	58	0.09	0.74	0.26	0.09	161	0	0.7	0.09	0.18
Morelos	38	0	0.70	0.27	0.14	97	0	0.68	0.04	0.17
Nayarit	37	0	0.6	0.08	0.03	117	0.01	0.60	0.07	0.14
Nuevo León	25	0	0.32	0.2	0.04	119	0.02	0.34	0.09	0.20
Oaxaca	152	0.39	0.69	0.60	0.10	299	0.11	0.55	0.11	0.18
Puebla	92	0.03	0.7	0.49	0.16	176	0.02	0.61	0.07	0.14
Querétaro	34	0.60	0.56	0.32	0.12	104	0.02	0.49	0.07	0.18
Quintano Roo	23	0	0.09	0.04	0	108	0.01	0.12	0.12	0.16
San Luis Potosí	42	0	0.41	0.34	0.12	138	0	0.41	0.09	0.17
Sinaloa	39	0	0.55	0.13	0	119	0.01	0.51	0.10	0.14
Sonora	36	0	0.39	0.11	0.03	159	0.10	0.37	0.13	0.18
Tamaulipas	44	0.11	0.41	0.27	0.14	137	0.04	0.34	0.11	0.21
Yucatán	17	0	0.12	0.06	0	85	0	0.12	0.12	0.18

and socioeconomic variables and the geographic and climatic variables and species richness, proportion of country endemics, proportion of state endemics, proportion of species in an IUCN category of concern, and proportion SEMARNAT-listed species. We used JMP Pro 15.1 (SAS Institute, Cary, NC). for statistical analyses.

Results

Amphibian species richness was positively related to latitude range and number of physiographic regions and negatively related to latitude (Table 3; Fig. 1A-C). The proportion of state endemics was negatively related to latitude (Table 3; Fig. 1D). The proportion of country endemics was positively related to human population density and the number of physiographic region and negatively related to per capita GDP and latitude range (Table 3; Fig.1E-H). The proportion of amphibian species in an IUCN category of concern was positively related to human population density and negatively

Table 2. Human demographic and socioeconomic variables and environmental variables for Mexican states.

State	State Area (km^2)[1]	Human Population (2018)[1]	Human Population Density (N/km^2)[1]	Per capita GDP (US$)[2]	Proportion Protected Territory[3]	GPS Coordinates[1] (°)	Elevation Range (m)[1]	Number of Physiographic Regions[4]
Aguascalientes	5618	1.337,792	238.1	9975	26.0	22.1243, 1.0042	1666	3
Baja California	71.450	3.633,772	50.9	9449	19.0	30.3593, 4.7186	3100	2
Baja California Sur	73.909	832.827	11.3	11.060	42.0	25.4360, 5.1280	2080	1
Campeche	57.507	948.459	16.5	51.460	39.6	19.6167, 0.7667	390	2
Chiapas	73.311	5.445,233	74.3	3592	18.0	17.2588, 5.4530	4080	3
Chihuahua	247.460	3.816,865	15.4	8833	8.1	28.6843, 6.4175	3050	2
Coahuila	151.595	3.063,662	20.2	12.838	19.0	27.2114, 5.3372	3380	3
Colima	5627	759.686	135	9177	6.6	19.0983, 0.8283	3820	2
Durango	123.317	1.815,966	14.5	7888	22.1	24.5950, 4.5000	3240	4
Guerrero	63.596	3.625,040	5.7	4586	0.15	17.6018, 2.5719	3550	2
Hidalgo	20.813	2.980,532	143.2	6508	6.9	20.4982, 1.8008	3251	3
Jalisco	78.588	8.197,483	104.3	9239	11.2	20.8380, 3.8244	4339	4
Mexico	22.500	17.604,619	782.4	6199	43.8	19.3264, 1.9189	5268	2
Mexico City	1495	8.788,141	5878.4	21.079	14.1	19.3206, 0.5444	1702	1
Michoacán	58.599	4.687,211	80	5522	5.9	19.1547, 2.4794	4100	2
Morelos	4879	1.987,596	407.4	6961	26.8	18.7319, 0.7994	4580	2
Nayarit	27.857	1.290,519	46.3	6220	30.8	21.8439, 2.4811	2760	4
Nuevo León	64.156	5.300,619	82.6	16.228	8.9	25.4810, 4.6364	3660	3
Oaxaca	93.757	4.084,674	43.6	4446	7.1	17.1635, 3.0125	3720	5
Puebla	34.306	6.371,381	185.7	5890	19.5	19.3500, 2.9667	5530	4
Querétaro	11.699	2.091,823	178.8	12.502	33.6	20.8425, 1.655	2600	3
Quintano Roo	50.212	1.709,479	34	11.381	32.6	19.7000, 3.7667	230	1
San Luis Potosí	61.137	2.824,976	46.2	8118	6.6	22.8258, 3.3311	3160	3
Sinaloa	58.328	3.059,322	52.5	8108	7.6	24.7547, 4.5750	2520	2
Sonora	179.355	3.050,473	17	11.543	10.3	29.3954, 6.1969	2620	4
Tamaulipas	80.249	3.661,162	45.5	9347	13.7	24.9430, 5.4722	3280	3
Yucatán	39.524	2.199,618	55.7	8.011	25.6	20.5667, 2.0667	210	1

[1]INEGI (2018)
[2]https://es.wikipedia.org/wiki/Anexo:Estadios_de_M%C3%A9xico_por_PIB_per_c%C3%A1pita
[3]http://sig.conanp.gob.mx/website/pagsig/listanp/
[4]https://www.monografias.com/trabajos100/regions-fisiograficas-mexico/regions-fisiograficas-mexico.shtml#llanurasoa

related to latitude (Table 3; Fig. 2A, B). The proportion of SEMARNAT-listed amphibian species was positively related to human population density and negatively related to latitude range (Table 3; Fig. 2C, D).

Reptile species richness was positively related to latitude range and the number of physiographic regions and negatively related to latitude and the proportion of land protected (Table 4; Fig. 3A-D). The proportion of state endemics of reptiles was not related to any variables (Table 4). The proportion of country endemic reptile species was positively related to human population density and elevation range and negatively related to latitude range (Table 4; Fig. 3E-G). The proportion of a state's reptile species in an IUCN category of concern was negatively related to human population density (Table 4; Fig. 3H). The proportion of a state's reptile species that are SEMARNAT listed was positively related to human population density (Table 4; Fig. 3I).

Table 3. Results of generalized linear models examining the relationship between human demographic and socioeconomic variables and environmental variables and species richness, proportion of species in a state that are state and country endemics, proportion of species that are in an IUCN category of concern, and the proportion of species that are SEMARNAT listed for amphibians in 27 Mexican states. Values on first line are coefficients, values on second line are *P*-values. Bolded entries are significant at α = 0.05.

Variable	Intercept	State area	Human population	Human population density	per capita GDP	Proportion Protected	Latitude	Latitude Range	Elevation range	Physiographic regions	Overall P
Species Richness	**153.03 < 0.0001**	0.00011 0.16	< 0.00001 0.63	-0.0010 0.725	-0.0002 0.18	-44.61 0.074	**-7.37 < 0.0001**	**5.91 0.043**	0.0025 0.39	**10.62 0.0006**	**< 0.0001**
Prop State endemic	**0.447 0.0003**	< 0.000001 0.17	<0.0000001 0.39	<0.000001 0.65	-<0.000001 0.49	-0.247 0.057	**-0.018 0.0009**	0.004 0.81	-<0.00001 0.52	0.013 0.36	**0.0108**
Prop Country endemic	**0.568 0.0046**	0.000001 0.10	<<0.000001 0.36	**0.000062 0.024**	**-0.0000010 0.004**	-0.41 0.066	0.00055 0.95	**-0.116 < 0.0001**	0.000047 0.078	**0.069 0.008**	**<0.0001**
Prop IUCN	**0.469 0.0065**	-<0.000001 0.35	<<0.000001 0.26	**0.000050 0.0336**	-0.0000016 0.55	-0.33 0.086	**-0.018 0.017**	0.022 0.30	0.000029 0.20	0.035 0.10	**0.0002**
Prop SEMARNAT	0.0045 0.93	-0.0000001 0.56	<<0.0000001 0.14	**0.000050 < 0.0001**	-0.0000012 0.19	-0.042 0.19	0.0034 0.18	**-0.018 0.016**	0.000012 0.12	0.0096 0.19	**<0.0001**

Table 4. Results of generalized linear models examining the relationship between human demographic and socioeconomic variables and environmental variables and species richness, proportion of species in a state that are state and country endemics, proportion of species that are in an IUCN category of concern, and the proportion of species that are SEMARNAT listed for reptiles in 27 Mexican states. Values on first line are coefficients, values on second line are *P*-values. Bolded entries are significant at α = 0.05.

Variable	Intercept	State area	Human population	Human population density	per capita GDP	Proportion protected	Latitude	Latitude Range	Elevation range	Physiographic regions	Overall P
Species Richness	**279.65 < 0.0001**	0.00023 0.06	0.0000005 0.73	-0.0084 0.061	0.00026 0.62	**-109.7 0.0046**	**-10.74 < 0.0001**	**13.35 0.0031**	0.0013 0.76	**16.57 0.0003**	**<0.0001**
Prop State endemic	-0.070 0.58	-0.0000002 0.61	<0.0000001 0.074	0.000015 0.40	-<0.00001 0.79	0.272 0.072	0.0009 0.87	0.031 0.08	0.000025 0.17	-0.024 0.15	0.22
Prop Country endemic	0.245 0.18	0.00000035 0.61	<0.0000001 0.39	**0.000068 0.011**	-0.0000065 0.039	0.082 0.69	0.0094 0.26	**-0.067 0.009**	**0.000091 0.0011**	-0.0016 0.95	**0.0002**
Prop IUCN	0.051 0.28	-0.0000003 0.095	<0.0000001 0.34	**-0.000015 0.035**	0.0000014 0.10	-0.064 0.24	0.0024 0.28	0.0122 0.063	-0.000005 0.42	-0.0060 0.34	0.076
Prop SEMARNAT	0.079 0.087	-0.0000002 0.23	-<<0.00001 0.084	**0.000015 0.028**	0.00000025 0.74	0.088 0.10	0.0031 0.14	0.010 0.09	0.000011 0.10	-0.010 0.083	0.054

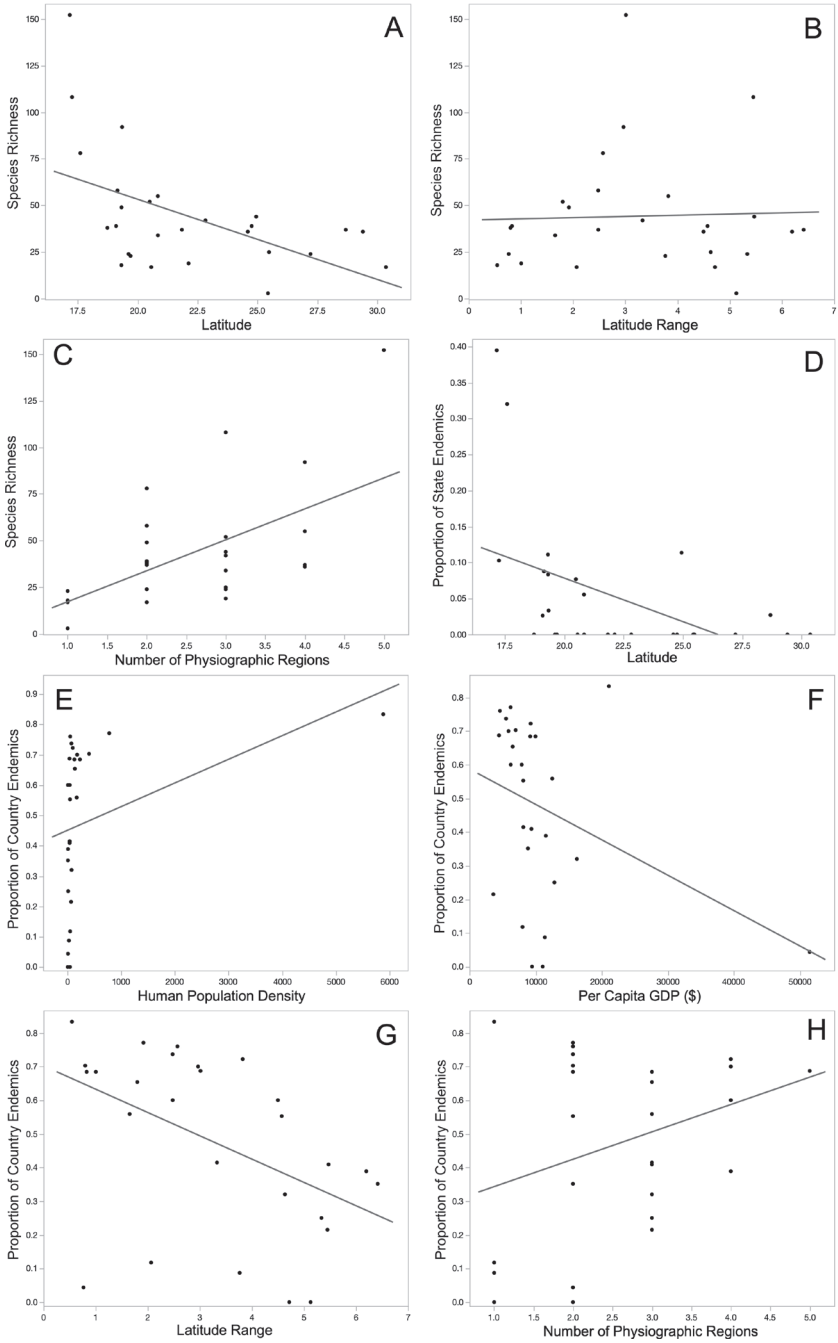

Figure 1. The relationships between amphibian species richness and a state's latitude **A** latitude range **B** and number of physiographic regions **C** between the proportion of a state's amphibian species that are state endemics and a state's latitude **D** and between the proportion of a state's amphibian species that are country endemics and the state's human population density **E** per capita GDP **F** latitude range **G** and the number of physiographic regions for Mexico **H**.

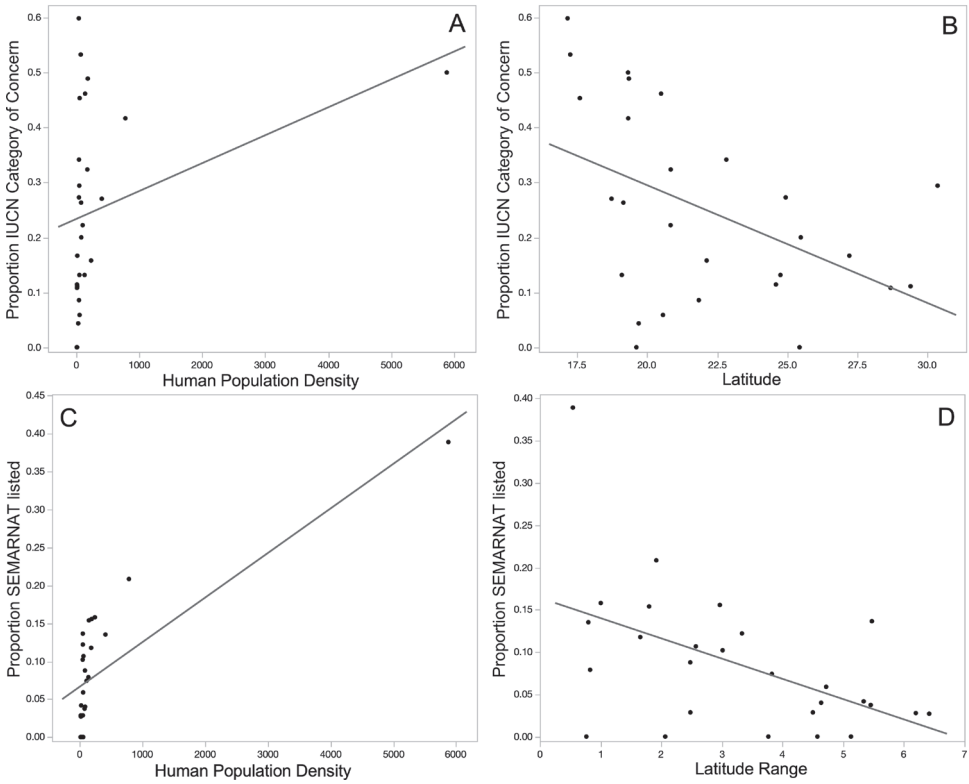

Figure 2. The relationships between the proportion of a state's amphibian species that are in an IUCN category of concern and a state's human population density **A** and latitude **B** and between the proportion of a state's amphibian species that are listed in SEMARNAT (2019) and a state's human population density **C** and latitude range for Mexico **D**.

Discussion

Our analyses found that species richness, endemism, and conservation status of amphibians and reptiles in Mexican states are related to both human demographic and socioeconomic variables and environmental variables. Below we discuss our observations on the factors related to species richness, endemism, and conservation status of amphibians and reptiles in Mexico.

Species richness and endemicity

For amphibians, species richness was positively related to latitude range and the number of physiographic regions in a state and negatively related to latitude (i.e., species richness decreased with latitude), whereas reptile species richness was positively related to latitudinal range and the number of physiographic regions and negatively related to latitude and the proportion of land protected. The proportion of a state's amphibian species that are state endemics was negatively related to latitude whereas none of the

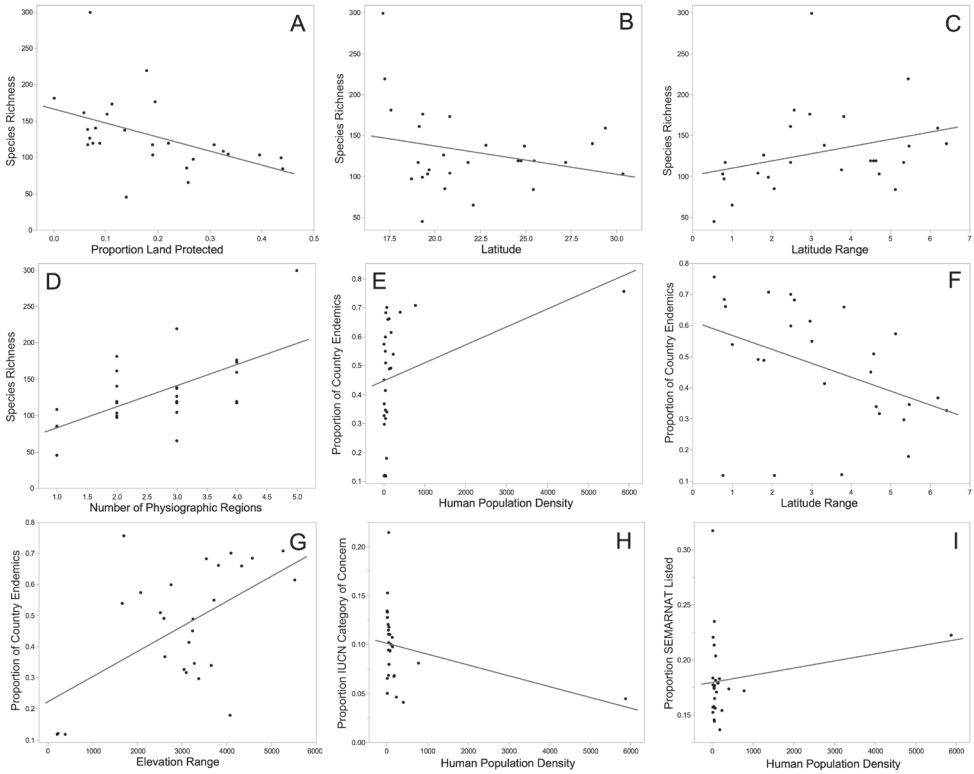

Figure 3. The relationships between reptile species richness and a state's proportion of protected land **A** latitude **B** latitude range **C** and number of physiographic regions **D** between the proportion of a state's reptile species that are country endemics and the state's human population density **E** latitude range **F** and elevation range **G** between the proportion of a state's reptile species that are in an IUCN category of concern and a state's human population density **H** and between the proportion of a state's reptile species that are listed in SEMARNAT (2019) and a state's human population density for Mexico **I**.

state variables we examined were related to the proportion of a state's reptile species that are state endemics. For the proportion of a state's species of amphibians that are country endemics there was a positive relationship with human population density and the number of physiographic regions and a negative relationship with per capita GDP and latitude range. For reptiles, this proportion was positively related to human population density and elevation range and negatively related to latitude range.

The positive relationships between species richness and latitude range and the number of physiographic regions for both amphibians and reptiles likely result from the increased variety of habitats and climates in a state leading to a greater number of niches, which can result in increased number of species occurring in a state. Our results for the herpetofauna of Mexico are similar to studies on *Sceloporus* lizards (Rivera et al. 2021) and on mammals finding that species richness at a variety of geographic scales increases with habitat or environmental heterogeneity (Amori et al. 2013, 2019; Udy et al. 2021).

The decrease in species richness of amphibians and reptiles with increasing latitude is consistent with the latitudinal species gradient (Pianka 1966; Willig et al. 2003; Hillebrand

2004; Pontarp et al. 2019). Species richness of amphibians in Mesoamerica is highest to the south (Wilson and Johnson 2010). Similarly, mammalian species richness in Mexico decreased with increasing latitude (Ceballos et al. 1998). These results are also similar to those found for amphibians and reptiles in a variety of regions and countries, such as Europe (Assunção-Albuquerque et al. 2012), United States (Schall and Pianka 1978), Australia (Schall and Pianka 1978), and North America (Rivera et al. 2021; Whiting and Fox 2021). The latitudinal gradient of species richness in both amphibians and reptiles in Mexico might be related to latitudinal gradients in climate related factors. For example, the species richness of reptiles and amphibians is often related to solar radiation, temperature, precipitation, annual potential and actual evapotranspiration (e.g., Schall and Pianka 1978; Rodríguez et al. 2005; Powney et al. 2010; Kafesh et al. 2020), all of which vary with latitude.

In addition, for reptiles, species richness decreased with increasing human population density and the proportion of the state's area protected. This relationship suggests there might be a negative impact of human population on species richness, perhaps due to the impact on amphibian and reptile populations. For example, in Europe, climate and human related factors explained 41–42% of variation in species richness of amphibians and reptiles (Assunção-Albuquerque et al. 2012). The species richness of reptiles in Mediterranean France is correlated with climate, elevation, and land use (Barnagaud et al. 2021). Reptile species richness is negatively affected by livestock production and urbanization (Cordier et al. 2021). Thus, the species richness of reptiles appears to be particularly susceptible to human pressures.

The patterns of state endemism that we observed show limited effects of the state variables we examined, with only a negative relationship between latitude and the proportion of a state's amphibian species being state endemics. In part this general lack of relationships may reflect the artificial nature of state boundaries (see Caveats below) such that states often share such physiographic regions or habitats and so likely share species, even over a small area along borders. For country-level endemism, we found positive relationships with human population density and measures related to habitat heterogeneity (e.g., number of physiographic regions or elevation range) for both amphibians and reptiles. Such relationships likely reflect the high level of endemism found in the Transvolcanic Mexican Belt (Flores-Villela et al. 2010) which is found in an area of high human population density (e.g., Mexico City and its environs). The negative relationship between country-wide endemism and latitude range likely also reflects the smaller states and federal entities found in central and southern Mexico where high levels of endemism are found.

Conservation status

Both human demographic and environmental variables affected the proportion of both amphibians and reptiles of conservation concern in a state. The proportion of amphibian species in an IUCN category of concern decreased with latitude and increased with human population density. For SEMARNAT, the proportion of listed species increased with human population density and decreased with latitudinal range. For reptiles, the proportion of a state's species in an IUCN category of concern decreased with human

population density, but the proportion that is SEMARNAT listed increased with human population density. The importance of human population density in determining conservation status is consistent with the impacts that anthropogenic effects on the environment have on amphibians and reptiles. For example, a high proportion of endangered amphibians in Mexico being found in areas that have experienced transformation to agriculture or urbanization (Londoño-Murcia and Sánchez-Cordero 2011). In addition, amphibian species diversity in central Mexico is reduced with the loss of canopy (Lara-Tufiño et al. 2019). Mayani-Parás et al. (2019) demonstrated that many species of amphibians and reptiles in Mexico have suffered major reductions in their distributions, and that this is particularly the result of the combined effects of mining and habitat loss. In addition, reptiles, and, to a lesser extent, amphibians, are subject to illegal trade and collection in Mexico (Masés-García et al. 2021). These patterns in Mexico are also consistent with patterns of conservation status and human pressures at the global and more regional scales for amphibians and reptiles. Globally, amphibian species richness is susceptible to deforestation, timber harvesting and production, and urbanization (Cordier et al. 2021). Reptile species richness is negatively affected by livestock production and urbanization (Cordier et al. 2021). In addition, reptile abundance globally is negatively affected by anthropogenic habitat changes (Doherty et al. 2020). Declines in European amphibians and reptiles were associated with the number of alien species and loss of habitat due to climate change (Falaschi et al. 2019). In China, the distribution of biodiversity loss is driven primarily by climate and anthropogenic sources (Lu et al. 2020). Similarly, in Australia extinction risk in reptiles is related to anthropogenic pressures and proximity to human populations as well as climatic variables (Senior et al. 2021).

Caveats

We recognize that our analysis is a snapshot in time of both taxonomic knowledge and conservation status. Species lists are dynamic and changing as new species are described, new localities are found, and populations are extirpated. In addition, conservation status for species, whether at the global (i.e., IUCN) or national (i.e., SEMARNAT) scale, are frequently reassessed. Thus, we realize that our analysis represents our knowledge at the time we generated our species lists and conducted our analyses. However, obtaining a snapshot now will provide a baseline that can be monitored and evaluated as our understanding of taxonomy, species distributions, and conservation status change over time.

We also recognize that by using global and national conservation status we are not taking into account variation in conservation status of species populations in each state such that species may be doing well in some states but poorly in other states. This is a challenge, but unfortunately conservation status at the state level is known for even fewer species than for the national and global measures. In addition, many regulations are focused on, or use, national or global level assessments rather than state level assessments.

Finally, we further recognize that the use of states in our analyses does not necessarily reflect ecological or biogeographical reality (i.e., they are not natural regions). However, given the nature of governmental processes, conservation efforts are usually a function of state or political boundaries and thus we argue that understanding patterns at the state level is pragmatic.

Acknowledgements

We thank L. Wilson, J. Sigala, and an anonymous reviewer for helpful comments on the manuscript. Support for this study was provided by Dirección General de Asuntos del Personal Académico – Programa de Apoyo a Proyectos de Investigación e Innovación Tecnológica (DGAPA-PAPIIT) through Project IN202021.

References

Amori G, Chiozza F, Patterson BD, Rondinini C, Schipper J, Luiselli L (2013) Species richness and distribution of Neotropical rodents, with conservation implications. Mammalia 77(1): 1–19. https://doi.org/10.1515/mammalia-2012-0050

Amori G, Boitani L, Milana G, Maiorano L, Luiselli L (2019) Endemism and diversity in European montane mammals: Macro-ecological patterns. Biological Journal of the Linnean Society. Linnean Society of London 128(1): 225–237. https://doi.org/10.1093/biolinnean/blz081

AmphibiaWeb (2020) AmphibiaWeb. University of California, Berkeley, CA, USA. https://amphibiaweb.org [Accessed on 2020-11-30]

Assunção-Albuquerque MJT, Rey Benayas JM, Rodríguez MÅ, Albuquerque FS (2012) Geographic patterns of vertebrate diversity and identification of relevant areas for conservation in Europe. Animal Biodiversity and Conservation 35(1): 1–11. https://doi.org/10.32800/abc.2012.35.0001

Barnagaud J-Y, Geniez P, Cheylan M, Crocket PA (2021) Climate overrides the effects of land use on the functional composition and diversity of Mediterranean reptile assemblages. Diversity & Distributions 27(1): 50–64. https://doi.org/10.1111/ddi.13176

Becker CG, Loyola RD (2008) Extinction risk assessments at the population and species level: Implications for amphibian conservation. Biodiversity and Conservation 17(9): 2297–2304. https://doi.org/10.1007/s10531-007-9298-8

Ceballos G, Rodríguez P, Medellín RA (1998) Assessing conservation priorities in megadiverse Mexico: Mammalian diversity, endemicity, and endangerment. Ecological Applications 8(1): 8–17. https://doi.org/10.1890/1051-0761(1998)008[0008:ACPIMM]2.0.CO;2

Chacón-Prieto F, Rodríguez-Soto C, Cuervo-Robayo AP, Carbajal Monroy JC, Alagador D (2021) Protected areas in Central Mexico – are they fit in promoting species persistence under climate and land use changes? Biological Conservation 260: e109186. https://doi.org/10.1016/j.biocon.2021.109186

Challenger A, Dirzo R, López Acosta JC, Mendoza E, Lira-Noriega A, Cruz I, Flores Martínez A, González Espinosa M (2009) Factores de cambio y estado de la biodiversidad. In: Capital Natural de México, vol. II: Estado de Conservación y Tendencias de Cambio. CONABIO, Mexico City, 37–73.

Chen Y, Peng S (2017) Evidence and mapping of extinction debts for global forest-dwelling reptiles, amphibians and mammals. Scientific Reports 7(1): e44305. https://doi.org/10.1038/srep44305

Cordier JM, Aguilar R, Lescano JN, Leynaud GC, Bonino A, Miloch D, Loyola R, Nori J (2021) A global assessment of amphibian and reptile response to land-use changes. Biological Conservation 253: e108863. https://doi.org/10.1016/j.biocon.2020.108863

Cuervo-Robayo AP, Ureta C, Goméz-Albores MA, Meneses-Mosquero AK, Téllez-Valdés O, Martínez-Meyer E (2020) One hundred years of climate change in Mexico. PLoS ONE 15(7): e0209808. https://doi.org/10.1371/journal.pone.0209808

Doherty TS, Balouch S, Bell K, Burns TJ, Feldman A, Fist C, Garvey TF, Jessop TS, Meiri S, Driscoll DA (2020) Reptile responses to anthropogenic habitat modification: A global meta-analysis. Global Ecology and Biogeography 29(7): 1265–1279. https://doi.org/10.1111/geb.13091

Falaschi M, Manenti R, Thuiller W, Ficetola GF (2019) Continental-scale determinants of population trends in European amphibians and reptiles. Global Change Biology 25(10): 3504–3515. https://doi.org/10.1111/gcb.14739

Flores-Villela O, Canseco-Márquez L, Ochoa-Ochoa LM (2010) Geographic distribution and conservation of the Mexican Central Highlands herpetofauna. In: Wilson LD, Townsend JH, Johnson JD (Eds) Conservation of Mesoamerican Amphibians and Reptiles. Eagle Mountain Publishing, Utah, 303–321.

Frost DR (2020) Amphibian Species of the World: an Online Reference. Version 6.1 (10 January 2020). American Museum of Natural History, New York. https://doi.org/10.5531/db.vz.0001

Geldmann J, Joppa LN, Burgess ND (2014) Mapping change in human pressure globally on land and within protected areas. Conservation Biology 28(6): 1604–1616. https://doi.org/10.1111/cobi.12332

Gómez-Mendoza L, Arriaga L (2007) Modeling the effect of climate change on the distribution of oak and pine species of Mexico. Conservation Biology 21(6): 1545–1555. https://doi.org/10.1111/j.1523-1739.2007.00814.x

González-Sánchez VH, Johnson JD, González-Solís D, Fucsko LA, Wilson LD (2021) A review of the introduced herpetofauna of Mexico and Central America, with comments on the effects of invasive species and biosecurity methodology. ZooKeys 1022: 79–154. https://doi.org/10.3897/zookeys.1022.51422

Hillebrand H (2004) On the generality of the latitudinal diversity gradient. American Naturalist 163(2): 192–211. https://doi.org/10.1086/381004

Hu X, Huang B, Verones F, Cavalett O, Cherubin F (2021) Overview of recent land-cover changes in biodiversity hotspots. Frontiers in Ecology and the Environment 19(2): 91–97. https://doi.org/10.1002/fee.2276

INEGI - Instituto Nacional de Estadística y Geografía (México) (2018) Anuario Estadísticos y Geográfico por Entidad Federative. Instituto Nacional de Estadistica Geografía, México.

Jiménez-García D, Li X, Lira-Noriega A, Townsend Peterson A (2021) Upward shifts in elevational limits of forest and grassland for Mexican volcanoes over three decades. Biotropica 53(3): 798–807. https://doi.org/10.1111/btp.12942

Kafesh A, Ashrafi S, Yousefi M, Rastegar-Pouyani E, Rajabizadeh M, Ahmadzadeh F, Grünig M, Pellissier L (2020) Reptile species richness associated to ecological and historical variables in Iran. Scientific Reports 10(1): e18167. https://doi.org/10.1038/s41598-020-74867-3

Lara-Tufiño JD, Badillo-Saldaña LM, Hernández-Austria R, Ramírez-Bautista A (2019) Effects of traditional agroecosystems and grazing areas on amphibian diversity in a region of central Mexico. PeerJ 7: e6390. https://doi.org/10.7717/peerj.6390

Lazcano D, Nevárez-de los Reyes M, García-Padilla E, Johnson JD, Mata-Silva V, DeSantis DL, Wilson LD (2019) The herpetofauna of Coahuila, Mexico: Composition, distribution, and conservation status. Amphibian & Reptile Conservation 13: 31–94.

Londoño-Murcia MC, Sánchez-Cordero V (2011) Distribución y conservación de especies amenazadas en Mesoamérica, Chocó y Andes tropicales. Revista Mexicana de Biodiversidad 82(3): 926–950. https://doi.org/10.22201/ib.20078706e.2011.3.1214

Lorenzo C, Sántiz EC, Bolaños-Citalán J, Navarrete-Gutiérrez D (2017) Influences of long-term changes in land cover on mammal populations: An example from Mexico. Oryx 53(2): 321–328. https://doi.org/10.1017/S0030605317000485

Lu Y, Yang Y, Sun B, Yuan J, Yu M, Stenseth NC, Bullock JM, Obersteiner M (2020) Spatial variation in biodiversity loss across China under multiple environmental stressors. Science Advances 6(47): eebd0952. https://doi.org/10.1126/sciadv.abd0952

Masés-García CA, Briones-Salas M, Sosa-Escalante JE (2021) Assessment of wildlife crime in a high-biodiversity region of Mexico. Journal for Nature Conservation 59: e125932. https://doi.org/10.1016/j.jnc.2020.125932

Mayani-Parás F, Botello F, Castañeda S, Sánchez-Cordero V (2019) Impact of habitat loss and mining on the distribution of endemic species of amphibians and reptiles in Mexico. Diversity (Basel) 11(11): e210. https://doi.org/10.3390/d11110210

Mayani-Parás F, Botello F, Castañeda S, Munguía-Carrana M, Sánchez-Cordero V (2021) Cumulative habitat loss increases conservation threats on endemic species of terrestrial vertebrates in Mexico. Biological Conservation 253: e108864. https://doi.org/10.1016/j.biocon.2020.108864

Mendoza-Ponce AV, Corona-Núñez RO, Kraxner F, Estrada F (2020) Spatial prioritization for biodiversity conservation in a megadiverse country. Anthropocene 32: e100267. https://doi.org/10.1016/j.ancene.2020.100267

Morrone JJ (2019) Regionalización biogeográfica y evolución biótica de México: Encrucijada de la biodiversidad del Nuevo Mundo. Revista Mexicana de Biodiversidad 90(0): e902980. https://doi.org/10.22201/ib.20078706e.2019.90.2980

Murali G, Gumbs R, Meiri S, Roll U (2021) Global determinants and conservation of evolutionary and geographic rarity in land vertebrates. Science Advances 7(42): eabe5582. https://doi.org/10.1126/sciadv.abe5582

Pavia EG, Graef F, Reyes J (2009) Annual and seasonal surface air temperature trends in Mexico. International Journal of Climatology 29(9): 1324–1329. https://doi.org/10.1002/joc.1787

Pianka E (1966) Latitudinal gradients in species diversity: A review of concepts. American Naturalist 100(910): 33–46. https://doi.org/10.1086/282398

Pontarp M, Bannefeld L, Sarmento Cabral J, Etienne RS, Fritz SA, Gillespie R, Graham CH, Hagen O, Hartig F, Huang S, Jansson R, Maliet O, Münkemüller T, Pellissier L, Rangel TF, Storch D, Wiegand T, Hurlbert AH (2019) The latitudinal diversity gradient: Novel understanding through mechanistic eco-evolutionary models. Trends in Ecology & Evolution 34(3): 211–223. https://doi.org/10.1016/j.tree.2018.11.009

Powney GD, Grenyer R, Orme CDL, Owens LPF, Meiri S (2010) Hot, dry and different: Australian lizard richness is unlike that of mammals, amphibians, and birds. Global Ecology and Biogeography 19(3): 386–396. https://doi.org/10.1111/j.1466-8238.2009.00521.x

Ramírez-Bautista A, Hernández-Salinas U, Cruz-Elizalde R, Berriozabal-Islas C, Moreno-Lara I, DeSantis DL, Johnson JD, García-Padilla E, Mata-Silva V, Wilson LD (2020) The herpetofauna of Hidalgo, Mexico: Composition, distribution, and conservation status. Amphibian & Reptile Conservation 14: 63–118.

Rivera JA, Rich HN, Lawing AM, Rosenberg MS, Martins EP (2021) Occurrence data uncover patterns of allopatric divergence and interspecies interactions in the evolutionary history of *Sceloporus* lizards. Ecology and Evolution 11(6): 2796–2813. https://doi.org/10.1002/ece3.7237

Rodrigues ASL, Brooks TM, Butchart SHM, Chanson J, Cox N, Hoffmann M, Stuart SN (2014) Spatially explicit trends in the global conservation status of vertebrates. PLoS ONE 9(11): e113934. https://doi.org/10.1371/journal.pone.0113934

Rodríguez MA, Belmontes JA, Hawkins BA (2005) Energy, water and large-scale patterns of reptile and amphibian species richness in Europe. Acta Oecologica 28(1): 65–70. https://doi.org/10.1016/j.actao.2005.02.006

Sarukhán J, Urquiza-Haas T, Koleff P, Carabias J, Dirzo R, Ezcurra E, Cerdeira-Estrada S, Soberón J (2015) Strategic actions to value, conserve, and restore the natural capital of megadiversity countries: The case of Mexico. Bioscience 65(2): 164–173. https://doi.org/10.1093/biosci/biu195

Schall JJ, Pianka ER (1978) Geographical trends in numbers of species. Science 201(4357): 679–686. https://doi.org/10.1126/science.201.4357.679

SEMARNAT (2019) Modificación al anexo normative III, lista de especies en riesgo de la Norma Oficial Mexicana NOM-059-SEMARNAT-2010. Protección Ambiental-Especies nativas de México de flora y fauna silvestres- Categorías de riesgo y especificaciones para su inclusion, exclusion o cambio- Lista de especies en riesgo, publicada el 30 de diciembre de 2010 (14 noviembre 2019). Secrearía de Medio Ambiente y Recursos Naturales, México. https://www.dof.gob.mx/nota_detalle.Php?codigo=5578808&fecha=14/11/2019.

Senior AF, Böhm M, Johnstone CP, McGee MD, Meiri S, Chapple DG, Tingley R, Byrne M (2021) Correlates of extinction risk in Australian squamate reptiles. Journal of Biogeography 48(9): 2144–2152. https://doi.org/10.1111/jbi.14140

Téllez-Valdés O, Dávila-Aranda P, Lira-Saade R (2006) The effects of climate change on the long-term conservation of *Fagus grandifolia* var. *mexicana*, an important species of the Cloud Forest in eastern Mexico. Biodiversity and Conservation 15(4): 1095–1107. https://doi.org/10.1007/s10531-004-1868-4

Udy K, Fritsch M, Meyer KM, Grass I, Hanß S, Hartig F, Kneib T, Kreft H, Kukunda CB, Pe'er G, Reininghaus H, Tietjen B, Tscharntke T, van Waveren C-S, Wiegand K (2021) Environmental heterogeneity predicts global species richness patterns better than area. Global Ecology and Biogeography 30(4): 842–851. https://doi.org/10.1111/geb.13261

Uetz P, Hošek J (2019) The Reptile Database. http://www.reptile.database.org [Accessed on 2020-11-30]

Villaseñor JL, Ortiz E, Delgadillo-Moya C, Juárez D (2020) The breadth of the Mexican Transition Zone as defined by its flowering plant genetic flora. PLoS ONE 15(6): e0235267. https://doi.org/10.1371/journal.pone.0235267

Whiting ET, Fox DL (2021) Latitudinal and environmental patterns of species richness in lizards and snakes across continental North America. Journal of Biogeography 48(2): 291–304. https://doi.org/10.1111/jbi.13996

Willig MR, Kaufman DM, Stevens RD (2003) Latitudinal gradients of biodiversity: Pattern, process, scale, and synthesis. Annual Review of Ecology, Evolution, and Systematics 34(1): 273–309. https://doi.org/10.1146/annurev.ecolsys.34.012103.144032

Wilson LD, Johnson JD (2010) Distributional patterns of the herpetofauna of Mesoamerica, a biodiversity hotspot. In: Wilson LD, Townsend JH, Johnson JD (Eds) Conservation of Mesoamerican Amphibians and Reptiles. Eagle Mountain Publishing, Utah, 31–235.

Supplementary material 1

Table S1

Authors: Geoffrey R. Smith, Julio A. Lemos-Espinal

Data type: Summary of sources for data used.

Explanation note: This file contains a list of the checklists from which we obtained our species lists for each Mecixan state. It also provides information on sources used to update those checklists.

Copyright notice: This dataset is made available under the Open Database License (http://opendatacommons.org/licenses/odbl/1.0/). The Open Database License (ODbL) is a license agreement intended to allow users to freely share, modify, and use this Dataset while maintaining this same freedom for others, provided that the original source and author(s) are credited.

Link: https://doi.org/10.3897/zookeys.1097.80424.suppl1

Supplementary material 2

Table S2

Authors: Geoffrey R. Smith, Julio A. Lemos-Espinal

Data type: Occurrences.

Explanation note: This file contains the data matrix used to generate the data used in our analyses. Basically it is a matrix of presence and absence of herpetofaunal species in each of the considered Mexican states. This matrix was created using the sources provided in Table S1.

Copyright notice: This dataset is made available under the Open Database License (http://opendatacommons.org/licenses/odbl/1.0/). The Open Database License (ODbL) is a license agreement intended to allow users to freely share, modify, and use this Dataset while maintaining this same freedom for others, provided that the original source and author(s) are credited.

Link: https://doi.org/10.3897/zookeys.1097.80424.suppl2

ZooKeys 1097: 103–116 (2022)
doi: 10.3897/zookeys.1097.79109
https://zookeys.pensoft.net

RESEARCH ARTICLE

A peer-reviewed open-access journal
ZooKeys
Launched to accelerate biodiversity research

A new species of the genus *Ivela* Swinhoe (Lepidoptera, Erebidae, Lymantriinae) from Guangdong, China

Lin-Zhe Xie[1], Kun-Yuan Li[2], Liu-Sheng Chen[2], Hou-Shuai Wang[1]

1 *Department of Entomology, College of Plant Protection, South China Agricultural University, Guangzhou 510642, China* **2** *Guangdong Academy of Forestry, Guangzhou 510642, China*

Corresponding authors: Liu-Sheng Chen (lshchen2008@163.com), Hou-Shuai Wang (houshuaiwang@scau.edu.cn)

Academic editor: James Adams | Received 10 December 2021 | Accepted 7 April 2022 | Published 20 April 2022

http://zoobank.org/5AEC83AB-5152-4074-B524-AE9B2648EE64

Citation: Xie L-Z, Li K-Y, Chen L-S, Wang H-S (2022) A new species of the genus *Ivela* Swinhoe (Lepidoptera, Erebidae, Lymantriinae) from Guangdong, China. ZooKeys 1097: 103–116. https://doi.org/10.3897/zookeys.1097.79109

Abstract

Ivela yini **sp. nov.**, is described from Guangdong, China based on morphological characters and molecular data. Adults, including genitalia and wing venation, and pupa are illustrated and compared to those of similar species. A key to Chinese *Ivela* species is provided. Assignment of the new species to *Ivela* Swinhoe is based primarily on a molecular phylogenetic analysis and is corroborated by morphology. Life histories of *I. yini* and *Dendrophleps semihyalina* Hampson are discussed.

Keywords

adults, *Dendrophleps*, Leucomini, molecular data, phylogenetic analyses, pupae

Introduction

The tribe Leucomini of Lymantriinae (Erebidae), proposed by Holloway (1999), is mainly distributed in the Oriental tropics and contains approximately 60 species in four genera (Wang et al. 2015). Adults of this tribe can be recognized by their appearance, often pale white, with translucent areas in male wings, and asymmetric male genitalia (Holloway 1999). Prior to this study, *Ivela* Swinhoe contained three species: *I. auripes* (Butler), *I. ochropoda* (Eversmann), and *I. eleuterioides* (Semper). Of these, *I. auripes* and *I. ochropoda* occur in China.

We report the discovery of a previously unrecognized species of tussock moth that resembles *Dendrophleps semihyalina* Hampson. Based on multiple morphological characters of adults and pupae and molecular data of four gene regions, we describe it as a species of *Ivela*.

Copyright *Lin-Zhe Xie et al.* This is an open access article distributed under the terms of the Creative Commons Attribution License (CC BY 4.0), which permits unrestricted use, distribution, and reproduction in any medium, provided the original author and source are credited.

Materials and methods

Collecting and morphology

All examined specimens were collected in light traps. They are deposited in the Insect Collection of Department of Entomology, South China Agricultural University (**SCAU**), Guangzhou, China. Adults and genitalia were treated following Wang et al. (2010, 2014). Terminology follows Holloway (1999) and Chao (2003).

Molecular taxa sampling

We sampled six species, including the type species of all genera of Leucomini, with two species of *Lymantria* Hübner as outgroups. Most sequences of Leucomini and those of the outgroup taxa were downloaded from NCBI. The detailed sampling data for molecular analyses are provided in Table 1.

Molecular data analyses

DNA was extracted from two or three legs of adult specimens using the TIANGEN DNA extraction kit following the manufacturer's instructions. One mitochondrial gene, DNA barcode region of cytochrome c oxidase subunit I (COI), and three nuclear genes, Elongation factor-1 alpha (EF-1α), ribosomal protein S5 (RpS5), and wingless (WNT), were amplificated and sequenced following Folmer et al. (1994) and Wahlberg and Wheat (2008). Concatenation and sequence alignment was performed using MEGA X (Kumar et al. 2018).

A neighbor-joining (NJ) analysis of DNA barcode was performed with MEGA X under the Kimura 2-Parameter (K2P) model (Kimura 1980), and bootstrap values were calculated with 1,000 replicates. A maximum-likelihood (ML) analysis was per-

Table 1. Sampling data used for molecular analyses in this study.

Specimen voucher no.	Taxa	Locality	GenBank accession no.			
			COI	EF1-a	RPS5	WNT
LE114	*Ivela yini* **sp. nov.**	Guangdong, China	OM242956#	–	–	–
LE074	*Ivela yini* **sp. nov.**	Guangdong, China	OM242952#	–	–	–
LE118	*Ivela yini* **sp. nov.**	Guangdong, China	OM242955#	–	–	–
H340	*Ivela yini* **sp. nov.**	China	KP081829.1	KP082270.1	–	KP082761.1
LE124	*Ivela auripes**	Guangdong, China	OM242951#	–	–	–
H49	*Ivela auripes**	China	KP081830.1	KP082302.1	–	KP082762.1
H181	*Perina nuda**	Guangdong, China	KP081831.1	KP082248.1	KP082623.1	KP082763
LE014	*Dendrophleps semihyalina**	Guangdong, China	OM250083#	OM328195#	OM328197#	OM328196#
LE115	*Dendrophleps semihyalina**	Guangdong, China	OM242954#	–	–	–
LE116	*Dendrophleps semihyalina**	Guangdong, China	OM242953#	–	–	–
GD385	*Dendrophleps semihyalina**	Guangdong, China	OM242949#	–	–	–
H377	*Leucoma* sp.	China	KP081825.1	KP082289.1	KP082620.1	KP082757.1
H351	*Leucoma salicis**	China	KP081826.1	KP082276.1	KP082621.1	KP082758.1
H127	*Lymantria dissoluta*	China	KP081854.1	KP082225	KP082643.1	KP082781
H58	*Lymantria similis*	China	KP081855.1	KP082304.1	KP082644.1	KP082782.1

* Type species of genus. # Sequences obtained in this study. – No data available.

formed using IQ-TREE (Nguyen et al. 2015) with 1,000 bootstrap replicates, and the best-fitting model was automatically selected by ModelFinder (Kalyaanamoorthy et al. 2017) implemented in IQ-TREE. A Bayesian-inference (BI) analysis was performed using MrBayes 3.2.6 (Ronquist et al. 2012) under the GTR + F + G4 model, with two parallel runs for 2,000,000 generations. The first 25% of trees were discarded as burn-in, and the remaining trees were used to calculate posterior probabilities (PP).

Results

Phylogenetic relationships

The genetic distances of the DNA barcode data (a 658 bp region of the COI gene) of Leucomini species in China are given in Appendix 1. The interspecific genetic distances within *Ivela* ranged from 10.6 to 12.2% (*I. yini* sp. nov. and *I. auripes*); the intraspecific genetic distances from 1.1% (*I. yini*) to 1.9% (*D. semihyalina*); and the intergeneric genetic distances within Leucomini ranged from 12.0% (*I. yini* and *Perina nuda* (Fabricius)) to 19.3% (*Leucoma salicis* (Linnaeus) and *D. semihyalina*). The concatenated dataset of four genes consists of 2,851 nucleotide positions (658 bp for COI, 400 bp for WNT, 600 bp for RPS5 and 1,193 bp for EF-1α). The NJ analysis of the DNA barcode data indicates that the new species and *I. auripes* (the type species of *Ivela*) form a clade in Leucomini (Fig. 1). This clade is strongly supported by both BI and ML analyses of the concatenated dataset (Fig. 2: BP = 1.00, PP = 87).

A key to *Ivela* from China

1 Forewings with R_3 and R_4 coincident ..... ***I. auripes***
– Forewings with R_3 and R_4 separated at near apex **2**
2 Palpi white ..... ***I. yini***
– Palpi yellow ..... ***I. ochropoda***

Species accounts

***Ivela yini* Xie & Wang, sp. nov.**
http://zoobank.org/2BA5C644-7CCA-4686-A445-6395DFB1E239
Figs 3–6, 9–11, 14–16, 21–24

Diagnosis. This new species is diagnosed by a combination of characters. Superficially, the thorax and abdomen of the adult are white without black markings (Figs 3–6, 9, 10), the palpi are white (Fig. 11), and the forelegs are orange with white rings on the tarsal segments (Figs 9–11). In the male, the asymmetrical valvae are wide and truncated, with a deeply concave cucullus (Fig. 15). The uncus of *I. yini* (Fig. 15) is more than twice as long as the uncus of *I. auripes* (Fig. 17) and *I. ochropoda* (Inoue 1956: fig. 25). The female corpus bursae of *I. yini* has a pair of caudal projections (Fig.

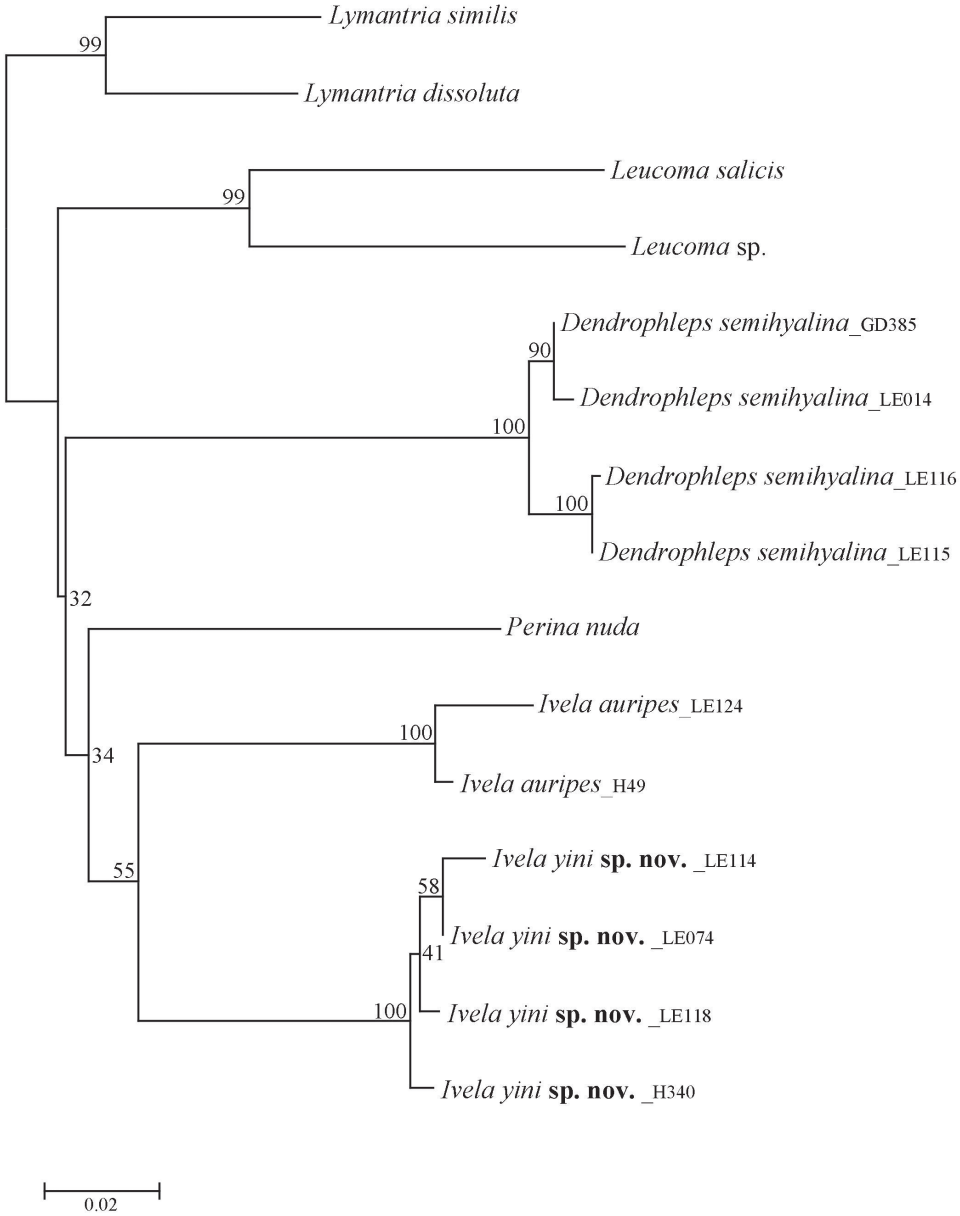

Figure 1. NJ tree of the selected samples of Leucomini based on DNA barcode data. Numbers near nodes represent support values.

16). The pupa has white hairs on the prothorax, on segments A2 and A3, and near the posterior end (Figs 21–24).

Dendrophleps semihyalina has black markings on the thorax and abdomen (Figs 7, 8, 12, 13), and its valvae are long, narrow, and without a deeply concave cucullus (Fig. 19). The corpora bursae of *I. auripes* and *D. semihyalina* lack caudal projections (Figs 18, 20).

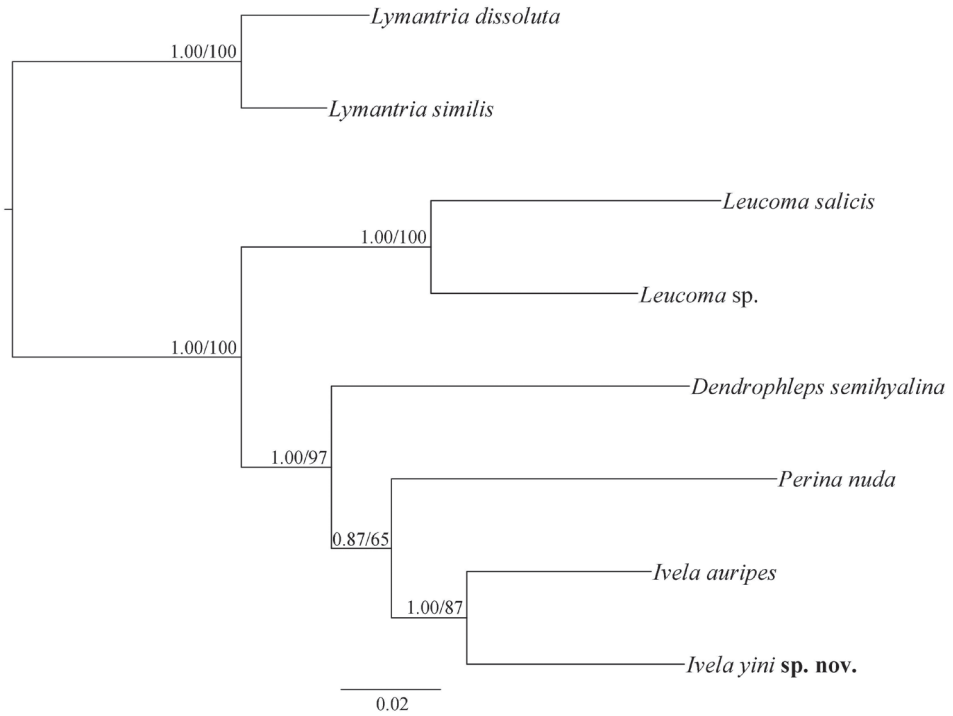

Figure 2. BI tree of the selected species of Leucomini inferred from the combined COI, EF-1α, RPS5, and WNT genes. Posterior probabilities from BI analysis and bootstrap values from ML analysis are indicated above the branches as PP/BP.

Description. Adult (Figs 3–6, 9–11, 14–16).

Head (Fig. 11). Antennae bipectinate, fuscous; frons and vertex covered densely with white hairs; labial palpi white, short.

Thorax (Figs 3–6, 9, 10, 14). Dorsum and venter covered with white scales, tegula white. Forewing length: 39–42 mm male, 48–50 mm female. Forewings translucent with dense white scales at basal area in male, white in female; R_1 and R_2 almost parallel, R_3, R_4, and R_5 stalked, M_1 arising from upper angle of discal cell, M_2 and M_3 arising from the lower angle of discal cell respectively, Cu_1 and Cu_2 approximately parallel, fringe white. Hindwings white, with a transparent area near apex in male; Rs and M_1 short stalked, M_2 and M_3 short stalked in male but arising separately from the lower angle of discal cell in female, fringe white. Forelegs densely covered with orange scales, tarsi with white rings; mid- and hindlegs white, tarsi yellow with white rings but inconspicuous in male.

Abdomen. Male genitalia (Fig. 15). Uncus hook-shaped apically; tegumen broad; valvae moderately symmetric, left valva smaller than right, broad, extremely short, cucullus concave medially, densely covered with setae on the dorsal and ventral parts of cucullus; saccus well developed; aedeagus tubular, distal gradually slightly curve toward distal area; vesica simple, without cornuti.

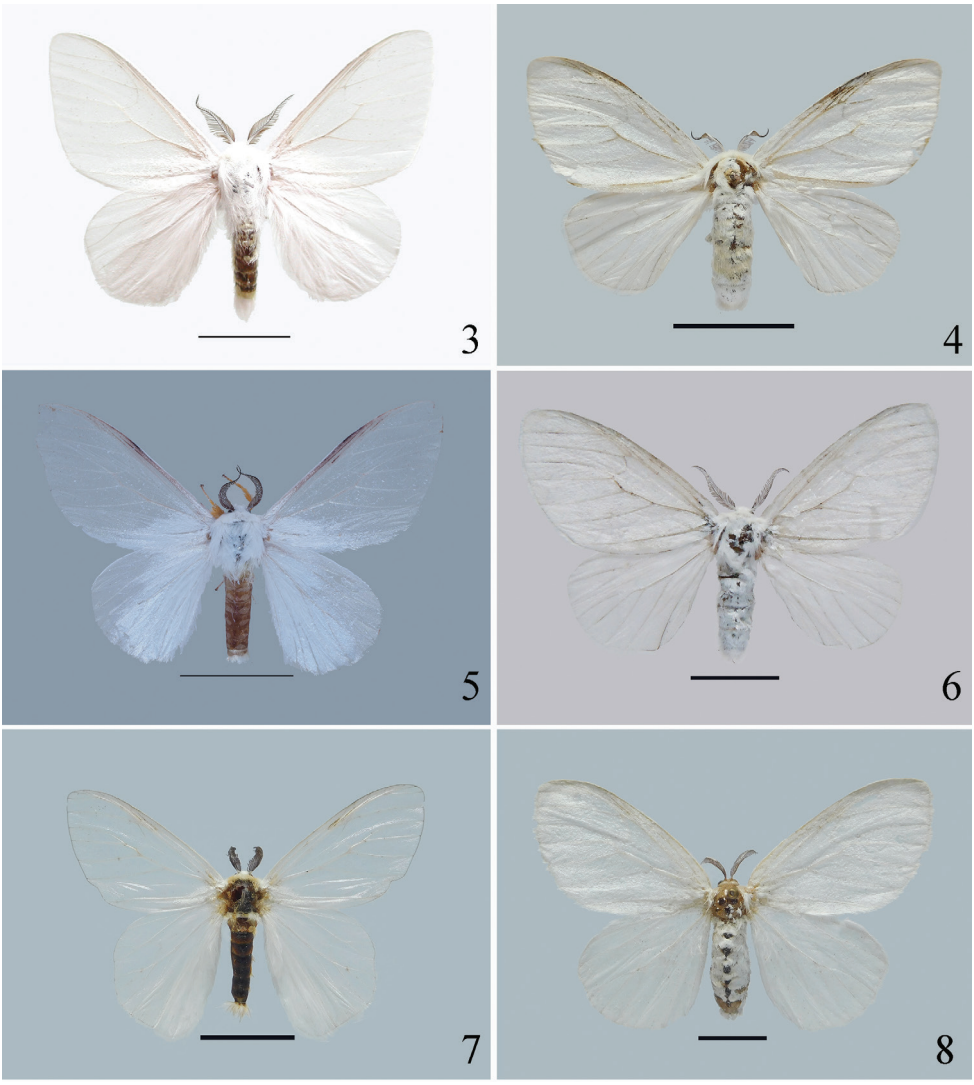

Figures 3–8. Adults **3–6** *Ivela yini* sp. nov. (**3** male, holotype **4** female, paratype **5** male, paratype **6** female, paratype) **7, 8** *Dendrophleps semihyalina* (**7** male **8** female). Scale bars: 10 mm.

Female genitalia (Fig. 16). Anterior apophysis almost as long as posterior apophysis; anal papillae larger; ostium larger; ductus bursae short, sclerotized; corpus bursae with a pair of terminal projections.

Pupa (Figs 21–24). Head white; prothorax white, with long, white hairs; mesothorax and metathorax chestnut-colored on dorsal surface, with dark brown hairs; wings white, with two black lines dorsally; forelegs and midlegs yellow, hindlegs white, with dark yellow dot terminally. Abdomen pale green laterally and ventrally, with chestnut-colored dots and spots dorsally; segments A1–A6 with a pair of black setae; segments A2 and A3 and terminal of abdomen with white hairs.

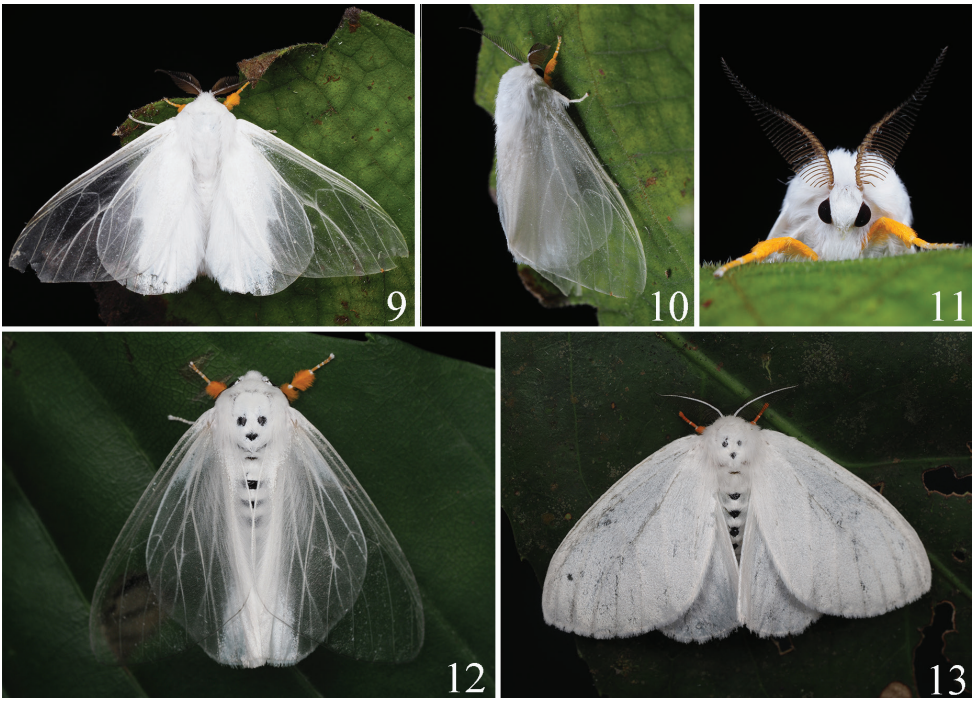

Figures 9–13. Field images of adults **9–11** *Ivela yini* sp. nov. male (**9** dorsal view **10** lateral view **11** ventral view of head) **12, 13** *Dendrophleps semihyalina* (**12** male, dorsal view **13** female, dorsal view).

A single pupa of *I. yini* was discovered on *Idesia polycarpa* Maxim. (Salicaceae) (Fig. 24). This suggests that this is the foodplant of this species.

Habitat. Forest zone 1000–1315 m elevation.

Materials examined. ***Holotype***: ♂, Nanling National Nature Reserve, Ruyuan County, Guangdong, 25.VI.2008, leg. Min Wang. ***Paratypes***: 1♂, same data as holotype, altitude 1315 m, 12.VII.2010, leg. Min Wang. 1♀, same data as holotype, 3.VII.2011, leg. Min Wang. 1♂, same data as holotype, altitude 1000 m, 10.VII.2019, leg. Ran Yin & Xiao-juan Xing. 1♀, same data as holotype, 11–14.VI.2019, leg. Hou-shuai Wang.

Distribution. China (Guangdong).

Etymology. The species is named after Ran Yin, who discovered the pupa of the new species. The name is in the genitive case.

Remarks. The female genitalia of *I. auripes* (Fig. 18) and *D. semihyalina* (Fig. 20) have to our knowledge not been illustrated previously. They are illustrated here for comparative purposes.

The early stages of *D. semihyalina* are also newly reported as below (Figs 25–30):

Host plant of *D. semihyalina* (Fig. 25): *Indocalamus tessellatus* (Munro) Keng f. (Poaceae).

Last instar larva of *D. semihyalina* (Figs 26, 27): body white laterally and ventrally; dorsally black, with scattered white dots. A1 and A2 with reddish orange tufts dorsally. Verrucae pale yellow laterally, black dorsally, with long white or black hairs.

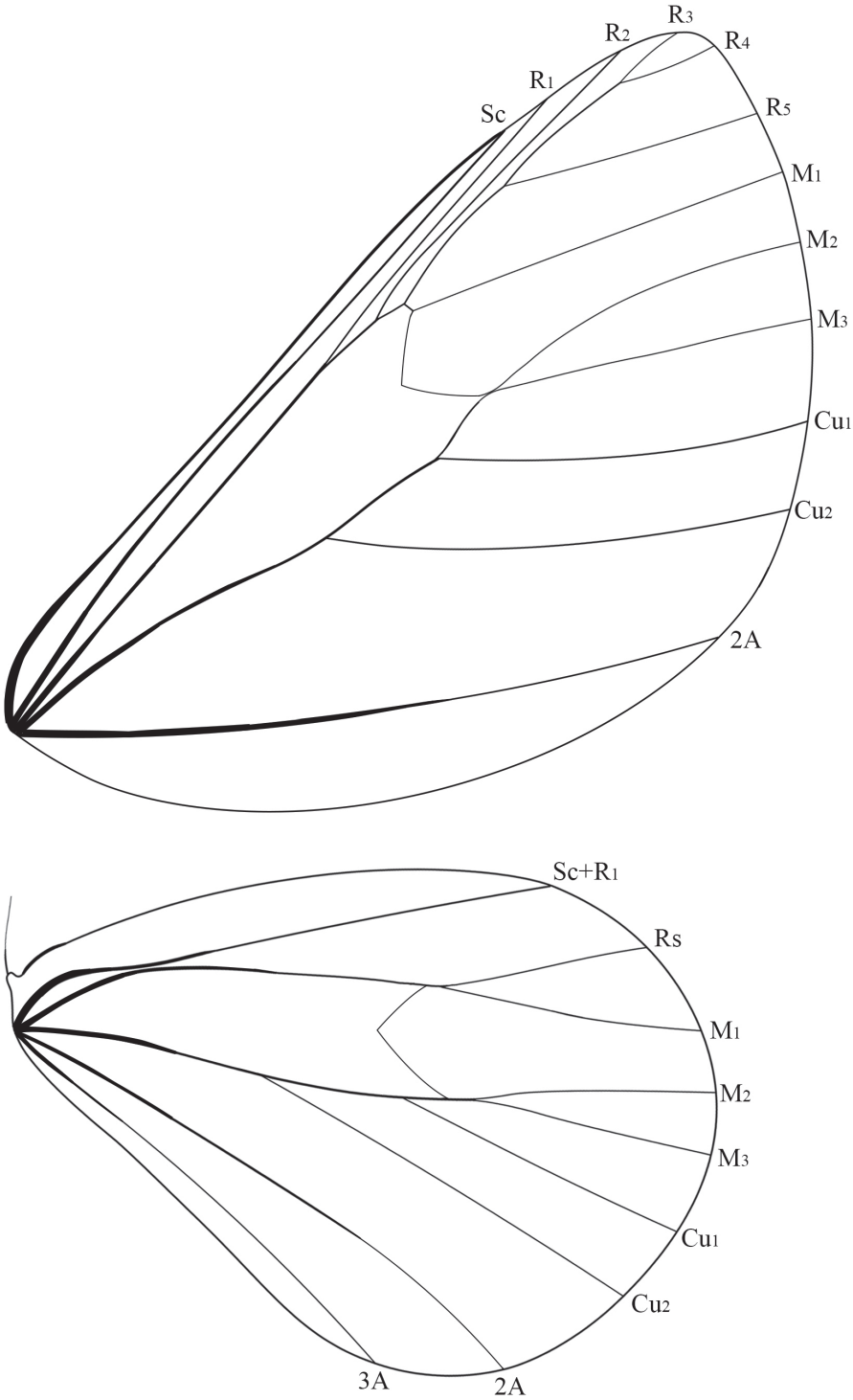

Figure 14. Wing venation of *Ivela yini* sp. nov. (male, paratype).

Figures 15–20. Genitalia **15, 16** *Ivela yini* sp. nov. (**15** male, holotype **16** female, paratype) **17, 18** *I. auripes* (**17** male **18** female) **19, 20** *Dendrophleps semihyalina* (**19** male **20** female).

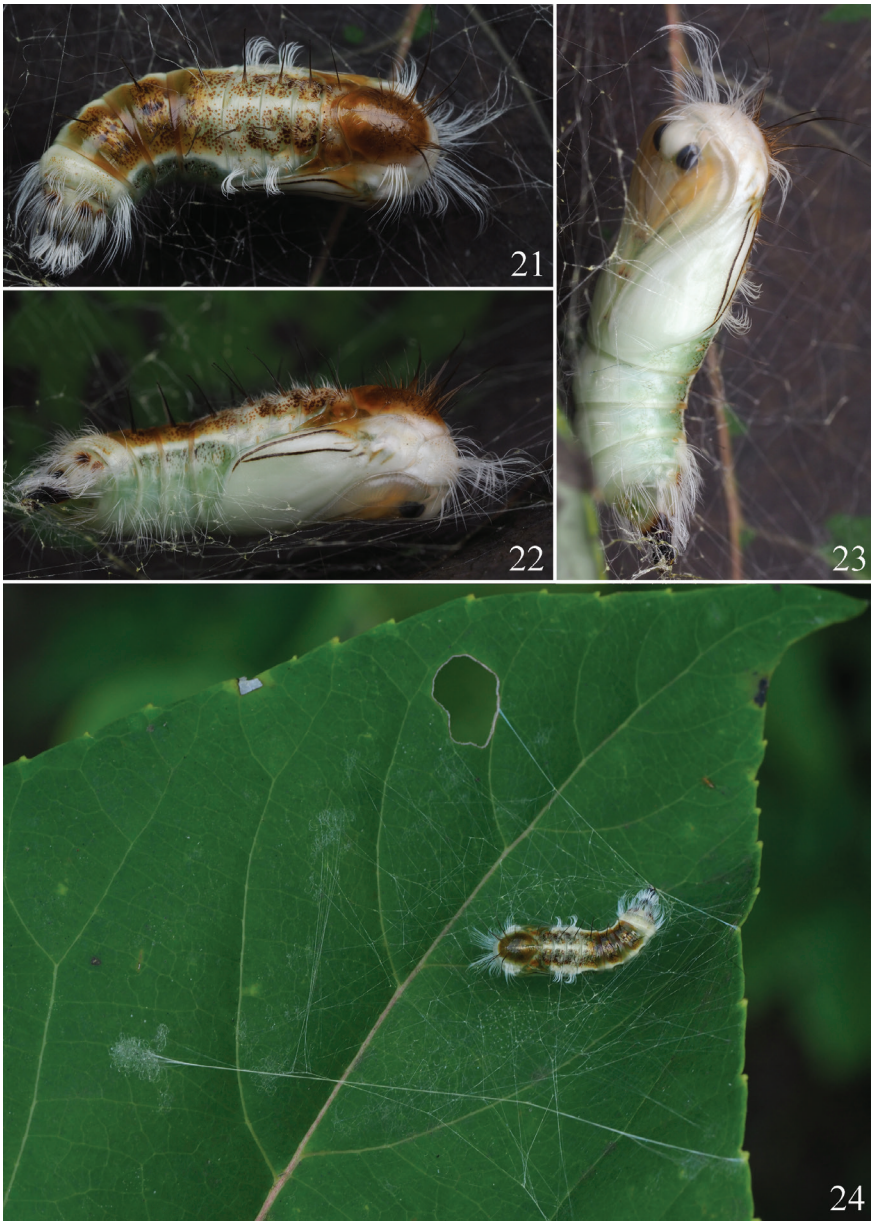

Figures 21–24. Pupa of *Ivela yini* sp. nov. **21** dorsal view **22** lateral view **23** ventral view **24** pupa on *Idesia polycarpa* Maxim.

Pupa of *D. semihyalina* (Figs 28–30): body white laterally and ventrally, green-brown dorsally. Thorax and abdomen with irregular black spots on lateral and ventral surfaces. A1–A3 with a pair of green patches on dorsal surface. Wings with some mixed orange and black veins.

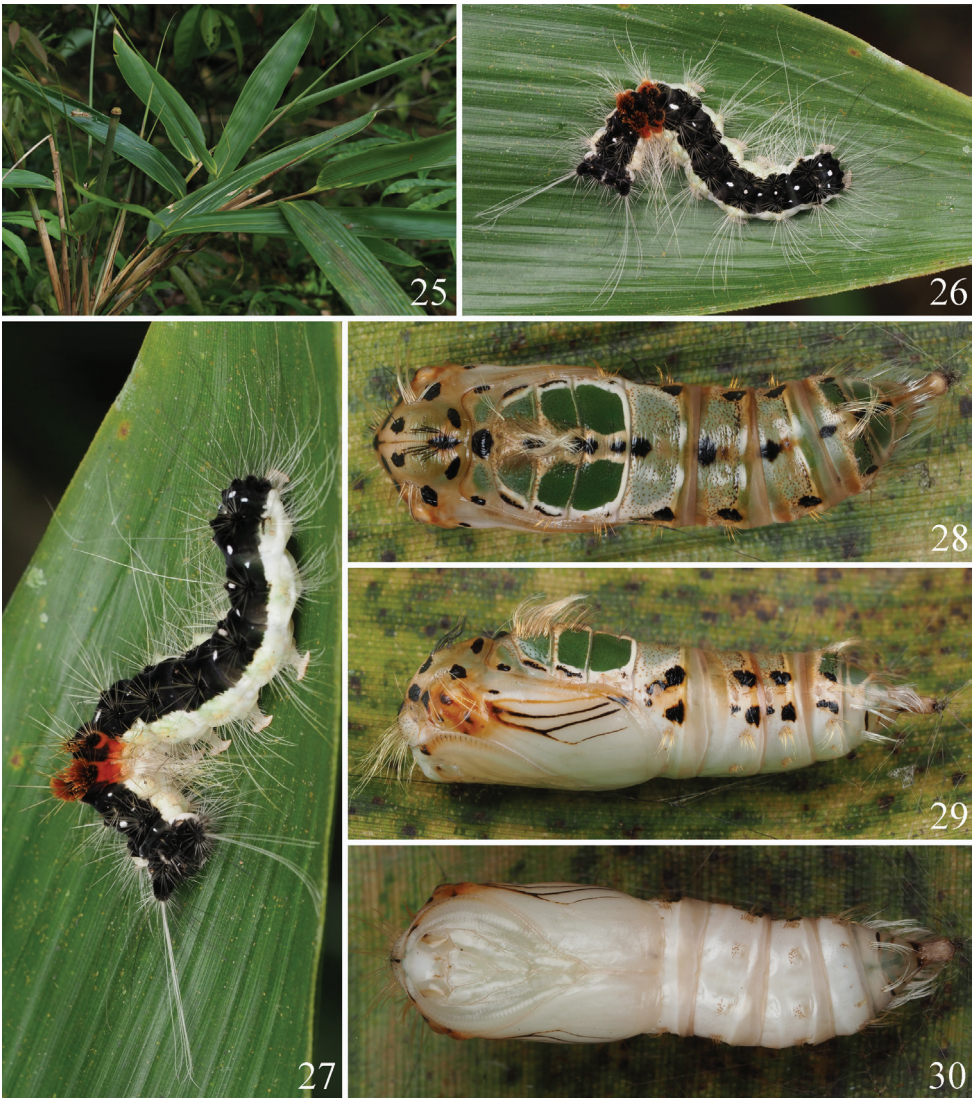

Figures 25–30. Immature stages and host plant of *Dendrophleps semihyalina* **25** host plant: *Indocalamus tessellatus* (Munro) Keng f. **26, 27** last instar larva on the host plant **28–30** pupa (**28** dorsal view **29** lateral view **30** ventral view).

Discussion

Ivela yini is superficially similar to several tussock moths with which it is sympatric. We illustrated it with *Dendrophleps semihyalina* and *Ivela auripes* for comparative purposes. These species can be distinguished reliably by the combinations of superficial characters outlined above. The identification can be confirmed by dissection of the male and female genitalia if required.

The genetic distance values of DNA barcode data between Lepidoptera species are ordinarily greater than 3% (Hebert et al. 2003). Our analysis of Chinese Leucomini indicates that the DNA barcode of *I. yini* is 10.6% from the closest species *I. auripes* (Appendix 1). The NJ tree also strongly supports the validity of the new species (Fig. 1). Our phylogenetic analyses show that *I. yini* and *I. auripes* are a monophyletic clade (PP = 1.00, BP = 87) and strongly suggest that *I. yini* belongs in *Ivela* (Fig. 2). This arrangement is supported by morphology. All *Ivela*, including *I. yini*, share wide valvae, and their hindwings lack a row of oblique veinlets (accessory veins) between A2 and the dorsal margin. These veinlets are considered diagnostic for *Dendrophleps* (Holloway 1999; Mackey 2019).

Several hardwoods were reported as foodplants for *I. auripes: Corylopsis multiflora* Hance (Hamamelidaceae), *Cornus controversa* Hemsley (Cornaceae), *C. brachypoda* C.A. Mey (Cornaceae), *Styrax japonicus* Sieb. et Zucc (Styracaceae), and *S. obassis* Siebold et Zucc (Styracaceae) (Inoue 1956; Chao 2003). While our discovery of a pupa of *I. yini* on *Idesia polycarpa* is less than absolute proof that it is the foodplant of this moth, it does suggest that *I. yini* feeds on a broadleaved tree. In contrast, *D. semihyalina* was discovered to be a grass feeder. These foodplant differences support placement of these similar-appearing moths into different genera.

Acknowledgements

We are grateful to three reviewers for their constructive feedback on our manuscript. We are thankful Prof. Min Wang from South China Agricultural University for collecting the specimens. We are also thankful to Mr Ran Yin and Ms Xiao-juan Xing for discovering the pupa of the new species. This work was supported by a grant from National Natural Science Foundation of China to HSW (no. 31601879) and Natural Science Foundation of Guangdong (no. 2022A1515012050).

References

Chao CL (2003) Lepidoptera Lymantriidae. Fauna Sinica, Insecta 30. Science Press, Beijing, 484 pp.

Folmer O, Black M, Hoeh W, Lutz R, Vrijenhoek R (1994) DNA primers for amplification of mitochondrial cytochrome c oxidase subunit I from diverse metazoan invertebrates. Molecular Marine Biology and Biotechnology 3(5): 294–299.

Hebert PDN, Cywinska A, Ball SL, deWaard JR (2003) Biological identifications through DNA barcodes. Proceedings. Biological Sciences 270(1512): 313–321. https://doi.org/10.1098/rspb.2002.2218

Holloway JD (1999) The moths of Borneo [Part 5]: Family Lymantriidae. Malayan Nature Journal 53: 1–188.

Inoue H (1956) A revision of the Japanese Lymantriidae (I). Japanese Journal of Medical Science & Biology 9(4–5): 133–163. https://doi.org/10.7883/yoken1952.9.133

Kalyaanamoorthy S, Minh BQ, Wong TKF, von Haeseler A, Jermiin LS (2017) ModelFinder: Fast model selection for accurate phylogenetic estimates. Nature Methods 14(6): 587–589. https://doi.org/10.1038/nmeth.4285

Kimura M (1980) A simple method for estimating evolutionary rates of base substitutions through comparative studies of nucleotide sequences. Journal of Molecular Evolution 16(2): 111–120. https://doi.org/10.1007/BF01731581

Kumar S, Stecher G, Li M, Knyaz C, Tamura K (2018) MEGA X: Molecular Evolutionary Genetics Analysis across computing platforms. Molecular Biology and Evolution 35(6): 1547–1549. https://doi.org/10.1093/molbev/msy096

Mackey P (2019) A note on *Dendrophleps lobipennis* (Swinhoe, 1892) (Lepidoptera, Erebidae, Lymantriinae) with a description of the female. Suara Serangga Papua 12(1): 1–7. [SUGAPA digital]

Nguyen LT, Schmidt HA, von Haeseler A, Minh BQ (2015) IQ-TREE: A fast and effective stochastic algorithm for estimating maximum-likelihood phylogenies. Molecular Biology and Evolution 32(1): 268–274. https://doi.org/10.1093/molbev/msu300

Ronquist F, Teslenko M, van der Mark P, Ayres DL, Darling A, Höhna S, Larget B, Liu L, Suchard MA, Huelsenbeck JP (2012) MrBayes 3.2: Efficient Bayesian phylogenetic inference and model choice across a large model space. Systematic Biology 61(3): 539–542. https://doi.org/10.1093/sysbio/sys029

Wahlberg N, Wheat CW (2008) Genomic outposts serve the phylogenomic pioneers: Designing novel nuclear markers for genomic DNA extractions of Lepidoptera. Systematic Biology 57(2): 231–242. https://doi.org/10.1080/10635150802033006

Wang HS, Xiong W, Wang M (2010) Two new species of the genus *Longipenis* (Lepidoptera: Lecithoceridae) from China. The Florida Entomologist 93(3): 352–356. https://doi.org/10.1653/024.093.0305

Wang HS, Fan XL, Owada M, Wang M, Nylin S (2014) Phylogeny, systematics and biogeography of the genus *Panolis* (Lepidoptera: Noctuidae) based on morphological and molecular evidence. PLoS ONE 9(3): e90598. https://doi.org/10.1371/journal.pone.0090598

Wang HS, Wahlberg N, Holloway JD, Bergsten J, Fan XL, Janzen DH, Hallwachs W, Wen LJ, Wang M, Nylin S (2015) Molecular phylogeny of Lymantriinae (Lepidoptera, Noctuoidea, Erebidae) inferred from eight gene regions. Cladistics 31(6): 579–592. https://doi.org/10.1111/cla.12108

Appendix 1

Table A1. Kimura 2-parameter genetic distances based on COI barcodes among 13 samples of Leucomini and two outgroups.

Species code	Species name	1	2	3	4	5	6	7	8	9	10	11	12	13	14
LE114	*Ivela yini* **sp. nov.**														
LE074	*Ivela yini* **sp. nov.**	0.006													
LE118	*Ivela yini* **sp. nov.**	0.000	0.006												
H340	*Ivela yini* **sp. nov.**	0.011	0.011	0.011											
LE124	*Ivela auripes*	0.122	0.119	0.122	0.120										
H49	*Ivela auripes*	0.110	0.106	0.110	0.108	0.020									
H181	*Perina nuda*	0.126	0.122	0.126	0.120	0.157	0.144								
LE116	*Dendrophleps semihyalina*	0.154	0.156	0.154	0.154	0.183	0.165	0.170							
LE115	*Dendrophleps semihyalina*	0.152	0.154	0.152	0.152	0.181	0.163	0.168	0.002						
GD385	*Dendrophleps semihyalina*	0.144	0.146	0.144	0.144	0.167	0.150	0.161	0.019	0.017					
LE014	*Dendrophleps semihyalina*	0.142	0.144	0.142	0.142	0.165	0.148	0.159	0.015	0.014	0.003				
H377	*Leucoma* sp.	0.169	0.173	0.169	0.171	0.174	0.155	0.172	0.187	0.187	0.182	0.181			
H351	*Leucoma salicis*	0.159	0.161	0.159	0.161	0.163	0.149	0.182	0.193	0.191	0.188	0.187	0.127		
H127	*Lymantria dissoluta*	0.138	0.135	0.138	0.142	0.153	0.136	0.131	0.157	0.155	0.149	0.147	0.159	0.167	
H58	*Lymantria similis*	0.133	0.129	0.133	0.133	0.139	0.121	0.137	0.154	0.154	0.146	0.145	0.144	0.163	0.071

ZooKeys 1097: 117–132 (2022)
doi: 10.3897/zookeys.1097.76426
https://zookeys.pensoft.net

RESEARCH ARTICLE

A peer-reviewed open-access journal
ZooKeys
Launched to accelerate biodiversity research

Tadpole soup: Chinantec caldo de piedra and behavior of *Duellmanohyla ignicolor* larvae (Amphibia, Anura, Hylidae)

Carlos A. Flores[1], Medardo Arreortúa[1], Edna González-Bernal[2]

1 *CIIDIR Unidad Oaxaca, Instituto Politécnico Nacional, Laboratorio de Ecología de Anfibios (ECA), Hornos 1003, Col. Noche Buena, 71230, Santa Cruz Xoxocotlán, Oaxaca, Mexico* **2** *CONACYT - CIIDIR Unidad Oaxaca, Instituto Politécnico Nacional, Laboratorio de Ecología de Anfibios (ECA). Hornos 1003, Col. Noche Buena, 71230, Santa Cruz Xoxocotlán, Oaxaca, Mexico*

Corresponding author: Edna González-Bernal (ednagbernal@gmail.com)

Academic editor: Annemarie Ohler | Received 14 October 2021 | Accepted 2 March 2022 | Published 21 April 2022

http://zoobank.org/BBF9F262-8B29-4E27-A437-A2A6DB319D07

Citation: Flores CA, Arreortúa M, González-Bernal E (2022) Tadpole soup: Chinantec caldo de piedra and behavior of *Duellmanohyla ignicolor* larvae (Amphibia, Anura, Hylidae). ZooKeys 1097: 117–132. https://doi.org/10.3897/zookeys.1097.76426

Abstract

Although amphibian consumption by humans has been reported globally, this practice is not well studied despite its direct implications to the decline of amphibian populations. The International Union for Conservation of Nature (IUCN) recognizes the need to document the use and trade of species to be considered in assessing their extinction risk. Here the consumption of *Duellmanohyla ignicolor* tadpoles is documented. It is a micro endemic species categorized as Near Threatened (NT) consumed in a traditional dish called "caldo de piedra" (stone soup) prepared by the Chinantec people (Tsa Ju Jmí') in Oaxaca, Mexico. Through conversations with local people and stream monitoring, the behavior of tadpoles of this species was documented and aspects of their exploitation and habitat use described. Places where caldo de piedra is still consumed were determined and using a spatial analysis with Geographic Information Systems, the distribution of the species in relation to those localities was analyzed. A number of other areas where tadpoles of this species might also occur and be exploited is predicted. In conclusion, the school behaviour, surface feeding, and the preference for deeper waterbodies that these tadpoles exhibit makes them vulnerable to being caught in large quantities. As they are consumed locally, are not commercialized, and the species distribution range is wider than caldo de piedra consumption, this implies a low risk for their populations. However, the tadpoles' reliance on streams with depths $\bar{x}$ = 60 cm and flux $\bar{x}$ = 0.65 m/s reduces the availability of sites for their optimal development.

Copyright *Carlos A. Flores et al.* This is an open access article distributed under the terms of the Creative Commons Attribution License (CC BY 4.0), which permits unrestricted use, distribution, and reproduction in any medium, provided the original author and source are credited.

Keywords
Amphibian, consumption, hot-rock cookery, Mexico, natural history, stream dwellers

Introduction

Amphibians are a vertebrate group at high extinction risk due to habitat transformation, alien species introduction, contamination, emergent diseases, climate change, and human exploitation (Kats and Ferrer 2003; Whittaker et al. 2013). Currently, at least 41% of all known anuran species are at risk and almost half show population declines (Hoffmann et al. 2010; Stuart et al. 2010; IUCN 2021a). Of the various ways that humans use amphibians, their use as food is poorly studied (Tyler et al. 2007; Gratwicke et al. 2010; Akinyemi and Ogaga 2015; Grano 2020). Amphibian consumption by humans has received far less attention than mammal and bird consumption (Ibarra et al. 2011; Chaves et al. 2019; Dobson et al. 2019; Ripple et al. 2019) and it is usually reported by social scientists who frequently fail to identify the species involved. Amphibian consumption data are often present in the grey literature and not evaluated in the context of species risk (González-Hernández 2019). Frogs have been part of the human diet since the early Pleistocene and archeological remains suggest that this consumption was not random (Kyselý 2008; Blasco et al. 2011). This practice continues in different cultures across the globe (Cooke 1989; Onadeko et al. 2011; Akinyemi and Ogaga 2015; Ohler and Nicolas 2017) and in some cases it can become a tangible species threat. For example, in Indonesia, *Fejervarya cancrivora* (Gravenhorst, 1829) (Least Concern) and *Limnonectes macrodon* (Duméril & Bibron, 1841) (Least Concern), are exploited for both local consumption and large scale exportation. Since these species are not raised in captivity, it can be assumed that all consumed individuals are collected from the wild (Kusrini and Alford 2006).

In general, amphibian consumption studies focus mainly on adult anurans with less attention paid to tadpole exploitation, even though larvae consumption might imply the need to capture larger numbers of individuals to match an equivalent nutritional yield to that of adult consumption. For example, tadpole consumption of the Western Ghats (India) endemic frog *Nasikabatrachus sahyadrensis* (Biju & Bossuyt, 2003; Purple frog), reaches up to 50% of the available individuals yearly and the proportion of collected/available tadpoles increased to 70% from 2008 to 2012, representing a direct threat to the species' survival (Thomas and Biju 2015).

Despite a genuine concern about amphibian overexploitation for human consumption and its effects on species population sizes (Stuart et al. 2004; Kusrini and Alford 2006; Onadeko et al. 2011; Talukdar and Sengupta 2020), data on species use are still scarce in relation to other threats considered by the IUCN. For example, although amphibian cultural importance and use has been widely documented in México, for Oaxaca, the state with the richest amphibian diversity in the country, only

7.55% (12/159) of the amphibian species present a general scheme of use according to the IUCN (Parra-Olea et al. 2020; Mata-Silva et al. 2021; IUCN 2021b).

Regarding tadpole consumption by humans, it is only superficially mentioned in historical writings with the species remaining unidentified (Aguilar and Luría 2016). Even now, in rural or indigenous communities where tadpoles are eaten, researchers tend to mention it only anecdotally with no formal studies on this practice.

During herpetofauna surveys in Santa Cruz Tepetotutla, our field guide Pedro Osorio-Hernández brought to our attention the local consumption of tadpoles in a soup called "caldo de piedra" (stone soup in English). Caldo de piedra is an ancient dish that is traditionally prepared on the bank of the river, using a container or rock holes in which river water, fish meat, vegetables, and raw seasonings are placed and cooked by adding heated stones. In order to study this activity, identify the tadpole species involved, and document other biological and cultural information, we conducted conversational interviews, rivers and streams surveys, spatial analysis through Geographic Information Systems, and a literature review. Here we report that tadpoles of the Sierra Juarez brook frog *Duellmanohyla ignicolor* (Duellman, 1961) are consumed in caldo de piedra in the Chinantla region, in Oaxaca Mexico. We also report on aspects of the tadpole's behavior and natural history relevant to its exploitation and survival.

Materials and methods

Study area

Santa Cruz Tepetotutla (17.7391°N, -96.5582°W) is a Chinantec indigenous community located in the southwest portion of San Felipe Usila municipality in the state of Oaxaca, Mexico (Fig. 1). It forms part of an indigenous region known as "La Chinantla", which is subdivided in three ecophysiographic subregions known as higher, medium, and lower Chinantla due to altitudinal differences (de Teresa 1999). It includes 14 municipalities and 258 communities. Throughout the region, Chinantec language is spoken in 11 variants (INEGI 2010). In their own language, Chinantecs refer to themselves as *Tsa ju jmí'*, which means "people of the ancient word" (INPI-INALI 2020).

Santa Cruz Tepetotutla preserves 9,670 ha of montane cloud forest under the Indigenous and Community Conserved Area (**ICCAs**) modality, certified by National Protected Area Commission in Mexico (**CONANP**). It supports the presence of several threatened species (Simón-Salvador et al. 2021). The main vegetation is montane cloud forest, with several streams filling two main waterways, the Tlacuache river (Fig. 2A) and the Perfume River, which discharge their waters into the Usila River that finally reaches the Presidente Miguel de la Madrid Hurtado dam in the lower Chinantla (INEGI 2014).

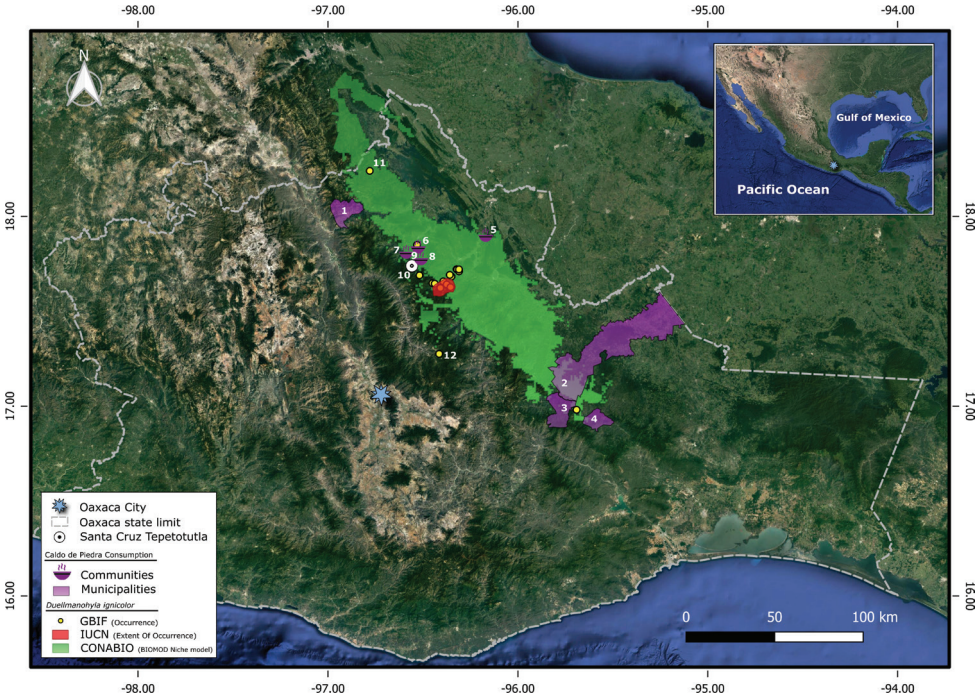

Figure 1. Study site. Santa Cruz Tepetotutla locality in Oaxaca, Mexico represented by a white dot. The red polygon represents the Extent Of Occurrence elaborated by IUCN. The green polygon represents the CONABIO model. GBIF occurrences are represented by yellow dots. Municipalities and communities where caldo de piedra is consumed are represented by areas in purple and by a purple soup icon respectively.

Species

Duellmanohyla ignicolor (Fig. 2B) is an hylid frog endemic to Oaxaca, Mexico and restricted to the Sierra Madre de Oaxaca (**SMO**) physiographic region (Duellman 1961; Duellman 2001; Ortiz- Pérez et al. 2004). According to the IUCN it is catalogued as Near Threatened (**NT**) and it has not been considered as used in trade or for human consumption (IUCN 2020).

Interviews

We conducted interviews with men and women in the community to ask mainly if caldo de piedra was still prepared locally. If it was, we asked which tadpoles were used in its preparation, where, when, and by whom they are collected, how they taste, and how they know which are edible or not.

River surveys

As the interviewees referred to tadpoles captured at the main river (Río Tlacuache); we surveyed it at accessible areas along five sections of approximately 50 m long, looking

for tadpoles with the described behavior. Once found we corroborated that those were the tadpoles used to prepare caldo de piedra by talking to a family that was eating caldo de piedra at that moment by the river. Species identification was made according to literature (Duellman 1961).

We conducted stream surveys to determine tadpole presence and stream characteristics in other waterways in the region. A total of ten waterways in addition to Río Tlacuache was surveyed in 50 m long sections. The characteristics assessed were depth, width, and water current speed measured with a flow meter Flow Watch 30 (JDC Electronics SA). Surveys took place between April and August in 2019.

Literature review and spatial analysis

To give a better perspective on caldo de piedra consumption and explore potential areas where it can be prepared with *D. ignicolor* tadpoles (Fig. 2C) as an ingredient, we reviewed ethnographic research conducted in the region related to this cooking style and cuisine. An approximation of the likelihood of *D. ignicolor* tadpoles being a component of contemporary caldo de piedra, was made with a spatial analysis that compared the species distribution with areas where this dish is consumed. Available geospatial information for *D. ignicolor* was obtained. These included the potential distribution area elaborated by the Comisión Nacional para el Conocimiento de la Biodiversidad (**CONABIO**) (Ochoa-Ochoa and Flores-Villela 2016), the Extent Of Occurrence (**EOO**) polygon elaborated by IUCN, and the species occurrence records from Global Biodiversity Information Facility (GBIF 2021). The data was compared with the sites where the elaboration of the caldo de piedra is reported in literature. The information was analyzed on QGIS 3.16.4 (Quantum GIS Development Team 2021).

Results

Interviews

Caldo de piedra with *Duellmanohyla ignicolor* tadpoles as an ingredient is still prepared and eaten in Santa Cruz Tepetotutla, although these days the main animal protein in the soup is farmed *mojarra* (*Oreochromis niloticus* (Linnaeus, 1758) or *Coptodon rendalli* (Boulenger, 1897)). During April when tadpoles are abundant, people prepare the soup both at the river and at home. Children are usually the ones that capture the *D. ignicolor* tadpoles, especially during the Easter holidays (April) when they go swimming in the river. The tadpoles are captured in plastic bags, by hand, and even with hats or caps. Innards are removed by squeezing the tadpole's body with the fingers. Once “cleaned”, they are placed in a bowl with tomato, onion, chili, salt, wild coriander, and water and then the mixture is brought to a boil by adding small hot stones until the soup is cooked.

Duellmanohyla ignicolor tadpoles are considered cleaner and thus more edible than tadpoles from other stream species because they swim at the water surface (Fig. 2D).

The tadpoles of other species in the streams are bottom dwellers and are perceived of as dirty because of their contact with the sediment. The tadpoles that are consumed are between Gosner stages 30 and 35. Later stage larvae with easily visible legs are not considered edible. Interviewees described the tadpoles as having a delicious fish-like flavor (Fig. 2E).

Duellmanohyla ignicolor tadpole habitat use and behavior

Of the ten surveyed streams in the locality, we found *D. ignicolor* tadpoles in only one of them (Bado stream) apart from the main river (Río Tlacuache). *Duellmanohyla ignicolor* tadpoles prefer deeper pools available at the edge of the stream ($\bar{x}$ = 60 cm ± SD = 7.6, n = 12 in used streams vs. $\bar{x}$ = 11.9 cm ± SD = 6, n = 54 in unused streams). Water bodies with faster currents ($\bar{x}$ = 0.65 m/s ± SD = 0.11, n = 12 in used streams vs. $\bar{x}$ = 0.31 m/s ± SD = 0.26, n = 54 in unused streams) and that are deeper at the center ($\bar{x}$ = 81.2 cm ± SD = 6.32, n = 12 in used streams vs. $\bar{x}$ = 20.8 cm, ± SD = 12.90, n = 54 in unused streams). Values of utilized waterways include measurements taken at the main river. Kruskal-Wallis test conducted on all measurements showed statistical differences P<.0001.

Duellmanohyla ignicolor tadpoles can be found at the river edge using pools formed by rocks. Most of the time, they are near to the water surface with head-up positions forming schools. It is possible to find groups composed of more than 100 individuals in ~ 4 m^2 (Fig. 2C, D). While in this position, they continuously move their mouthparts which suggests they might be feeding on suspending particles dragged by the water current or that land on the water surface. If disturbed by any unusual movement in the water, they move towards the rocks and cling to them using their large oral disc. They can also hide in the leaf litter or beneath the rocks located at the bottom of the pool. Large oral discs in this species are considered an adaptation to living in fast-moving currents (Caldwell 1974). At the study site, individuals at Gosner stage 36 reached up to 52 mm in total length.

At Río Tlacuache in Santa Cruz Tepetotutla, this species shares microhabitat with *Ptychohyla zophodes* (Campbell & Duellman, 2000) and *Incilius valliceps* (Wiegmann, 1833). In Arroyo Bado, they co-occur with *P. zophodes*. In contrast to *D. ignicolor* tadpoles, *P. zophodes* and *I. valliceps* tadpoles are benthic feeders so they spend most of the time at the bottom of the pools.

Caldo de Piedra and amphibian consumption by Chinantec people (Tsa Ju Jmí')

Caldo de Piedra was exclusively prepared by men, who dug a hole in the river sand and covered it with pozol leaves (*Calathea lutea* (Aubl) E. Mey. ex Schult, 1822) to prevent the water from escaping (river rock holes are also used). Chili, vegetables, and salt were placed inside and with a branch, some egg-sized rocks, previously heated in a campfire, were added in order to cook the food. When the water began to boil, a fish without entrails was added and cooked for 10–15 minutes. Finally, the broth was served in a plate made with pozol leaves or in a "Jícara", a bowl made of *Crescentia cujete* Linnaeus, 1753, and it was accompanied with "tortillas" (Weitlaner 1951; Bost 2009). There is

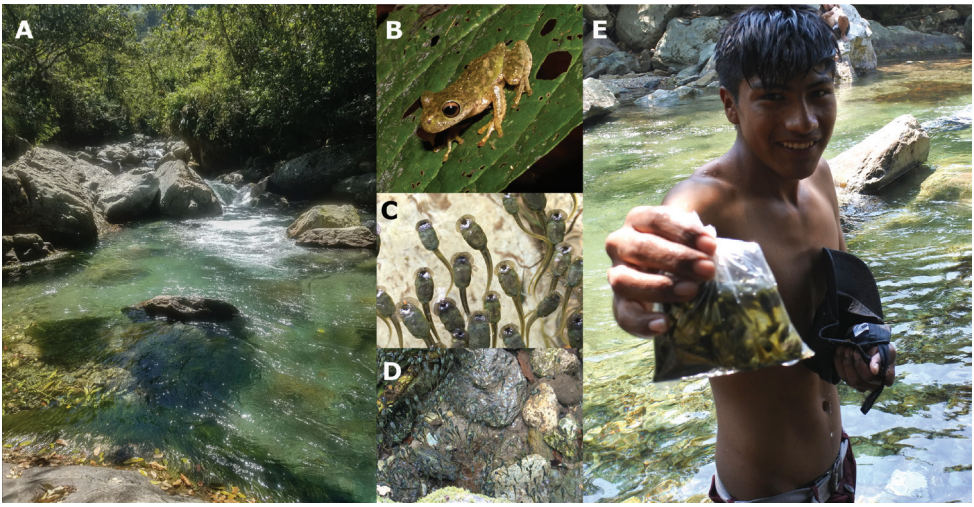

Figure 2. Aspects of *Duellmanohyla ignicolor* natural history and use **A** characteristic pools in the Tlacuache river where tadpoles aggregate **B** *D. ignicolor* adult **C** *D. ignicolor* tadpoles **D** school forming behavior **E** a teenager collecting tadpoles with a cap and keeping them in a plastic bag. Photographs: (**A, C, D, E**) by Edna González-Bernal; (**B**) by Medardo Arreortúa.

no agreement on when and by whom caldo de piedra was invented. Its ancient origin is claimed by some inhabitants of San Felipe Usila as a "millenary cooking practice uniquely developed by fishermen in his community" (Brulotte and Starkman 2014). The dish is based on a gendered division of labor where "women bathe and wash clothes in the river, but it's only adult men who fish and prepare the caldo. With the finished soup finally being offered to women and children" (Brulotte and Starkman 2014). Nevertheless, similar dishes are present in other Oaxacan cultures like Ayuk (Mixe) where it is named "caldo de playa" since it is made at the riverbanks (Nahmad 2003; Sánz 2015). There is evidence that this type of hot-rock cooking has been long used in by North American cultures (Thoms 2008), with the same cooking principle know to occur in Europe since the late Aurignacian (ca. 32,000–33,000 B.P.) and similar cooking technology occurring elsewhere in the world (Thoms 2009).

One of the common characteristics among the different descriptions of caldo de piedra from Oaxaca is the use of ingredients like tomato, chili, spices, salt, and fish (bobo fish *Joturus pichardi* Poey, 1860 and trout *Oncorhynchus mykiss* Walbaum, 1792) as the main base, but also river shrimp, prawns, and snails (Mejía and González 2019). However, no amphibians as either as tadpoles or adult frogs have been previously mentioned.

Spatial analysis

There are currently two species distribution models for *D. ignicolor* (Fig. 1). The first, presented by CONABIO uses the BIOMOD platform and suggests that the distribution of the species is 6605 km^2 including the states of Oaxaca, Puebla, and

Table 1. Location of communities and municipalities referred in Fig. 1. Inclusion (✓) or exclusion (✗) in the CONABIO and UICN distribution models for *Duellmanohyla ignicolor*. Species occurrence refers to real occurrence data.

Map id	Municipalities	Conabio	IUCN	Species Occurrence	Caldo De Piedra Consumption	Coordinates
1	Mazatlán Villa de Flores	✗	✗	✗	✓	18.032542°N, -96.915527°W
2	San Juan Cotzocón	✓	✗	✗	✓	17.160736°N, -95.783228°W
3	San Miguel Quetzaltepec	✓	✗	✓	✓	17.018643°N, -95.830581°W
4	Santiago Ixcuintepec	✓	✗	✗	✓	16.934397°N, -95.623581°W
	Communities					
5	San José Chiltepec	✗	✗	✗	✓	17.948046°N, -96.169111°W
6	San Felipe Usila	✓	✗	✗	✓	17.887505°N, -96.524692°W
7	San Juan Bautista Tlacoatzintepec	✓	✗	✗	✓	17.859707°N, -96.586562°W
8	Santiago Tlatepusco	✓	✗	✗	✓	17.825197°N, -96.509955°W
9	San Antonio del Barrio	✗	✗	✗	✓	17.758098°N, -96.556130°W
10	Santa Cruz Tepetotutla	✗	✗	✓	✓	17.739398°N, -96.558096°W
11	Ejido Clemencia	✓	✗	✓	✗	18.240000°N, -96.780000°W
12	Capulalpam de Méndez	✓	✗	✓	✗	17.275553°N, -96.414522°W

Veracruz (Ochoa-Ochoa and Flores-Villela 2016). The second model, elaborated by IUCN, uses EOO parameter and suggests that the species is restricted to only 91 km^2 within Sierra Madre de Oaxaca physiographic region (IUCN 2021b).

Occurrence records for the species obtained from GBIF (gbibID: 1897584918, 1572339861), CONABIO and MZFC (Museo de Zoología de la Facultad de Ciencias, UNAM) (Ochoa-Ochoa and Flores-Villela 2016), include three localities outside the IUCN model (Table 1). The first corresponds to a specimen collected in Capulalpam de Méndez (Departamento de Zoología, Instituto de Biología IBUNAM, CNAR24801). The second record is an observation of several adults in a stream in San Miguel Quetzaltepec municipality (Levy N. Gray, pers. comm.). It is outside south the area of the UICN model and represents the most southern known occurrence of the species. The third record corresponds to a series of specimens collected in Ejido Clemencia, a locality in Santa María Chilchotla municipality, that represents the most northern known occurrence of the species (Ochoa-Ochoa and Flores-Villela 2016).

From our spatial analysis we determined that caldo de piedra is consumed in ten localities among three regions: La Chinantla (six localities), the Mixe region (three localities), and the Cañada region (one locality). From these ten localities, only six overlap with the CONABIO distribution model of *D. ignicolor* (Fig. 1), and none of them overlap with the IUCN distribution model. In only two localities (Santa Cruz Tepetotutla and San Miguel Quetzaltepec) the species occurrence has been confirmed; only in Santa Cruz Tepetotutla has it been confirmed that caldo de piedra is prepared with *D. ignicolor* tadpoles (Table 1).

Discussion

Documenting the human use of a species is fundamental to developing conservation measures. One cause of species' declines is human consumption linked to poor regulation. Educational programs deficient in environmental and ecological foci and few or no economic alternatives for people consuming the taxa are contributing to species' declines. Seventeen native amphibian species out of 411 in Mexico are known to be consumed by humans: *Agalychnis dacnicolor* (Cope, 1864), *Ambystoma dumerilii* (Dugès, 1870), *A. mexicanum* (Shaw & Nodder, 1798), *A. taylori* (Brandon, Maruska, & Rumph, 1981), *A. velasci* (Dugès, 1888), *A. altamirani* (Dugès, 1895), *A. granulosum* (Taylor, 1944), *A. lermaense* (Taylor, 1940), *Charadrahyla taeniopus* (Günther, 1901), *Dryophytes eximius* (Baird, 1854), *Lithobates forreri* (Boulenger, 1883), *L. tlaloci* (Hillis & Frost, 1985), *L. sierramadrensis* (Taylor, 1939), *L. montezumae* (Baird, 1854), *L. spectabilis* (Hillis & Frost, 1985), *Rheohyla miotympanum* (Cope, 1863) and *Rhinella horribilis* (Wiegmann, 1833) (Huacuz 2002; Casas-Andreu et al. 2004; Carpenter et al. 2007; Altherr et al. 2011; Velarde 2012; Aguilar and Luría 2016; González-Hernández 2019; IUCN 2021a). All these species are consumed at their adult stage. Tadpole consumption has only been formally reported for one native species: *Lithobates montezumae* (Baird, 1854) and one introduced species *L. catesbeianus* (Shaw, 1802) (Casas-Andreu et al. 2004; González-Hernández 2019).

We report the first record of *Duellmanohyla ignicolor* tadpole consumption in the country in a traditional soup called caldo de piedra. In Mexico, this meal is consumed in different localities in Oaxaca, but in Santa Cruz Tepetotutla, it is prepared with *D. ignicolor* tadpoles. This tadpole soup is consumed during the hottest months (April and May: Fernández et al 2012), when people go swimming in the river. Therefore, human predation of this species takes place at the main river of the locality. The rest of the year, the soup is prepared with fish.

Biological characteristics can make tadpoles of some species more exploitable than others, for example, *Nasikabatrachus sahyadrensis* (Biju & Bossuyt, 2003) tadpoles are collected in large numbers due to their practice of attaching themselves in groups to rock surfaces in waterfalls. Consequently, people easily sweep large numbers off the rocks using branches (Thomas and Biju 2015). Concerning *D. ignicolor* tadpoles, we registered three aspects that contribute to their exploitation by humans: their feeding behavior, their school formation (McDiarmid and Altig 1999), and their preference for deeper water pools.

Duellmanohyla ignicolor tadpoles feed on suspended particles by swimming near the water surface with head-up postures. While feeding, they form schools that facilitate their catch in big numbers. This schooling behavior is associated with protection against predators, temperature, and the effectiveness of feeding strategies (Blaustein and Waldman 1992; Blaustein and Walls 1995; Spieler 2003; Hase and Kutsukake 2019). However, this behavior makes them more vulnerable to human exploitation. As they swim near the water surface, people perceive them as clean and prefer them

over co-occurring tadpoles that exhibit a benthic behavior. Tadpoles with benthic behavior (*P. zophodes* and *I. valliceps*) are considered dirty due to their association with sediments.

Contrary to previous studies that mention that *D. ignicolor* tadpoles use shallow gravel-bottomed pools in streams (Duellman 2001), we found them in deeper water bodies with faster currents. The preference for deeper water has been associated with an anti-predatory strategy and as a way to reduce the chances of pool drying during the dry season (Borges-Júnior and Rocha 2013). However, this strategy might increase the chances of human exploitation, as humans use deeper water bodies to swim.

Concerning habitat use, *D. ignicolor* tadpoles can be found in waterbodies with faster currents. The existence of another stream used by *D. ignicolor* tadpoles from where they are not extracted ensures their local presence. However, most of the available streams in the locality present lower currents, and are not used by tadpoles of this species, even when we observed adult individuals on those streams. Differences in microhabitat preference among developmental stages have been reported in other amphibian species but their causes remain to be studied (Afonso and Eterovick 2007; Eterovick et al. 2010).

It will be necessary to determine the impact of reduced availability of optimal streams combined with human extraction. In this sense, everyone we spoke with referred to tadpole consumption as local and without commercial purposes. Nobody reported selling tadpoles and we have not heard about any trading with them. *D. ignicolor* tadpole consumption is not as threatening as in cases where large numbers of larvae are extracted yearly, i.e., *Nasikabatrachus sahyadrensis* (Thomas & Biju, 2015).

From the six communities where caldo de piedra is consumed that overlap with the CONABIO species distribution model (Ochoa-Ochoa and Flores-Villela 2016), only in one, has the species presence been confirmed. It is necessary to verify that the species occurs in the remaining five communities, and if so, whether or not it is used in tadpole soup. The new record from Santa Cruz Tepetotutla confirms that the species occurs in a locality not included in any distribution model, and it represents the only instance where *D. ignicolor* tadpoles are consumed in caldo de piedra.

The information gathered can give a better perspective of the pressure factors to which the species is exposed. The conservation status of *D. ignicolor* has been recently changed from Endangered (EN) to Near Threatened (NT) as it occurs in an Indigenous and Community Conserved Area (ICCA's) (IUCN 2020). Even when some populations distribute within protected land, pressure factors occurring in the area like chytridiomycosis, land-use change, reduced availability of ideal streams and tadpole consumption, can affect this species.

Finally, we consider that the recent increase in studies on larval stages (Rivera-Correa et al. 2021) is of vital importance for the conservation of amphibians. A broader knowledge of biology, behavior, and the natural history of adult and larval stages (Malagoli et al. 2021) should allow the design of appropriate conservation measures for organisms with complex life cycles like amphibians.

Acknowledgements

We thank Pedro Osorio-Hernandez for sharing his knowledge during the field work, and the interviewees and the authorities of Santa Cruz Tepetotutla for allowing us to work in their community. María de los Ángeles Ríos, Library Coordinator for the CIESAS-Pacífico Sur, as well as those responsible for the Welte Institute and Juan de Córdova libraries allowing us to review literature in their care for this research. Allegra Noe Burger provided comments on this manuscript. Dr. Richard Wassersug and Dr. Annemarie Ohler reviewed and provided comments to improve the final manuscript. This work was financed by SEP-CONACYT Mexico Ciencia básica project # 256071. In memory of Eugui Roy.

References

Afonso LG, Eterovick PC (2007) Microhabitat choice and differential use by anurans in forest streams in southeastern Brazil. Journal of Natural History 41(13–16): 937–948. https://doi.org/10.1080/00222930701309544

Aguilar LJL, Luría MR (2016) Los anfibios en la cultura mexicana. Ciencia 67(2): 1–8.

Akinyemi AF, Ogaga ED (2015) Frog consumption pattern in Ibadan, Nigeria. Journal for Studies in Management and Planning 3(1): 522–531.

Baird SF (1854) Descriptions of new genera and species of North American frogs. Proceedings. Academy of Natural Sciences of Philadelphia 7: 59–62.

Biju SD, Bossuyt F (2003) New frog family from India reveals an ancient biogeographical link with the Seychelles. Nature 425(6959): 711–714. https://doi.org/10.1038/nature02019

Blasco R, Blain HA, Rosell J, Díez JC, Huguet R, Rodríguez J, Arsuaga JL, Bermúdez De Castro JM, Carbonell E (2011) Earliest evidence for human consumption of tortoises in the European Early Pleistocene from Sima del Elefante, Sierra de Atapuerca, Spain. Journal of Human Evolution 61(4): 503–509. https://doi.org/10.1016/j.jhevol.2011.06.002

Blaustein AR, Waldman B (1992) Kin recognition in anuran amphibians. Animal Behaviour 44: 207–221. https://doi.org/10.1016/0003-3472(92)90027-7

Blaustein AR, Walls CS (1995) Aggregation and kin recognition. In: Heatwole H, Sullivan BK (Eds.) Amphibian biology, Vol 2. Social behavior. Surrey, Beatty and Sons, Chipping, Norton, 568–602.

Borges-Júnior VNT, Rocha CFD (2013) Tropical tadpole assemblages: Which factors affect their structure and distribution? Oecologia Australis 17(2): 217–228. https://doi.org/10.4257/oeco.2013.1702.04

Bost JA (2009) Edible plants of the Chinantla, Oaxaca, Mexico with an emphasis on the participatory domestication prospects of *Persea schideana*. PhD Thesis, University of Florida, USA, 113 pp. https://ufdc.ufl.edu/UFE0024534/00001

Boulenger GA (1883) Descriptions of new species of lizards and frogs collected by Herr A. Forrer in Mexico. Annals & Magazine of Natural History 5(11): 342–344. https://doi.org/10.1080/00222938309459162

Brandon RA, Maruska EJ, Rumph WT (1981) A new species of neotenic *Ambystoma* (Amphibia, Caudata) endemic to Laguna Alchichica, Puebla, Mexico. Bulletin of the Southern California Academy of Sciences 80: 112–125.

Brulotte RL, Starkman A (2014) Caldo de Piedra and Claiming Pre-Hispanic Cuisine as Cultural Heritage. In: Brulotte RL, Di Giovine M (Eds) Edible Identities: Food as Cultural Heritage. Ashgate Publishing, Farnham, UK, 109–123. https://doi.org/10.4324/9781315578781-8

Caldwell JP (1974) Tropical treefrog communities: patterns of reproduction, size, and utilization of structural habitat. Ph.D. dissertation. University of Kansas, Lawrence.

Campbell JA, Duellman WE (2000) New species of stream-breeding hylid frogs from the northern versant of the highlands of Oaxaca, Mexico. Scientific Papers. Natural History Museum, University of Kansas 16: 1–28. https://doi.org/10.5962/bhl.title.16165

Casas-Andreu G, Méndez de la Cruz FR, Aguilar-Miguel X (2004) Anfibios y Reptiles. In: García-Mendoza AJ, Ordoñez J, Briones-Salas M (Eds) Biodiversidad de Oaxaca. Instituto de Biología, Universidad Nacional Autónoma de México. Fondo Oaxaqueño para la Conservación de la Naturaleza. World Wildlife Fund, México, 375–390.

Chaves WA, Monroe MC, Sieving KE (2019) Wild Meat Trade and Consumption in the Central Amazon, Brazil. Human Ecology 47: 733–746. https://doi.org/10.1007/s10745-019-00107-6

Cooke GR (1989) Anurans as human food in tropical America: Ethnographic, ethnohistoric and archaeologic evidence. Archaeozoologia 3(1): 123–142.

Cope ED (1863) On *Trachycephalus*, *Scaphiopus* and other Batrachia. Proceedings. Academy of Natural Sciences of Philadelphia 15: 43–54.

Cope ED (1864) Contributions to the herpetology of tropical America. Proceedings. Academy of Natural Sciences of Philadelphia 16: 166–181.

Departamento de Zoología, Instituto de Biología (IBUNAM) (2009) *Duellmanohyla ignicolor* (Duellman, 1961), ejemplar de: Colección Nacional de Anfibios y Reptiles (CNAR). Portal de Datos Abiertos UNAM México, Universidad Nacional Autónoma de México. http://datosabiertos.unam.mx/IBUNAM:CNAR:24801

de Teresa AP (1999) Población y recursos en la región chinanteca de Oaxaca. Desacatos 1: 1–24.

Dobson ADM, Milner-Gulland EJ, Ingram DJ, Keane A (2019) A Framework for Assessing Impacts of Wild Meat Hunting Practices in the Tropics. Human Ecology 47(3): 449–464. https://doi.org/10.1007/s10745-019-0075-6

Duellman WE (1961) Descriptions of two new species of frogs, genus *Ptychohyla*. Studies of American hylid frogs, V. University of Kansas Publications. Museum of Natural History 13: 349–357. https://doi.org/10.2307/3626762

Duellman WE (2001) Hylid frogs of Middle America. Second Edition. Society for the Study of Amphibians and Reptiles. Contributions to Herpetology. Ithaca, 1250 pp.

Dugès AAD (1870) Una nueva especie de ajolote de la Laguna de Patzcuaro. La Naturaleza 1: 241–244.

Dugès AAD (1888) Herpetología del Valle de México. La Naturaleza Serie II 1: 97–146.

Dugès AAD (1895) Description d'un Axolotl des Montagnes de las Cruces (*Amblystoma Altamirani*, *A. Dugès*). Institut Médico-Nacional, Imprimèrie du Ministère de Fomento, México, 64 pp.

Duméril AMC, Bibron G (1841) Erpétologie Genérale ou Histoire Naturelle Complète des Reptiles. Librarie Enclyclopedique de Roret, Paris, 112 pp.

Eterovick PC, Lazarotti I, Franco BP, Dias CJ (2010) Seasonal variation of tadpole spatial niches in permanent streams: The roles of predation risk and microhabitat availability. Austral Ecology 35(8): 879–887. https://doi.org/10.1111/j.1442-9993.2009.02094.x

Fernández EA, Romero CR, Zavala HJ, Trejo VI, Conde AC (2012) Superficies Climáticas de Temperatura Media: Atlas Climático y de Cambio Climático del Estado de Oaxaca, México. 1a edición, Centro de Ciencias de la Atmósfera. Universidad Nacional Autónoma de México. http://atlasclimatico.unam.mx/oaxaca

GBIF.org (2021) GBIF Occurrence Download.

González-Hernández AJ (2019) Estudio etnozoológico de anfibios en el Estado de México. Tesis de maestría, Universidad Autónoma del Estado de México, 105 pp. http://ri.uaemex.mx/handle/20.500.11799/105051

Grano M (2020) The Asian market of frogs as food for humans during COVID-19. Risk and consequences for public health. Medicine Papers 6(4): 77–87.

Gratwicke B, Evans MJ, Jenkins PT, Kusrini MD, Moore RD, Sevin J, Wildt DE (2010) Is the international frog legs trade a potential vector for deadly amphibian pathogens? Frontiers in Ecology and the Environment 8(8): 438–442. https://doi.org/10.1890/090111

Gravenhorst JLC (1829) Deliciae Musei Zoologici Vratislaviensis. Fasciculus primus. Chelonios et Batrachia. Leopold Voss, Leipzig, 106 pp.

Günther ACLG (1901) Reptilia and Batrachia. In: Salvin O, Godman FD (Eds) Biologia Centrali Americana, Volume 7, Part 166. R.H. Porter and Dulau and Company, London, 326 pp.

Hase K, Kutsukake N (2019) Developmental effects on social preferences in frog tadpoles, *Rana ornativentris.* Animal Behaviour 154: 7–16. https://doi.org/10.1016/j.anbehav.2019.06.001

Hillis DM, Frost JS (1985) Three new species of leopard frogs (*Rana pipiens* complex) from the Mexican Plateau. Occasional Papers of the Museum of Natural History, University of Kansas 117: 1–14.

Hoffmann M, Hilton-Taylor C, Angulo A, Böhm M, Brooks TM, Butchart SHM, Cox NA, Carpenter KE, Chanson J, Collen B, Darwall WRT, Dulvy NK, Harrison LR, Katariya V, Pollock CM, Quader S, Richman NI, Rodrigues ASL, Tognelli MF, Vié JC, Aguiar JM, Allen DJ (2010) The impact of conservation on the status of the world's vertebrates. Science 330(6010): 1503–1509. https://doi.org/10.1126/science.1194442

Huacuz D (2002) Programa de conservación y manejo de *Ambystoma dumerilii* el achoque del lago de Pátzcuaro. Universidad Michoacana de San Nicolás de Hidalgo, Fondo Mexicano para la Conservación de la Naturaleza, A.C. Secretaría de Ambiente y Recursos Naturales. Morelia, Michoacán, 138 pp.

Ibarra J, del Campo C, Barreau A, Medinaceli A, Camacho CI, Puri R, Martin GJ (2011) Etnoecología Chinanteca: Conocimiento, Práctica y Creencias Sobre Fauna y Cacería en un Área de Conservación Comunitaria de La Chinantla, Oaxaca, México. Etnobiología 9(1): 36–58.

INEGI (2010) Clasificación de lenguas indígenas Instituto Nacional de Estadística y Geografía. INEGI, c2014, México, VII, 14 pp.

INEGI (2014) Conjunto de datos vectoriales de información topográfica E14D18 (San Felipe Usila) escala 1:50 000 serie III. https://datos.gob.mx/busca/dataset/mapas-topograficos-escala-1-50-000-serie-iii-oaxaca/resource/b6c05400-36b9-40c4-bfa5-547ff3036072

INPI-INALI (2020) Atlas de los pueblos indígenas de México. Instituto Nacional de los Pueblos Indígenas. http://atlas.inpi.gob.mx/chinantecos-etnografia/

IUCN (2021a) The IUCN Red List of Threatened Species. Version 2021–1. https://www.iucnredlist.org

IUCN SSC Red List Technical Working Group (2021b) Mapping Standards and Data Quality for the IUCN Red Spatial Data. V1.19 (May 2021). https://www.iucnredlist.org/resources/mappingstandards

IUCN SSC Amphibian Specialist Group (2020) *Duellmanohyla ignicolor*. The IUCN Red List of Threatened Species 2020: e.T55308A53951963.

Kats BL, Ferrer PR (2003) Alien predators and amphibian declines: Review of two decades of science and the transition to conservation. Diversity & Distributions 9(2): 99–110. https://doi.org/10.1046/j.1472-4642.2003.00013.x

Kusrini MD, Alford RA (2006) Indonesia's Exports of Frogs' Legs. Traffic Bulletin 21(1): 13–24.

Kyselý R (2008) Frogs as a part of the Eneolithic diet. Archaeozoological records from the Czech Republic (Kutná Hora-Denemark site, Řivnáč Culture). Journal of Archaeological Science 35(1): 143–157. https://doi.org/10.1016/j.jas.2007.02.016

Linnaeus CF (1753) Species Plantarum. Holmia, 626 pp.

Malagoli LR, Pezzuti TL, Bang DL, Faivovich J, Lyra ML, Giovanelli JGR, de Anchietta Garcia PC, Sawaya RJ, Haddad CFB (2021) A new reproductive mode in anurans: natural history of *Bokermannohyla astartea* (Anura: Hylidae) with the description of its tadpole and vocal repertoire. PLoS ONE 16(2): 1–30. https://doi.org/10.1371/journal.pone.0246401

Mata-Silva V, García-Padilla E, Rocha A, DeSantis D, Johnson J, Ramírez-Bautista A, Wilson L (2021) A reexamination of the herpetofauna of Oaxaca, Mexico: composition update, physiographic distribution, and conservation commentary. Zootaxa 4996(2): 201–252. https://doi.org/10.11646/zootaxa.4996.2.1

McDiarmid RW, Altig R (1999) Tadpoles: the biology of anuran larvae. University of Chicago Press, Chicago, 458 pp.

Mejía MC, González SF (2019) La Chinantla: Crónicas gastronómicas. Universidad del Papaloapan, Secretaría de las Culturas y Artes de Oaxaca, 127 pp.

Mey E, ex Schult (1822) In: Mant. 1: 8.

Museo de Zoología de la Facultad de Ciencias, UNAM (2018) Colección de Herpetología, MZFC-UNAM.

Nahmad S (2003) Fronteras étnicas análisis y diagnóstico de dos sistemas de desarrollo: proyecto nacional vs. proyecto étnico. El caso de los "ayuuk" (mixes) de Oaxaca. México, Ciesas, 673 pp.

Ochoa-Ochoa LM, Flores-Villela OA (2016) *Duellmanohyla ignicolor* (rana arroyera de Sierra de Juárez). Distribución potencial actual, escala: 1:1000000. edición: 2. Facultad de Ciencias, Universidad Nacional Autónoma de México. Proyecto: JM022, Anfibiofauna endémica frente al cambio climático: análisis de sensibilidad e incertidumbre. CONABIO. Ciudad de México, México.

Ohler A, Nicolas V (2017) Which frog's legs do froggies eat? The use of DNA barcoding for identification of deep frozen frog legs (Dicroglossidae, Amphibia) commercialized in France. European Journal of Taxonomy 271(271): 1–11. https://doi.org/10.5852/ejt.2017.271

Onadeko AB, Egonmwan RI, Saliu JK (2011) Edible amphibian species: Local knowledge of their consumption in Southwest Nigeria and their nutritional value. West African Journal of Applied Ecology 19(1): 67–76.

Ortiz-Pérez MA, Hernández-Santana JR, Figueroa-Mah-Eng JM (2004) Reconocimiento fisiográfico y geomorfológico. In: García-Mendoza AJ, Ordoñez MJ, Briones-Salas MJ, Biodiversidad de Oaxaca (Eds) Universidad Autónoma de México, Fondo oaxaqueño para la Conservación de la Naturaleza y WWF, México, 43–544.

Parra-Olea G, García-Castillo MG, Rovito SM, Maisano JA, Hanken J, Wake DB (2020) Descriptions of five new species of the salamander genus *Chiropterotriton* (Caudata: Plethodontidae) from eastern Mexico and the status of three currently recognized taxa. PeerJ, 2020(5): 1–71. https://doi.org/10.7717/peerj.8800

Quantum GIS Development Team (2021) Quantum GIS Geographic Information System. Open-Source Geospatial Foundation Project. www.qgis.com

Ripple WJ, Wolf C, Newsome TM, Betts MG, Ceballos G, Courchamp F, Hayward MW, Valkenburgh BW, Wallach AD, Worm B (2019) Are we eating the world's megafauna to extinction? Conservation Letters 12(3): 1–10. https://doi.org/10.1111/conl.12627

Rivera-Correa M, Baldo D, Candioti FV, Goyannes V, Gambale P, Gower DJ, Quah ESH, Rowley JJL, Twomey E (2021) Amphibians in Zootaxa: 20 years documenting the global diversity of frogs, salamanders, and caecilians. Zootaxa 4979(1): 57–69. https://doi.org/10.11646/zootaxa.4979.1.9

Sánz JP (2015) Cómo se calentaba el caldo prehistórico. Boletín de Arqueología Experimental 10: 174–182.

Shaw G (1802) General Zoology or Systematic Natural History. Volume III, Part 1. Amphibia. London: Thomas Davison. https://doi.org/10.5962/bhl.title.1593

Shaw G, Nodder FP (1798) The Naturalist's Miscellany; or Coloured Figures of Natural Objects Drawn and Described Immediately from Nature. Volume 9. Nodder and Company, London, 287 pp.

Simón-Salvador PR, Arreortúa M, Flores CA, Santiago-Dionicio H, González-Bernal E (2021) The role of Indigenous and Community Conservation Areas in herpetofauna conservation: A preliminary list for Santa Cruz Tepetotutla, Oaxaca Mexico. ZooKeys 1029: 185–208. https://doi.org/10.3897/zookeys.1029.62205

Spieler M (2003) Risk of predation affects aggregation size: a study with tadpoles of *Phrynomantis microps* (Anura: Microhylidae). Animal Behaviour 65(1): 179–184. https://doi.org/10.1006/anbe.2002.2030

Stuart SN, Chanson JS, Cox NA, Young BE, Rodrigues ASL, Fischman DL, Waller RW [Eds] (2004) Status and trends of amphibian declines and extinctions worldwide. Science 306(5702): 1783–1786. https://doi.org/10.1126/science.1103538

Stuart SN, Chanson JS, Cox NA, Young BE (2010) The global decline of amphibians: Current trends and future prospects. In: Wilson LD, Townsend JH, Johnson JD (Eds)

Conservation of Mesoamerican Amphibians and Reptiles. Eagle Mountain Publishing, LC, Eagle Mountain, Utah, USA, 2–15.

Talukdar S, Sengupta S (2020) Edible frog species of Nagaland. Journal of Environmental Biology 41(4(SI)): 927–930. https://doi.org/10.22438/jeb/4(SI)/MS_1918

Taylor EH (1939) New salamanders from Mexico, with a discussion of certain known forms. The University of Kansas Science Bulletin 26: 407–430.

Taylor EH (1944) A new ambystomid salamander from the Plateau Region of Mexico. The University of Kansas Science Bulletin 30: 57–61. https://doi.org/10.5962/bhl.part.6502

Thomas A, Biju SD (2015) Tadpole consumption is a direct threat to the endangered purple frog, *Nasikabatrachus sahyadrensis.* Salamandra (Frankfurt) 51(3): 252–258.

Thoms AV (2008) The fire stones carry: Ethnographic records and archaeological expectations for hot-rock cookery in western North America. Journal of Anthropological Archaeology 27(4): 443–460. https://doi.org/10.1016/j.jaa.2008.07.002

Thoms AV (2009) Rocks of ages: Propagation of hot-rock cookery in western North America. Journal of Archaeological Science 36(3): 573–591. https://doi.org/10.1016/j.jas.2008.11.016

Tyler MJ, Wassersug R, Smith B (2007) How frogs and humans interact: Influences beyond habitat destruction, epidemics and global warming. Applied Herpetology 4(1): 1–18. https://doi.org/10.1163/157075407779766741

Velarde MT (2012) Importancia ecológica y cultural de una especie endémica de ajolote (*Ambystoma dumerilii*) del Lago de Pátzcuaro, Michoacán. Etnobiología 10: 40–49.

Weitlaner R (1951) Sobre la alimentación chinanteca. Anales del Instituto Nacional de Antropologia e Historia 33(5): 177–195.

Whittaker K, Koo MS, Wake DB, Vredenburg VT (2013) Global Declines of Amphibians. In: Levin SA (Ed.) Encyclopedia of Biodiversity. USA Academic Press, 691–699. https://doi.org/10.1016/B978-0-12-384719-5.00266-5

Wiegmann AFA (1833) Herpetologische Beyträge. I. Ueber die mexicanischen Kröten nebst Bemerkungen über ihnen verwandte Arten anderer Weltgegenden. Isis von Oken 26: 651–662.

ZooKeys 1097: 133–134 (2022)
doi: 10.3897/zookeys.1097.83215
https://zookeys.pensoft.net

CORRIGENDA

A peer-reviewed open-access journal
ZooKeys
Launched to accelerate biodiversity research

Smicromyrme frankburgeri Schmid-Egger (Hymenoptera, Mutillidae), a replacement name for *S. burgeri* Schmid-Egger, 2021, preoccupied by *S. burgeri* Lelej, 2020

Christian Schmid-Egger[1], Stefan Schmidt[2]

1 *Fischerstr. 1, 10317 Berlin, Germany* **2** *SNSB-Zoologische Staatssammlung München, Munich, Germany*

Corresponding author: Stefan Schmidt (schmidt.s@snsb.de)

Academic editor: Thorleif Dörfel | Received 10 March 2022 | Accepted 30 March 2022 | Published 21 April 2022

http://zoobank.org/463A17E4-4958-4C9F-8D14-B00303EFB9BC

Citation: Schmid-Egger C, Schmidt S (2022) *Smicromyrme frankburgeri* Schmid-Egger (Hymenoptera, Mutillidae), a replacement name for *S. burgeri* Schmid-Egger, 2021, preoccupied by *S. burgeri* Lelej, 2020. ZooKeys 1097: 133–134. https://doi.org/10.3897/zookeys.1097.83215

Abstract

Smicromyrme burgeri Schmid-Egger, 2021, a junior homonym of *S. (Eremotilla) burgeri* Lelej, 2020, is replaced with *Smicromyrme (Smicromyrme) frankburgeri* Schmid-Egger, **nom. nov.**

Keywords

Velvet ants, homonymy, replacement name

In a recent publication (Schmid-Egger and Schmidt 2021) a new species of Mutillidae from Germany was described as *Smicromyrme (Smicromyrme) burgeri* Schmid-Egger. The name of the new species turned out to be preoccupied by *Smicromyrme (Eremotilla) burgeri* Lelej, 2020, a species described from Karnataka, India (Lelej 2020), only one year before the German species was described. Both species were named after the German entomologist Frank Burger.

In accordance with Article 60 of the International Code of Zoological Nomenclature (International Commission on Zoological Nomenclature 1999), the junior homonym is replaced with a new name, *Smicromyrme (Smicromyrme) frankburgeri* Schmid-Egger, nom. nov.

Copyright *Christian Schmid-Egger & Stefan Schmidt.* This is an open access article distributed under the terms of the Creative Commons Attribution License (CC BY 4.0), which permits unrestricted use, distribution, and reproduction in any medium, provided the original author and source are credited.

Smicromyrme is a genus of velvet ants (Mutillidae) with currently approximately 270 described species from the Palearctic, Afrotropical, and Oriental regions (Pagliano et al. 2020). The Indian species, *S. burgeri* was described in the subgenus *Eremotilla* (Lelej 2020), whereas the German species belongs to the nominate subgenus.

References

International Commission on Zoological Nomenclature (1999) International Code of Zoological Nomenclature (4th Edn.). The International Trust for Zoological Nomenclature, London, 306 pp. https://www.iczn.org/the-code/the-international-code-of-zoological-nomenclature/the-code-online/

Lelej A (2020) Three new species of velvet ants from the tribe Smicromyrmini (Hymenoptera: Mutillidae) with unusual color syndrome. Far Eastern Entomologist = Dal'nevostochnyi Entomolog 421: 1–9. https://doi.org/10.25221/fee.421.1

Pagliano G, Brothers D, Cambra R, Lelej A, Lo Cascio P, Matteini Palmerini M, Scaramozzino P, Williams K, Romano M (2020) Checklist of names in Mutillidae (Hymenoptera), with illustrations of selected species. Bollettino del Museo regionale di Scienze naturali di Torino 36: 5–425.

Schmid-Egger C, Schmidt S (2021) Unexpected diversity in Central European Vespoidea (Hymenoptera, Mutillidae, Myrmosidae, Sapygidae, Scoliidae, Tiphiidae, Thynnidae, Vespidae), with description of two species of *Smicromyrme* Thomson, 1870. ZooKeys 1062: 49–72. https://doi.org/10.3897/zookeys.1062.70763

ZooKeys 1097: 135–152 (2022)
doi: 10.3897/zookeys.1097.78127
https://zookeys.pensoft.net

RESEARCH ARTICLE

A peer-reviewed open-access journal
ZooKeys
Launched to accelerate biodiversity research

How many more species are out there? Current taxonomy substantially underestimates the diversity of bent-toed geckos (Gekkonidae, *Cyrtodactylus*) in Laos and Vietnam

Hanh Thi Ngo[1,2,3,4], Quyen Hanh Do[5,6], Cuong The Pham[6], Vinh Quang Luu[7], L. Lee Grismer[8,9], Thomas Ziegler[3,4], Van Thi Hong Nguyen[2], Truong Quang Nguyen[6], Minh Duc Le[1,5,10]

1 *Central Institute for Natural Resources and Environmental Studies, Vietnam National University, 19 Le Thanh Tong, Hanoi, Vietnam* **2** *Faculty of Biology, Hanoi University of Science, 334 Nguyen Trai Road, Thanh Xuan, Hanoi, Vietnam* **3** *AG Zoologischer Garten Köln, Riehler Strasse 173, D-50735 Cologne, Germany* **4** *Institute of Zoology, University of Cologne, Zülpicher Strasse 47b, D-50674 Cologne, Germany* **5** *Faculty of Environmental Sciences, Hanoi University of Science, 334 Nguyen Trai Road, Thanh Xuan, Hanoi, Vietnam* **6** *Institute of Ecology and Biological Resources and Graduate, University of Science and Technology, Vietnam Academy of Science and Technology, 18 Hoang Quoc Viet, Cau Giay, Hanoi, Vietnam* **7** *Faculty of Forest Resources and Environmental Management, Vietnam National University of Forestry, Xuan Mai, Chuong My, Hanoi, Vietnam* **8** *Department of Herpetology, San Diego Natural History Museum, PO Box 121390, San Diego, California, 92112, USA* **9** *Herpetology Laboratory, Department of Biology, La Sierra University, 4500 Riverwalk Parkway, Riverside, California 92505, USA* **10** *Department of Herpetology, American Museum of Natural History, Central Park West at 79th Street, New York, New York 10024*

Corresponding authors: Truong Quang Nguyen (nqt2@yahoo.com), Minh Duc Le (le.duc.minh@hus.edu.vn)

Academic editor: Johannes Penner | Received 17 November 2021 | Accepted 8 March 2022 | Published 26 April 2022

http://zoobank.org/5666F9CE-D518-4B90-A1D3-EF053D4B0266

Citation: Ngo HT, Do QH, Pham CT, Luu VQ, Grismer L, Ziegler T, Nguyen VTH, Nguyen TQ, Le MD (2022) How many more species are out there? Current taxonomy substantially underestimates the diversity of bent-toed geckos (Gekkonidae, *Cyrtodactylus*) in Laos and Vietnam. ZooKeys 1097: 135–152. https://doi.org/10.3897/zookeys.1097.78127

Abstract

Cyrtodactylus is the most diverse genus of the family Gekkonidae and the world's third largest vertebrate genus. The number of species has increased more than fourfold over the last two decades. Indochina, especially Vietnam and Laos, has witnessed a surge in new species discoveries over the last three decades. The species number reported from Laos and Vietnam has remarkably increased from five in 1997 to 71 species in 2021. However, within the genus, several taxonomic issues have not yet been fully resolved. Based on recently collected samples from Laos and Vietnam, we conducted a comprehensive molecular review of *Cyrtodactylus*

Copyright *Hanh Thi Ngo et al.* This is an open access article distributed under the terms of the Creative Commons Attribution License (CC BY 4.0), which permits unrestricted use, distribution, and reproduction in any medium, provided the original author and source are credited.

occurring in Laos and Vietnam. Our molecular analysis with support from morphological comparisons showed that *C. thuongae* is a junior synonym of *C. dati* and *C. rufford* is a junior synonym of *C. lomyenensis*. In total, 68 described species distributed in Laos and Vietnam are undisputed with strong support from both molecular and morphological evidence. On the other hand, the molecular analyses revealed that there are at least seven undescribed species in Vietnam and Laos, one in the *C. angularis* group, one in the *C. chauquangensis*, and five in the *C. irregularis* group. This number will likely increase significantly, as previous work suggested that the *C. angularis* and *C. irregularis* groups harbor three and six unnamed lineages, respectively. Based on survey gaps identified in our study, it is clear that additional new species will be discovered in poorly studied regions of central Vietnam and northern and southern Laos. As many species in the genus are facing high extinction risks, several undescribed populations might already be severely threatened by human activities in both countries. Therefore, urgent taxonomic research is needed before conservation assessments of newly discovered taxa can be undertaken to protect them from anthropogenic threats.

Keywords

COI, conservation, Gekkonidae, integrative taxonomy, Southeast Asia, synonymy

Introduction

The bent-toed geckos of the genus *Cyrtodactylus* comprise the most diverse genus of the Gekkonidae with at least 330 nominal species (Uetz et al. 2021). They have a broad distribution extending from tropical South Asia, Indochina, the Philippines, and the Indo-Australian Archipelago to the Solomon Islands (Grismer et al. 2021a, b). Species in the genus can adapt to different habitat types, including limestone karst, granitic montane forests, and lowland evergreen forest. Interestingly, several species have been observed in sympatry, for example, in Phong Nha – Ke Bang National Park in Vietnam (*C. cryptus* Heidrich, Rösler, Vu, Böhme & Ziegler, 2007; *C. phongnhakebangensis* Ziegler, Rösler, Herrmann & Vu, 2003; *C. roesleri* Ziegler, Nazarov, Orlov, Nguyen, Vu, Dang, Dinh and Smith, 2010) and Ba Den Mountain in Vietnam (*C. badenensis* Nguyen, Orlov & Darevsky, 2006; *C. nigriocularis* Nguyen, Orlov & Darevsky; *C. thuongae* Phung, van Schingen, Ziegler & Nguyen, 2006) (Ziegler et al. 2003, 2010, 2013; Nguyen et al. 2006; Heidrich et al. 2007; Phung et al. 2014). Additionally, many new species of *Cyrtodactylus* have been described over the last ten years. *Cyrtodactylus* is therefore recognized as an ideal group for taxonomic, biogeographic, and ecological research as well as a model group for lizard evolution (Grismer et al. 2021a, b; 2022).

Indochina, including Cambodia, Laos, and Vietnam, has long been recognized as a region of global importance in terms of biodiversity richness (Myers et al. 2000). Laos and Vietnam have also been a hotspot of new *Cyrtodactylus* discoveries. From 1997 to present, 66 new species of *Cyrtodactylus* have been described, making it a total of 71 recognized species (Uetz et al. 2021). Remarkably, many cryptic species have recently been described based on either comparison with newly acquired collections or implementation of an integrative approach, i.e., combining evidence from morphological and molecular data. For example, *C. phongnhakebangensis* was split into two species, namely *C. phongnhakebangensis* and *C. roesleri* in 2010 (Ziegler et al. 2010), which were found to occupy different ecological niches (Loos et al. 2012), and *C. irregularis* Smith, 1921 was broken up into

multiple species (Nazarov et al. 2008; Geissler et al. 2009; Grismer et al. 2021a, b). On the other hand, several species have been synonymized. *C. paradoxus* Darevsky & Szczerbak, 1997 was shown to be a junior synonym of *C. condorensis* Smith, 1921 and *C. thochuensis* Ngo & Grismer, 2012 was recommended as a junior synonym of *C. leegrismeri* Chan & Norhayati, 2010 (Orlov et al. 2007; Grismer et al. 2015). In addition, *C. thuongae* was synonymized with *C. dati* Ngo, 2013 based on molecular evidence (Ngo et al. 2017).

In Laos, most new species described in recent years belong to the *Cyrtodactylus angularis* group, which contains at least 16 species recorded in the country. This karst-adapted clade occurs in central Laos and north-central Vietnam (Grismer et al. 2021a). Another five recently discovered species are members of the *C. chauquangensis* group, which occupies northern Laos and northwestern and north-central Vietnam. Two remaining groups include *C. brevipalmatus* and *C. irregularis*. While it is still unclear what species of the former group are present in Laos, the latter likely consists of three species in Laos, *C. buchardi* David, Teynié, Ohler, 2004; *C. cryptus*, and *C. pseudoquadrivirgatus* Rösler, Nguyen, Vu, Ngo & Ziegler, 2008 (David et al. 2004; Rösler et al. 2008; Pauwels et al. 2018; Schneider et al. 2020; Grismer et al. 2021a)

As new species of the genus have been consistently described at a rapid rate, there is a need to review the taxonomic progress and identify areas where future research should focus. Although there have been some attempts to assess the diversity of the group in Vietnam and Laos using molecular data (Nguyen et al. 2015, 2017; Brennan et al. 2017; Ngo et al. 2017), the studies either did not include a thorough taxonomic sampling of species in both countries (Brennan et al. 2017; Grismer et al. 2021a, b) or only focused on Vietnamese or Lao taxa (Nguyen et al. 2017; Ngo et al. 2017; Schneider et al. 2020). To better understand the outstanding taxonomic issues and accurately evaluate the taxonomic diversity of the group, we analyzed 68 of 71 described species and several undescribed populations from across the range of this group in Laos and Vietnam. To determine the distribution ranges of the taxa, we incorporated as many samples as possible from different localities and samples from newly discovered and undescribed populations from previous studies. In some cases where the molecular evidence was equivocal, morphological comparisons were employed to address the pending taxonomic issues.

Materials and methods

Sampling

Field work was conducted between 2009 and 2018 in Laos and Vietnam. Specimens were euthanized with ethyl acetate, fixed in approximately 85% ethanol, then transferred to 70% ethanol for permanent storage. Specimens were subsequently deposited in the collections of the Institute of Ecology and Biological Resources (**IEBR**), Vietnam Academy of Science and Technology, Hanoi, Vietnam; the Vietnam National Museum of Nature (**VNMN**), Hanoi, Vietnam; the Vietnam National University of Forestry (**VNUF**), Hanoi, Vietnam; the National University of Laos (**NUOL**), Laos; and the Zoological Research Museum Alexander Koenig (**ZFMK**), Bonn, Germany.

Morphological analysis

Main morphological characters were rechecked: Measurements were taken with a digital caliper to the nearest 0.1 mm. Abbreviations are as follows: snout-vent length (**SVL**, from tip of snout to anterior margin of cloaca); tail length (**TaL**, from posterior margin of cloaca to tip of tail).

Scale counts were taken using stereo microscopes (Leica S6E, Keyence VHX-500F): ventral scales in longitudinal rows at midbody (**V**) counted transversely across the center of the abdomen from one ventrolateral fold to the other; dorsal tubercle rows (**DTR**) counted transversely across the center of the dorsum from one ventrolateral fold to the other; supralabials (**SL**) and infralabials (**IL**) counted from the first labial scale to the corner of mouth; enlarged femoral scales (**EFS**); femoral pores (**FP**); precloacal pores (**PP**) or the total number of femoral pores and precloacal pores (i.e. the contiguous rows of femoral and precloacal scales bearing pores combined as a single meristic character referred to as the femoroprecloacal pores); number of subdigital lamellae on the fourth finger (**LD4**) and number of subdigital lamellae on the fourth toe (**LT4**) counted from the base of the first phalanx to the claw.

Molecular data and phylogenetic analysis.

Most described taxa of the genus *Cyrtodactylus* in Laos and Vietnam, except for *C. buchardi*, *C. raglai*, and *C. septimontium* were included in the study. In addition, samples of the species from different localities were sequenced to determine their distribution range. In total, 84 new samples from 26 provinces were incorporated (Suppl. material 1: Table S1). The tissue samples of muscle, liver or tail tissue was preserved separately in 70% ethanol. The mitochondrial DNA cytochrome c oxidase subunit I (COI) gene was selected as the markers have been widely used in previous studies and for some geographic populations, only COI data were available (Nguyen et al. 2015, 2017; Luu et al. 2016a; Brennan et al. 2017; Ngo et al. 2017). In several cases, where comparative data for COI were not available, the mitochondrial gene NADH dehydrogenase subunit 2 (ND2) was generated for specimens under consideration. In addition, we obtained 90 sequences of the mitochondrial COI for the ingroup taxa and one outgroup species, *Hemidactylus frenatus*, from GenBank (Wood et al. 2012).

Total genomic DNA was extracted using DNeasy Blood and Tissue Kit (Qiagen, Germany), following protocols by the manufacturer's instructions. PCR was performed using HotStar Taq Mastermix (Qiagen, Germany) to amplify approximately 657 bp fragment of the mitochondrial gene COI and approximately 1200 bp fragment of the mitochondrial gene ND2. We used two primer pairs for PCR with VF1d (5'–TTCTCAACCAACCACAARGAYATYGG-3'), VR1d (5'– TAGACTTCTGGGTGGCCRAARAAYCA–3') (Ivanova et al. 2006) for generating the COI and MetF1 (5'– AAGCTTTCGGGCCCATACC–3'), COIR1 (5'– AGRGTGCCAATGTCTTTGTGRTT–3') (Macey et al. 1997 for the ND2. The PCR volume consisted of 21 µl (2 µl each primer, 5 µl water, 10 µl of Taq mastermix and 1 – 2 µl of DNA depending on the quality of DNA in the final extraction solution). The reactions were performed at 95 °C for 15 min, followed by 35 cycles of 30 s

at 95 °C, 45 s at 48 °C, and 60 s at 72 °C with a final elongation step of 6 min at 72 °C. A negative and positive control was used for every DNA extraction and PCR reactions. PCR products were visualized using electrophoresis through a 1% agarose gel, marker 1 kb, 1X TBE and stained with ethidium bromide and photographed under UV light. Successful amplifications were purified using GeneJet PCR Purification Kit (ThermoFisher Scientific, Lithuania). Cleaned PCR products was sent to 1st Base (Malaysia) for sequencing.

Newly generated sequences were checked by eye using Sequencher v5.4 (Gene Codes Corp, Ann Arbor, MI, USA), aligned by ClustalX v2.1 (Thompson et al. 1997) with default setting. The data were then analyzed using Bayesian inference (BI) as implemented in MrBayes v3.1.2 (Ronquist et al. 2012) and maximum likelihood (ML) analysis using IQ-TREE v.1.6.7.1 (Nguyen et al. 2015) with a single molecular model and 10,000 ultrafast bootstrap (UFBP) replications. For BI, the analysis was conducted with a random starting tree and run for 1×10^7 generations. Four Markov chains, one cold and three heated (utilizing default heating values), were sampled every 1000 generations. Log likelihood scores of sample points were plotted against generation time to detect stationarity of the Markov chains. The burn-in value was set to 59 in the BI analysis, as –lnL scores reached stationarity after 59,000 generations in both runs. The optimal model, GTR+I+G, for nucleotide evolution was set to BI and ML analysis as selected by jModeltest v2.1.4 (Darriba et al. 2012). Nodal support was evaluated using UFBP as estimated in IQ-TREE v1.6.7.1 and posterior probability (PP) in MrBayes v3.2. UFBP and PP ≥ 95% are regarded as strong support for a clade (Ronquist et al. 2012; Nguyen et al. 2015). Uncorrected pairwise distance (*p*) was calculated in PAUP*v4.0b10 (Swofford 2001).

Results

Phylogenetic relationships

We successfully sequenced a fragment of the COI gene for 90 samples and ND2 gene for four samples. The final concatenated matrix consisted of 216 terminals, including 90 from this study, 126 from previous studies, including one outgroup, *Hemidactylus frenatus*, following Wood et al. (2012). Both BI and ML analyses based on a total of 657 aligned characters with no gaps and using a single model of molecular evolution produced very similar topologies (Fig. 1). All species groups were generally recovered with strong support values from both analyses, except for the *C. irregularis* group, which was corroborated only by the BI analysis (Fig. 1). The results show that *Cyrtodactylus* species in Laos and Vietnam fall into six species groups, namely *C. angularis*, *C. brevipalmatus*, *C. chauquangensis*, *C. condorensis*, *C. intermedius*, and *C. irregularis*. While Vietnam harbors members of all groups, Lao species mostly belong to the two karst-dwelling *C. angularis* and *C. chauquangensis* groups (Grismer et al. 2021a, b). Two other groups contain one taxon each from Laos, including *C.* cf. *cryptus* of the *C. irregularis* group (samples of *C. buchardi* and *C. pseudoquadrivirgatus* from Laos not included in the analysis) and *C.* cf. *ngati* of the *C. brevipalmatus* group. Two remaining mostly insular groups, the *C. condorensis* and *C. intermedius* groups, do not have any species from Laos (Fig 1, Suppl. material 1: Table S1).

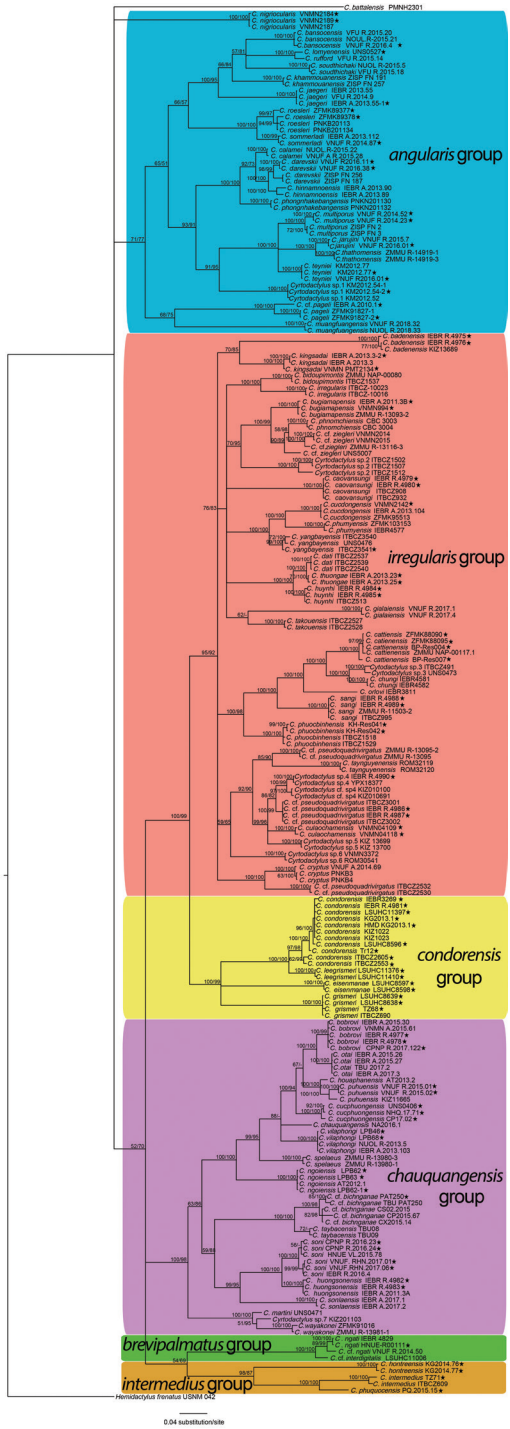

Figure 1. Bayesian cladogram based on 657 bp of the partial COI gene. Numbers above branches are Bayesian posterior probabilities and ultrafast bootstrap values of ML analysis, respectively. ★ = new sequences used in the phylogenetic analyses.

The main difference between this and previous studies is that the *Cyrtodactylus angularis* group was rendered paraphyletic. Nguyen et al. (2015) and Ngo et al. (2017) used the same COI region and confirmed that the monophyly of the group is significantly supported in the BI analysis, while its monophyletic relationship based on 1474 base pairs of the ND2 gene received perfect statistical values from both BI and ML phylogenetic estimates (Grismer et al. 2021a). All other species groups were recovered with strong support values from both analyses, except for the *C. irregularis* group, which was corroborated only by the BI analysis but received perfect statistical support in both analysis in Grismer et al. (2021a).

In the *Cyrtodactylus angularis* group, almost all species are well defined and supported by both analyses. According to our tree, the group contains 19 known species and one undescribed taxon (*Cyrtodactylus* sp. 1) in both countries. There are only three species that have notable genetic sub-structuring, i.e., *C. darevskii*, *C. multiporus*, and *C. pageli*, and samples from genetically distinct populations are labeled as cf. (Fig. 1). Another population from Khammouane Province, Laos with three representative samples, KM2012.52, KM2012.54–1, and KM2012.54–2, is clearly differentiated from other species and likely forms a new species. The former two samples were incorrectly assigned to *C. lomyenensis* in previous studies (Nazarov et al. 2014, Schneider et al. 2014). It is marked as *Cyrtodactylus* sp. 1 on the tree (Fig. 1). The highest pairwise genetic divergence between species of the *Cyrtodactylus angularis* group is 24.04% based on the fragment of COI gene (Suppl. material 2: Table S2). The lowest pairwise genetic divergence between species that are not morphologically well differentiated (SVL, LT4, LD4, Infralabials, EFS, color pattern of dorsum, and enlarged subcaudals specifications, see Tables 2, 4) is 2.44% (*C. rufford* and *C. lomyenensis*). The lowest divergence between species that are morphologically distinct is 4.57% (*C. jarujini* and *C. thathomensis*).

Members of the *Cyrtodactylus brevipalmatus* group, recently discovered in Vietnam (Le et al. 2021), are present in both countries. The genetic divergence between the Vietnamese and Lao populations of *C. ngati* is 2.13% and they are ~ 3.81–4.41% separated from *C.* cf. *interdigitalis* from Thailand. This group contains the lowest number of taxa (Fig. 1, Suppl. material 1: Table S1, Suppl. material 6: Table S6). The *C. chauquangensis* group is also distributed in both countries with 16 described species and one undescribed form, *Cyrtodactylus* sp. 7, from Vietnam. Samples of purported *C. bichnganae* are all labeled as cf. because genetic sequences of the true *C. bichnganae* have not been made available (see Pham et al. 2019). The second and third smallest groups, the *C. intermedius* and *C. condorensis* groups, have three and four species, respectively. All of the species occur in Vietnam and mostly inhabit offshore islands in the southern part of the country.

The largest group, the *Cyrtodactylus irregularis* group, consists of more than 30 species with at least five undescribed forms, *Cyrtodactylus* sp. 2 – *Cyrtodactylus* sp. 6. The highest and lowest pairwise genetic divergence that exists between species of the *C. irregularis* group are 21.41% and 0.74% (Suppl. material 3: Table S3). In addition, *C.* cf. *pseudoquadrivirgatus* is recovered in three distinct places of the tree, one close to *C. taynguyenensis*, one embedded within a clade comprising *Cyrtodactylus* sp. 4, *Cyrtodactylus* sp. 5, *C. culaochamensis*, and the other was recovered as a sister taxon to *C. cryptus*. Finally, *C. dati* and *C. thuongae* are not highly divergent in terms of pairwise genetic distance and only separated by 0.74% (Table 3, Suppl. material 3: Table S3).

The *Cyrtodactylus condorensis* group is composed of four well defined species with pairwise divergences of 5.48 – 18.05% (Suppl. material 4: Table S4). The *Cyrtodactylus chauquangensis* group is composed of 17 species which have remained stable in many analyses of phylogenetic relationships. The genetic divergences between the members of the group are ~ 3.81–19.54% (Suppl. material 5: Table S5).

Taxonomic issues

Our results based on a fragment of the mitochondrial gene COI show that the lineage containing *Cyrtodactylus thuongae* with the holotype and paratype from Tay Ninh Province and *C. dati* from the Lam Dong, Binh Phuoc populations is divided into two sub-lineages. However, the PP value is insignificant (Fig. 1). These populations are separated by no greater than 1% in sequence divergence using COI data (Table 3). In addition, genetic distances between the holotype of *C. dati* (UNS 0543) and the holotype and paratype of *C. thuongae* (IEBR A.2013.23, IEBR A.2013.25) are 2.21% and 1.85%, respectively, based on 951 bp of a fragment of the mitochondrial ND2 gene. At the time of the latter species' description, molecular data for both species were not available for comparison. Instead, *C. thuongae* was described on the basis of its highly variable morphology (Table 1). Morphological examination of specimens of *C. thuongae* and published data of *C. dati* show that morphologically they do not have a high level of distinction (size, number of ventral scales, infralabials, EFS, FP, LT4, enlarged subcaudals, color pattern of dorsum. The only differences between the two species are: DTR: 17 or 18 in *C. thuongae* vs. 20–22 in *C. dati*, SL: 7–9 in *C. thuongae* vs. 10–12 in *C. dati* and 0 or 1 pitted scales in males in *C. thuongae* vs. five or six in *C. dati*.

Much the same is true for *C. lomyenensis* from Khammouan (paratype – UNS0527) and *C. rufford* also from Khammouan (holotype – VFU R.2015.14). Genetic divergence between the two species is less than 2.44% based on a fragment of mitochondrial gene COI. According to our morphological examinations between specimens of

Table 1. Morphological characters of *Cyrtodactylus dati*, *C. huynhi*, *C. thuongae.*

	C. dati	***C. thuongae***	***C. huynhi* without UNS 0327**	***C. huynhi* UNS 0327 paratype, M**
Article	Ngo 2013	Phung et al. 2014	Ngo et al. 2008	Ngo and Bauer 2008
Locality	Binh Phuoc	Tay Ninh	Dong Nai	Dong Nai
SVL	max 70.1	57.3 – 77.6	67.2 – 79.8	54.8
TaL	max 57.3	max 78.1	61.5 – 78.6	29.1
V	42 – 48	29 – 44	43 – 46	44
DTR	20 – 22	17 – 18	16 – 18	18
SL	10 – 12	7 – 9	?	?
IL	8 – 10	7 – 10	?	?
EFS	4 – 7	2 – 5	3 – 5	/
FP	3 – 4 each	0 – 3 (pitted scales)	3 – 8	4+4
PP in males	5 – 6	0 – 1 (pitted scales)	7 – 9	9
PP in females	?	0	0 – 8 (pitted scales)	?
LD4	?	14 – 17	14 – 17	15
LT4	18 – 19	14 – 20	17 – 21	17
Color pattern of dorsum	blotched	blotched	banded	banded
Enlarged subcaudals	absent	absent	absent	absent

Table 2. Morphological characters of *Cyrtodactylus rufford* and *C. lomyenensis.*

	C. lomyenensis	*C. rufford*
Article	Ngo and Pauwels 2010	Luu et al. 2016b
Locality	Khammouan Province	Khammouan Province
SVL	max 71.2	max 72.5
TaL	max 86.1 (Reg)	max 96.8
V	35 – 36	27 – 29
DTR	20 – 24	14 – 16
SL	13 – 14	11 – 12
IL	11	9 – 11
EFS	17 – 18	17 – 18
Total of FP and PP in males	39 – 40	42 – 43
LD4	16 – 19	19 – 20
LT4	19 – 23	18 – 19
Color pattern of dorsum	four narrow yellowish-cream transversal bands	three or four light transverse bands
Enlarged subcaudals	medially enlarged	medially enlarged

Table 3. Uncorrected ("p") distance matrix showing percentage genetic divergence (COI) between *Cyrtodactylus dati*, *C. thuongae*, and closely related species. Numbers in bold are the lowest percentages.

Species	1	2	3	4	5	6	7	8	9	10	11	12
1. *C. bidoupimontis* HQ967215	–											
2. *C. bugiamapensis* IEBR A.2011.3B	13.24	–										
3. *C. caovansungi* NT.2016.2	15.07	14.0	–									
4. *C. cucdongensis* VNMN PMT 2142	13.70	14.16	15.68	–								
5. *C. cryptus* KX064038	14.31	15.53	15.07	14.92	–							
6. *C. dati* KF929508	14.71	15.05	17.07	17.04	16.78	–						
7. *C. huynhi* KF169948	14.18	15.24	16.71	16.68	16.77	**4.18**	–					
8. *C. irregularis* KP199951	8.86	15.13	16.96	14.05	14.97	14.71	14.89	–				
9. *C. takouensis* KF929533	13.26	11.98	13.45	12.32	15.31	13.64	12.36	13.42	–			
10. *C. thuongae* IEBR A.2013.23	14.61	14.61	16.44	16.44	15.53	**0.74**	**3.83**	14.52	13.46	–		
11. *C. yangbayensis* ITBCZ 3540	12.79	12.33	15.22	7.92	15.22	15.22	14.31	12.83	11.60	14.46	–	
12. *C. ziegleri* HQ967210	14.41	7.36	14.41	15.34	15.17	15.42	15.07	15.51	12.59	15.02	13.15	–

Table 4. Uncorrected ("p") distance matrix showing percentage genetic divergence (COI) between *Cyrtodactylus lomyenensis*, *C. rufford* and closely related species. Number in bold is the lowest percentage.

Species	1	2	3	4	5	6	7	8
1. *C. bansocensis* KU175573	–							
2. *C. jaegeri* KT004364	15.09	–						
3. *C. khammouanensis* HM888469	12.04	14.92	–					
4. *C. lomyenensis* UNS0527	11.58	15.22	11.72	–				
5. *C. sommerladi* KJ817437	15.55	15.83	16.44	15.98	–			
6. *C. soudthichaki* KX077904	12.65	14.16	13.55	14.00	15.55	–		
7. *C. roesleri* KF929531	15.97	15.27	16.39	16.13	6.22	15.11	–	
8. *C. rufford* KU175572	11.43	14.61	11.87	**2.44**	17.20	14.46	16.28	–

C. rufford and published data of *C. lomyenensis*, *C. rufford* differs from *C. lomyenensis* by having fewer ventral scale rows (27–29 vs. 35 or 36), fewer supralabials (10–12 vs. 13 or 14), and more femoral and precloacal pores in males (42 or 43 vs. 39 or 40) (Table 2). The differences are quite small, except for the ventral scale row. In addition, *C. rufford* is similar to *C. lomyenensis* in size and coloration: head dorsum yellowish with irregular brown blotches, dorsal pattern with transverse bands, rings on original tail with dark brown transversal bands wider than light brown spaces, and median

row of enlarged subcaudal scales. In addition, genetic distance between the paratype of *C. lomyenensis* (UNS0527) and holotype of *C. rufford* (VFU R.2015.14) is 0.21% based on 413 bp of a fragment of the mitochondrial ND2 gene.

Discussion

In general, the phylogenetic relationships supported by this study are similar to those corroborated by previous studies using the same genetic marker (Nguyen et al. 2013; Luu et al. 2016a; Brennan et al. 2017; Ngo et al. 2017). However, some outstanding issues remain unresolved. Specifically, this study shows that *C. badenensis* is a member of the *C. irregularis* group, although Grismer et al. (2021a) based on ND2 suggested that the species belongs to *C. condorensis* or an independent lineage. The *C. irregularis* group contains several taxonomically unconfirmed populations. For example, *C.* cf. *ziegleri* revealed to be at least two taxa, while the phylogenetic placement of the true *C. ziegleri*, similarly to the previously reported cases in *C. bichnganae* in the *C. chauquangensis* group, has not been clarified in previous studies. Our study also confirms that although COI is a good marker for DNA barcoding it is limited by its length and lacks characters to resolve deeper nodes.

Cyrtodactylus has a complex taxonomic history and at least two species have been synonymized before this study. Grismer et al. (2015) examined the taxonomy of *C. condorensis* and *C. intermedius* complex using 100 samples from 30 localities and their analyses based on the mitochondrial ND2 suggested that *C. paradoxus* is a junior synonym of *C. condorensis* and *C. thochuensis* is a junior synonym of *C. leegrismeri*. Based on the similarities of morphological and molecular data, we consider *C. thuongae* Phung, van Schingen, Ziegler & Nguyen, 2014 a junior synonym of *C. dati* Ngo, 2013 and place *C. rufford* Luu, Calame, Nguyen, Le, Bonkowski & Ziegler, 2016b in the synonymy of *C. lomyenensis* Ngo & Pauwels, 2010. With two more species synonymized in this study, *Cyrtodactylus* from Vietnam and Laos currently consists of 69 valid species, including 47 from Vietnam and 22 from Laos (of these, *C. cryptus* and *C. roesleri* are known from both countries). Independent of morphological evidence, our molecular phylogenetic results confirm that other lineages represent undisputed species.

The number of *Cyrtodactylus* species within six identified species groups will likely change as new discoveries continue to be made at a rapid rate. At least seven unnamed lineages are confirmed by our study, one in the *C. angularis* group, one in the *C. chauquangensis* group, and five others in the *C. irregularis* group. In addition, several species complexes, such as *C. pseudoquadrivirgatus* and *C. ziegleri*, warrant further taxonomic clarification and future studies will probably reveal that some of the lineages within the complexes turn out to be new taxa. Of these, *C. pseudoquadrivirgatus* is most problematic because it was described using the type series from a wide distribution while at the moment, many members of the genus *Cyrtodactylus* are known for their notable site-restricted endemism. It is recommended that the species definition be redefined to the holotype of *C. pseudoquadrivirgatus* from A Luoi in Thua Thien Hue Province (including voucher/field numbers ITBCZ3001, ITBCZ3002, AL.2017.125, AL.2017.126), or to topotypic specimens, viz. the series in case they can be clearly proven to represent that taxon.

Grismer et al. (2021a) also suggest that several other unnamed lineages are present in Vietnam and Laos. The *Cyrtodactylus angularis* group comprises three undescribed taxa from Laos, while the *C. irregularis* group includes six. The results of this and our study clearly demonstrate that the *C. irregularis* group is the most speciose within the genus, but there exist many more cryptic species that have not been formally described thus far, in particular from southern Vietnam, a hotspot of this group. It is also noted that several areas in Vietnam and Laos are still poorly studied. More surveys in the areas, in particular the karst region in the northern Annamites, the southern Annamites, and the Central Highlands in Vietnam and northern karst region in northern Laos and the lowland area in southern Laos, will certainly yield more new taxa for science (Fig. 2).

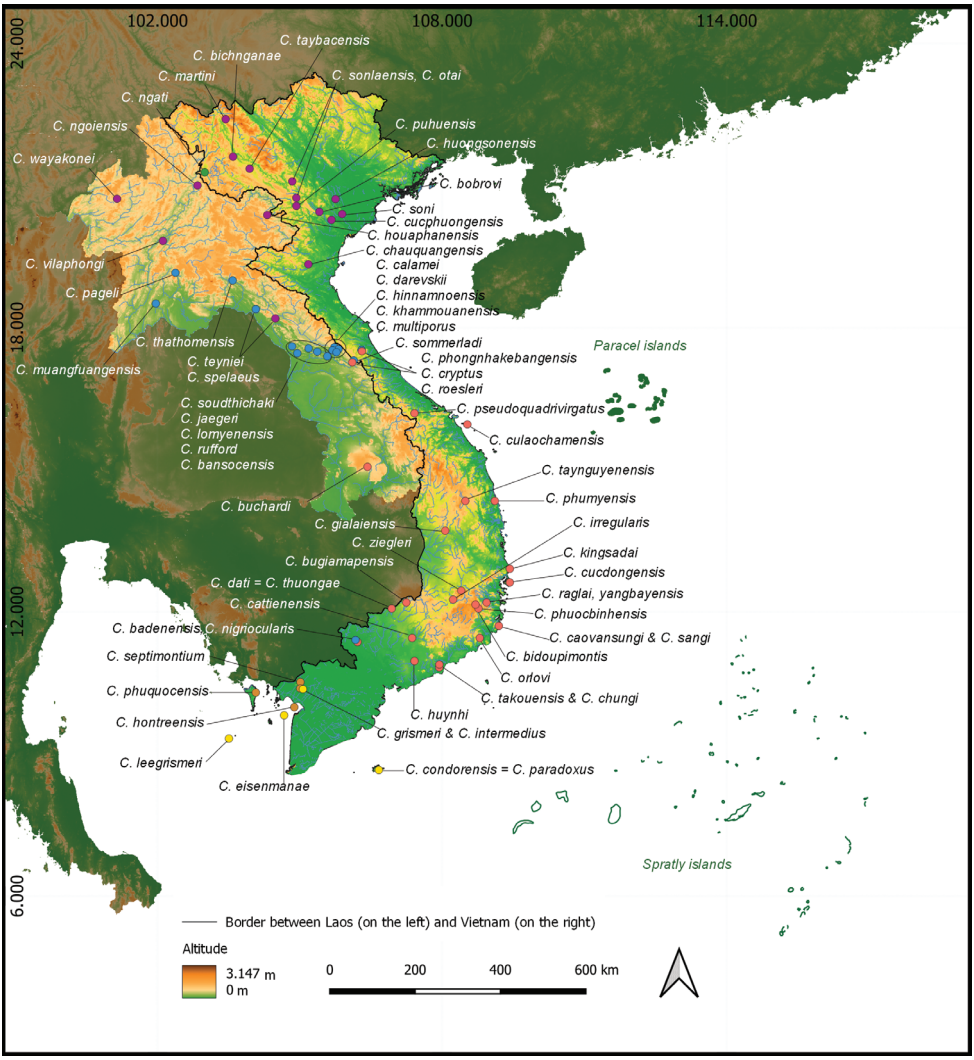

Figure 2. Type localities of all *Cyrtodactylus* taxa occurring in Laos and Vietnam (the altitude data based on GADM database of Global Administrative Areas, 2021).

According to the IUCN Red List, several species of this genus in Laos and Vietnam are facing exceedingly high extinction risks, including four species listed as Critically Endangered, three Endangered, and eight Vulnerable (IUCN Red List 2021). The recently described *Cyrtodactylus gialaiensis* is only known from a single locality with a distribution range of less than 10 km^2 and a population of fewer than 50 individuals (Luu et al. 2017, 2020). However, a majority of *Cyrtodactylus* still need to be carefully evaluated and it is likely that additional assessment will result in a higher number of species to be listed in the IUCN Red List in the future. Taxonomic uncertainty is also hindering conservation efforts, as some undescribed populations might already be critically threatened by human activities in both countries. Urgent research is therefore needed to resolve pending taxonomic issues before conservation assessments for the taxa can be undertaken.

Information on biogeographic ranges of six *Cyrtodactylus* groups occurring in Laos and Vietnam was detailed in Grismer et al. (2021a). According to geographic distribution of our newly collected samples, several species have broader ranges than previously documented. For example, while the occurrences of *C. cattienensis* were reported for the first time from Dong Nai and Ba Ria-Vung Tau provinces, we herein record it from Dong Phu District, Binh Phuoc Province. Distribution of *C. cucdongensis* is extended to Dak Nong Province, *C. huongsonensis* to Lac Thuy District, Hoa Binh Province, *C. kingsadai* to Khanh Hoa and Dak Nong provinces, and *C. phuocbinhensis* to Khanh Hoa Province. With more sampling of the members of the genus in Laos and Vietnam, our knowledge of its taxonomy, distribution, and conservation in the two countries will be improved in the future.

Acknowledgements

We thank A.V. Pham, T.V. Nguyen, D.T. Le, T.M. Phung for their assistance in the field. T.V. Nguyen, H.T. Duong, G.H.T. Cao, T.T. Nguyen, N.D. Pham, T.P.T. Bui, A.N.T. Ho assisted laboratory work. This research was funded by the Vietnam National Foundation of Science and Technology Development (NAFOSTED) under grant number 106.05-2020.24. Research of H. T. Ngo in Germany is funded by the German Academic Exchange Service (DAAD). Comments from Aaron Bauer, Mark D. Scherz, the editor, and two anonymous reviewers greatly improved the paper.

References

Brennan IG, Bauer AM, Ngo TV, Wang Y-Y, Wang W-Z, Zhang Y-P, Murphy RW (2017) Barcoding utility in a mega-diverse, cross-continental genus: Keeping pace with *Cyrtodactylus* geckos. Scientific Reports 7(1): e5592. https://doi.org/10.1038/s41598-017-05261-9

Darriba D, Taboada GL, Doallo R, Posada D (2012) jmodelTest 2: More models, new heuristics and high-performance computing. Nature Methods 9(8): e772. https://doi.org/10.1038/nmeth.2109

David P, Teynié A, Ohler A (2004) A new species of *Cyrtodactylus* Gray, 1827 (Reptilia: Squamata: Gekkonidae) from southern Laos. The Raffles Bulletin of Zoology 52: 621–627.

GADM Global Administrative Areas (2021) University of California, Berkely. http://www.gadm.org [accessed 08 September 2021]

Geissler P, Nazarov R, Orlov NL, Böhme W, Phung TM, Nguyen TQ, Ziegler T (2009) A new species of the *Cyrtodactylus irregularis* complex (Squamata: Gekkonidae) from southern Vietnam. Zootaxa 2161(1): 20–32. https://doi.org/10.11646/zootaxa.2161.1.2

Grismer LL, Poyarkov NA, Quah ESH, Grismer JL, Wood Jr PL (2022) The biogeography of bent-toed geckos, Cyrtodactylus (Squamata: Gekkonidae). PeerJ 10(40): e13153. https://doi.org/10.7717/peerj.13153

Grismer LL, Wood PL, Ngo VT, Murdoch ML (2015) The systematics and independent evolution of cave ecomorphology in distantly related clades of Bent-toed Geckos (Genus *Cyrtodactylus* Gray, 1827) from the Mekong Delta and islands in the Gulf of Thailand. Zootaxa 3980(1): 106–126. https://doi.org/10.11646/zootaxa.3980.1.6

Grismer LL, Wood Jr PL, Poyarkov NA, Le MD, Kraus F, Agarwal I, Oliver PM, Nguyen SN, Nguyen TQ, Karunarathna S, Welton LJ, Stuart BL, Luu VQ, Bauer AM, O'Connell KA, Quah ESH, Chan KO, Ziegler T, Ngo H, Nazarov RA, Aowphol A, Chomdej S, Suwannapoom C, Siler CD, Anuar S, Tri NV, Grismer JL (2021a) Phylogenetic partitioning of the third-largest vertebrate genus in the world, *Cyrtodactylus* Gray, 1827 (Reptilia; Squamata; Gekkonidae) and its relevance to taxonomy and conservation. Vertebrate Zoology 71: 101–154. https://doi.org/10.3897/vertebrate-zoology.71.e59307

Grismer L, Wood PL, Poyarkov Jr NA, Le MD, Karunarathna S, Chomdej S, Suwannapoom C, Qi S, Liu S, Che J, Quah ESH, Kraus F, Oliver PM, Riyanto A, Pauwels OSG, Grismer JL (2021b) Karstic landscapes are foci of species diversity in the world's third-largest vertebrate genus *Cyrtodactylus* Gray, 1827 (Reptilia: Squamata: Gekkonidae). Diversity (Basel) 13(5): e183. https://doi.org/10.3390/d13050183

Heidrich A, Rösler H, Vu NT, Böhme W, Ziegler T (2007) Another new *Cyrtodactylus* (Squamata: Gekkonidae) from Phong Nha-Ke Bang National Park, central Truong Son, Vietnam. Zootaxa 1445(1): 35–48. https://doi.org/10.11646/zootaxa.1445.1.3

Ivanova NV, Waard J, Hebert PDN (2006) An inexpensive, automation-friendly protocol for recovering high-quality DNA. Molecular Ecology Notes 6(4): 998–1002. https://doi.org/10.1111/j.1471-8286.2006.01428.x

Le DT, Sitthivong S, Tran TT, Grismer LL, Nguyen TQ, Le MD, Ziegler T, Luu VQ (2021) First record of the *Cyrtodactylus brevipalmatus* group (Squamata: Gekkonidae) from Vietnam with description of a new species. Zootaxa 4969(3): 492–510. https://doi.org/10.11646/zootaxa.4969.3.3

Loos J, von Wehrden H, Dang KN, Ziegler T (2012) Niche segregation in microhabitat use in of three sympatric *Cyrtodactylus* in the Phong Nha – Ke Bang National Park, central Vietnam. Herpetological Conservation and Biology 7: 101–108.

Luu VQ, Bonkowski M, Nguyen TQ, Le MD, Schneider N, Ngo HT, Ziegler T (2016a) Evolution in karst massifs: Cryptic diversity among bent-toed geckos along the Truong Son Range with descriptions of three new species and one new country record from Laos. Zootaxa 4107(2): 101–140. https://doi.org/10.11646/zootaxa.4107.2.1

Luu VQ, Calame T, Nguyen TQ, Le MD, Bonkowski M, Ziegler T (2016b) *Cyrtodactylus rufford*, a new cave-dwelling bent-toed gecko (Squamata: Gekkonidae) from Khammouane Province, central Laos. Zootaxa 4067(2): 185–199. https://doi.org/10.11646/zootaxa.4067.2.4

Luu VQ, Tran DV, Nguyen TQ, Le MD, Ziegler T (2017) A new species of the *Cyrtodactylus irregularis* complex (Squamata: Gekkonidae) from Gia Lai Province, Central Highlands of Vietnam. Zootaxa 4362(3): 385–403. https://doi.org/10.11646/zootaxa.4362.3.4

Luu VQ, Lo OV, Hoang TT, Pham TV, Le Duc O, Bordes C, Leprince B, Amori G, Luiselli L (2020) Ecological characteristics of a recently described, critically endangered gecko species, endemic to Central Highland, Vietnam. Tropical Zoology 33(2): 53–62. https://doi.org/10.4081/tz.2020.71

Macey JJ, Larson A, Ananjeva NB, Fang Z, Papenfuss TJ (1997) Two novel gene orders and the role of light-strand replication in rearrangement of the vertebrate mitochondrial genome. Molecular Biology and Evolution 14(1): 91–104. https://doi.org/10.1093/oxfordjournals.molbev.a025706

Myers N, Mittermeier RA, Mittermeier CG, da Fonseca GAB, Kent J (2000) Biodiversity hotspots for conservation priorities. Nature 403(6772): 853–858. https://doi.org/10.1038/35002501

Nazarov RA, Orlov NL, Nguyen SN, Ho CT (2008) Taxonomy of naked-toe geckos *Cyrtodactylus irregularis* complex of South Viet Nam and description of a new species from Chu Yang Sin Natural Park (Krong Bong District, Dac Lac Province), Viet Nam. Russian Journal of Herpetology 15: 141–156.

Nazarov RA, Poyarkov NA, Orlov NL, Nguyen SN, Milto KD, Martynov AA, Konstantinov EL, Chulisov AS (2014) A review of genus *Cyrtodactylus* (Reptilia: Sauria: Gekkonidae) in fauna of Laos with description of four new species. Proceedings of the Zoological Institute RAS 318: 391–423.

Ngo TV (2013) *Cyrtodactylus dati*, a new forest dwelling Bent-toed Gecko (Squamata: Gekkonidae) from southern Viet Nam. Zootaxa 3616(2): 151–164. https://doi.org/10.11646/zootaxa.3616.2.4

Ngo TV, Bauer AM (2008) Descriptions of two new species of *Cyrtodactylus* Gray 1827 (Squamata: Gekkonidae) endemic to southern Vietnam. Zootaxa 1715(1): 27–42. https://doi.org/10.11646/zootaxa.1715.1.2

Ngo TV, Pauwels OSG (2010) A new cave-dwelling species of *Cyrtodactylus* Gray, 1827 (Squamata: Gekkonidae) from Khammouane Province, southern Laos. Zootaxa 2730(1): 44–56. https://doi.org/10.11646/zootaxa.2730.1.3

Ngo HT, Le MD, Pham ND, Nguyen HVT, Pham CT, Nguyen TQ (2017) Taxonomy and Phylogenetic Relationships of *Cyrtodactylus* (Squamata: Gekkonidae) in Vietnam. VNU Journal of Science: Natural Sciences and Technology 33: 182–192. https://doi.org/10.25073/2588-1140/vnunst.4530

Nguyen SN, Orlov NL, Darevsky IS (2006) Descriptions of two new species of the genus *Cyrtodactylus* Gray, 1827 (Squamata: Sauria: Gekkonidae) from southern Vietnam. Russian Journal of Herpetology 13: 215–226.

Nguyen SN, Le NTT, Tran DTA, Orlov NL, Lathrop A, Macculloch RD, Le DTT, Jin J-Q, Nguyen LT, Nguyen TT, Hoang DD, Che J, Murphy RW, Zhang Y-P (2013) Phylogeny of the *Cyrtodactylus irregularis* species complex (Squamata: Gekkonidae) from Viet Nam with the description of two new species. Zootaxa 3737(4): 399–414. https://doi.org/10.11646/zootaxa.3737.4.4

Nguyen TQ, Le MD, Pham AV, Ngo HN, Hoang CV, Pham CT, Ziegler T (2015) Two new species of *Cyrtodactylus* (Squamata: Gekkonidae) from the karst forest of Hoa Binh Province, Viet Nam. Zootaxa 3985(3): 375–390. https://doi.org/10.11646/zootaxa.3985.3.3

Nguyen TQ, Pham AV, Ziegler T, Ngo HT, Le MD (2017) A new species of *Cyrtodactylus* (Squamata: Gekkonidae) and the first record of *C. otai* from Son La Province, Vietnam. Zootaxa 4341: 025–040. https://doi.org/10.11646/zootaxa.4341.1.2

Orlov NL, Nguyen QT, Nazarov RA, Ananjeva NB, Nguyen SN (2007) A new species of the genus *Cyrtodactylus* Gray, 1827 and redescription of *Cyrtodactylus paradoxus* (Darevsky & Szczerbak, 1997). Russian Journal of Herpetology 14: 145–152. [Squamata: Sauria: Gekkonidae]

Pauwels OSG, Nazarov RA, Bobrov VV, Poyarkov NA (2018) Taxonomic of two populations of Bent-toed Geckos of the *Cyrtodactylus irregularis* complex (Squamata: Gekkonidae) with description of a new species from Nui Chua National Park, southern Vietnam. Zootaxa 4403(2): 307–335. https://doi.org/10.11646/zootaxa.4403.2.5

Pham AV, Le MD, Ngo HT, Ziegler T, Nguyen TQ (2019) A new species of *Cyrtodactylus* (Squamata: Gekkonidae) from northwestern Vietnam. Zootaxa 4544(3): 360–380. https://doi.org/10.11646/zootaxa.4544.3.3

Phung TM, van Schingen M, Ziegler T, Nguyen TQ (2014) A third new *Cyrtodactylus* (Squamata: Gekkonidae) from Ba Den Mountain, Tay Ninh Province, southern Viet Nam. Zootaxa 3764(3): 347–363. https://doi.org/10.11646/zootaxa.3764.3.5

Red List IUCN (2021) The IUCN Red List of Threatened Species. https://www.iucnredlist.org [accessed Oct 3, 2021]

Ronquist F, Teslenko M, van der Mark P, Ayres DL, Darling A, Höhna S, Larget B, Liu L, Suchard MA, Huelsenbeck JP (2012) MrBayes 3.2: Efficient Bayesian phylogenetic inference and model choice across a large model space. Systematic Biology 61(3): 539–542. https://doi.org/10.1093/sysbio/sys029

Rösler H, Vu TN, Nguyen TQ, Ngo TV, Ziegler T (2008) A new *Cyrtodactylus* (Squamata: Gekkonidae) from central Vietnam. Hamadryad 32: 125–140.

Schneider N, Phung TM, Le MD, Nguyen TQ, Ziegler T (2014) A new *Cyrtodactylus* (Squamata: Gekkonidae) from Khanh Hoa Province, southern Viet Nam. Zootaxa 3785(4): 518–532. https://doi.org/10.11646/zootaxa.3785.4.2

Schneider N, Luu VQ, Sithivong S, Teynie A, Le MD, Nguyen TQ, Ziegler T (2020) Two new species of *Cyrtodactylus* (Squamata: Gekkonidae) from northern Laos, including new finding and expanded diagnosis of *C. bansocensis*. Zootaxa 4822(4): 503–530. https://doi.org/10.11646/zootaxa.4822.4.3

Swofford DL (2001) PAUP*. Phylogenetic Analysis Using Parsimony (* and Other Methods). Version 4. Sinauer Associates, Sunderland, Massachusetts.

Thompson JD, Gibson TJ, Plewniak F, Jeanmougin F, Higgins DG (1997) The ClustalX windows interface: Flexible strategies for multiple sequence alignment aided by quality analysis tools. Nucleic Acids Research 25(24): 4876–4882. https://doi.org/10.1093/nar/25.24.4876

Uetz P, Hallermann J, Hosek J (Eds) (2021) The Reptile Database. http://www.reptile-database.org [accessed 08 September 2021]

Wood Jr PL, Heinicke MP, Jackman TR, Bauer AM (2012) Phylogeny of bent-toed geckos (*Cyrtodactylus*) reveals a west to east pattern of diversification. Molecular Phylogenetics and Evolution 65(3): 992–1003. https://doi.org/10.1016/j.ympev.2012.08.025

Ziegler T, Rösler H, Herrmann HW, Nguyen TV (2003) *Cyrtodactylus phongnhakebangensis* sp. n. Ein neuer Bogenfingergecko aus dem annamitischen Karstwaldmassiv, Vietnam. Herpetofauna 24: 11–25.

Ziegler T, Nazarov R, Orlov N, Nguyen TQ, Vu TN, Dang KN, Dinh TH, Schmitz A (2010) A third new *Cyrtodactylus* (Squamata: Gekkonidae) from Phong Nha – Ke Bang National Park, Vietnam. Zootaxa 2413(1): 20–36. https://doi.org/10.11646/zootaxa.2413.1.2

Ziegler T, Phung TM, Le MD, Nguyen TQ (2013) A new *Cyrtodactylus* (Squamata: Gekkonidae) from Phu Yen Province, southern Viet Nam. Zootaxa 3686(4): 432–446. https://doi.org/10.11646/zootaxa.3686.4.2

Supplementary material 1

Table S1

Authors: Hanh Thi Ngo, Quyen Hanh Do, Cuong The Pham, Vinh Quang Luu, L. Lee Grismer, Thomas Ziegler, Van Thi Hong Nguyen, Truong Quang Nguyen, Minh Duc Le

Data type: Docx file.

Explanation note: Samples used in this study.

Copyright notice: This dataset is made available under the Open Database License (http://opendatacommons.org/licenses/odbl/1.0/). The Open Database License (ODbL) is a license agreement intended to allow users to freely share, modify, and use this Dataset while maintaining this same freedom for others, provided that the original source and author(s) are credited.

Link: https://doi.org/10.3897/zookeys.1097.78127.suppl1

Supplementary material 2

Table S2

Authors: Hanh Thi Ngo, Quyen Hanh Do, Cuong The Pham, Vinh Quang Luu, L. Lee Grismer, Thomas Ziegler, Van Thi Hong Nguyen, Truong Quang Nguyen, Minh Duc Le

Data type: Docx file.

Explanation note: Uncorrected ("p") distance matrix showing percentage genetic divergence (COI) (highlighted in bold are the lowest and highest percentage) between species in the *Cyrtodactylus angularis* group.

Copyright notice: This dataset is made available under the Open Database License (http://opendatacommons.org/licenses/odbl/1.0/). The Open Database License (ODbL) is a license agreement intended to allow users to freely share, modify, and use this Dataset while maintaining this same freedom for others, provided that the original source and author(s) are credited.

Link: https://doi.org/10.3897/zookeys.1097.78127.suppl2

Supplementary material 3

Table S3

Authors: Hanh Thi Ngo, Quyen Hanh Do, Cuong The Pham, Vinh Quang Luu, L. Lee Grismer, Thomas Ziegler, Van Thi Hong Nguyen, Truong Quang Nguyen, Minh Duc Le

Data type: Docx file.

Explanation note: Uncorrected ("p") distance matrix showing percentage genetic divergence (COI) (highlighted in bold are the lowest and highest percentage) between species in the *Cyrtodactylus irregularis* group.

Copyright notice: This dataset is made available under the Open Database License (http://opendatacommons.org/licenses/odbl/1.0/). The Open Database License (ODbL) is a license agreement intended to allow users to freely share, modify, and use this Dataset while maintaining this same freedom for others, provided that the original source and author(s) are credited.

Link: https://doi.org/10.3897/zookeys.1097.78127.suppl3

Supplementary material 4

Table S4

Authors: Hanh Thi Ngo, Quyen Hanh Do, Cuong The Pham, Vinh Quang Luu, L. Lee Grismer, Thomas Ziegler, Van Thi Hong Nguyen, Truong Quang Nguyen, Minh Duc Le

Data type: Docx file.

Explanation note: Uncorrected ("p") distance matrix showing percentage genetic divergence (COI) (highlighted in bold are the lowest and highest percentage) between species in the *Cyrtodactylus condorensis* group.

Copyright notice: This dataset is made available under the Open Database License (http://opendatacommons.org/licenses/odbl/1.0/). The Open Database License (ODbL) is a license agreement intended to allow users to freely share, modify, and use this Dataset while maintaining this same freedom for others, provided that the original source and author(s) are credited.

Link: https://doi.org/10.3897/zookeys.1097.78127.suppl4

Supplementary material 5

Table S5

Authors: Hanh Thi Ngo, Quyen Hanh Do, Cuong The Pham, Vinh Quang Luu, L. Lee Grismer, Thomas Ziegler, Van Thi Hong Nguyen, Truong Quang Nguyen, Minh Duc Le

Data type: Docx file.

Explanation note: Uncorrected ("p") distance matrix showing percentage genetic divergence (COI) (highlighted in bold are the lowest and highest percentage) between species in the *Cyrtodactylus chauquangensis* group.

Copyright notice: This dataset is made available under the Open Database License (http://opendatacommons.org/licenses/odbl/1.0/). The Open Database License (ODbL) is a license agreement intended to allow users to freely share, modify, and use this Dataset while maintaining this same freedom for others, provided that the original source and author(s) are credited.

Link: https://doi.org/10.3897/zookeys.1097.78127.suppl5

Supplementary material 6

Table S6

Authors: Hanh Thi Ngo, Quyen Hanh Do, Cuong The Pham, Vinh Quang Luu, L. Lee Grismer, Thomas Ziegler, Van Thi Hong Nguyen, Truong Quang Nguyen, Minh Duc Le

Data type: Docx file.

Explanation note: Uncorrected ("p") distance matrix showing percentage genetic divergence (COI) (highlighted in bold are the lowest and highest percentage) between species in the *C. brevipalmatus and C. intermedius* group.

Copyright notice: This dataset is made available under the Open Database License (http://opendatacommons.org/licenses/odbl/1.0/). The Open Database License (ODbL) is a license agreement intended to allow users to freely share, modify, and use this Dataset while maintaining this same freedom for others, provided that the original source and author(s) are credited.

Link: https://doi.org/10.3897/zookeys.1097.78127.suppl6

ZooKeys 1097: 153–165 (2022)
doi: 10.3897/zookeys.1097.74243
https://zookeys.pensoft.net

RESEARCH ARTICLE

A peer-reviewed open-access journal
ZooKeys
Launched to accelerate biodiversity research

A new species of *Sarsinebalia* (Crustacea, Leptostraca) from Japan

Takuma Hirata[1], Tomohiko Kikuchi[2]

1 *National Institute for Environmental Studies, Biodiversity Division, Ecological Risk Assessment and Control Section, Onogawa, Tsukuba, Ibaraki 305-8506, Japan* **2** *Graduate School of Environment and Information Sciences, Yokohama National University, 79-2 Tokiwadai, Hodogaya, Yokohama, Kanagawa 240-8501, Japan*

Corresponding author: Takuma Hirata (hirata.takuma@nies.go.jp)

Academic editor: Saskia Brix | Received 10 September 2021 | Accepted 24 March 2022 | Published 26 April 2022

http://zoobank.org/0FFD9293-DF45-420B-997B-C8A150C0B110

Citation: Hirata T, Kikuchi T (2022) A new species of *Sarsinebalia* (Crustacea, Leptostraca) from Japan. ZooKeys 1097: 153–165. https://doi.org/10.3897/zookeys.1097.74243

Abstract

A new species of Leptostraca, *Sarsinebalia agoensis* **sp. nov.**, from Ago Bay, Japan is described from specimens found at a depth of 120 m. The new species differs from other known *Sarsinebalia* species as follows: the compound eye has three distal lobes; the anterior margin of the first antennal segment has one distal process covered with setae; and the lateral margin of pleopod 1 exopod bears 5–6 simple, robust spines. A taxonomic key to all species of *Sarsinebalia* is also provided.

Keywords

Ago Bay, biodiversity, Malacostraca, taxonomic key

Copyright *Takuma Hirata & Tomohiko Kikuchi.* This is an open access article distributed under the terms of the Creative Commons Attribution License (CC BY 4.0), which permits unrestricted use, distribution, and reproduction in any medium, provided the original author and source are credited.

Introduction

The genus *Sarsinebalia* Dahl, 1985 belongs to the family Nebaliidae (Leptostraca: Nebaliacea). The type species of the genus, *Sarsinebalia typhlops* (Sars, 1870), was initially included in the genus *Nebalia* Leach, 1814. However, in the revision of the European shelf species by Dahl (1985) it was pointed out that *Nebalia typhlops* showed several morphological characters not present in any known *Nebalia* species at the time, i.e., rostrum with a ventral keel and terminal spine; compound eye disc-shaped and lacking pigment or externally discernible visual elements; first pleopod exopod lacking a row of serrated spines on the lateral border; and second maxilla exopod shorter than first article of endopod. Therefore, Dahl established the genus *Sarsinebalia* based on these characters. However, the validity of the genus *Sarsinebalia* was challenged by the phylogenetic analyses of Walker-Smith and Poore (2001), and later reconsidered by Moreira et al. (2003, 2021) and McCormack et al. (2016). The genus *Sarsinebalia* is currently composed of seven species that have been recorded from the Bay of Biscay (Ledoyer 1998), the sea near New Caledonia (Ledoyer 2000), the Atlantic coast of the Iberian Peninsula (Moreira et al. 2003; Sampaio et al. 2016), the Kuril-Kamchatka Trench (Petryashov 2016), the British Isles (McCormack et al. 2016), French Atlantic and Mediterranean waters (Latry and Droual 2020), and the Gulf of Cadiz (Moreira et al. 2021).

Three leptostracan species had long been reported from waters off the coast of Japan: *Nebalia bipes* (Fabricius, 1780), *Paranebalia longipes* (Willemoes-Suhm, 1875), and *Nebaliopsis typica* (Sars, 1887). Later, Hirata et. al. (2019) described *Nebalia tagiri* Hirata, Fujiwara & Kikuchi, 2019 from a hydrothermal field in Kagoshima Bay, Japan. Here, we report three specimens belonging to the genus *Sarsinebalia* collected from a depth of 120 m near Ago Bay, Japan in 1986. These specimens represent a new species that is described here as *Sarsinebalia agoensis* sp. nov.. There have been few studies of Leptostraca in waters near Japan, and previous findings have not explained the full diversity. This report is considered to be a very important discovery for the evaluation of the diversity of Leptostraca in waters near Japan.

Materials and methods

Samples were collected by ORI dredge; specimens ware sorted in the laboratory, and then identified and sexed. The following measurements were considered: Total length (**TL**: measured from the articulation between the rostrum and the carapace to the posterior end of the caudal furca), lateral carapace length (**LCL**: measured from the anterodorsal margin to the posteromedian margin of the carapace), carapace height (**CH**: measured between the dorsal and ventral margins), and rostrum length (**RL**: measured along the midline). Drawings were made with the aid of a camera lucida on a stereomicroscope (Model SMZ-10; Nikon Corporation, Japan). The type material of the new species is deposited at the National Museum of Nature and Science, Tokyo (**NSMT**).

Taxonomy

Order Leptostraca Claus, 1880
Suborder Nebaliacea Calman, 1904
Family Nebaliidae Samouelle, 1819
Genus *Sarsinebalia* Dahl, 1985

***Sarsinebalia agoensis* sp. nov.**
http://zoobank.org/04D34FE7-C3B2-42C0-AD9D-B5E1DEA2DF7E
Figs 1–5

Diagnosis. Carapace reaching pleonite 5. Rostrum long and narrow, about 3.8 times as long as wide, bearing a thin terminal spine. Compound eyes subrectangular, with three lobes on terminal margin. Article 4 of antennule with a row of nine simple setae and one robust distal spine. Antennular scale about twice as long as wide. Article 1 of antenna with one rounded process on anterior margin, covered by setae. Article 1 of endopod of second maxilla sub-equal in length to article 2, exopod not beyond article 1 of endopod. Article 2 of mandibular palp with one long plumose and one thin plumose seta. Pleonites 2–7 with distally rounded denticles along posterior border. Epipod of thoracopod 8 distinctly broader than thoracopods 1–7. Exopod of pleopod 1 with a single row of simple spines along lateral margin. Anal plate with lateral "shoulder". Furcal rami shorter than combined length of pleonite 7 and telson.

Examined material. Three ♀♀ (TL: 4.5–8.0 mm) collected from the Japanese Pacific coast near Ago Bay, during the R/V "Tansei Maru" KT 86-6 cruise (Atmosphere and Ocean Research Institute, The University of Tokyo); 34°12'00N, 136°43'00E; 120 m; May 1986.

Types material. *Holotype*: (NSMT-Cr 28987), adult ♀, 8.0 mm **TL. *Paratypes*:** two adult ♀♀ (**TL**: 5.6–6.5 mm) (NSMT-Cr 28988, NSMT-Cr 28989).

Description. Female holotype:

Carapace (Fig. 1A): Oval, reaching lateral side of pleonite 5. LCL about 4.2 mm; carapace ca. twice longer than high.

Rostrum (Fig. 1B, C): Long and narrow, ventral keel long and narrow, with thin terminal spine. RL about 1.6 mm; approximately 3.8 times as long as wide.

Compound eye (Fig. 1D, E): Subrectangular in shape, ommatidial part covering most of eyestalk, with three serrated lobes on terminal margin (Fig. 1E). Supraocular plate extending to about half of eyestalk.

Antennule (Fig. 2A): Peduncle composed of four articles. Article 1 about twice as long as wide. Article 2 longer than article 3, with a single plumose seta on anterior margin, four long and two short plumose setae arising subterminally, one spine-like seta, four plumose setae, and a cluster of simple setae on anterior margin, respectively. Article 3 expanded distally, with a terminal cluster of simple setae on anterior margin. Article 4 about half as long as article 3, with a row of nine simple setae and one spine distally, a row of five simple setae on anterior face, and a long robust seta on posterior

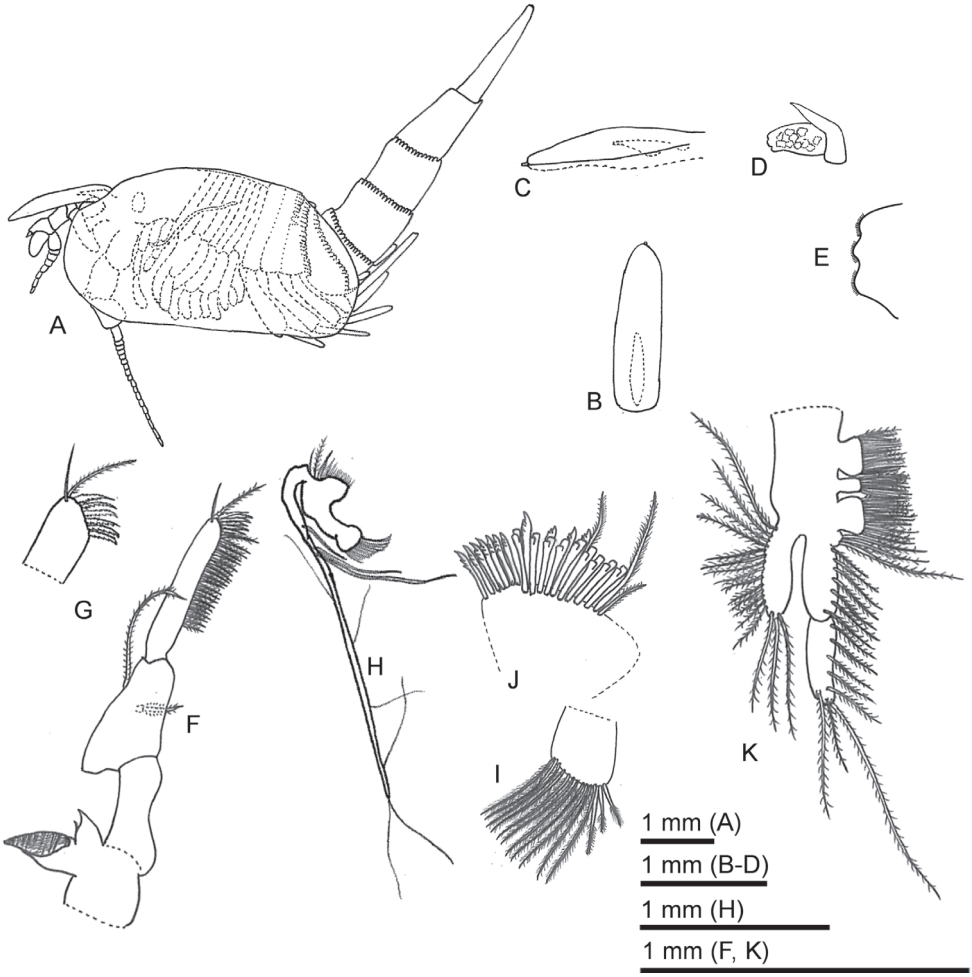

Figure 1. *Sarsinebalia agoensis* sp. nov. **A** female holotype, lateral view **B** rostrum, dorsal view **C** rostrum, lateral view **D** compound eye **E** detail of eye lobes **F** mandible **G** detail of mandibular palp article 3, distal end **H** first maxilla **I** detail of first maxilla proximal endite **J** detail of first maxilla distal endite **K** second maxilla.

margin. Antennular scale oval, about twice as long as wide, with a row of setae along lateral to terminal margin. Flagellum shorter than peduncle, composed of eight articles, each article with three pairs of thin setae and one long seta with aesthetascs.

Antenna (Fig. 2B–D): Peduncle composed of three articles. Article 1 with one rounded process on anterior margin, covered by eight setae (Fig. 2C). Article 2 about twice as long as wide, with a stout spine at dorsodistal margin. Article 3 longer than article 2, with one plumose seta on proximal margin and several rows of spines or setae along medial anterior margin (Fig. 2D), as follows:

1. Proximal row of seven setae and robust plumose seta on inner surface.

2. Five spines and nine spine-like setae along proximal half, distalmost the longest.
3. Six spine-like setae on external lateral face.
4. Seven plumose setae, two thin plumose setae, and two simple setae, each associated with a row of proximal spines.
5. Eight robust spines increasing in length distally, one robust plumose seta, two simple setae, one long simple seta and one long plumose seta at apex, 16 plumose setae arising from posterior distal margin, and two robust plumose and three thin simple setae arising from posterior proximal margin.

Flagellum longer than peduncle, composed of 18 articles, each article with two pairs of robust setae and one thin seta on anterior margin, and a single thin seta on posterior margin of articles 1–14.

Mandible (Fig. 1F): Well developed. Mandibular palp composed of three articles. Article 2 sub-equal in length to article 3, article 2 with one thin and one long plumose seta at mid-length on lateral margin and sub-terminally on superior margin, respectively. Article 3 cylindrical, with marginal row of setae covering distal four-fifths of article, terminal margin with a simple long, a plumose long seta and serration spines (Fig. 1G). Molar process shorter than palp article 1, distal margin with row of teeth forming grinding surface. Incisor process broad basally with acute terminal process and a minute tooth along lateral margin.

First maxilla (Fig. 1H): Proximal endite (Fig. 1I) with rounded medial margin, bearing 11 long plumose and three short robust plumose setae. Distal endite (Fig. 1J) with two rows of stout setae, spatulate setae, and a long plumose seta. Palp long, ca. six times longer than both endites combined, bearing nine setae.

Second maxilla (Fig. 1K): Protopod subdivided into four endites bearing plumose setae. Endite 1 approximately as long as endite 3; endite 2 oval, smaller than endites 1 and 3; endite 4 smaller than endites 1–3. Endopod composed of two articles; article 1 subequal to article 2, lateral margin with plumose setae, article 2 with three terminal plumose setae. Exopod just reaching distal end of endopod article 1, bearing 14 plumose setae on lateral margins and three on terminal margin.

Thoracopod 1 (Fig. 3A): Endopod composed of one large and four distal small articles, with numerous plumose setae along outer margin. Exopod oval, not surpassing distal article of endopod, with three long plumose setae on terminal margin and 20 thin plumose setae along inner margin. Epipod smaller than that of thoracopods 3–7, tip of proximal lobe reaching beyond basis, distal lobe short and not reaching distal half of endopod.

Thoracopods 3–7 (Fig. 3B–F): Similar in shape. One long and 18 thin plumose setae on thoracopod 3 exopod, one long and 12 thin in thoracopod 4, one long and 15 thin on thoracopod 5, one long and 11 thin on thoracopod 6, and ten thin on thoracopod 7. Three thin plumose setae on thoracopod 6 epipod, eight thin on thoracopod 7, thoracopods 3–5 lacking setae, and thoracopod 2 damaged.

Thoracopod 8 (Fig. 3G): Smaller than that of other thoracopods. Endopod composed of a large article and four small articles, with numerous plumose setae along

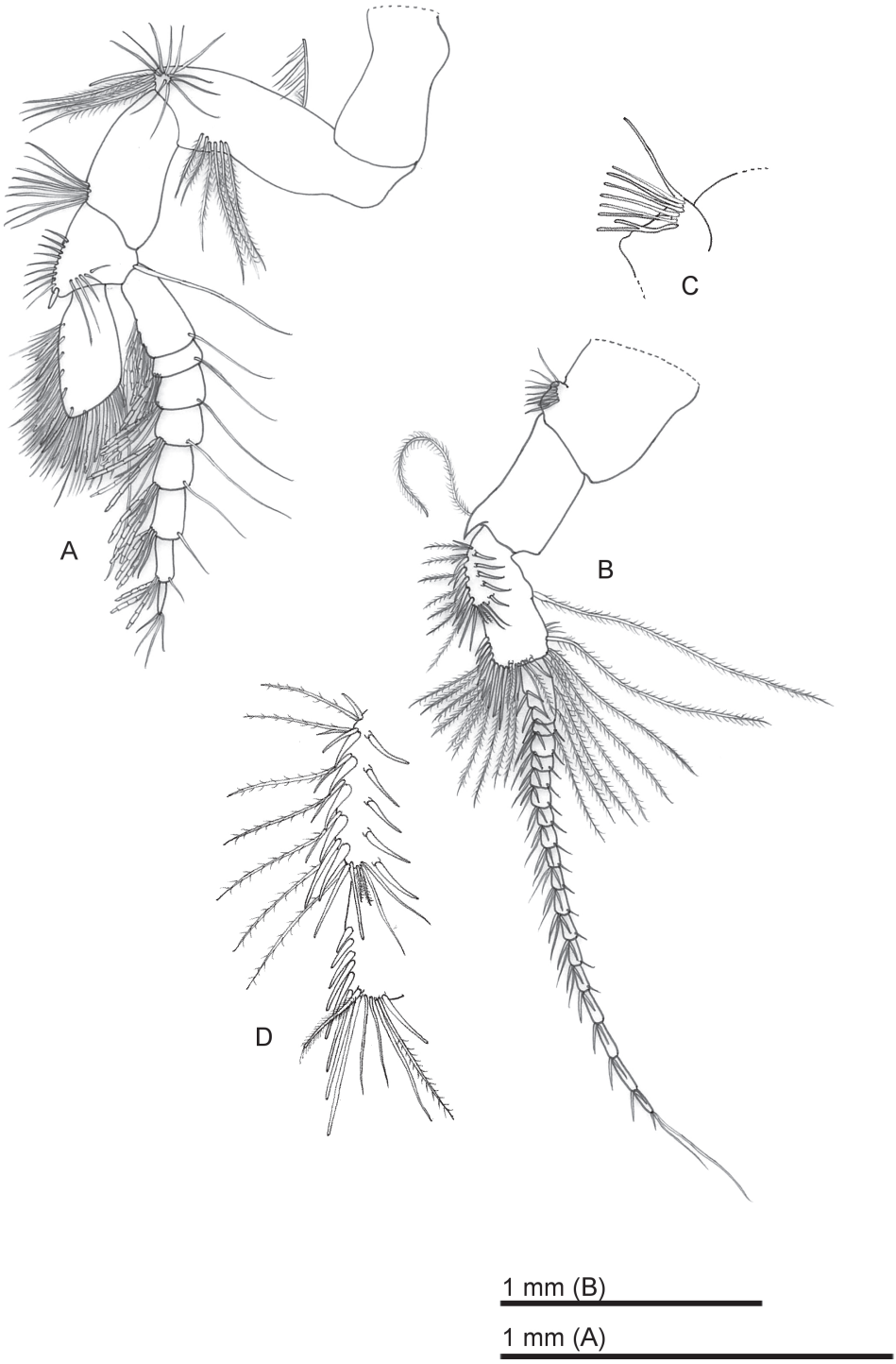

Figure 2. *Sarsinebalia agoensis* sp. nov. **A** antennule **B** antenna **C** detail of process on antenna peduncle article 1 **D** detail of row of spines and setae on antenna peduncle article 3.

outer margin. Exopod narrow with lateral margin concave, with two long plumose setae on terminal margin. Epipod large, distal lobe elongate, with 12 plumose setae.

Pleon (Fig. 1A): Composed of seven segments. Posterior margin of pleonite 1 smooth, pleonite 2 with rounded and acute denticles on half-length of posterior margin with flat margin between acute denticles. Pleonite 3 with rounded denticles. Pleonite 4 with rounded denticles, posterolateral margin expanded forming a narrow acute process. Pleonites 5–7 with rounded denticles (Fig. 5C).

Pleopod 1 (Fig. 4A): Protopod twice as long as wide, with single seta on proximal lateral margin, three setae on medial inner margin, with a simple seta, a simple spine-like seta, and a plumose seta near base of endopod; and a spine-like seta and simple seta near base of exopod. Endopod composed of two segments, longer than exopod, distal segment with an acute process at apex, bearing a long robust simple spine, lateral and medial margins each with plumose setae, appendix interna of proximal segment with three short, recurved hooks (Fig. 4B). Exopod with five simple spines along lateral margin, three simple spines on distolateral margin, the distal one the longest, and plumose setae along inner margin.

Pleopod 2 (Fig. 4C): Protopod twice as long as wide, six simple setae on proximal face, a single spine-like seta on proximal inner margin, one thin seta and a long spine-like seta on proximal outer margin, four setae on medial outer margin, two short and three long setae near base of endopod, single spine-like seta and robust simple spine near base of exopod, seven simple setae on distal face, with blade-like process between exopod and endopod. Endopod composed of two segments, longer than exopod, distal segment with acute process at apex, bearing a long robust simple spine, lateral and medial margins each with plumose setae, appendix interna of proximal segment with three short, recurved hooks. Exopod with a row of five pairs of simple spines and a thin plumose seta along lateral margin and single thin plumose seta near basis, two simple spines on distal margin, and plumose setae along inner margin.

Pleopod 3 (Fig. 4D): Protopod twice as long as wide, with seven simple setae on proximal face, one simple spine-like seta on proximal inner margin, a single spine-like seta on proximal outer margin, three simple setae near base of endopod, two simple setae, a robust seta, and a simple spine-like seta near base of exopod, eight simple setae on distal face, with a blade-like process between the exopod and endopod. Endopod composed of two segments, longer than exopod, distal segment with an acute process at apex, bearing a long robust simple spine, lateral and medial margins each with plumose setae, appendix interna of proximal segment with three short, recurved hooks. Exopod with a row of six pairs of simple spines and thin plumose setae along lateral margin, two simple spines on distal margin, and plumose setae along inner margin.

Pleopod 4 (Fig. 4E): Protopod sub-rectangular, both terminal sides acute, twice as long as wide, with nine simple setae on proximal face, one spine-like seta and five simple setae on proximal inner margin, four simple setae on proximal lateral margin, and six simple setae on distal face. Endopod composed of two segments, longer than exopod, distal segment with an acute process at apex, bearing a long robust simple spine,

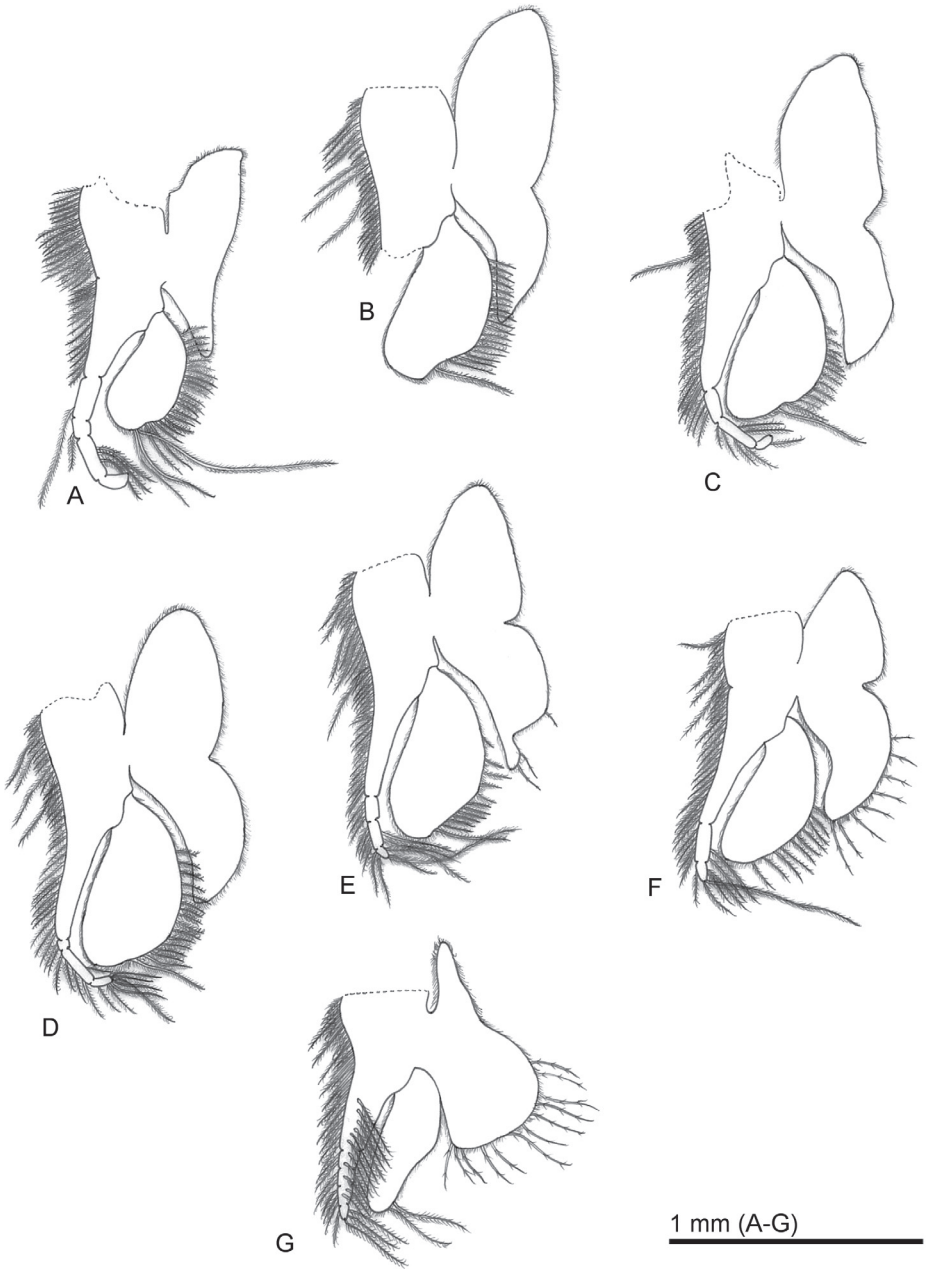

Figure 3. *Sarsinebalia agoensis* sp. nov. **A** thoracopod 1 **B** thoracopod 3 **C** thoracopod 4 **D** thoracopod 5 **E** thoracopod 6 **F** thoracopod 7 **G** thoracopod 8.

lateral and medial margins each with plumose setae, appendix interna of proximal segment with three short, recurved hooks. Exopod with a row of seven pairs of simple spines and thin plumose setae along lateral margin, two stout simple spines on distal margin, and plumose setae along inner margin.

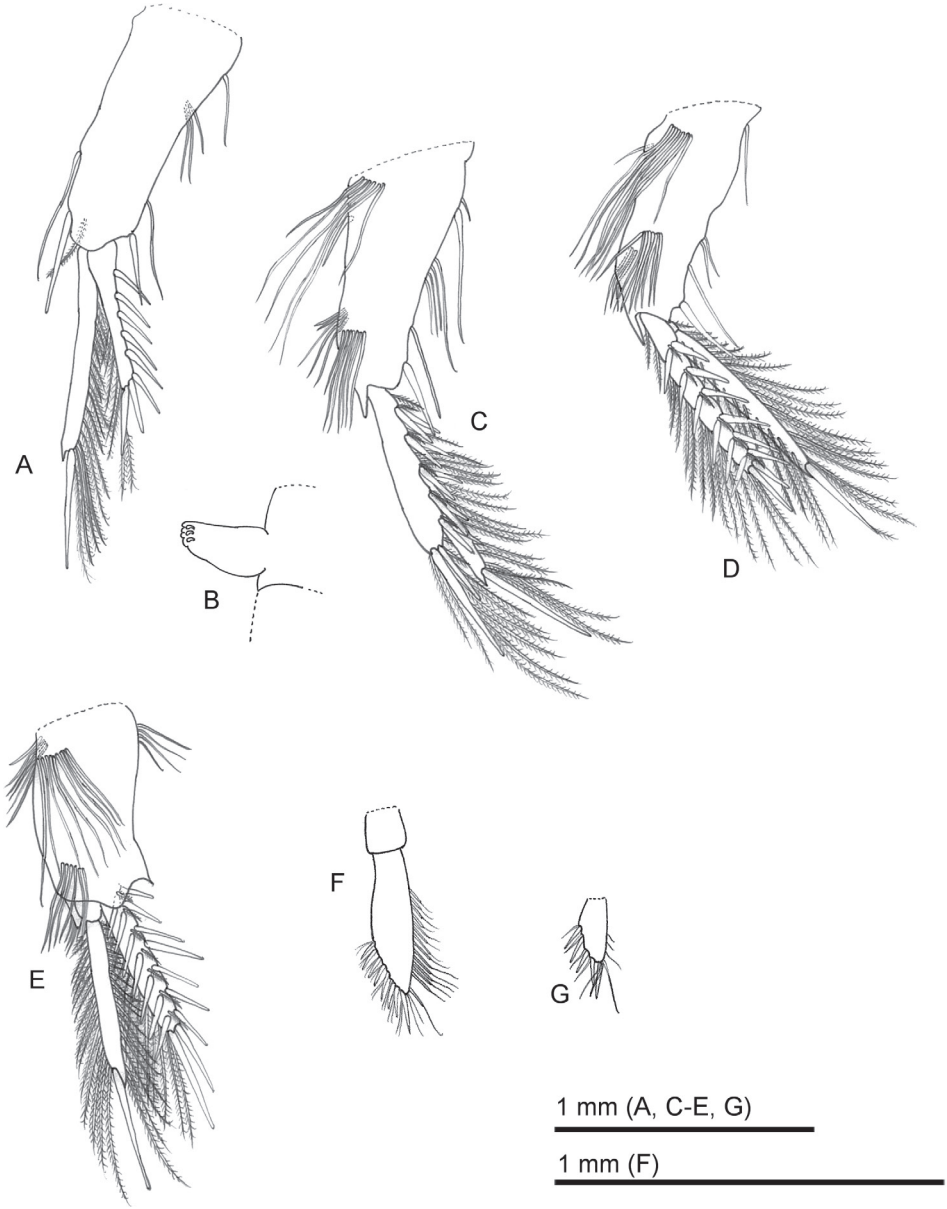

Figure 4. *Sarsinebalia agoensis* sp. nov. **A** pleopod 1, lateral view **B** detail of pleopod 1 appendix interna **C** pleopod 2, lateral view **D** pleopod 3, lateral view **E** pleopod 4, lateral view **F** pleopod 5, ventral view **G** pleopod 6, ventral view.

Pleopod 5 (Fig. 4F): Composed of two segments. Distal segment about three times as long as wide, bearing eight simple spines and 18 simple thin setae, lateral margin with approximately 13 simple setae.

Pleopod 6 (Fig. 4G): Rami bearing five simple spines and six simple thin setae, lateral margin with three simple thin and one simple long seta.

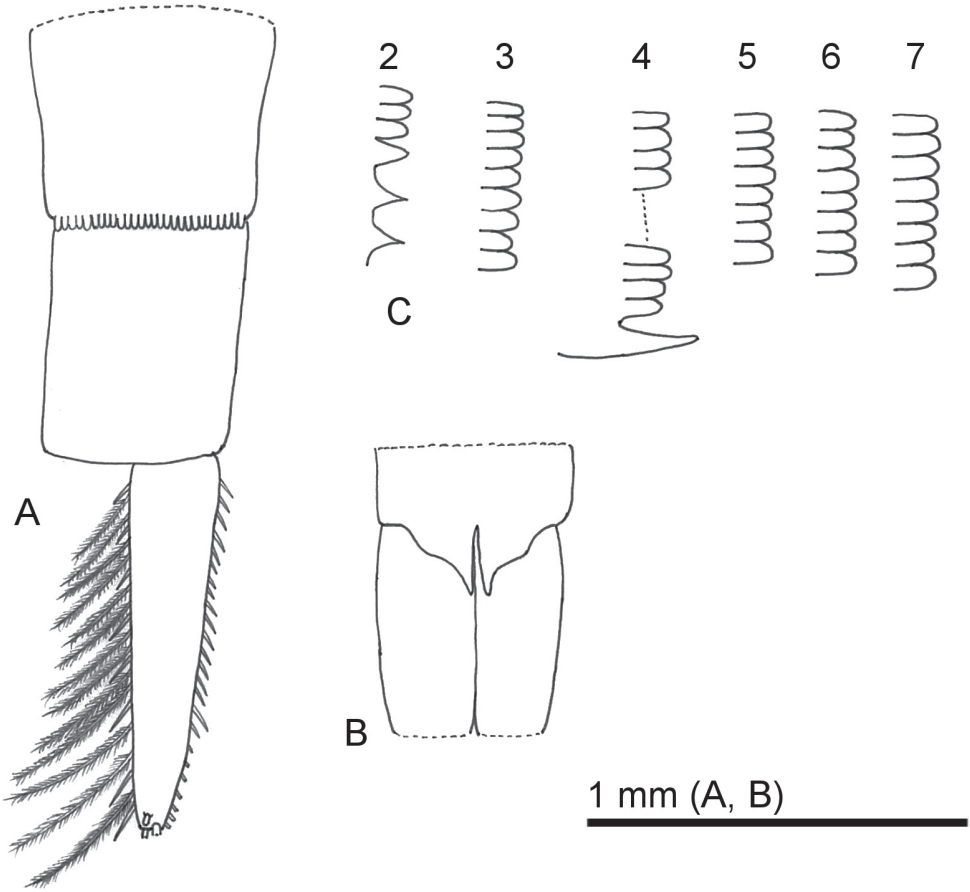

Figure 5. *Sarsinebalia agoensis* sp. nov. **A** telson and right furcal ramus, dorsal view (left ramus not illustrated) **B** anal plates, ventral view **C** detail of denticles of pleonites 2–7 posterior margin.

Anal plate (Fig. 5B): No distinct 'shoulder', point acute. Furcal rami (Fig. 5A) shorter than pleonite 7 and telson combined, 24 spines along lateral margin, eight spine-like setae and 13 plumose setae along inner margin, and two robust setae on distolateral margin.

Morphological variation. The number of distal setae of the antennule peduncle article 4 and of lateral spines of the pleopod 1 exopod show some variation among specimens: six to nine setae on distal margin, and six simple spines on lateral margin, respectively.

Etymology. The name *agoensis* refers to the type locality of the new species, the sea near Ago Bay.

Remarks. The seven known species of the genus *Sarsinebalia* can be grouped according to presence or absence of the ommatidia and the pigment of eyes. Three species, *S. biscayensis* Ledoyer, 1998, *S. typhlops* (Sars, 1869) and *S. pseudotyphlops* Petryashov, 2016, lack both ommatidia and pigments. On the contrary, *S. cristoboi* Moreira, Gestoso & Troncoso, 2003, *S. kunyensis* Ledoyer, 2000, *S. ledoyeri* Moreira, Esquete & Cunha, 2021, and *S. urgorrii* Moreira, Gestoso & Troncoso, 2003, have

compound eyes provided with ommatidia; *S. cristoboi*, *S. kunyensis* and *S. urgorrii* also bear red eye pigment. Therefore, *S. agoensis* sp. nov. is close the latter four species for the presence of ommatidia, but differs from them in a number of features (Table 1):

Table 1. Comparison of *Sarsinebalia agoensis* sp. nov. with related species of *Sarsinebalia*. Abbreviations: a = article; An2 = antenna; enp = endopod; exp = exopod; Mx2 = second maxilla; pn 6–7 = pleonite 6–7; pp1 = pleopod 1; sp = supraocular plate.

Species	Ommatidia	Eye pigment	Eye shape	Eye-stalk terminal lobes	Sp length	An2 a1 distal process	Mx2 exp	Pp1 exp lateral margin	Shape of pn 6–7 denticles	Source
S. agoensis sp. nov.	Present	Absent	Almost oblong, disto-ventral margin concave	3 lobes	Two thirds of eye-stalk	Covered by 8 setae	< enp a1	4 simple spines	Distally rounded	This paper
S. kunyensis Ledoyer, 2000	Present	Absent	Oval, elongated	Absent	Two thirds of eye-stalk	Margin smooth	> enp a1	7 serrated spines	Elongated, distally rounded	Ledoyer (2000)
S. cristoboi Moreira et al., 2003	Present	Present (red-orange)	Expanded distally	Absent	Beyond distal end of eye-stalk	One tooth (2?)	> enp a1	Smooth	Distally rounded	Moreira et al. (2003)
S. urgorrii Moreira et al., 2003	Present	Present (red-orange, dark)	Oblong	Absent	Two thirds of eye-stalk	One thooth	> enp a1	Smooth	Distally bluntly rounded	Moreira et al. (2003)
S. ledoyeri Moreira et al., 2021	Present	Absent	Almost oblong, disto-ventral margin concave	Absent	Half of eye-stalk	One tooth	> enp a1	Smooth	Elongated, slightly triangular distally	Moreira et al. (2021)

1. *S. agoensis* sp. nov. is the only known species in the genus with three lobes on the terminal margin of the eyestalk; in *S. cristoboi* the eyestalk is slightly longer than wide and the distal border is straight; in *S. kunyensis* it is oval and tapering distally, oblong in *S. urgorrii*, and oblong with concave disto-ventral margin in *S. ledoyeri*.

2. The tip of the supraocular plate extends along the proximal half of the eyestalk in *S. agoensis* sp. nov. and *S. ledoyeri*, along the proximal two-thirds in *S. kunyensis* and *S. urgorrii*, and beyond the terminal margin of the eyestalk in *S. cristoboi*.

3. Article 1 of the antenna peduncle has a rounded process covered with eight setae in *S. agoensis* sp. nov. This process ends in one tooth in *S. ledoyeri*, *S. cristoboi*, and *S. urgorrii*; apparently, there is a second tooth/spine in *S. cristoboi* that is not mentioned in the original description but illustrated (cfr. fig. 2A in Moreira et al. 2003). The process is smooth and lacking teeth/spines in *S. kunyensis*.

4. The tip of the exopod of the second maxilla just reaches the distal end of the first article of the endopod in *S. agoensis* sp. nov., but extends well beyond the level of the second article of the endopod in *S. cristoboi*, *S. kunyensis*, *S. ledoyeri*, and *S. urgorrii*.

5. The lateral margin of the pleopod 1 exopod bears a row of four to six simple spines in *S. agoensis* sp. nov., whereas *S. kunyensis* bears seven serrated spines; the lateral margin is smooth in *S. cristoboi*, *S. ledoyeri*, and *S. urgorrii*.

6. The denticles of the posterior margins of pleonites 6–7 are distally rounded in *S. agoensis* sp. nov. and *S. cristoboi*, elongated and distally rounded in *S. kunyensis*, distally bluntly rounded in *S. urgorrii*, and elongated and distally slightly triangular in *S. ledoyeri*.

In conclusion, *S. agoensis* sp. nov. stands out from other known species of *Sarsinebalia* by having the eyestalk provided with distal lobes and pleopod 1 exopod with a lateral row of several spines.

Until now, there have been few studies on Leptostraca in waters near Japan; in addition, only limited sea areas have been studied. For this reason, previous studies have never been able to accurately evaluate the diversity of Leptostraca in waters near Japan. Ago Bay is also one of the sea areas that has never been investigated, and this paper is the first report from this area. This is also the first report of the genus *Sarsinebalia* in waters near Japan. The discovery of *S. agoensis* sp. nov. suggests that further investigations may uncover further diversity of Leptostraca in waters near Japan.

Key to species of the genus *Sarsinebalia*

1 Eyestalk lacking ommatidia or pigment **2**
– Eyestalk provided with ommatidia or pigment **4**
2 Eyestalk oblong ..... ***S. pseudotyphlops* Petryashov, 2016**
– Eyestalk not oblong **3**
3 Eyestalk sub-rectangular; disto-ventral margin concave ..... ***S. typhlops* (Sars, 1870)**
– Eyestalk elongated; disto-ventral margin convex ... ***S. biscayensis* Ledoyer, 1998**
4 Eyestalk with three lobes on terminal margin ..... ***S. agoensis* sp. nov.**
– Eye-stalk lacking terminal lobes **5**
5 Eyestalk expanding distally ... ***S. cristoboi* Moreira, Gestoso & Troncoso, 2003**
– Eyestalk tapering distally **6**
6 Eyestalk oval ..... ***S. kunyensis* Ledoyer, 2000**
– Eyestalk not oval **7**
7 Eyestalk oblong ..... ***S. urgorrii* Moreira, Gestoco & Troncoso, 2003**
– Eyestalk almost oblong; disto-ventral margin concave ..... ***S. ledoyeri* Moreira, Esquete & Cunha, 2021**

Acknowledgements

We thank the captain and crew of the R/V “Tansei Maru” for organizing the cruise and sampling.

References

Dahl E (1985) Crustacea Leptostraca, principles of taxonomy and a revision of European shelf species. Sarsia 70(2–3): 135–165. https://doi.org/10.1080/00364827.1985.10420626

Fabricius O (1780) Fauna Groenlandica. J. G. Rothe, Hafniae et Lipsiae [Copenhagen and Leipzig], 452 pp.

Hirata T, Fujiwara Y, Kikuchi T (2019) A new species of Nebalia (Crustacea, Leptostraca) from a hydrothermal field in Kagoshima Bay, Japan. ZooKeys 897: 1–18. https://doi.org/10.3897/zookeys.897.37061

Latry L, Droual G (2020) Leptostraca (Crustacea: Phyllocarida: Nebaliidae) from French coastal waters: new records and new data on their ecology and distribution. Cahiers de Biologie Marine 61(1): 91–103. https://doi.org/10.21411/CBM.A.A741CE15

Leach WE (1814) The zoological miscellany, being descriptions of new and interesting animals. McMillan, London, 149 pp.

Ledoyer M (1998) Leptostracés (Crustacea) des côtes de Mauritanie récoltés au cours de la champagne Eumeli 4 en 1992 et *Sarsinebalia biscayensis* n. sp. de la terrasse de Meriadzek, golfe de Gascogne (Nord-Est Atlantique). Marine Life (Marseille) 8(1–2): 29–33.

Ledoyer M (2000) Leptostracés (Crustacea) de Nouvelle-Calédonie (mer de Corail, Ouest Pacifique). Marine Life (Marseille) 10(1–2): 57–68.

McCormack E, Ashelby CW, McGrath D (2016) A review of the Leptostraca of the British Isles with discussion of the genus *Sarsinebalia* Dahl. Nauplius 24(0): e2016006. https://doi.org/10.1590/2358-2936e2016006

Moreira J, Gestoso L, Troncoso JS (2003) Two new species of *Sarsinebalia* (Crustacea, Leptostraca) from the Northeast Atlantic, with comments on the genus. Sarsia 88(3): 189–209. https://doi.org/10.1080/00364820310001390

Moreira J, Esquete P, Cunha MR (2021) Leptostracans (Crustacea: Phyllocarida) from mud volcanoes at the Gulf of Cadiz (NE Atlantic) with description of a new species of *Sarsinebalia* Dahl, 1985. European Journal of Taxonomy 736: 102–136. https://doi.org/10.5852/ejt.2021.736.1255

Petryashov VV (2016) Two new species of deep-sea leptostracans (Crustacea: Phyllocarida: Leptostraca) from the North-West Pacific. Russian Journal of Marine Biology 42(5): 383–391. https://doi.org/10.1134/S1063074016050084

Sampaio L, Mamede R, Ricardo F, Magalhães L, Rocha H, Martins R, Dauvin JC, Rodrigues AM, Quintino V (2016) Soft-sediment crustacean diversity and distribution along the Portuguese continental shelf. Journal of Marine Systems 163: 43–60. https://doi.org/10.1016/j.jmarsys.2016.06.011

Sars GO (1870) Nye Dybvandscrustaceer fra Lofoten. Forhandlinger i Videnskabs-Selskabet i Christiana (1869): 147–174.

Sars GO (1887) Report on the Phyllocarida collected by H.M.S. Challenger during the years 1873–76. Report on the Scientific Results of the Voyage of H.M.S. Challenger during the years 1873–76. Zoology (Jena, Germany) 19: 1–38. https://doi.org/10.5962/bhl.title.10403

Walker-Smith GK, Poore GCB (2001) A phylogeny of the leptostraca (Crustacea) with keys to families and genera. Memoirs of the Museum of Victoria 58(2): 383–410. https://doi.org/10.24199/j.mmv.2001.58.21

Willemoes-Suhm R von (1875) On some Atlantic crustacea from the 'Challenger' Expedition. Transactions of the Linnean Society of London. Zoology 2nd ser, v 1: 23–59. [pl 6–13] https://doi.org/10.1111/j.1096-3642.1875.tb00433.x

ZooKeys 1097: 167–181 (2022)
doi: 10.3897/zookeys.1097.80216
https://zookeys.pensoft.net

RESEARCH ARTICLE

A peer-reviewed open-access journal
ZooKeys
Launched to accelerate biodiversity research

The complete mitochondrial DNA sequences of two sibling species of lumbricid earthworms, *Eisenia fetida* (Savigny, 1826) and *Eisenia andrei* (Bouché, 1972) (Annelida, Crassiclitellata): comparison of mitogenomes and phylogenetic positioning

Csaba Csuzdi[1*], Jachoon Koo[2*], Yong Hong[3]

1 *Department of Zoology, Eszterházy Károly Catholic University, Eger, Hungary* **2** *Division of Science Education and Institute of Fusion Science, College of Education, Jeonbuk National University, Jeonju 54896, Republic of Korea* **3** *Department of Agricultural Biology, College of Agriculture & Life Science, Jeonbuk National University, Jeonju 54896, Republic of Korea*

Corresponding author: Yong Hong (yonghong@jbnu.ac.kr)

Academic editor: Sergei Subbotin | Received 7 January 2022 | Accepted 3 April 2022 | Published 29 April 2022

http://zoobank.org/C43A88B7-0CF9-46A1-8F5E-51B35E43C488

Citation: Csuzdi C, Koo J, Hong Y (2022) The complete mitochondrial DNA sequences of two sibling species of lumbricid earthworms, *Eisenia fetida* (Savigny, 1826) and *Eisenia andrei* (Bouché, 1972) (Annelida, Crassiclitellata): comparison of mitogenomes and phylogenetic positioning. ZooKeys 1097: 167–181. https://doi.org/10.3897/zookeys.1097.80216

Abstract

Composting earthworms of the genus *Eisenia* play an important role in soil ecosystems. However, taxonomic classification of this genus, especially the sibling species *Eisenia fetida* and *Eisenia andrei*, is complicated because of their morphological similarity. In this study, we assessed the utility of the complete mitochondrial genome (mitogenome) for identification and differentiation of the two species. The complete mitogenomes of *E. andrei* and *E. fetida* were 15,714 and 16,560 bp, respectively. They contained 37 genes, comprising 13 protein-coding genes (PCGs), two rRNA genes, 22 tRNA genes, and a putative non-coding region, as observed in other earthworms. Sequence comparisons based on the complete nucleotide sequences excluding the non-coding region showed 85.8% similarity, whereas the predicted amino acid sequences of the 13 PCGs were 92.7% similar between the two species. In particular, distinct features were found in the non-coding regions of the mitogenomes. They include a control region associated with putative mitogenome replication and an extended sequence. The extended sequence showed sig-

* These authors contributed equally to this work.

Copyright *Csaba Csuzdi et al.* This is an open access article distributed under the terms of the Creative Commons Attribution License (CC BY 4.0), which permits unrestricted use, distribution, and reproduction in any medium, provided the original author and source are credited.

nificant differences between the two species and other known earthworm species, suggesting its potential as a feasible molecular marker for species identification. Phylogenetic analysis of the 36 mitogenomes of earthworm species corroborated the monophyly of the genus *Eisenia* and the taxonomic distinctness of the sibling species pair, *E. fetida* and *E. andrei*.

Keywords
Compost worms, mitogenome, Oligochaeta, phylogeny, sibling species

Introduction

The earthworm species *Eisenia fetida* was described as *Enterion fetidum* by Savigny (1826). Eisen (1873) relegated this species to his newly described genus *Allolobophora* Eisen, 1873 and remarked that it is easily recognized by its peculiar color pattern consisting of reddish-brown bands separated by yellowish intersegments. Later, Malm (1877) selected *Enterion fetidum* as the type species of the genus *Eisenia* Malm, 1877. For a long time, the characteristic striated pattern was a primary identifiable characteristic of the species until Avel (1937) recognized that the classical *Eisenia fetida* existed in two morphological variants: a typical striped form and an evenly pigmented form that might represent a separate species (Avel 1937).

André (1963) carried out breeding experiments with earthworms and recognized that reproductive isolation exists between the striped and evenly colored forms of *E. fetida*, and that the crossbred offspring are sterile. Consequently, he described the uniformly pigmented form as *Eisenia fetida* var. *unicolor*. Variety names proposed after 1961 were considered intrasubspecific and invalid; therefore, Bouché (1972) proposed a new name for var. *unicolor*, *Eisenia fetida andrei* Bouché, 1972. Since then, various authors have treated the subspecies *E. f. andrei* differently. Reynolds (1977), Sims (1983), Easton (1983), Csuzdi and Zicsi (2003), and Blakemore (2008, 2013) regarded it as a color morph and synonym of *Eisenia fetida* (Savigny, 1826). Others, such as Sims and Gerard (1985), Qiu and Bouché (1998), Lehmitz et al. (2014), and Martin et al. (2016), considered *E. fetida* and *E. andrei* to be two distinct valid species.

Eisenia fetida is an important composting worm and ecotoxicological test organism (Domínguez et al. 2005; Römbke et al. 2016). Therefore, intensive studies have been carried out since the early 1980s to determine whether the two types of *E. fetida* (striped and unicolor) represent two morphological variants or two separate species. The first clear indication that *E. fetida* and *E. andrei* might represent two separate species was presented by Jaenike (1982) who used an electrophoretic survey to demonstrate complete reproductive isolation between the two species. Later, Reinecke and Viljoen (1991) and Domínguez et al. (2005), using crossbreed experiments, reported complete reproductive isolation between the two species (no viable cocoons were observed in interspecific crosses) and noted that the two species differed in their life histories. Furthermore, *E. andrei* exhibited higher reproduction rates.

Recently, Römbke et al. (2016) carried out a detailed barcoding study of the *Eisenia fetida* / *E. andrei* complex using samples from 28 laboratories in 15 countries. The two species formed two distinct clades on the neighbor-joining tree, and the *E. fetida* clade consisted of two subclades, *fetida* 1 and *fetida* 2. The mean uncorrected p-distances were 14.2% between *fetida*1 and *andrei*, 14.3% between *fetida*2 and *andrei*, and 11.2% between the two *fetida* subclades; these values exceed the species-level threshold suggested by Chang and James (2011). Therefore, Römbke et al. (2016) concluded that the complex consists of three taxa: *E. andrei* and two cryptic taxa, *E. fetida* 1 and *E. fetida* 2. Moreover, they found that *E. andrei* was always correctly identified from its morphology, whereas *E. fetida* was often misidentified as *E. andrei* (Römbke et al. 2016).

It is worth mentioning that the native range of *E. fetida* and *E. andrei* is unknown. All of the above-mentioned studies were based on laboratory stocks or specimens collected from compost or manure heaps. Perel (1998) hypothesized that the native range of *E. fetida* is somewhere in the forest-steppe zone of Central Asia; therefore, Latif et al. (2017) barcoded 62 new specimens of this complex collected from different anthropogenic and natural habitats in Iran. Surprisingly, all Iranian material appeared in the *E. andrei* clade, irrespective of striped or uniform pigmentation. Moreover, the *E. andrei* clade showed high genetic structuring in contrast to the almost uniform genetic composition found by Römbke et al. (2016). Automatic barcode gap discovery (ABGD) analysis identified two species corresponding to *Eisenia andrei* and *Eisenia fetida* with high genetic structuring inside both species, but neither of the subclades reached the unambiguous species threshold [15% K2P distance according to Chang and James (2011)].

Comparison of mitogenomes may reveal important genome-level characteristics, helping us understand genome structure, gene order, phylogenetic relationships, and evolutionary lineages. The earthworm mitogenome is a circular, double-stranded, covalently closed DNA molecule containing 13 protein-coding genes (PCGs), two ribosomal RNA genes (rRNAs), 22 transfer RNA genes (tRNAs), and one non-coding region (Zhang et al. 2016). Although Lumbricidae is the most important earthworm family in the Northern Hemisphere temperate zone and contains many widespread and invasive cosmopolitan species, only a few complete or nearly complete mitogenomes are available for this family (Boore and Brown 1995; Shekhovtsov and Peltek 2019; Zhang et al. 2019; Shekhovtsov et al. 2020). In the present study, we sequenced the complete mitochondrial genome of the sibling species *E. fetida* and *E. andrei* to clarify its taxonomic position and to gain a better understanding of the mitogenomes of Lumbricidae.

Material and methods

Sample preparation and DNA extraction

Adult *E. andrei* were collected from a farm in Sangseo-myeon, Buan-gun, Jeollabuk-do, Korea (33°41'23.80"N, 126°38'33.67"E; 40 m a.s.l.) on March 26, 2021. *Eisenia fetida* adults were collected near a house at Seolcheon-myeon, Muju-gun, Jeollabuk-do, Korea

(33°58'00.61"N, 127°47'47.88"E; 408 m a.s.l.) on April 2, 2021, and preserved in 99% ethanol until DNA extraction. A voucher specimen of each species was deposited at Jeonbuk National University, Jeonju City, Korea, under accession numbers JBNU0011 and JBNU0012. Total genomic DNA was prepared from a small portion of body segments of a single adult earthworm using the QIAamp DNA Mini Kit (Qiagen, Hilden, Germany). The remaining tissue was stored at -20 °C in 90% ethanol to preserve the specimens.

TruSeq DNA Library construction

The sequencing library was prepared by random fragmentation of genomic DNA, followed by 5' and 3' adapter ligations. Briefly, 100 ng genomic DNA was fragmented using adaptive focused acoustic (AFA) technology (Covaris Inc., Woburn, MA, USA). The fragmented DNA was end-repaired and ligated to TruSeq indexing adapters using the Illumina TruSeq DNA Nano Library Prep Kit according to the manufacturer's instructions (Illumina Inc., San Diego, CA, USA). The resulting libraries were quantified through a qPCR-based assay using the KAPA Library Quantification Kit for Illumina Sequencing platforms according to the manufacturer's instructions (Kapa Biosystems, Woburn, MA, USA). The libraries were qualified using an Agilent Technologies 2200 TapeStation (Agilent Technologies, Santa Clara, CA, USA).

DNA sequencing and assembly

Paired-end (2 × 150 bp) sequencing was performed using an Illumina HiSeq-X platform (Illumina Inc., USA) at Macrogen Inc. (Seoul, Korea). For each species, > 39 million reads (5.1–5.9 Gb) were generated. To reduce bias in the analysis, adapter trimming and quality filtering were performed using Trimmomatic version 0.36 (Bolger et al. 2014). After filtering, the number of total reads of *E. andrei* and *E. fetida* was > 29 million (4.4 Gb) and > 34 million (5.2 Gb), respectively. De novo assembly of raw sequencing reads was performed using various *k*-mer lengths in SPAdes version 3.13.0 (Bankevich et al. 2012). Mitochondrial contigs were assembled into a single contig using BlastN alignment (https://blast.ncbi.nlm.nih.gov/Blast.cgi) against the *Lumbricus terrestris* Linnaeus, 1758 mitogenome (GenBank accession number, NC_001673) as the reference sequence. The assembled mitochondrial sequences for *E. andrei* were connected to a single circular molecule, whereas the conformation of the contig for *E. fetida* was unclear because the 12 bp TA-repeat sequence overlapped at both ends. This region corresponds to heteroplasmic tandem repeats in the mitochondrial control region (Liu et al. 2020). To close the circular genome, pairs of PCR primers (5'-ACCACCAGAGTTCTCGTTCG-3' and 5'-GCCAATATCGGCCCAAAACC-3') were designed to amplify the control region. The reaction was performed in an nTaq-tenuto (Enzynomics Inc., Seoul, Korea) with the following program: 95 °C for 3 min; 35 cycles of 95 °C for 20 s, 55 °C for 30 s, and 72 °C for 1 min; and a final extension of 5 min at 72 °C. The amplicons were directly sequenced using Sanger sequencing (Macrogen Inc., Seoul, Korea) to determine the complete mitogenome of *E. fetida*.

Mitogenome annotation

The annotation and visualization of mitochondrial genomes were performed using the online MITOS software (Donath et al. 2019), and manual curation was performed using BLAST searches in the NCBI database for various earthworm mitochondrial genomes deposited in NCBI (Table 1). A comparative map of mitochondrial genomes was created using Geneious Prime 2021 software (https://www.geneious.com). The *cox1* sequence was used as an anchor for linearized maps of the mitochondrial genomes. The annotated complete genome sequences were registered in GenBank under accession numbers OK513069 for *E. andrei* and OK513070 for *E. fetida*. The associated biosample numbers were SAMN26185682 for *E. andrei* and SAMN26185683 for *E. fetida*. All sequencing datasets, including SRA, are available in the NCBI BioProject database under the accession number PRJNA769829.

Phylogenetic analyses

To clarify the phylogenetic position of the two species, the available complete or near-complete mitogenomes were obtained from GenBank, comprising 24 species of Megascolecidae, 14 species of Lumbricidae, and one species of Rhinodrilidae. *Drawida japonica* (Michaelsen, 1892) from the exquisiclitellate family Moniligastridae was used as the outgroup.

Two sets of sequence matrices were composed: one containing the PCGs, 12S, and 16S RNA genes, and the other consisting only of PCGs. Sequences were aligned with MAFFT ver. 7 (Katoh and Standley 2013) using the G-INS-i option and concatenated in MegaX (Kumar et al. 2018); the resulting matrices were 13,505 and 11,241 bp, respectively. The protein-coding alignment was translated into amino acid sequences and aligned in MAFFT ver. 7 using the G-INS-i option; the resulting matrix was with 3714 amino acid positions.

The best-fitting evolutionary model for each partition (PCG, 16S, 12S) was selected using ModelFinder (Kalyaanamoorthy et al. 2017) implemented in the IQTree web server (http://iqtree.cibiv.univie.ac.at/) by applying the Akaike information criterion (AIC; Akaike 1973) and Bayesian information criterion (BIC; Schwarz 1978). GTR + I + Γ was selected as the best-fitting evolutionary model for PCGs and 12S RNA, TIM2 I + Γ was selected for 16S RNA, and MtMAM I + Γ for the amino acid sequences.

Bayesian inference of the phylogeny was estimated with MrBayes v.3.2.6 (Ronquist et al. 2012) as implemented in CIPRES Science Gateway V. 3.3. (Miller et al. 2010). The analysis was performed with default parameters, and each of the two independent runs was set to 10 million generations and sampling every 1000th generation (10,000 trees). Twenty percent of the trees were discarded as burn-in, and the remaining trees were combined and summarized in a 50% majority-rule consensus tree. As the TIM2 model was not implemented in MrBayes, the closest complex model GTR + I + Γ was used instead. Maximum likelihood phylogenetic inference was performed using the IQTree web server with default options (Nguyen et al. 2015 http://iqtree.cibiv.univie.ac.at/).

Table 1. List of Megadrili mitogenomes used in this study.

Species	Genbank No.	Total length (bp)	*Non-coding region (bp)	Topology
Amynthas aspergillus	KJ830749	15,115	565	Circular
Amynthas carnosus	KT429008	15,160	601	Circular
Amynthas corticis	KM199290	15,126	573	Circular
Amynthas cucullatus	KT429012	15,122	569	Circular
Amynthas gracilis	KP688582	15,161	582	Circular
Amynthas hupeiensis	KT429009	15,069	477	Circular
Amynthas instabilis	KT429007	15,159	577	Circular
Amynthas jiriensis	KT783537	15,151	618	Circular
Amynthas longisiphonus	KM199289	15,176	491	Circular
Amynthas moniliatus	KT429020	15,133	562	Circular
Amynthas pectiniferus	KT429018	15,188	618	Circular
Amynthas redactus	KT429010	15,131	572	Circular
Amynthas robustus	KT429019	15,013	432	Circular
Amynthas rongshuiensis	KT429014	15,086	546	Circular
Amynthas spatiosus	KT429013	15,152	595	Circular
Amynthas triastriatus	KT429016	15,160	582	Circular
Amynthas yunoshimensis	LC573969	15,109	581	Circular
Metaphire californica	KP688581	15,147	567	Circular
Metaphire guillelmi	KT429017	15,174	594	Circular
Metaphire hilgendorfi	LC573968	15,186	649	Circular
Metaphire vulgaris	KJ137279	15,061	484	Circular
Duplodicodrilus schmardae	KT429015	15,156	595	Circular
Perionyx excavatus	EF494507	15,083	504	Circular
Tonoscolex birmanicus	KF425518	15,170	595	Circular
Aporrectodea rosea	MK573632	15,086	512	Circular
Lumbricus rubellus	MN102127	15,464	433	Circular
Lumbricus terrestris	U24570	14,998	384	Circular
**Eisenia balatonica*	MK642872	14,589	-	Linear
**Eisenia nana*	MK618511	14,599	-	Linear
**Eisenia nordenskioldi*	MK618509	14,572	-	Linear
**Eisenia nordenskioldi*	MK618510	14,592	-	Linear
**Eisenia nordenskioldi*	MK618513	14,567	-	Linear
**Eisenia nordenskioldi*	MK642867	14,576	-	Linear
**Eisenia nordenskioldi*	MK642868	14,556	-	Linear
**Eisenia nordenskioldi pallida*	MK618512	14,567	-	Linear
**Eisenia nordenskioldi pallida*	MK642869	14,553	-	Linear
**Eisenia spelaea*	MK642870	14,738	-	Linear
**Eisenia tracta*	MK642871	14,589	-	Linear
Eisenia andrei	OK513069	15,714	1151	Circular
Eisenia fetida	OK513070	16,560	1988	Circular
Drawida japonica	KM199288	14,648	3	Circular
Pontoscolex corethrurus	KT988053	14,835	318	Circular

*Putative non-coding region between *trnR* and *trnH*.

** Incomplete mitochondrial genome sequence lacking the entire non-coding region and *trnR*.

Results

The complete mitochondrial genomes of *Eisenia fetida* and *Eisenia andrei* consisted of 16,560 and 15,714 base pairs, respectively. The setup of the mitogenomes of both species followed the typical Bauplan of the earthworm mitogenome assembly, consisting of 13 PCGs, 22 transfer RNAs, two ribosomal RNA genes, and a control region (Fig. 1; Table 2).

All genes were encoded on the heavy DNA strand, and both genomes showed biased base composition, with 63.5% AT and 36.4% GC content in *E. fetida* and 62.8% and 37.2% in *E. andrei*.

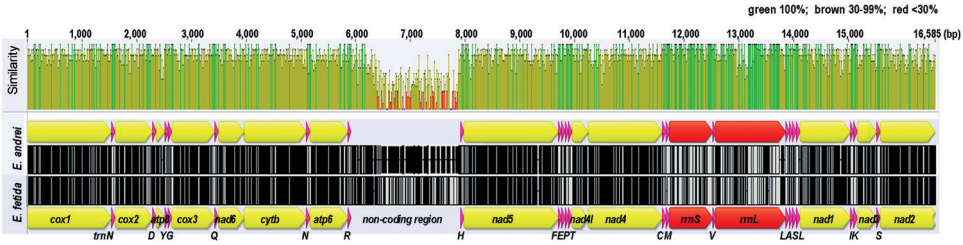

Figure 1. Comparison of mitogenomes of *Eisenia andrei* and *E. fetida*. The map is based on sequence similarity and was constructed using Geneious Prime 2021 software. Sequence similarity is represented by green (100%), brown (30–99%), and red (<30%). *cox1* was used as an anchor to linearized genomes. Organization of mitochondrial genes is shown in Table 2. Non-coding region is defined as the region between *trnR* and *trnH*.

Table 2. Comparative analysis of gene organization of *Eisenia andrei* and *E. fetida* mitogenomes (bp = base pairs).

Gene	Strand	*E. fetida*		*E. andrei*		Similarity
		Size (bp)	start/stop codon	Size (bp)	start/stop codon	
cox1	+	1540	ATG/T	1540	ATG/T	86%
trnN	+	61		61		98%
cox2	+	687	ATG/TAG	687	ATG/TAA	86%
trnD	+	61		61		89%
atp8	+	163	ATG/T	160	ATG/T	78%
trnY	+	63		63		95%
trnG	+	63		64		92%
cox3	+	778	ATG/T	778	ATG/T	86%
trnQ	+	69		69		91%
nad6	+	469	ATG/T	469	ATG/T	85%
cytb	+	1140	ATG/TAA	1140	ATG/TAA	85%
trnW	+	62		63		90%
atp6	+	696	ATG/TAA	696	ATG/TAA	82%
trnR	+	61		63		93%
*NC	+	1988		1151		60%
trnH	+	62		62		90%
nad5	+	1722	ATG/TAA	1722	ATG/TAA	83%
trnF	+	62		63		92%
trnE	+	63		63		95%
trnP	+	64		64		94%
trnT	+	65		63	-	97%
nad4L	+	297	ATG/TAA	297	ATG/TAA	88%
nad4	+	1359	ATG/TAG	1359	ATG/TAG	83%
trnC	+	65		65		97%
trnM	+	63		63		100%
rrnS	+	794		794		94%
trnV	+	64		63		94%
rrnL	+	1282		1278		89%
trnL	+	62		63		94%
trnA	+	62		62		94%
trnS	+	67		67		94%
trnL	+	64		62		95%
nad1	+	919	ATG/T	919	ATG/T	85%
trnI	+	64		64		97%
trnK	+	65		65		97%
nad3	+	354	ATG/TAG	354	ATG/TAG	82%
trnS	+	64		64		97%
nad2	+	1003	ATG/T	1003	ATG/T	81%

* Non-coding regions between *trnR* and *trnH*.

Table 3. Comparison of deduced amino acid sequences of 13 protein-coding genes between *Eisenia andrei* and *E. fetida*.

Protein	*Eisenia fetida*	*Eisenia andrei*	Similarity (%)
COX1	513 aa	513 aa	99.4
COX2	228 aa	228 aa	95.2
ATP8	54 aa	53 aa	79.6
COX3	259 aa	259 aa	97.7
NAD6	156 aa	156 aa	93.6
CYTB	379 aa	379 aa	96.0
ATP6	231 aa	231 aa	93.1
NAD5	567 aa	573 aa	90.8
NAD4L	98 aa	98 aa	92.9
NAD4	452 aa	452 aa	92.0
NAD1	306 aa	306 aa	92.6
NAD3	117 aa	117 aa	92.3
NAD2	334 aa	334 aa	89.1

The overall mitogenome sequence similarity between the two species was 80.8%, and it increased to 85.8% when the control region was excluded. The 13 PCGs were 78%–86% similar (Table 2). Among the PCGs, *nad4l* showed the highest similarity (88%) and *atp8* the lowest (78%). The average similarity of the 13 PCGs between the two species was 84%.

However, the deduced amino acid sequences of the 13 PCGs showed, on average, 92.7% similarity between the species; COX1 was the most similar (99.4%) and ATP8 the most dissimilar (79.6%) (Table 3). Sequence variation between the two species was lower at the amino acid level than at the DNA level. In particular, *cox1* showed 86% similarity at the DNA level but more than 99% similarity at the amino acid level.

Phylogenetic reconstruction of the available Lumbricidae complete or nearly complete mitogenomes using the 13 PCGs and the 12S and 16S RNA genes highly supported the Lumbricidae family (1 posterior probability and 100% bootstrap support). In addition, the genus *Eisenia* was resolved monophyletic, and the close relationship of the *E. fetida*/*andrei* species pairs was confirmed (Fig. 2). Interestingly, the included *Eisenia* sequences formed two well-supported subclades: one consisting of the European *E. spelaea* (Rosa, 1901) and the *E. fetida*/*andrei* species pair, and the other comprising the Asian taxa of the *E. nordenskioldi* (Eisen, 1879) species complex (including *E. tracta* Perel, 1985 and *E. nana* Perel, 1985), and the Asian specimens of the European *E. balatonica* (Pop, 1943). A nearly identical tree topology was obtained using the translated amino acid sequences. The only notable difference was in the swapped position of *Perionyx excavatus* Perrier, 1872 and *Tonoscolex birmanicus* within the Megascolecidaeae clade (Fig. 3).

Discussion

The mitogenomes of *E. fetida* and *E. andrei* show the same setup as other lumbricid mitogenomes (Boore and Brown 1995; Shekhovtsov and Peltek 2019; Zhang et al. 2019; Shekhovtsov et al. 2020). The nucleotide composition of the mitogenomes was also

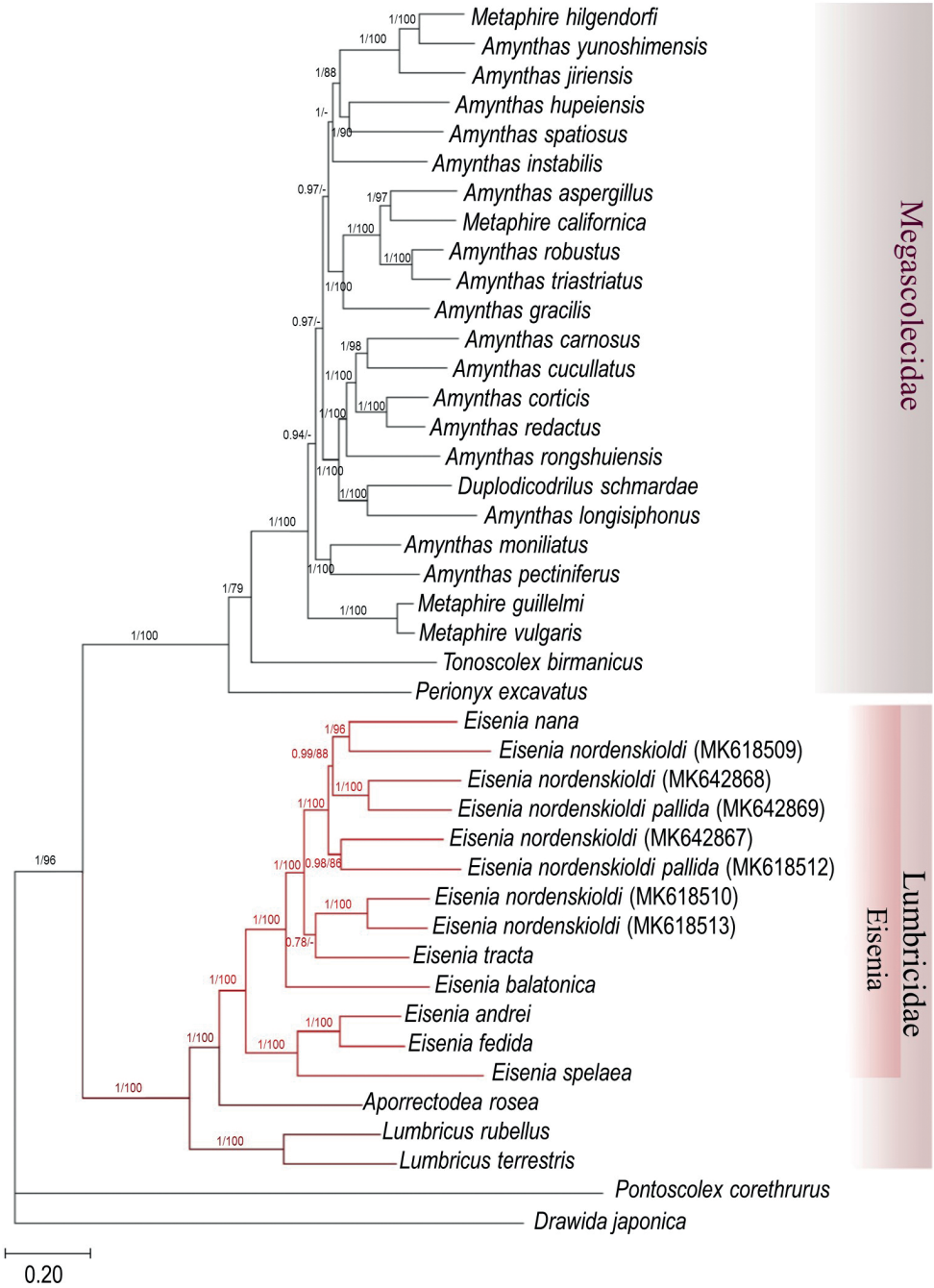

Figure 2. Phylogenetic analysis of 42 Megadrili species, including *E. andrei* and *E. fetida*, based on nucleotide sequences of 13 protein-coding genes and the 12S and 16S RNA genes. The numbers above branches present Bayesian posterior probabilities/maximum likelihood bootstrap values (values under 0.75 and 75% are not shown).

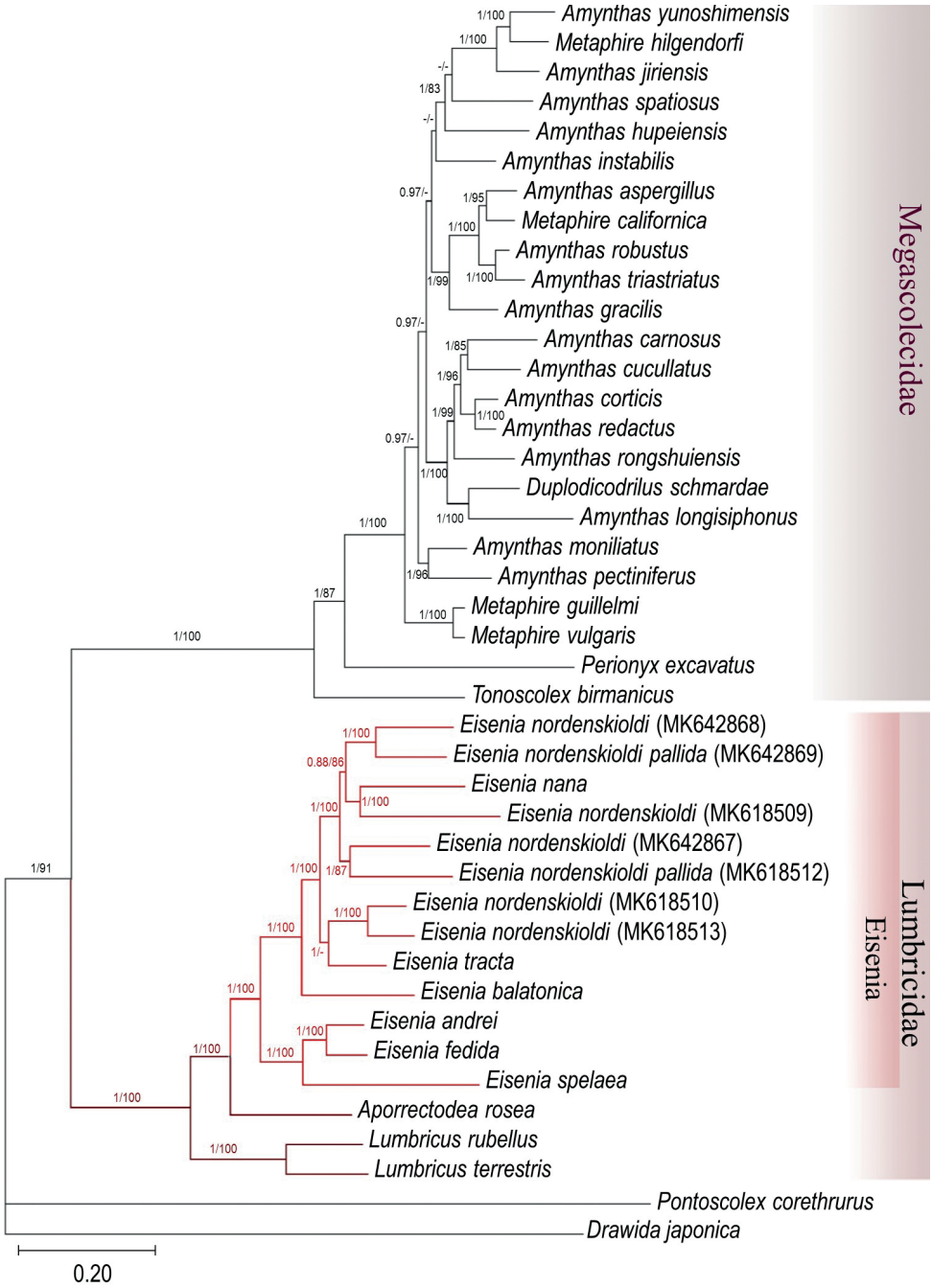

Figure 3. Phylogenetic analysis of 42 Megadrili species, including *E. andrei* and *E. fetida*, based on translated amino acid of 13 protein-coding genes. The numbers above branches are Bayesian posterior probabilities/maximum likelihood bootstrap values (values under 0.75 and 75% are not shown).

similar to that of other Lumbricidae species: the AT content of *E. fetida* and *E. andrei* (63.5% and 62.8%, respectively) was comparable to that in Lumbricidae species (59.88–65.69%), including *Eisenia nordenskioldi*, *E. balatonica*, *E. tracta*, *E. spelaea*, *Lumbricus terrestris* Linneaus, 1758, and *Aporrectodea rosea* (Savigy, 1826) (Shekhovtsov et al. 2020). Zhang et al. (2016) reported higher AT contents in other earthworm families; for example, Megascolecidae has an AT content of 62.6–67.6%, and the Moniligastridae (*Drawida japonica*) genome has an AT content as high as 69.7%. However, the mitogenomes of *E. fetida* (16,560 bp) and *E. andrei* (15,714 bp) were larger than those of other lumbricid species, such as *L. terrestris* (14,998 bp), *L. rubellus* Hoffmeister, 1845 (15,464 bp), and *Ap. rosea* (15,089 bp). These size differences are primarily due to the extreme length variation of the non-coding region (Shekhovtsov et al. 2020). The length of the non-coding region was 1988 bp in *E. fetida* and 1152 bp in *E. andrei* and significantly longer than those of known mitogenomes of other earthworm species [from 318 bp in *Pontoscolex corethrurus* (Müller, 1857) to 649 bp in *Metaphire hilgendorfi* (Michaelsen, 1892); Table 1]. In addition, slight differences were observed in the coding regions. The *atp8* gene consists of 54 amino acids in *fetida* and 53 amino acids in *andrei*, whereas *nad5* comprises 567 amino acids in *fetida* and 573 amino acids in *andrei*.

The family Lumbricidae is well-known for its notoriously polyphyletic genera (Domínguez et al. 2015). Unfortunately, only 16 complete or nearly complete Lumbricidae mitogenomes are available in GenBank (including our two new sequences), which prevents us from reaching a comprehensive conclusion on Lumbricidae phylogeny. However, our phylogenetic reconstructions using the available complete or nearly complete mitogenomes corroborated the monophyly of the family Lumbricidae and *Eisenia* (Domínguez et al. 2015; Shekhovtsov et al. 2020), the genus with the most mitogenome sequences (13 sequences) reported, including the type species *Eisenia fetida*. It is interesting to note that the *E. fetida* and *E. andrei* clade along with the Central European *E. spelaea* is distant from the Asian *E. nordenskioldi* species complex, *E. tracta*, and *E. nana*.

Perel (1998) hypothesized that the native range of *E. fetida* is somewhere in the forest-steppe zone of Central Asia, and that the species originally occurred under the bark of fallen logs. In addition, Latif et al. (2017) found surprisingly high morphological and genetic variability of *E. andrei* in northwestern Iran, which demonstrates that the native range of both species is somewhere in western Central Asia. This could explain their closer affinity to the Central European *E. spelaea* than to the Siberian–Far Eastern *E. nordenskioldi* species group.

Eisenia fetida and *E. andrei* are sister taxa in both tree topologies (Figs 2, 3), and the branch length between *E. fetida* and *E. andrei* is similar to those of other species on the trees. This supports their distinct species status. However, considering the genetic p-distances of the studied mitogenomes (Table 4), the *E. fetida*/*E. andrei* species pair showed the second smallest genetic distance (14.1%), whereas the p-distance between *L. rubellus* and *L. terrestris* was 18.9% or even larger between the two closely related species *E. nana* and *E. tracta* (19.2%).

Conclusion

On the basis of the mitogenomic analysis of *E. fetida* and *E. andrei*, we can conclude that, although the reproductive isolation between the two taxa is not complete, they should be considered as two independently evolving phylogenetic lineages and, consequently, two separate species.

It is clear that mitogenomes, owing to their highly conserved and highly variable regions, are useful in understanding earthworm systematics at the species and genus/family levels. Addition of other species in future analyses will help to further elucidate the phylogenetic relationships within earthworm families.

Table 4. Genetic p-distances of the Lumbricidae mitogenomes.

Lumbricus terrestris (U24570)															
Lumbricus rubellus (MN102127)	0.189														
Aporrectodea rosea (NC046733)	0.238	0.231													
Eisenia fetida (OK513070)	0.245	0.244	0.223												
Eisenia andrei (OK513069)	0.245	0.243	0.217	0.141											
Eisenia nana (MK618511)	0.251	0.246	0.231	0.222	0.224										
Eisenia tracta (MK642871)	0.245	0.238	0.221	0.209	0.212	0.192									
Eisenia nordenskioldi (MK618509)	0.260	0.255	0.238	0.233	0.236	0.205	0.204								
Eisenia nordenskioldi (K618513)	0.246	0.241	0.221	0.213	0.216	0.202	0.179	0.212							
Eisenia nordenskioldi (MK618510)	0.246	0.24	0.221	0.216	0.217	0.202	0.178	0.213	0.138						
Eisenia nordenskioldi (MK642867)	0.252	0.249	0.229	0.224	0.225	0.194	0.187	0.206	0.198	0.199					
Eisenia nordenskioldi (MK642868)	0.257	0.251	0.234	0.226	0.227	0.199	0.196	0.211	0.204	0.199	0.194				
Eisenia nordenskioldi (MK642869)	0.25	0.245	0.232	0.221	0.22	0.195	0.187	0.204	0.197	0.193	0.191	0.170			
Eisenia nordenskioldi (MK618512)	0.258	0.25	0.232	0.228	0.232	0.205	0.196	0.218	0.201	0.202	0.196	0.200	0.199		
Eisenia balatonica (MK642872)	0.252	0.248	0.228	0.225	0.224	0.217	0.2	0.225	0.206	0.206	0.209	0.219	0.214	0.220	
Eisenia spelaea (MK642870)	0.264	0.261	0.252	0.221	0.218	0.25	0.245	0.257	0.243	0.242	0.249	0.252	0.251	0.255	0.250

Acknowledgements

This study was supported by the National Research Foundation of Korea (NRF) funded by the Ministry of Education (NRF-2019R1I1A3A01060987).

References

Akaike H (1973) Information theory and an extension of the maximum likelihood principle. In: Petrow BN, Csáki F (Eds) Proceedings of the 2nd International Symposium on Information. Akademiai Kiado, Budapest, 267–281.

André F (1963) Contribution à l'analyse expérimentale de la reproduction des lombriciens. Bulletin Biologique de la France et de la Belgique 97: 3–101.

Avel M (1937) Titres et travaux scientifiques. Delmas, Bordeaux, 76 pp.

Bankevich A, Nurk S, Antipov D, Gurevich AA, Dvorkin M, Kulikov AS, Lesin VM, Nikolenko SI, Pham S, Prjibelski AD, Pyshkin AV, Sirotkin AV, Vyahhi N, Tesler G, Alekseyev MA, Pevzner PA (2012) Spades: A new genome assembly algorithm and its applications to single-cell sequencing. Journal of Computational Biology 19(5): 455–477. https://doi.org/10.1089/cmb.2012.0021

Blakemore RJ (2008) Cosmopolitan earthworms – an eco-taxonomic guide to the species. 3rd edn. VermEcology, Yokohama, 757 pp.

Blakemore RJ (2013) Earthworms newly from Mongolia (Oligochaeta, Lumbricidae, *Eisenia*). ZooKeys 285: 1–21. https://doi.org/10.3897/zookeys.285.4502

Bolger AM, Lohse M, Usadel B (2014) Trimmomatic: A flexible trimmer for Illumina sequence data. Bioinformatics (Oxford, England) 30(15): 2114–2120. https://doi.org/10.1093/bioinformatics/btu170

Boore JL, Brown WM (1995) Complete sequence of the mitochondrial DNA of the annelid worm *Lumbricus terrestris.* Genetics 138: 423–433. https://doi.org/10.1093/genetics/138.2.423

Bouché MB (1972) Lombriciens de France Écologie et Systématique. Institut National de la Recherche Agronomique. Annales de Zoologie Ecologie Animale. Numéro hors-série, Paris, 671 pp.

Chang CH, James SW (2011) A critique of earthworm molecular phylogenetics. Pedobiologia 54S: 3–9. https://doi.org/10.1016/j.pedobi.2011.07.015

Csuzdi Cs, Zicsi A (2003) Earthworms of Hungary (Annelida: Oligochaeta, Lumbricidae). Hungarian Natural History Museum, Budapest, 273 pp.

Domínguez J, Velando A, Ferreiro A (2005) Are *Eisenia fetida* and *Eisenia andrei* (Oligochaeta, Lumbricidae) different biological species? Pedobiologia 49(1): 81–87. https://doi.org/10.1016/j.pedobi.2004.08.005

Domínguez J, Aira M, Breinholt JW, Stojanović M, James SW, Pérez-Losada M (2015) Underground evolution: New roots for the old tree of lumbricid earthworms. Molecular Phylogenetics and Evolution 83: 7–19. https://doi.org/10.1016/j.ympev.2014.10.024

Donath A, Jühling F, Al-Arab M, Bernhart SH, Reinhardt F, Stadler PF, Middendorf M, Bernt M (2019) Improved annotation of protein-coding genes boundaries in metazoan mitochondrial genomes. Nucleic Acids Research 47(20): 10543–10552. https://doi.org/10.1093/nar/gkz833

Easton EG (1983) A guide to the valid names of Lumbricidae (Oligochaeta). In: Satchell JE (Ed.) Earthworm Ecology - From Darwin to Vermiculture. Chapman & Hall, London, 475–487. https://doi.org/10.1007/978-94-009-5965-1_41

Eisen G (1873) On Skandinaviens Lumbricider. Ofversigt af Kongliga Vetenskaps-Akademiens Forhandligar 30: 43–56. https://archive.org/details/biostor-135527

Eisen G (1879) On the Oligochaeta collected during the Swedish Expeditions to the Arctic regions in the years 1870, 1875 and 1876. Öfversigt af Kongliga Svenska Vetenskaps-Akademiens Förhandligar 15(7): 1–49.

Jaenike J (1982) *"Eisenia foetida*" is two biological species. Megadrilogica 4: 6–8.

Kalyaanamoorthy S, Minh BQ, Wong TKF, von Haeseler A, Jermiin LS (2017) ModelFinder: Fast model selection for accurate phylogenetic estimates. Nature Methods 14(6): 587–589. https://doi.org/10.1038/nmeth.4285

Katoh K, Standley DM (2013) MAFFT multiple sequence alignment software version 7: Improvements in performance and usability. Molecular Biology and Evolution 30(4): 772–780. https://doi.org/10.1093/molbev/mst010

Kumar S, Stecher G, Li M, Knyaz C, Tamura K (2018) MEGA X: Molecular Evolutionary Genetics Analysis across Computing Platforms. Molecular Biology and Evolution 35(6): 1547–1549. https://doi.org/10.1093/molbev/msy096

Latif R, Malek M, Csuzdi Cs (2017) When morphology and DNA are discordant: Integrated taxonomic studies on the *Eisenia fetida/andrei* complex from different parts of Iran (Annelida, Clitellata: Megadrili). European Journal of Soil Biology 81: 55–63. https://doi.org/10.1016/j.ejsobi.2017.06.007

Lehmitz R, Römbke J, Jänsch S, Krück S, Beylich A, Graefe U (2014) Checklist of earthworms (Oligochaeta: Lumbricidae) from Germany. Zootaxa 3866(2): 221–245. https://doi.org/10.11646/zootaxa.3866.2.3

Liu H, Xu N, Zhang Q, Wang G, Xu H, Ruan H (2020) Characterization of the complete mitochondrial genome of *Drawida gisti* (Metagynophora, Moniligastridae) and comparison with other Metagynophora species. Genomics 112(5): 3056–3064. https://doi.org/10.1016/j.ygeno.2020.05.020

Malm AW (1877) Om daggmaskar, Lumbricina. Öfversigt af Sallskapet Hortikulturens Vänners i Göteborg Förhandligar 1: 34–47.

Martin P, Martinez-Ansemil E, Pinder A, Timm T, Wetzel MJ (2016) World checklist of freshwater Oligochaeta species. [Available online at] http://fada.biodiversity.be/group/show/12 [accessed 09 October 2021]

Miller MA, Pfeiffer W, Schwartz T (2010) Creating the CIPRES Science Gateway for inference of large phylogenetic trees. In: 2010 Gateway Computing Environments Workshop (GCE), 1–8. https://doi:10.1109/GCE.2010.5676129

Nguyen LT, Schmidt HA, von Haeseler A, Minh BQ (2015) IQ-TREE: a fast and effective stochastic algorithm for estimating maximum-likelihood phylogenies. Molecular Biology and Evolution 32(1): 268–274. https://doi/org/10.1093/molbev/msu300

Perel TS (1985) Specific Features of the Earthworm Fauna (Oligochaeta, Lumbricidae) in Altai Refugia of Nemoral Vegetation. Doklady Akademii Nauk SSSR 283(3): 752–756. [In Russian]

Perel TS (1998) The earthworms of the fauna of Russia: Cadaster and key. Nauka, Moscow, 97 pp. [in Russian]

Pop V (1943) Hazai és külföldi lumbricidák a Magyar Nemzeti Múzeumban. Annales Historico-Naturales Musei Nationalis Hungarici 34: 12–24.

Qiu JP, Bouché MB (1998) Revision des taxons supraspecifiques de Lumbricoidea. Documents pedozoologiques et intergrologiques 3: 179–216.

Reinecke AJ, Viljoen SA (1991) A comparison of the biology of *Eisenia fetida* and *Eisenia andrei* (Oligochaeta). Biology and Fertility of Soils 11(4): 295–300. https://doi.org/10.1007/BF00335851

Reynolds JW (1977) The earthworms (Lumbricidae and Sparganophilidae) of Ontario. Royal Ontario Museum, Toronto, 141 pp.

Ronquist F, Teslenko M, van der Mark P, Ayres DL, Darling A, Höhna S, Larget B, Liu L, Suchard MA, Huelsenbeck JP (2012) MrBayes 3.2: efficient bayesian phylogentic inference and model choice across a large model space. Systematic Biology 61(3): 539–542. https://doi.org/10.1093/sysbio/sys029

Römbke J, Aira M, Backeljau T, Breugelmans K, Dominguez J, Funke E, Graf N, Hajibabaei M, Perez-Losada M, Porto PG, Schmelz RM, Vierna J, Vizcaino A, Pfenninger M (2016) DNA barcoding of earthworms (*Eisenia fetida/andrei* complex) from 28 ecotoxicological test laboratories. Applied Soil Ecology 104: 3–11. https://doi.org/10.1016/j.apsoil.2015.02.010

Rosa D (1901) Un lombrico cavernicolo. Atti della Societa dei Naturalisti e Matematici di Modena 4: 36–39. http://www.morebooks.unimore.it/site/home/la-produzione-scientifica/documento610066458.html

Savigny JC (1826) Analyse d'un memoire sur les Lumbricus par Cuvier. Mémoires de l'Académie des Sciences de l'Institut de France 5: 176–184.

Schwarz G (1978) Estimating the dimension of a model. Annals of Statistics 6(2): 461–464. https://doi.org/10.1214/aos/1176344136

Shekhovtsov S, Peltek SE (2019) The complete mitochondrial genome of *Aporrectodea rosea* (Annelida: Lumbricidae). Mitochondrial DNA. Part B, Resources 4(1): 1752–1753. https://doi.org/10.1080/23802359.2019.1610091

Shekhovtsov SV, Golovanova EV, Ershov NI, Poluboyarova TV, Berman DI, Bulakhova NA, Szederjesi T, Peltek SE (2020) Phylogeny of the *Eisenia nordenskioldi* complex based on mitochondrial genomes. European Journal of Soil Biology 96: e103137. https://doi.org/10.1016/j.ejsobi.2019.103137

Sims RW (1983) The scientific names of earthworms. In: Satchell JE (Ed.) Earthwom Ecology: from Darwin to Vermiculture. Chapman and Hall, London, 365–373. https://doi.org/10.1007/978-94-009-5965-1_40

Sims RW, Gerard BM (1985) Earthworms. Keys and notes to the identification and study of the Species. Synopsis of the British Fauna (New series), EJ. Brill, Leiden, 171 pp.

Zhang L, Sechi P, Yuan M, Jiang J, Dong Y, Qiu J (2016) Fifteen new earthworm mitogenomes shed new light on phylogeny within the *Pheretima* complex. Scientific Reports 6(1): e20096. https://doi.org/10.1038/srep20096

Zhang Q, Liu H, Zhang Y, Ruan H (2019) The complete mitochondrial genome of *Lumbricus rubellus* (Oligochaeta, Lumbricidae) and its phylogenetic analysis. Mitochondrial DNA. Part B, Resources 4(2): 2677–2678. https://doi.org/10.1080/23802359.2019.1644242

ZooKeys 1097: 183–207 (2022)
doi: 10.3897/zookeys.1097.79713
https://zookeys.pensoft.net

RESEARCH ARTICLE

A peer-reviewed open-access journal
ZooKeys
Launched to accelerate biodiversity research

Three new species of non-marine ostracods (Crustacea, Ostracoda) from small water bodies of northern China

Na Yu[1], Shunxin Ma[1,2], Qianwei Wang[3,4], Dayou Zhai[3,4]

1 *College of Teacher Education, East China Normal University, Shanghai, China* **2** *Fengxian High School, Shanghai, China* **3** *Yunnan Key Laboratory for Palaeobiology, Institute of Palaeontology, Yunnan University, Kunming 650500, China* **4** *MEC International Joint Laboratory for Palaeobiology and Palaeoenvironment, Yunnan University, Kunming 650500, China*

Corresponding author: Dayou Zhai (dyzhai@ynu.edu.cn)

Academic editor: Ivana Karanovic | Received 27 December 2021 | Accepted 5 April 2022 | Published 29 April 2022

http://zoobank.org/4B27A1D5-A4A8-4BF8-99E8-B1C6A29FEB0F

Citation: Yu N, Ma S, Wang Q, Zhai D (2022) Three new species of non-marine ostracods (Crustacea, Ostracoda) from small water bodies of northern China. ZooKeys 1097: 183–207. https://doi.org/10.3897/zookeys.1097.79713

Abstract

Three new species, *Pseudocandona cheni* **sp. nov.**, *Cyclocypris pangi* **sp. nov.**, and *Tonnacypris rectangularis* **sp. nov.**, collected from northern China, are described in this study. *Pseudocandona cheni*, of the *compressa* group, is difficult to be distinguished from other members of the same group by carapace morphology alone, but can be readily recognised by the structure of the hemipenis comprised of a long lobe *a*, distally inflated lobe *h*, and exteriorly pointed lobe *b*, as well as thick trunks of the male fifth limb endopodites. *Cyclocypris pangi*, despite its similarity in carapace morphology to its congeners, can be identified based on the morphology of the hemipenis, which bears a slender, slightly curved lobe *h*, and an S-shaped process accompanying lobe *b*, in addition to the rectangular trunk of the male fifth limb endopodite. On the other hand, *Tonnacypris rectangularis*, described on the basis of females only, can be distinguished from other *Tonnacypris* Diebel & Pietrzeniuk, 1975 representatives by its distinct sub-rectangular carapace alone. Other differences include the length of the swimming setae, the length of the distal claws on the second antennae, and the morphology of the pincer organ on the seventh limb. This study contributes to the poorly known extant non-marine ostracod fauna of Inner Mongolia and Beijing, and generally to the central-eastern Palaearctic region. In addition, the known distribution range of *Tonnacypris* is extended eastwardly by *T. rectangularis*. The valve-morphology data are useful for identifying fossil/sub-fossil representatives.

Keywords

biodiversity, *Cyclocypris*, freshwater ecosystem, *Pseudocandona*, taxonomy, *Tonnacypris*

Copyright *Na Yu et al.* This is an open access article distributed under the terms of the Creative Commons Attribution License (CC BY 4.0), which permits unrestricted use, distribution, and reproduction in any medium, provided the original author and source are credited.

Introduction

Taxonomic studies of the extant non-marine ostracods of China lag behind other Eurasian regions where ostracods have been extensively investigated, such as Europe (e.g., Meisch 2000), Japan (e.g., Okubo 2004; Smith et al. 2011), Korea (e.g., Karanovic and Lee 2012), and Thailand (e.g., Savatenalinton and Suttajit 2016). More than 90 years after the pioneering work of Sars (1903) and the first taxonomic study by a native ostracod worker (Chen 1957), only 47 species of extant non-marine ostracods were known from China based on the checklist by Yin and Martens (1997). Yu et al. (2009) compiled an updated checklist of 154 extant, non-marine ostracod species from China, but only 94 of these were based on the living material (Martens and Savatenalinton 2011). Yu (2014) has provided the most comprehensive taxonomic description of the extant ostracods of China to date, which included 91 species, the majority of which have soft-part morphology described. The number of species presented by Yu (2014) is in accordance with the Martens and Savatenalinton (2011) estimate. Recently, a number of publications added taxa to the catalogue of the living non-marine ostracods of China (e.g., Zhai and Xiao 2013; Kong et al. 2014; Zhai and Zhao 2014; Ma and Yu 2018, 2020; Peng et al. 2021), and the total number may be slightly more than 100. Probably many more species await discovery and description, considering the comparatively small number of taxonomic works done in China since Sars (1903) and Chen (1957), and disparity of geographical settings with diverse aquatic ecosystems found across the vast land area of this country. A number of ostracods recorded during the studies of the valve material from the superficial sediments have been left in open nomenclature (e.g., Mischke et al. 2003, 2007; Zhai et al. 2013; Li et al. 2021). Even in some taxonomic publications, species were left with open nomenclature due to the incomplete illustrations and descriptions. For example, in the discussion on the identification methods of ostracods of Zhai et al. (2017), a number of unidentified species were mentioned, with only some limb-structure measurements provided. In addition, several species, although named, are known only after empty valves without information on the soft parts (Yang et al. 1982; Yang and Huang 1983; Huang et al. 1985), hindering further understanding of their ecology and phylogeny. Therefore, there is an urgent need to accumulate more taxonomic data on the living non-marine ostracods of China, preferentially based on both carapace and soft-part morphology, to facilitate the application of ostracods in various fields of scientific research including palaeoclimatology, ecology and biology.

In this study, we present detailed taxonomic descriptions of three unnamed species originally reported by Zhai et al. (2017), where only some limb structures had been measured and no illustrations of their carapace or soft parts were presented. We also provide a brief description of the ecological characterisation of these species. This work will provide valuable information for future research based on ostracods, especially in Beijing and Inner Mongolian areas.

Material and methods

Ostracods were collected from four sites (Table 1). At the sites Y11, Y26, and Y30, bottom substrates were collected with a simplified sucking device modified from Viehberg (2002), and were sieved with a mesh of 0.15 mm. The sample Y34 was collected by sieving the detritus-rich substrate and the macrophytes with a mesh of 0.15 mm. The samples were fixed with 70% ethanol after excess water was drained. Electrical conductivity of the ambient water was measured with a HANA HI98128 device.

In the laboratory, samples were transferred to a Petri dish, from which ostracods were picked under the Olympus SZX16 stereomicroscope and then stored in 70% ethanol in centrifuge tubes. Soft parts of the specimens were dissected with a pair of sharpened, fine needles attached to bamboo handles, sealed in Hydro-Matrix (Micro-Tech-Lab, Graz, Austria) and drawn with the aid of a camera lucida attached to the Olympus CX31RTSF microscope. Carapaces were stored dry on the micropalaeontological slides. Carapaces and valves that are illustrated were coated with gold and imaged under the JEOL 5800 LV, or the FEI Quanta 200 scanning electron microscope (SEM). All specimens are deposited at the Yunnan Key Laboratory for Palaeobiology, Institute of Palaeontology, Yunnan University.

Terminology and abbreviations

A1	antennule;	**L6**	sixth limb;	**Mx**	maxillula;
A2	antenna;	**L7**	seventh limb;	**RV**	right valve;
Hp	hemipenis;	**LV**	left valve;	**UR**	uropodal ramus.
L5	fifth limb;	**Md**	mandible;		

Terminology of the limb chaetotaxy follows Broodbakker and Danielopol (1982), Martens (1987) and Meisch (1996, 2000). Terminology of the structures of reproductive organs follows Danielopol (1969, 1978). Systematics follows Meisch et al. (2019).

Table 1. Information on sampling sites (GPS coordinates based on WGS84 system).

Site	Coordinates	Habitat description	Date	EC	Specimens
Y11	43°22'26.0"N, 116°44'36.8"E	pond with abundant plant detritus, formed in rechanneled bed of Gongger River, Hexigten Banner, Inner Mongolia	12.v.2015	2314	dyzoc575–580, dyzoc819, dyzoc821 (*Tnr*)
Y26	43°00'20.5"N, 115°47'34.9"E	small pond with abundant plant detritus, connected with small creek in Zhenglan Banner, Inner Mongolia	18.v.2015	458	dyzoc567–570, dyzoc706–707, dyzoc813 (*Psc*)
Y30	42°58'55.8"N, 115°49'14.0"E	small swamp with abundant grass in Zhenglan Banner, Inner Mongolia	18.v.2015	562	dyzoc625, dyzoc626, dyzoc814 (*Psc*);
					dyzoc675, dyzoc816–817 (*Clp*)
Y34	between 40°33'59.7"–34'11.5"N, 116°47'9.7"–48'25.8"E	pond with a few macrophytes, flowed through by mountain brook in vicinity of Beijing	25.v.2015	199	dyzoc558–563 (*Clp*)

Key: EC, electrical conductivity in μS cm^{-1}. *Clp*, *Cyclocypris pangi* sp. nov.; *Psc*, *Pseudocandona cheni* sp. nov.; *Tnr*, *Tonnacypris rectangularis* sp. nov.

Taxonomy

Suborder Cypridoidea Baird, 1845
Family Candonidae Kaufmann, 1900
Subfamily Candoninae Kaufmann, 1900
Genus *Pseudocandona* Kaufmann, 1900

***Pseudocandona cheni* sp. nov.**
http://zoobank.org/1023A7A8-5811-4B6E-8E8A-062596F1BA7B
Figs 1–3

Pseudocandona sp. 2 – Zhai et al. 2017: 486, fig. 9.

Type locality. A small shallow pond (Y26, Table 1) in Inner Mongolia, China.

Type material. ***Holotype*:** one male (dyzoc567). ***Allotype*:** one female (dyzoc569). ***Paratypes*:** one male (dyzoc568) and three females (dyzoc570, dyzoc706, dyzoc707). All from the type locality, with soft parts dissected, valves preserved on the micropalaeontological slides.

Other material. One male (dyzoc625) and one female (dyzoc626), both from the site Y30 (Table 1), with soft parts dissected, valves preserved on the micropalaeontological slides. One female (dyzoc813), from the type locality. One female (dyzoc814), from the site Y30 (Table 1). Both undissected, with carapace enclosed, preserved on the micropalaeontological slides.

Etymology. This species is named after Prof. Shouzhong Chen (= Shoutsung Chen; Institute of Hydrobiology, Chinese Academy of Sciences), who was the first among the Chinese ostracod workers to describe soft parts of non-marine ostracods from China (Chen 1957).

Dimensions. Male, n = 3, LV, length 860–872 μm, height 510–535 μm; RV, length 842–849 μm, height 485–513 μm. Female, LV, n = 5, length 874–941 μm, height 526–574 μm; RV, n = 3, length 874–903 μm, height 497–520 μm.

Diagnosis. Carapace sub-trapezoidal in lateral view, relatively short and stout, with hinged part of dorsal margin nearly straight and sloping anteriorly (Fig. 1). Setal group on second segment of Md palp with five setae (Fig. 2D). Right palp of L5 with wide trunk and ventrally curved finger-like end (Fig. 3C). Left palp with elongated and ventrally curved trunk (Fig. 3D). Hemipenis with M-process triangular distally. Lobe *a* tongue-like. Lobe *b* shortest, with sub-quadrate distal part on inner edge and triangular distal part on outer edge. Lobe *h* with rounded distal part (Fig. 3G).

Description. Carapace surface densely covered with small shallow pits in anterior, posterior, and dorsal areas (Fig. 1B). In lateral view, greatest height posterior of mid-length. Postero-dorsal angle of male valve (Fig. 1A, B) slightly blunter than female (Fig. 1E, F). Ventral margin nearly straight. Anterior margin narrower than posterior. Anterior calcified inner lamella wide. Carapace compressed in anterior area and

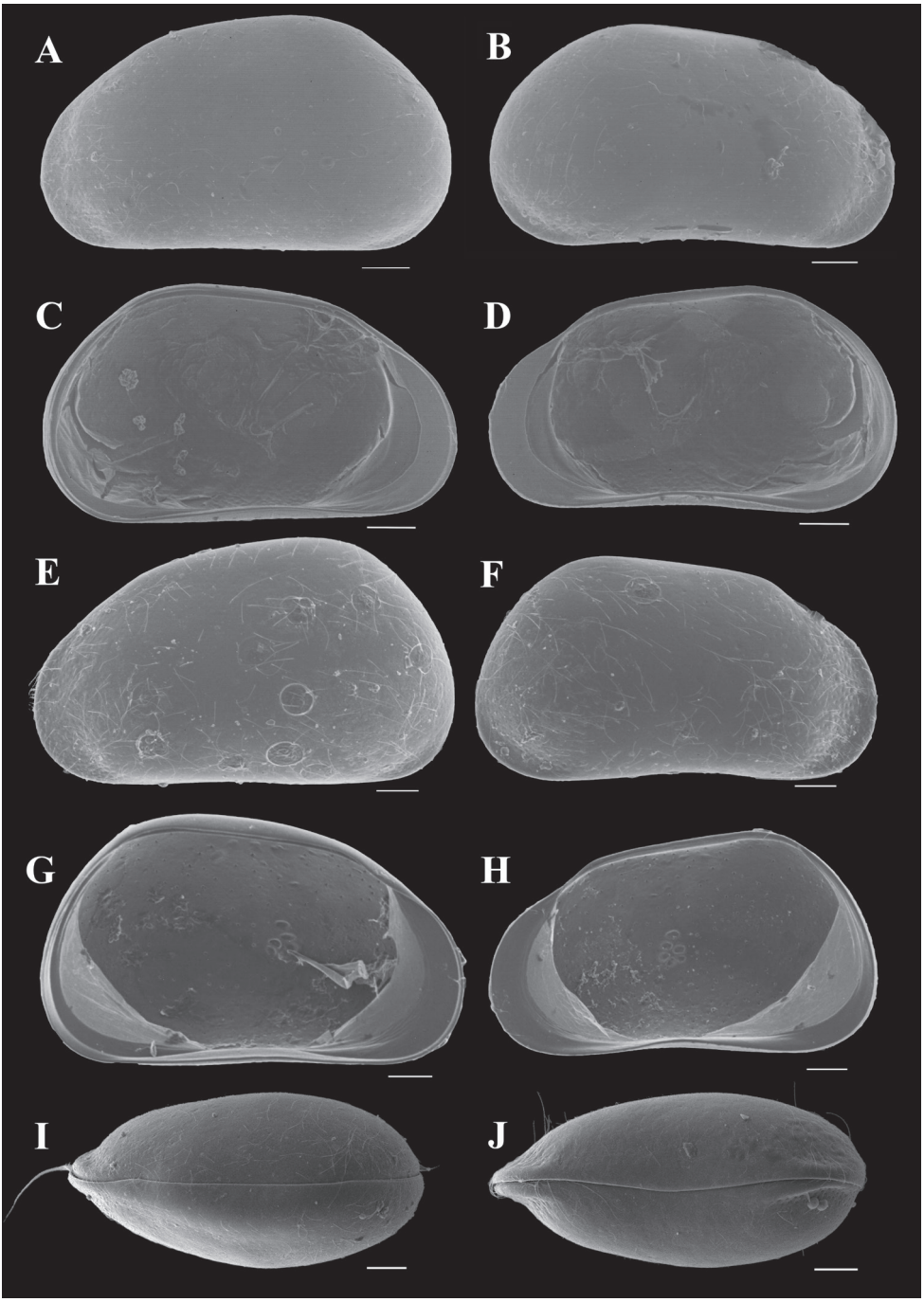

Figure 1. *Pseudocandona cheni* sp. nov. **A–D** male, dyzoc567 (holotype) **A** outer view of LV **B** outer view of RV **C** inner view of LV **D** inner view of RV **E–H** female, dyzoc569 (allotype) **E** outer view of LV **F** outer view of RV **G** inner view of LV **H** inner view of RV **I** female, dyzoc813, dorsal view of carapace, anterior to left **J** female, dyzoc814, ventral view of carapace, anterior to left. Scale bars: 100 μm.

postero-ventral corner (Fig. 1I, J). LV overlaps RV on dorsal, ventral, and posterior sides, and slightly exceeds RV anteriorly (Fig. 1I, J).

A1 (Fig. 2A) seven-segmented. First segment with two dorsal and two long ventral setae. Second segment with one short dorso-apical seta. Third segment without seta. Fourth and fifth segments with two long dorso-apical setae and one short ventro-apical seta, respectively. Sixth segment with one short and three long apical setae. Terminal segment with one short and two long setae and aesthetasc *ya*.

Male A2 (Fig. 2B) five-segmented. Seta *t2* and *t3* transformed into male bristles, both similar in morphology, each terminating with slightly inflated, triangular process. Claws *z1* and *z2* long, slightly shorter than claw *G2*. Seta *G3* slim, slightly exceeding end of terminal segment. Claw *G1* short, slightly exceeding half-length of claw *G2*. Claw *Gm* slightly exceeding half-length of claw *GM*.

Female A2 (Fig. 2C) four-segmented. Claw *G2* short, not reaching half-length of claw *G3*. Claw *G3* slightly shorter than claw *G1*. Claw *Gm* exceeding half-length of claw *GM*. Setae *t1–4* unequally long, with *t1* and *t3* being longest while *t4* being shortest. Seta *z1* short, extending to ca. mid-way of terminal segment. Setae *z2* and *z3* extending to ca. mid-way of *G*-claws but *z2* slightly longer than *z3*.

Md (Fig. 2D) palp with short and slender α-seta. Seta β short and slender with 5 grouped setae and one sub-equally long accompanying seta on second segment. Seta γ long, smooth, and slender.

Mx (Fig. 3A) palp two-segmented. Second segment spatulate. Two tooth-bristles on third masticatory lobe smooth.

Male L5 (Fig. 3C, D) asymmetrical. Right palp basally wide, grading to finger-like end, with two sub-apical setae. Left palp distally narrower than right, with two sub-apical setae.

Female L5 (Fig. 3B) with long *b*- and *d*- setae, and one long *a*-seta.

L6 (Fig. 3E) five-segmented. First segment with *d1*-seta extending slightly beyond this segment. Setae *e* and *f* extending to ca. tips of second and third endopodal segments, respectively. Seta *g* exceeding beyond terminal segment with ~ 50% of length. Terminal segment with *h1*-seta conspicuously longer than *h3*-seta.

L7 (Fig. 3F) five-segmented. First segment with *d1*-, *d2*- and *dp*- setae. Setae *e* and *f* absent. Seta *g* long. Terminal segment with short *h1*-seta and long *h2*- and *h3*- setae.

UR (Fig. 3H) with tiny seta *Sa*. Claw *Gp* slightly shorter than claw *Ga*. Seta *Sp* slightly exceeding end of ramus.

Hemipenis (Fig. 3G) sub-ovate in outline. Lobe *a* tongue-like, with sub-quadrate distal end. M-process with triangular distal part. Lobe *b* shorter than lobes *a* and *h*, with sub-quadrate distal part on inner edge and triangular distal part on outer edge. Lobe *h* slightly shorter than lobe *a*, with rounded distal part. Bursa copulatrix elongated with long finger distally.

Remarks. The genus *Pseudocandona* Kaufmann, 1900, with 72 species described to date, is the third most diverse genus of the non-marine ostracods after *Candona* Baird, 1845 and *Strandesia* Stuhlmann, 1888 (see Meisch et al. 2019). [Karanovic (2005, 2012) proposed an alternative taxonomic scheme where *Pseudocandona* is treated as

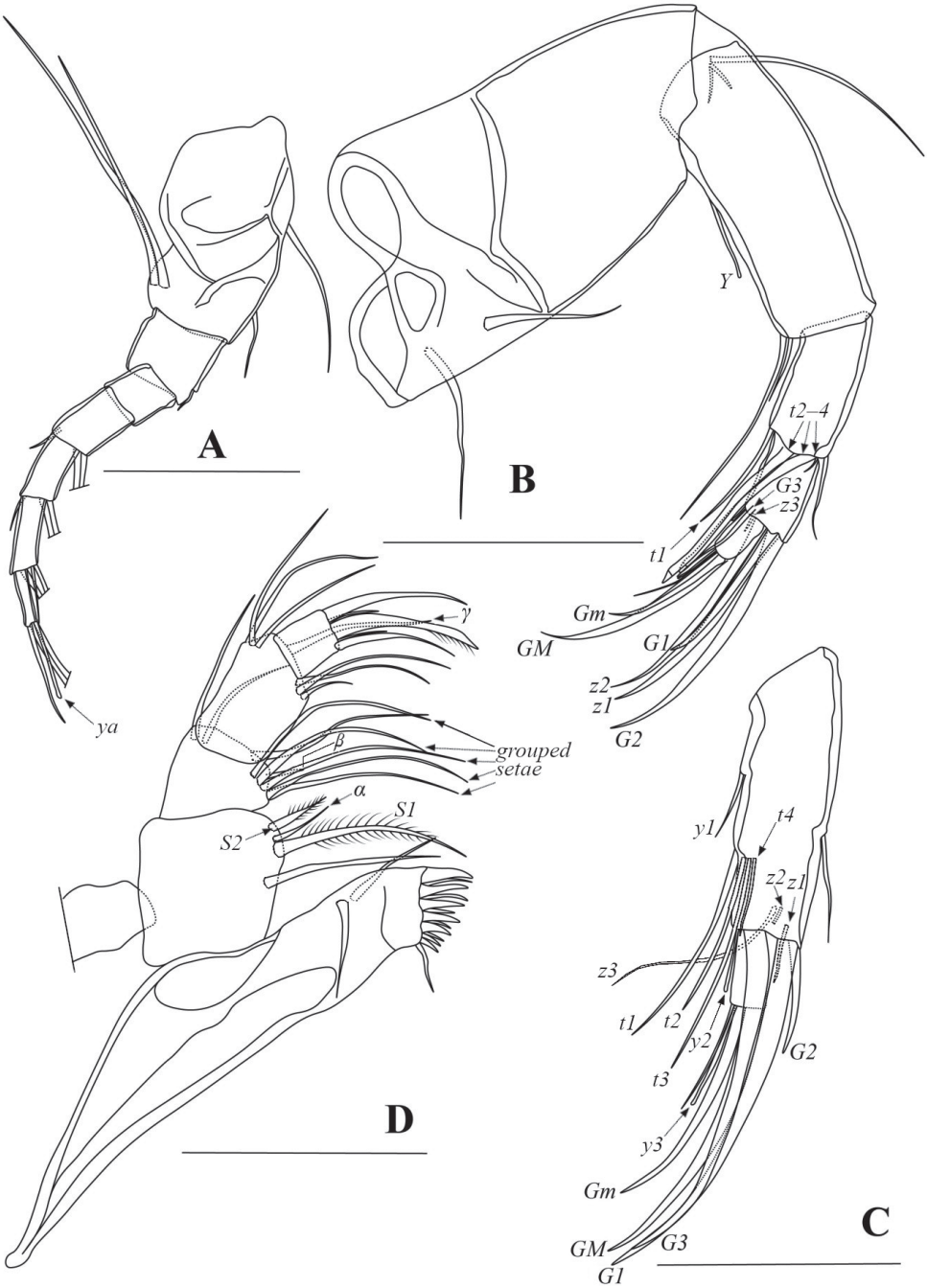

Figure 2. *Pseudocandona cheni* sp. nov. **A** male, dyzoc567 (holotype), A1 **B** male, dyzoc567, A2 **C** female, dyzoc570, part of A2 **D** male, dyzoc567, Md. Scale bars: 100 μm.

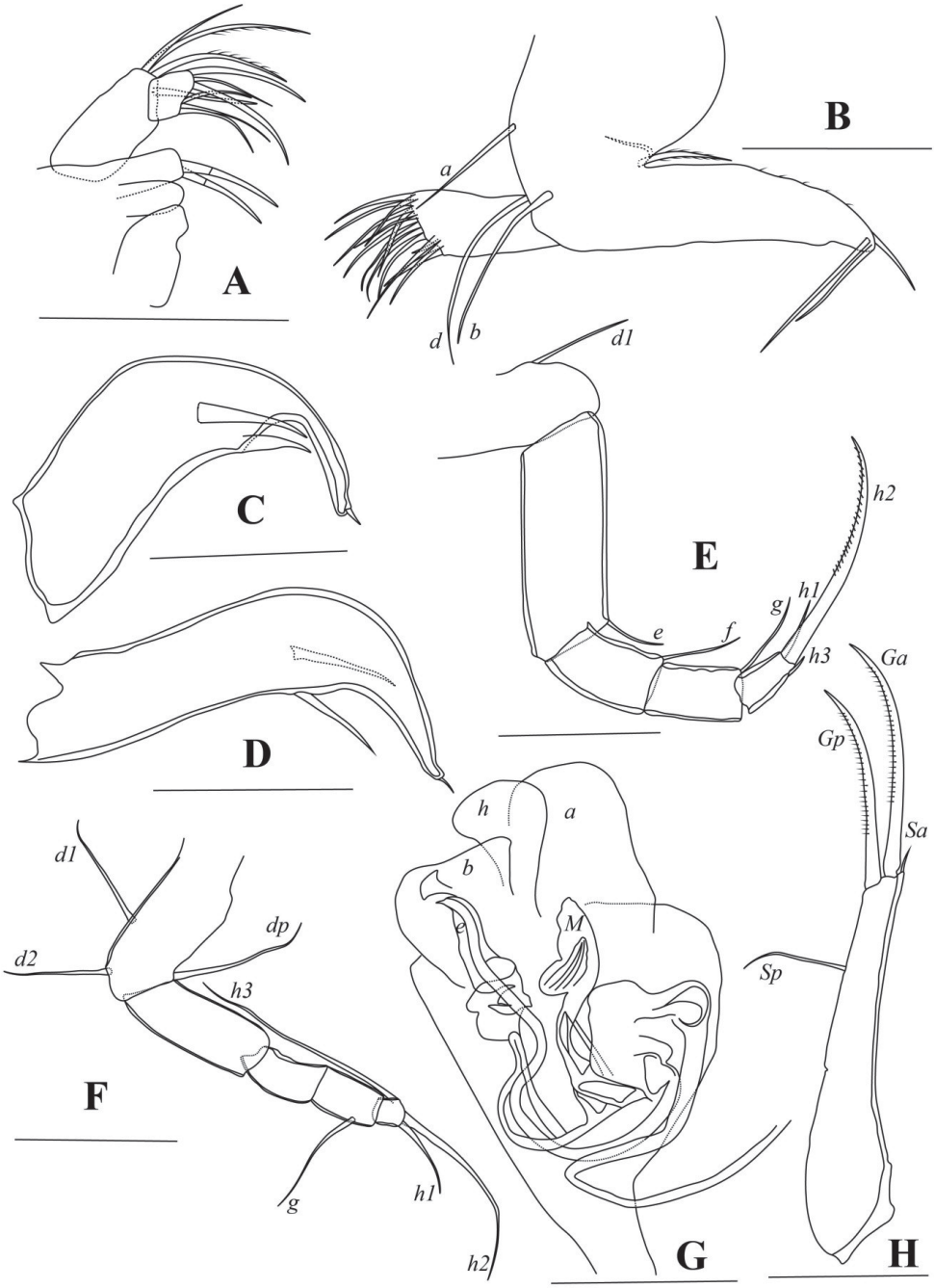

Figure 3. *Pseudocandona cheni* sp. nov. **A** male, dyzoc567 (holotype), Mx **B** female, dyzoc570, L5 **C** male, dyzoc567, right L5 palp **D** male, dyzoc567, left L5 palp **E** male, dyzoc567, L6 **F** male, dyzoc567, L7 **G** male, dyzoc567, Hp **H** male, dyz567, UR. Scale bars: 100 μm.

a subgenus under the genus *Typhlocypris* Vejdovský, 1882 and it only contains the six species of the *compressa* group, but we follow Namiotko et al. (2014) who redefined the genus *Typhlocypris*.] The genus, as accepted at the moment, consists of five species groups (*caribbeana*, *compressa*, *prespica*, *rostrata*, and *zschokkei*) and some species with uncertain positions (Namiotko and Danielopol 2004; Meisch et al. 2019). This division is mostly based on the number of posterior setae on the second segment of Md palp. Species with 5+1+β setae, as well as with the *h1*-seta on the L7 being more than twice the length of terminal segment, are classified in the *compressa* group (Meisch 1996, 2000; Namiotko and Danielopol 2004), to which the present new species also belongs. Other species of this group are *P. albicans* (Brady, 1864), *P. compressa* (Koch, 1838), *P. insculpta* (G. W. Müller, 1900), *P. pratensis* (Hartwig, 1901), *P. regisnikolai* Karanovic & Petkovski, 1999, and *P. sucki* (Hartwig, 1901) (Karanovic and Petkovski 1999; Meisch 2000; Karanovic 2012). *Pseudocandona albicans* can be distinguished from the present species by a shorter seta that accompanies the group of the five setae on the Md palp (sub-equally long to the grouped setae in the present species), a much slenderer first endopodal segment of the L6, as well as a slenderer carapace in dorsal view (Meisch 2000). Male bristles on the A2 are absent in *P. insculpta* (Meisch 2000), which easily distinguishes it from the present species. No other species of the *compressa* group has the morphology of the male L5 and the Hp similar to *P. cheni*. In *P. compressa*, *P insculpta*, and *P. pratensis*, the lob *h* is not distally inflated (albeit slightly curved in *P. pratensis*), their right L5 have slenderer trunks. The lobe *h* in *P. sucki* is very wide, while the lobe *b* is small (Meisch 2000). *Pseudocandona regisnikolai* is much larger (females range between 1.33 and 1.4 mm and males are up to 1.53 mm) (Karanovic and Petkovski 1999). In addition, *P. regisnikolai* possesses only one dorsal seta on the basal segment of the A1, setae *t2* and *t3* on the male A2 are not transformed into bristles, the left prehensile palp of male is much slenderer than the right one, and the *Hp* bears a conspicuous lobe *g* (Karanovic and Petkovski 1999).

Subfamily Cyclocypridinae Kaufmann, 1900
Genus *Cyclocypris* Brady & Norman, 1889

***Cyclocypris pangi* sp. nov.**
http://zoobank.org/98BB8DE9-79A3-4985-9EC3-EAE47971E91C
Figs 4–6

Cyclocypris sp. – Zhai et al. 2017: 485, fig. 8.

Type locality. A pond (Y34, Table 1) in Beijing, China.

Type material. ***Holotype*:** one male (dyzoc559). ***Allotype*:** one female (dyzoc558). ***Paratypes*:** two females (dyzoc560, dyzoc561) and two males (dyzoc562, dyzoc563). All from the type locality, dissected, valves preserved on the micropalaeontological slides.

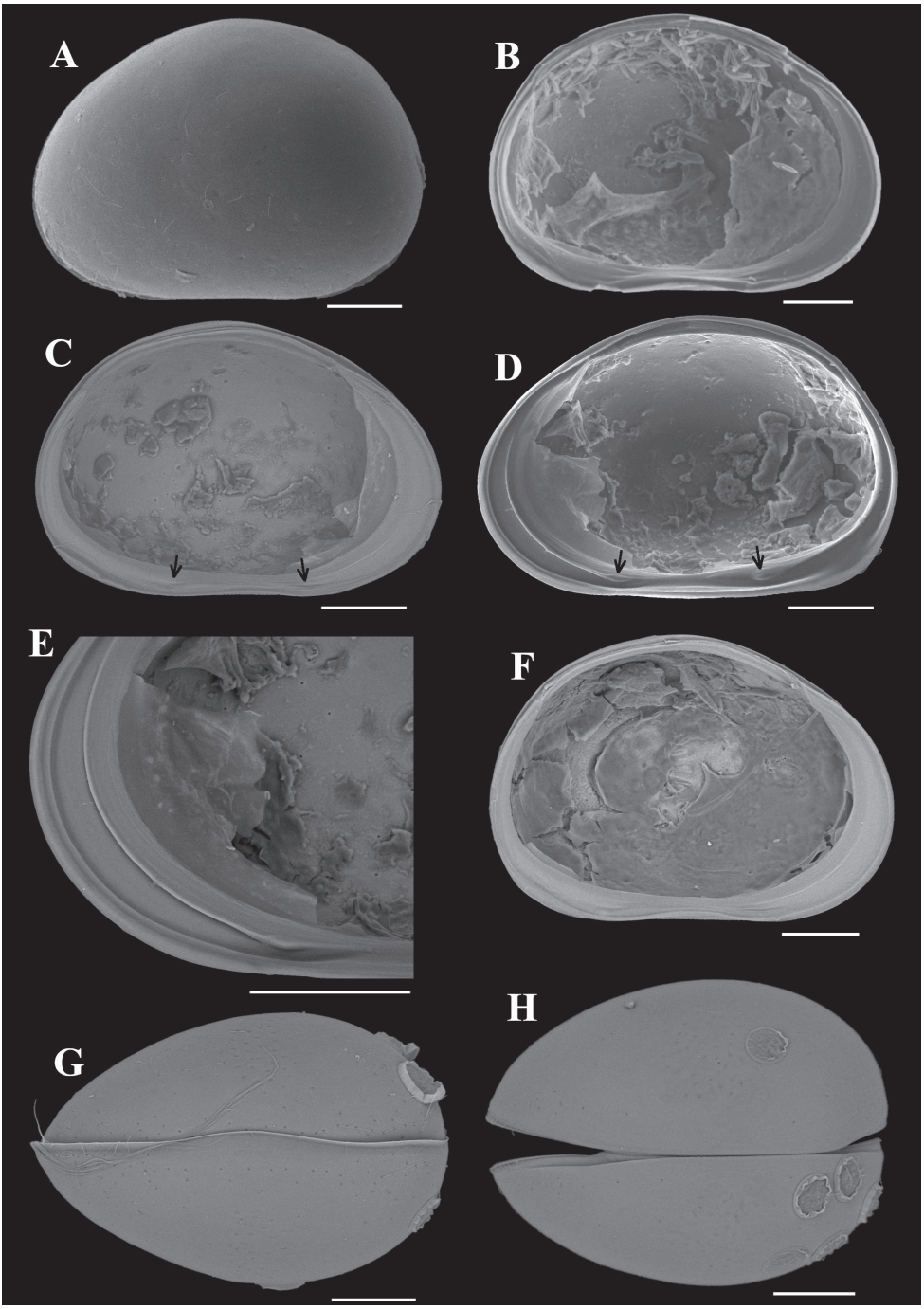

Figure 4. *Cyclocypris pangi* sp. nov. **A, B** female, dyzoc558 **A** outer view of LV **B** inner view of LV **C–E** female, dyzoc675 **C** inner view of LV, with sockets arrowed **D** inner view of RV, with pegs arrowed **E** anterior part of (D) showing details of calcified inner lamella **F** female, dyzoc560, inner view of LV **G** sex unknown, dyzoc816, ventral view of carapace **H** sex unknown, dyzoc817, dorsal view of slightly open carapace. Scale bars: 100 μm.

Other material. One female (dyzoc675), from the site Y30 (Table 1), with soft parts dissected and valves preserved on a micropalaeontological slide. Two undissected specimens (dyzoc816, dyzoc817), from the site Y30 (Table 1), preserved dry on the micropalaeontological slides.

Etymology. This species is named in the honour of Prof. Qiqing Pang (Hebei GEO University, China) in recognition of his productive work on Mesozoic and Cenozoic ostracods since the 1960s.

Dimensions. Male, *n* = 3, LV, length 520−540 μm, height 355−387 μm. Female, *n* = 4, LV, length 483−558 μm, height 331−390 μm.

Diagnosis. *Cyclocypris* species with intermediate-sized (Fig. 4A), dark-brown carapace. RV overlapping LV anteriorly and ventrally. A2 natatory setae exceeding terminal claws by 55% of length (Fig. 5B). Prehensile palps slightly asymmetrical, with subrectangular trunks, finger of left prehensile palp wider (Fig. 6A, B). L6 *e*-seta exceeding end of terminal segment. L7 fourth segment with length almost twice of width, *h1* short and slightly curved, not "S-shaped" (Fig. 6C). Terminal claws of UR not reaching half-length of UR stem (Fig. 6D). Hp carrying S-shaped structure to interior side of lobe *b*, lobes *a* and *b* with wide distal end (Fig. 6F).

Description. Carapace smooth. RV overlapping LV on all directions, and with one lobe-like expansion ventrally (Fig. 4G, H). Dorsal margin arched. Ventral margin almost straight in RV (Fig. 4D) and only slightly concave in LV (Fig. 4A−C, F). Greatest height near middle length. Posterior end more rounded than anterior. Selvage peripheral along antero-ventral and postero-ventral margins (Fig. 4A). Two inner lists present on each valve (Fig. 4C−F): interior one most pronounced on anterior margin of RV (Fig. 4E), weakly expressed on same position of LV (Fig. 4C, F); exterior one running close to selvage on both valves (Fig. 4C−F) except postero-ventral part of LV (Fig. 4C, F). Antero- and postero-ventral parts of RV each with one blunt peg (arrows in Fig. 4D), corresponding to antero- and postero-ventral sockets on LV (arrows in Fig. 4C).

A1 (Fig. 5A) seven-segmented. First segment with one dorsal and two long ventral setae. Second segment with one dorso-apical seta and tiny Rome organ. Third segment with one medium-long dorso-apical seta and one short ventro-apical seta. Fourth segment with two long dorso-apical setae and two short ventro-apical setae. Fifth segment with two long dorso-apical setae, and one long and one short ventro-apical setae. Sixth segment with four long apical setae. Seventh segment with three long apical setae and aesthetasc *ya*.

Male A2 (Fig. 5B) five-segmented. Five long natatory setae extending beyond terminal claws with ~ 55% of their lengths. Sixth seta extending to end of next segment. Seta *z3* long, reaching to end of terminal claws. Seta *z1* well-developed and claw-like, slightly shorter than claws *G2* and *GM*. Claw *G1* short, not reaching mid-way of *G2*. Claw *G3* very small and seta-like. Claw *Gm* almost reaching mid-length of claw *GM*.

Female A2 (Fig. 5C) four-segmented. Seta *z1* shorter than setae *z2* and *z3*, exceeding mid-length of claw *G3*. Claws *G1*, *G3*, and *G2* progressively shorter. Claw *Gm* long, almost 80% length of claw *GM*.

Md (Fig. 5D) palp four-segmented. Seta *a* short and slim. Seta *β* very short and stout. Second segment with three long setae. Fourth segment with three claws and two setae.

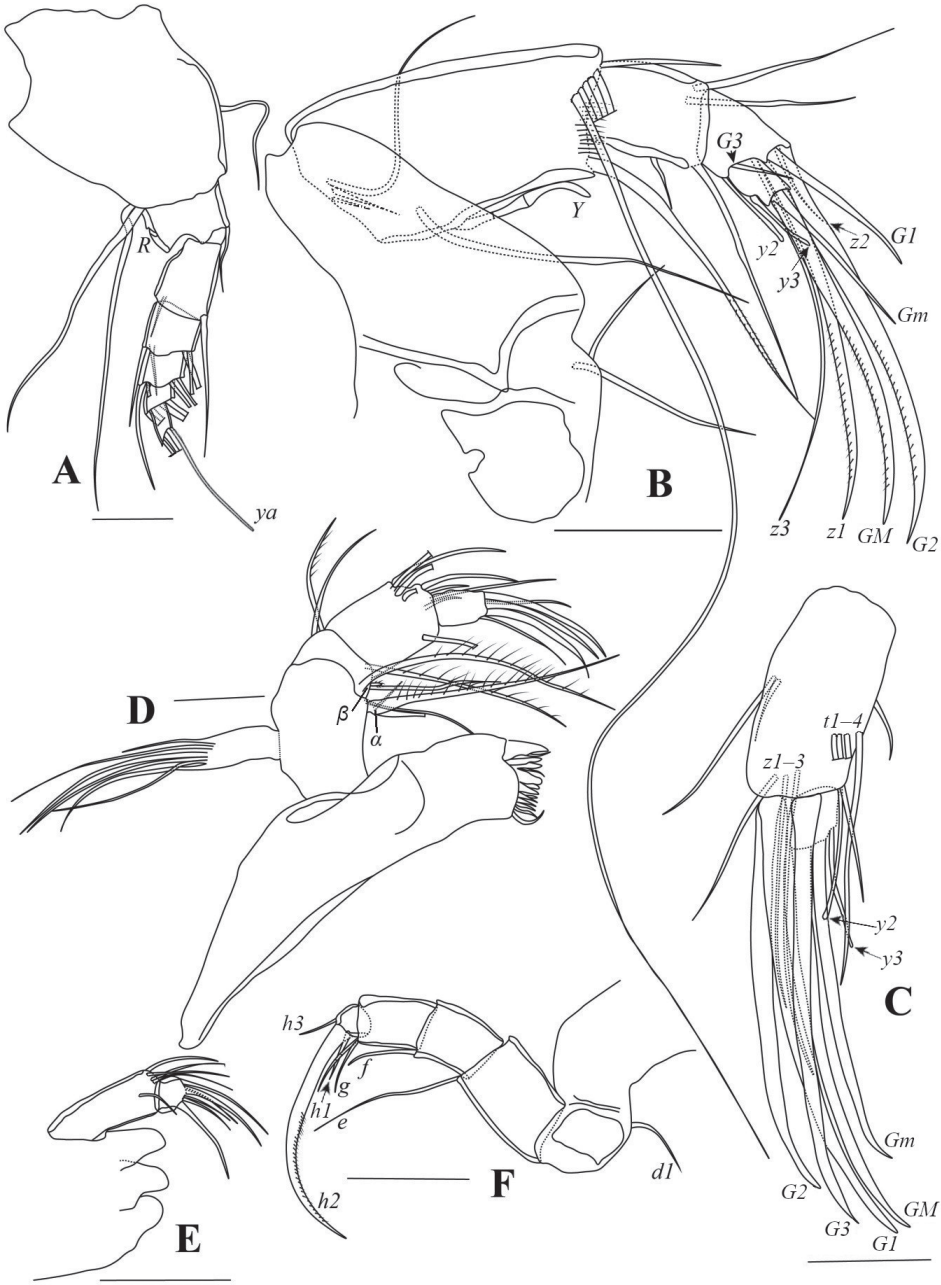

Figure 5. *Cyclocypris pangi* sp. nov. **A** male, dyzoc559 (holotype), A1 **B** male, dyzoc559, A2 **C** female, dyzoc558 (allotype), A2 **D** female, dyzoc558, Md **E** female, dyzoc558, Mx **F** male, dyzoc559, L6. Scale bars: 100 μm.

Mx (Fig. 5E) palp two-segmented. First segment with four setae on outer apical edge and one seta in sub-apical position near outer edge. Second segment with three long and three short setae.

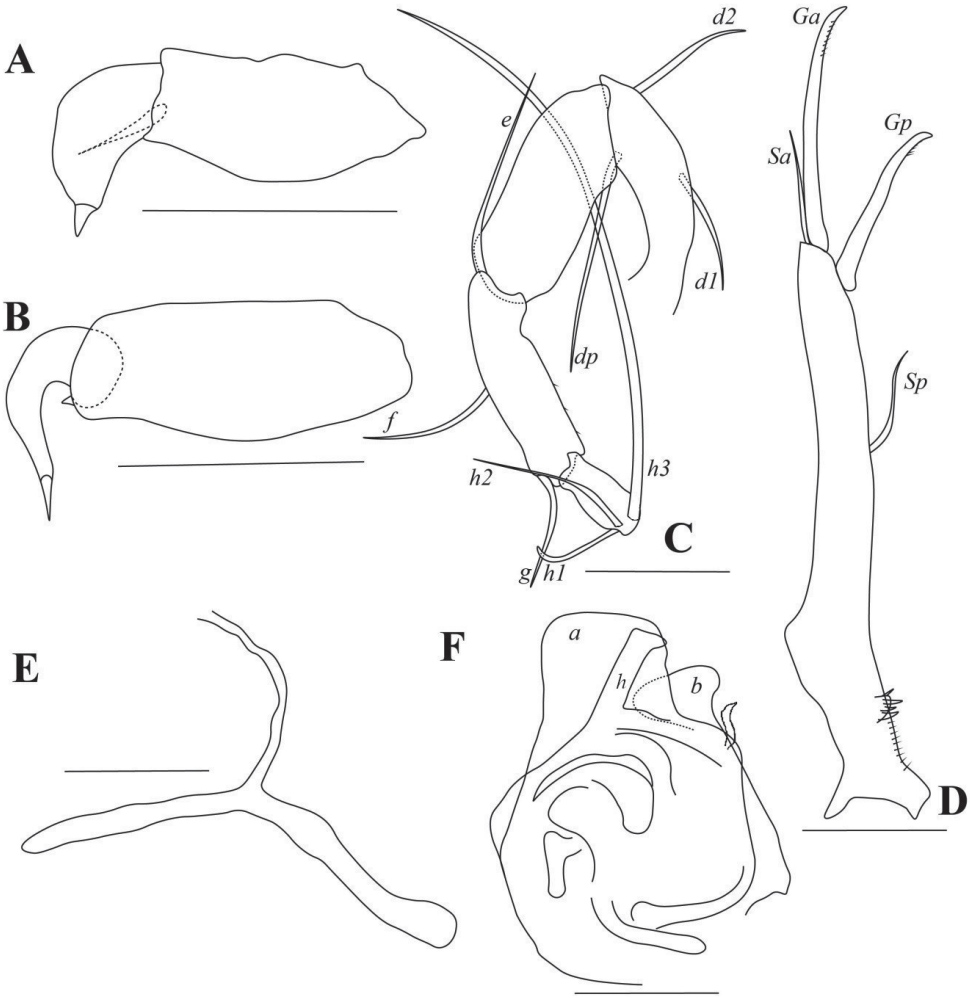

Figure 6. *Cyclocypris pangi* sp. nov. **A** male, dyzoc559, left L5 **B** male, dyzoc559, right L5 **C** female, dyzoc558, L7 **D** female, dyzoc558, UR **E** female, dyzoc558, UR attachment **F** male, dyzoc559, Hp. Scale bars: 100 μm.

Male L5 (Fig. 6A, B) palps asymmetrical. First segment sub-rectangular. Left palp with bluntly rounded end and one sub-apical seta. Right palp slimmer than left, with one minute sub-apical seta. Distal end of right palp hook-like.

Female L5 (not shown, deformed in all specimens examined.) Exopod bearing five soft, thick rays. Other chaetotaxy structures difficult to discern.

L6 (Fig. 5F) five-segmented. First segment with *d1*-seta. Second segment with long *e*-seta, exceeding end of terminal segment. Third segment with *f*-seta slightly exceeding end of fourth segment. Fourth segment with two long *g*-setae, both exceeding beyond end of terminal segment. Fifth segment with short *h1*- and *h3*- setae and long claw *h2*.

L7 (Fig. 6C) four-segmented. First segment with *d1*-, *d2*- and *dp*- setae. Second segment with *e*-seta, not extending to end of third segment. Third segment with *f*-seta slightly exceeding end of this segment, and *g*-seta, slightly exceeding end of fourth

segment. Fourth segment long, the length almost two times length of width with short *h1*- and *h2*- setae and long *h3*-seta.

UR (Fig. 6D) robust. Claw *Gp* exceeding mid-length of claw *Ga*. Seta *Sa* not reaching mid-length of claw *Ga*. Seta *Sp* short, not reaching base of claw *Gp*. UR attachment with two long branches.

Hemipenis (Fig. 6F) stout. Lobe *a* with wide, truncated distal end. Lobe *b* shorter than lobe *a* with wide distal end. Medial lobe *h* elongated, distally curved. Thin, slightly S-shaped structure with pointed end present to interior side of lobe *b*.

Remarks. *Cyclocypris* is the third most diverse genus in Cyclocypridinae Kaufmann, 1900 and contains 21 species (Meisch et al. 2019). Except for *C. pusilla* Sars, 1895 reported from Afrotropical region (Sars 1895; Meisch et al. 2019), most *Cyclocypris* species are known from the Nearctic and Palaearctic regions. In China, three *Cyclocypris* species, *C. serena* (Koch, 1838), *C. globosa* (Sars, 1863), and *C. ovum* (Jurine, 1820), have been reported so far (Chen 1982; Huang 1986; Wang et al. 1995; Zhang et al. 2006; Kong et al. 2013). Majority of those species are known as fossils or sub-fossils, with the exception of *C. serena* (Kong et al. 2013).

The new species has some typical *Cyclocypris* characteristics. It is small, has a rounded carapace and long swimming setae on the A2; besides, it lacks male bristles on the A2 and has elongated terminal segment on the L7 and a long *g*-seta on the same appendage. The new species is somewhat similar to *C. serena* in terms of its size, the overlap of RV and LV, smooth surface of the valves, long swimming setae on the A2, rectangular basal segment of the L5, and short *h1*-seta on the L7. However, it can be distinguished from *C. serena* based on the following characters: (1) the lobes *a* and *b*, and the general shape of Hp, are much wider than in *C. serena* (Meisch 2000); (2) the length of the L6 *e*-seta, the UR *Sa*- and *Sp*- setae, the number and length of the apical setae on both prehensile palps of the male L5, all differ from *C. serena*; (3) with respect to valve morphology, *C. serena* [0.58−0.63 mm according to Meisch (2000)] is significantly larger than the new species, the inner list on the RV is less pronounced (Fuhrmann 2012), and the exterior inner list is absent. These differences in valve morphology would help distinguish the two species when dealing with sub-fossil / fossil material. The new species can be easily recognised, among the other 21 congeners, by the presence of a small, S-shaped process next to the lobe *b*, as well as a slender, distally curved lobe *h* (Fig. 6F).

Family Cyprididae Baird, 1845
Subfamily Eucypridinae Bronstein, 1947
Genus *Tonnacypris* Diebel & Pietrzeniuk, 1975

***Tonnacypris rectangularis* sp. nov.**
http://zoobank.org/46D8213C-E160-4FDA-8CC6-D47BA32686E7
Figs 7−9

Tonnacypris sp. – Zhai et al. 2017: 488, fig. 11.

Type locality. A small pond (Y11, Table 1) in Inner Mongolia, China.

Type material. ***Holotype*:** one female (dyzoc575) dissected, valves preserved on the micropalaeontological slides. ***Paratype*:** five females (dyzoc576–580) dissected, valves preserved on the micropalaeontological slides. All from the type locality.

Other material. Two undissected females (dyzoc819, dyzoc821) from the type locality, preserved dry on the micropalaeontological slides.

Etymology. From the English word *rectangle*, referring to sub-rectangular valve shape in lateral view.

Dimensions. Female, LV, $n = 6$, length 1800–2030 μm, height 940–1040 μm; RV, $n = 4$, length 1804–2010 μm; height 980–1060 μm.

Diagnosis. Carapace sub-rectangular, dorsal margin sub-parallel to ventral or slightly inclined anteriorly. Peg present on antero-ventral part of LV (Fig. 7C, E, F). Natatory setae on A2 reduced, first and second setae approximately in same lengths, others increasing in lengths towards anterior edge (Fig. 8B). Claw *G2* on A2 short, not reaching to middle length of claw *G3* (Fig. 8C). Second segment of Md palp with 3+1+β setae at interior side (Fig. 8E). Mx palp with terminal segment slightly spatulate. Two tooth-bristles on third masticatory lobe of Mx smooth (Fig. 8F). Length ratio between *d1-* and *d2-* setae on L6 0.41 (Fig. 9B).

Description. Valves (Fig. 7) sub-rectangular, dorsal margin sub-parallel to ventral or slightly inclined anteriorly. When inclined, greatest height posterior of mid-length. Dorsal margin slightly arched posteriorly. Ventral margin concaved (Fig. 7A–E). Anterior end more rounded than posterior. Calcified inner lamella wider anteriorly than posteriorly. Peg present on antero-ventral part of LV (Fig. 7C, E, F). Valve surface smooth, with setae. Carapace sub-ovate in dorsal / ventral view (Fig. 7G, H), with greatest width behind mid-length. Each valve with one outer list running through anterior and ventral margins (Fig. 7G, H, I).

A1 (Fig. 8A) seven-segmented. First segment with one short dorsal and two long ventral setae. Second segment with one short dorso-apical seta and a tiny Rome organ. Third segment with one comparative long dorso-apical seta and one short ventro-apical seta. Fourth segment with two long dorso-apical and two short ventro-apical setae. Fifth segment with two long dorso-apical setae and two setae (one long and one short) ventrally. Sixth segment with four long apical setae. Seventh segment with two long setae, one short seta and aesthetasc *ya*.

A2 (Fig. 8B, C) four-segmented. Natatory setae reduced, first and second setae almost in same lengths, others decreasing in lengths towards anterior edge. Claws *G1* and *G3* almost in same lengths. Claw *G2* short, not reaching mid-length of claw *G3*. Claw *Gm* slim, reaching mid-length of claw *GM*.

Md coxa (Fig. 8D) elongated and arched, with masticatory processes on interior end. Palp (Fig. 8E) four-segmented. Seta *a* long and slim. Seta β hirsute. Second segment with 3+1+β setae on interior side. Seta γ slim and smooth.

Mx (Fig. 8F) palp two-segmented. First segment with seven setae on outer apical edge and one seta in sub-apical position near outer edge. Second segment slightly spatulate with three long and three short setae. Two tooth-bristles on third masticatory lobe smooth.

L5 (Fig. 9A) with two *a*-setae, one long *b*-seta, one short *c*-seta and one hirsute *d*-seta.

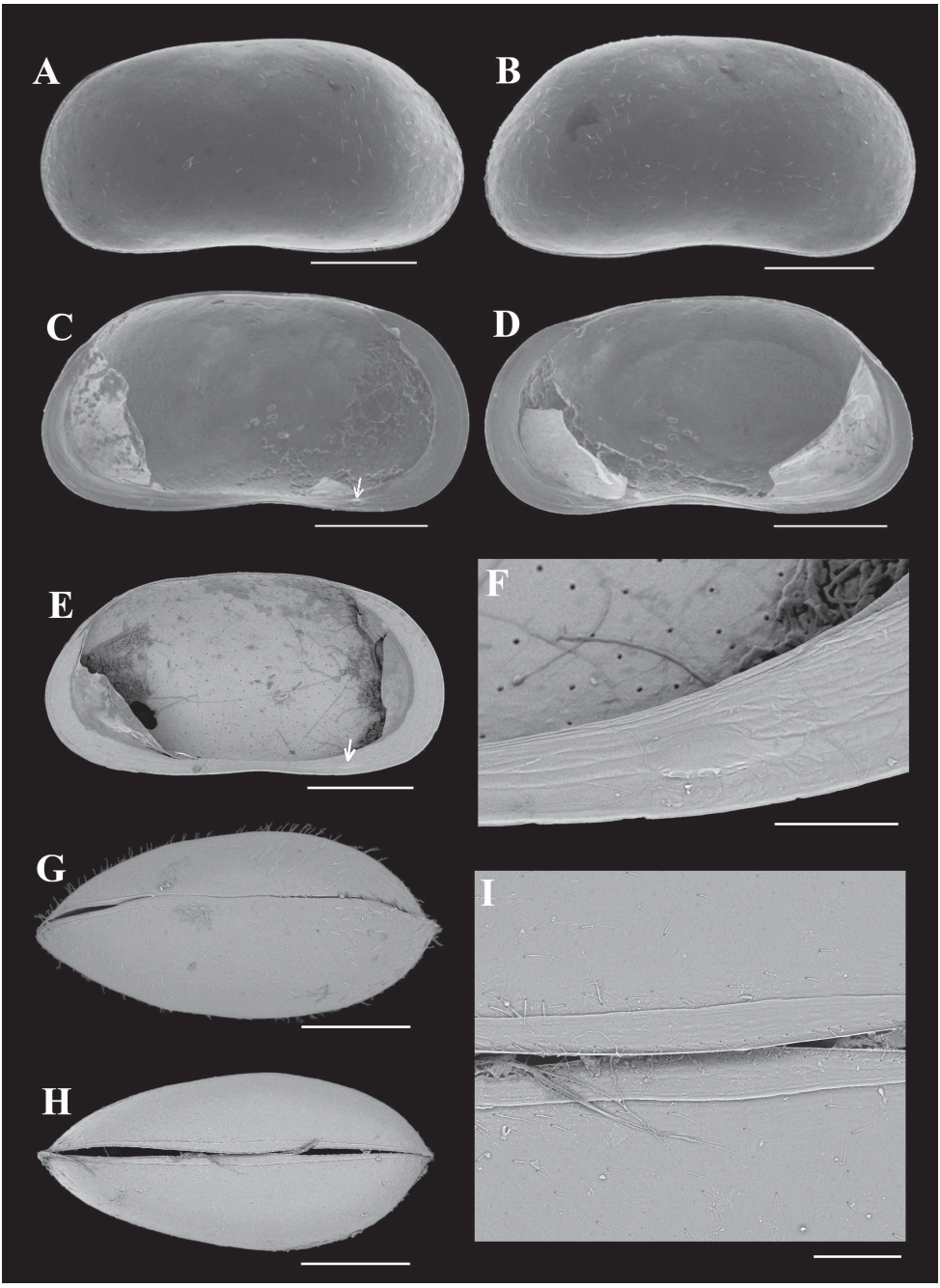

Figure 7. *Tonnacypris rectangularis* sp. nov. Female **A–D** dyzoc575 (holotype) **A** outer view of LV **B** outer view of RV **C** inner view of LV, with peg arrowed **D** inner view of RV **E, F** dyzoc577 **E** inner view of LV, with peg arrowed **F** detail of peg in (**E**) **G** dyzoc821, slightly oblique-dorsal view of carapace **H, I** dyzoc819 **H** ventral view of carapace **I** detail of central part of (**H**), showing outer lists on both valves. Scale bars: 100 μm (**F, I**); 500 μm (**A–E, G, H**).

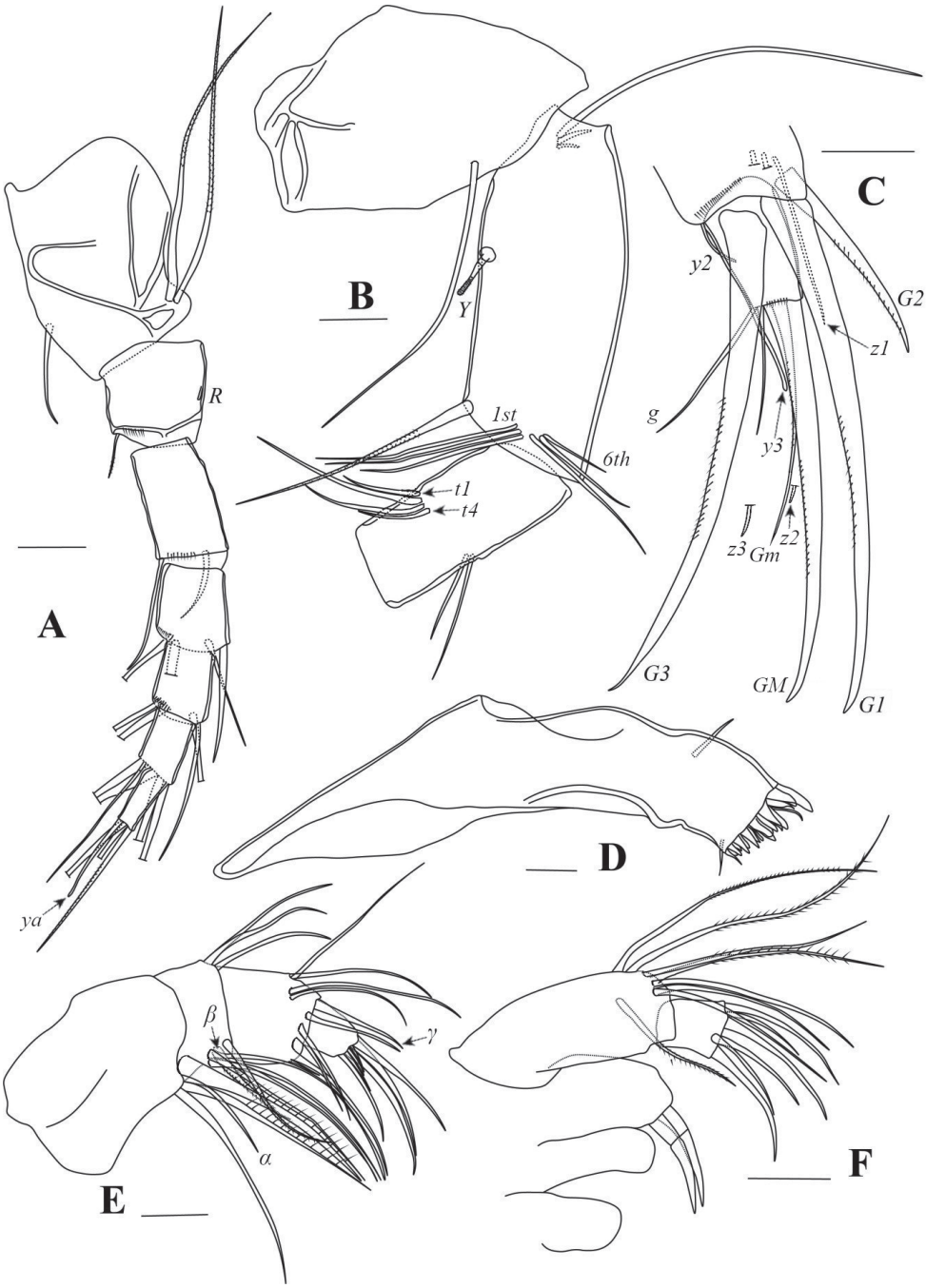

Figure 8. *Tonnacypris rectangularis* sp. nov. Female. dyzoc575 (holotype) **A** A1 **B** part of A2 **C** part of A2 **D** Md coxa **E** Md palp **F** Mx. Scale bars: 100 μm.

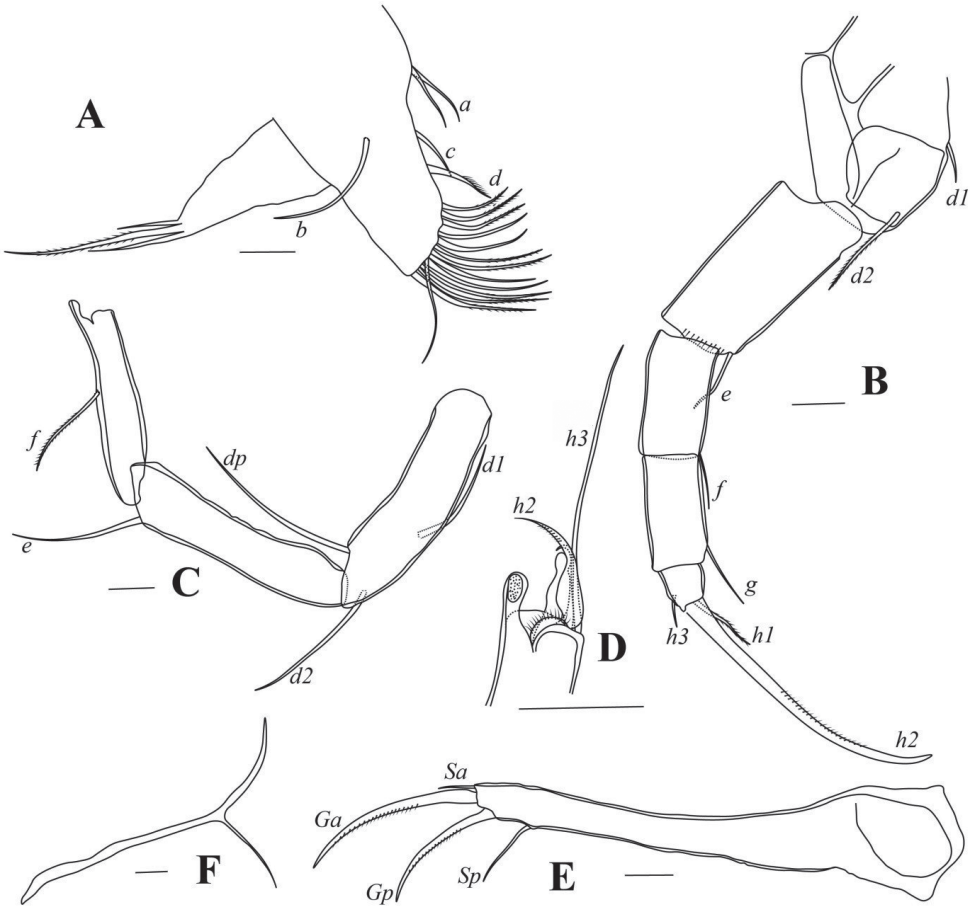

Figure 9. *Tonnacypris rectangularis* sp. nov. Female **A** dyzoc580, L5 **B** dyzoc580, L6 **C** dyzoc580 part of L7 **D** dyzoc580, part of L7 **E** dyzoc575, UR **F** dyzoc575, UR attachment. Scale bars: 100 μm.

L6 (Fig. 9B) five-segmented. Seta *d1* slightly shorter than half length of seta *d2*. Setae *e* and *f* short, not reaching end of next segment. Seta *g* long, slightly exceeding end of terminal segment. Seta *h1* longer than seta *h3*.

L7 (Fig. 9C, D) first segment with *d1*-, *d2*- and *dp*- setae. Second segment with *e*-seta not reaching end of third segment. Third segment medially with *f*-seta almost reaching end of this segment. Pincer organ typical of the genus, with comparatively long *h3*-seta and slender, gently curved *h2*-seta.

UR (Fig. 9E) with tiny seta *Sa*. Claw *Gp* exceeding half-length of claw *Ga*. Seta *Sp* slightly exceeding end of stem. UR attachment (Fig. 9F) with two long branches.

Remarks. The genus *Tonnacypris* was first established with the fossil species *Tonnacypris loessica* Diebel & Pietrzeniuk, 1975. *T. rectangularis* sp. nov. can be identified as belonging to this genus by the presence of peg on the LV [although not all specimens of this genus have pegs, see e.g., Peng et al. (2021)], presence of the *c*-seta

on the L5, a short *d1*- and long *d2*- setae on the L6. There are nine extant species in this genus (Meisch et al. 2019). Among these, *T. angulata* Yang, 1985 has been described based on valves alone (Huang et al. 1985), and its generic assignment remains uncertain (Van der Meeren et al. 2009). The new species can be readily distinguished from all other extant congeners by the valve morphology (e.g., long and sub-parallel or anteriorly sloping dorsal margin, and narrow anterior calcified inner lamella) alone, but its soft parts offer additional diagnostic information. According to the length of the swimming setae on the A2, this species was the most similar to *T. mazepovae* Van der Meeren et al., 2009. But in *T. rectangularis* the surface of the carapace and the tooth-bristles on Mx are smooth, while in *T. mazepovae* the carapace surface is covered with superficial grooves and the tooth-bristles on the Mx are serrated (Van der Meeren et al. 2009). The present specimens are similar in valve shape and size to *T. tonnensis* (Diebel & Pietrzeniuk, 1975). However, in *T. tonnensis* the postero-ventral part of the valve is more narrowly rounded, and its A1 has a very long dorsal seta on the second segment (Van der Meeren et al. 2009: fig. 8). In addition, the UR attachment is not bifurcated in *T. tonnensis*. Among the fossil species, the type species *T. loessica* may resemble the new species in valve morphology (Fuhrmann 2012). Both species have sub-rectangular valves and their anterior calcified inner lamella is narrow. However, while the dorsal margin of *T. rectangularis* is sub-parallel to the ventral margin or is inclined anteriorly, the dorsal margin of *T. loessica* is sloping posteriorly. And the antero-dorsal part of both valves of *T. loessica* is angular, forming an antero-dorsal corner (cf. Fuhrmann 2012).

Discussion

The world's extant non-marine ostracods are distributed across all eight zoogeographical regions (Martens et al. 2008). According to the latest checklist (Meisch et al. 2019), 799 extant non-marine ostracods have been reported from the Palaearctic, the greatest number in all the regions at present. Inner Mongolia and Beijing are located in the central-eastern part of Palaearctic region. The three new species described in this study thus enrich the ostracod records for the PA region, as well as for these two provinces, where only 21 named species were reported until this study (Table 2). The number of ostracods known from the Beijing and Inner Mongolia (Table 2) is very low and a large area has remained unexplored. Further studies are needed to expand our knowledge due to the complex geography and the diversity of aquatic ecosystems in this region. This is especially true for Inner Mongolia, the third largest Chinese province, which occupies the widest longitude range across the country (97°24'−126°04'E) but has a very small human population, which could provide suitable conditions for the survival of endemic ostracods.

According to Martens and Segers (2009), ~ 90% of the 1936 non-marine ostracod species recognised at that time were endemic to one zoogeographical region, while only a few dozen species could be considered cosmopolitan. Yu et al. (2009) suggested that the number of Chinese endemic species should represent ~ 40% of the entire ostracods (including subfossil species) of this country. However, with the increasing knowledge

Table 2. Named species of extant ostracods recorded in Inner Mongolia and Beijing, northern China.

No.	Species name	Beijing	Inner Mongolia	Reference	Zoogeographical region
1	*Bradleycypris vittata* (Sars, 1903)	✓		Zhai and Zhao 2014; Zhai et al. 2017	AU, OL, PA
2	*Candona quasiakaina* Karanovic & Lee, 2012	✓	✓	Zhai and Zhao 2014; Zhai et al. 2017	PA
3	*Cyclocypris pangi* sp. nov.	✓	✓	this study	PA
4	*Cypridopsis vidua* (O.F. Müler, 1776)	✓		Zhai and Zhao 2014; Zhai et al. 2017	AT, AU, NA, NT, OL, PA, PAC
5	*Cypris granulata* Daday, 1898	✓		Yu 2014 [as *Cypris subglobosa* Sowerby, 1840]	AT, AU, NA, OL, PA
6	*Eucypris pigra* (Fischer, 1851)	✓		Zhai and Zhao 2014; Zhai et al. 2017	PA
7	*Fabaeformiscandona alexandri* (Sywula, 1981)		✓	Zhai and Zhao 2014; Zhai et al. 2017	PA
8	*Fabaeformiscandona myllaina* Smith & Kamiya, 2007	✓		Zhai and Zhao 2014; Zhai et al. 2017	PA
9	*Fabaeformiscandona subacuta* (Yang, 1982)	✓		Zhai and Zhao 2014; Zhai et al. 2017	AU, NT, OL, PA
10	*Heterocypris auricularis* Zhai & Zhao, 2014		✓	Zhai and Zhao 2014; Zhai et al. 2017	PA
11	*Heterocypris vandouwei* (Brehm, 1923)	✓		Chen 1982	PA
12	*Heterocypris incongruens* (Ramdohr, 1808)		✓	Zhai and Zhao 2014; Zhai et al. 2017	AT, AU, NA, NT, OL, PA, PAC
13	*Ilyocypris angulata* Sars, 1903	✓		Zhai and Zhao 2014; Zhai et al. 2017	OL, PA
14	*Ilyocypris innermongolica* Zhai & Xiao, 2013		✓	Zhai and Xiao 2013; Zhai and Zhao 2014; Zhai et al. 2017	PA
15	*Ilyocypris mongolica* Martens, 1991		✓	Yu 2014; Zhai and Zhao 2014; Zhai et al. 2017	PA
16	*Ilyocypris salebrosa* Stepanaitys, 1960	✓		Zhai and Zhao 2014; Zhai et al. 2017	NA, OL, PA
17	*Leucocythere mirabilis* Kaufmann, 1892		✓	Yu 2014	PA
18	*Limnocythere inopinata* (Baird, 1843)	✓	✓	Zhai and Zhao 2014; Zhai et al. 2017	AT, NA, PA
19	*Limnocythere stationis* Vávra, 1891	✓		Zhai and Zhao 2014; Zhai et al. 2017	AT, PA, OL
20	*Physocypria kraepelini* G.W. Müller, 1903	✓	✓	Zhai and Zhao 2014; Zhai et al. 2017	NA, OL, PA
21	*Plesiocypridopsis newtoni* (Brady & Robertson, 1870)		✓	Zhai and Zhao 2014; Zhai et al. 2017	AT, PA, OL
22	*Pseudocandona cheni* sp. nov.		✓	this study	PA
23	*Potamocypris variegata* (Brady & Norman, 1889)	✓		Zhai and Zhao 2014; Zhai et al. 2017	NA, PA
24	*Tonnacypris rectangularis* sp. nov.		✓	this study	PA
Total number of species		15	13	/	/

Key: AT, Afrotropical region; AU, Australasian region; NA, Nearctic region; NT, Neotropical region; OL, Oriental region; PA, Palaearctic region; PAC, Pacific Oceanic Islands.

Note: We include here only the records with descriptions and/or illustrations of soft parts. Reports of sub-fossil valves (e.g., Zhai et al. 2013) are not included.

on the extant non-marine ostracods of China (Kong et al. 2014; Zhai and Zhao 2014; Ma and Yu 2018, 2020; Peng et al. 2021), the ratio of endemic species seems to be declining. Among all the ostracods listed in Table 2, 12 species are endemic to the PA region: *Candona quasiakaina* Karanovic & Lee, 2012, *Eucypris pigra* (Fischer, 1851), *Fabaeformiscandona alexandri* (Sywula, 1981), *F. myllaina* Smith & Kamiya, 2007, *Heterocypris auricularis* Zhai & Zhao, 2014, *H. vandouwei* (Brehm, 1923), *Ilyocypris innermongolica* Zhai & Xiao, 2013, *I. mongolica* Martens, 1991, *Leucocythere mirabilis* Kaufmann, 1892, in addition to the three new species described in this study. Another 12 ostracods are shared by the PA and other regions, among which *Cypridopsis vidua* (O.F. Müler, 1776), *Cypris granulata* Daday, 1898 [as *C. subglobosa* Sowerby, 1840 in Yu (2014)], and *Heterocypris incongruens* (Ramdohr, 1808) are well known cosmopolitan species tolerant to a wide range of environmental conditions (Yu 2014).

The three new species also add to our knowledge on the geographical distribution of extant ostracods in general. *Cyclocypris pangi* is the first named ostracod species of the genus *Cyclocypris* reported from Beijing (Table 2). Similarly, *Pseudocandona cheni* and *T. rectangularis* are the first representatives of their respective genera recorded from Inner Mongolia, although Zhai et al. (2013) reported the valves of *Pseudocandona* sp. from Lake Hulun from the northern Inner Mongolia. The genus *Tonnacypris* has been rarely reported from China. The only named species of the genus reported from this country, *T. estonica* (Järvekülg, 1960), has been found from the Qinghai–Tibet Plateau (Li et al. 2021; Peng et al. 2021). Mischke et al. (2003) found a fragment of the anterior part of RV of *Tonnacypris* (?) sp. from the Qilian Mountains from the northeastern margin of this plateau, the generic assignment of which is uncertain. Although members of this genus have been found in a number of sites in the PA region (e.g., Järvekülg 1960; Van der Meeren et al. 2009; Peng et al. 2021), their easternmost record was at 100°31'E in the northern part of Mongolia, represented by *T. mazepovae* (Van der Meeren et al. 2009). Thus, our study expands the known longitudinal range of the genus *Tonnacypris* eastwards, to ca. 116°45'E (Table 1).

Our detailed descriptions of the valves and carapaces of *P. cheni* (Fig. 1) and *C. pangi* (Fig. 4) provide clues for their identification from the sub-fossil and fossil assemblages. As stated above, the valves of *T. rectangularis* (Fig. 7) can be readily distinguished from its congeners by long, sub-parallel or anteriorly sloping dorsal margin and narrow anterior calcified inner lamella (see remarks of this species in the Taxonomy section). Previous studies (e.g., Mischke et al. 2010) suggested that the members of *compressa* group are difficult to identify to species level by using valve material only. The valves/carapace of *P. cheni* (Fig. 1), however, can be distinguished from other species in the group by the following carapace differences: *P. regisnikolai* is much longer (with females ranging between 1.33 and 1.4 mm and males being up to 1.53 mm) (Karanovic and Petkovski 1999); in dorsal view, *P. insculpta* is less inflated at the first 1/4 of its length, but more inflated at greatest width (slightly behind mid-length), and it is not compressed at the anterior end (Meisch 2000; Fuhrmann 2012); *P. compressa* is more laterally compressed in the dorsal view, and is less inflated at the first 1/4 (Meisch 2000;

Fuhrmann 2012); *P. pratensis* is stouter, and the dorsal valve margin is conspicuously more inclined (Meisch 2000); *P. sucki* is more elongated in lateral view, with H/L ratio between 0.53 and 0.56 (n = 7, measured from Tafel, Germany (i.e., plate 42 in Fuhrmann 2012)), and in the dorsal view. both *P. pratenis* and *P. sucki* (see Meisch 2000 and Fuhrmann 2012), have a beak-shaped anterior end. The valves/carapaces of *C. pangi* (Fig. 4) resemble those of *C. serena* in lateral and dorsal/ventral outlines, but can still be distinguished from the latter. *Cyclocypris serena* [0.58−0.63 mm according to Meisch (2000)] is significantly larger than *C. pangi*, the inner list situated in the medial zone of the calcified inner lamella on the RV is less pronounced (Fuhrmann 2012), and the inner list running close to the valve margin is absent (see Fig. 4C−F for the inner lists of *C. pangi*). These differences are helpful for distinguishing the two when dealing with the sub-fossil/fossil material. Considering intra-species morphological variations and possible loss of some fine-scaled structures such as the inner lists in the fossil material, however, some of the abovementioned differences may be obscure, and we suggest that geometric morphometric methods (e.g., Baltanás and Danielopol 2011; Namiotko et al. 2014) would be useful for the fine tuning of shell morphological characters.

Acknowledgements

This work is supported by the National Natural Science Foundation of China [41372365, 31672263, 32160116], Yunnan Provincial Grants 202101AT070158 and YNWR-QNBJ-2019-295, and the Key Research Program of the Institute of Geology & Geophysics, Chinese Academy of Sciences (IGGCAS-201905). We thank Ph.D. Robin J. Smith (Lake Biwa Museum, Japan) for the help with SEM and his valuable suggestions. Thanks are extended to Fangzhi Peng (Advanced Analysis and Measurement Center of Yunnan University, China) for imaging some of the specimens. The meticulous and constructive comments of Tadeusz Namiotko and an anonymous reviewer are much appreciated.

References

Baltanás A, Danielopol DL (2011) Geometric Morphometrics and its use in ostracod research: A short guide. Joannea—Geologie und Palaontologie 11: 235–272.

Broodbakker NW, Danielopol DL (1982) The chaetotaxy of Cypridacea (Crustacea, Ostracoda) limbs: Proposal for a descriptive model. Bijdragen tot de Dierkunde 52: 103–120. https://doi.org/10.1163/26660644-05202003

Chen ST (1957) Notes on some Ostracoda from Lake Tunghu, Wuchang. Shui Sheng Sheng Wu Hsueh Bao 2: 314–321. [in Chinese with English abstract]

Chen SZ (1982) Subclass Ostracoda. In: Dong YM, Dai AY, Jiang XZ, Chen SZ, Chen YS, Cai RX (Eds) Atlas of animals in China, Crustacea. Volume 1, 2nd edn. Science Press, Beijing, 48–63. [In Chinese]

Danielopol DL (1969) Recherches sur la morphologie de l'organe copulateur mâle chez quelques Ostracodes du genre *Candona* Baird (Fam. Cyprididae Baird). In: Neale JW (Ed.)

The Taxonomy, Morphology and Ecology of Recent Ostracoda. Oliver and Boyd Ltd, Edinburgh, 136–153.

Danielopol DL (1978) Über Herkunft und Morphologie der europäischen Süßwasser-Ostracoden. – Sitzungsberichte der Österreichischen Akademie der Wissenschaften, mathematisch-naturwissenschaftliche Klasse, Abteilung I, 187: 1–162.

Fuhrmann R (2012) Atlas quartärer und rezenter Ostrakoden Mitteleuropas. Altenburger Naturwissenschaftliche Forschungen 15: 1–320.

Huang MX (1986) Description of the living environment of several kinds of Ostracoda (Crustacea) in Sichuan. Sichuan. Journal of Zoology 1: 8–10. [in Chinese]

Huang BR, Yang LF, Fan YQ (1985) Ostracodes from surface deposits of Recent lakes in Xizang. Acta Micropalaeontologica Sinica 4: 369–376. [in Chinese with English abstract]

Järvekülg A (1960) *Ilyodromus estonicus* sp. nov., eine neue Süsswasser-Ostracode aus Estland. Eesti Nsv Teaduste Akadeemia Toimetised Bioloogiline Seeria 9: 27–34. https://doi.org/10.3176/biol.1960.1.03

Karanovic I (2005) On the genus *Typhlocypris* Vejdovský, 1892 (Crustacea: Ostracoda: Candoninae), with description of two new species. Systematics and Biodiversity 3: 375–406. https://doi.org/10.1017/S1477200005001738

Karanovic I (2012) Recent Freshwater Ostracods of the World. Springer-Verlag, Berlin, 608 pp. https://doi.org/10.1007/978-3-642-21810-1

Karanovic I, Lee W (2012) A review of candonid ostracods (Crustacea: Ostracoda: Podocopida) from East Asia, with descriptions of five new species from South Korea. Zootaxa 3368: 7–49. https://doi.org/10.11646/zootaxa.3368.1.3

Karanovic I, Petkovski TK (1999) Two new species of the subfamily Candoninae (Ostracoda) from Montenegro (SE Europe). Crustaceana 71: 603–616. https://doi.org/10.1163/156854099503645

Kong Q, Yu N, Zhao QH (2013) New record of freshwater ostracods from the Hongfeng Lake, Guizhou Province. Acta Micropalaeontologica Sinica 30: 166–174. [in Chinese with English Abstract]

Kong Q, Karanovic I, Yu N (2014) Phylogeny of the genus *Chrissia* (Ostracoda: Cyprididae) with description of a new species from China. Journal of Crustacean Biology 34: 782–794. https://doi.org/10.1163/1937240X-00002276

Li XZ, Zhai DY, Wang QW, Wen RL, Ji M (2021) Depth distribution of ostracods in a large fresh-water lake on the Qinghai–Tibet Plateau and its ecological and palaeolimnological significance. Ecological Indicators 129: 108019. https://doi.org/10.1016/j.ecolind.2021.108019

Ma SX, Yu N (2018) Freshwater ostracods (Crustacea) from Tiantong National Forest Park and Dongqian Lake, eastern China, with descriptions of two new species. Journal of Natural History 52: 1825–1868. https://doi.org/10.1080/00222933.2018.1489085

Ma SX, Yu N (2020) Freshwater ostracods (Crustacea) from Hainan Island, southern China, with description of a new species. Zootaxa 4767: 201–243. https://doi.org/10.11646/zootaxa.4767.2.1

Martens K (1987) Homology and functional morphology of the sexual dimorphism in the antenna of *Sclerocypris* Sars, 1924 (Crustacea, Ostracoda, Megalocypridinae). Bijdragen tot de Dierkunde 57: 183–190. https://doi.org/10.1163/26660644-05702003

Martens K, Savatenalinton S (2011) A subjective checklist of the Recent, free-living, non-marine Ostracoda (Crustacea). Zootaxa 2855: 1–79. https://doi.org/10.11646/zootaxa.2855.1.1

Martens K, Segers H (2009) Endemism in aquatic ecosystems. In: Likens GE (Ed.) Encyclopedia of Inland Waters, vol. 1. Elsevier, Oxford, 423–430. https://doi.org/10.1016/B978-012370626-3.00211-8

Martens K, Schön I, Meisch C, Horne DJ (2008) Global diversity of ostracods (Ostracoda, Crustacea) in freshwater. Hydrobiologia 595: 185–193. https://doi.org/10.1007/s10750-007-9245-4

Meisch C (1996) Contribution to the taxonomy of *Pseudocandona* and four related genera, with the description of *Schellencandona* nov. gen., a list of the Candoninae genera, and a key to the European genera of the subfamily (Crustacea, Ostracoda). Bulletin (Societe des Naturalistes Luxembourgeois) 97: 211–237.

Meisch C (2000) Freshwater Ostracoda of Western and Central Europe. In: Schwoerbel J, Zwick P (Eds) Süßwasserfauna von Mitteleuropa 8(3). Spektrum Akademischer Verlag, Heidelberg, Berlin, 522 pp.

Meisch C, Smith RJ, Martens K (2019) A subjective global checklist of the extant non-marine Ostracoda (Crustacea). European Journal of Taxonomy 492: 1–135. https://doi.org/10.5852/ejt.2019.492

Mischke S, Herzschuh U, Kürschner H, Fuchs D, Zhang JW, Meng F, Sun ZC (2003) Sub-Recent Ostracoda from Qilian Mountains (NW China) and their ecological significance. Limnologica 33: 280–292. https://doi.org/10.1016/S0075-9511(03)80023-3

Mischke S, Herzschuh U, Massmann G, Zhang CJ (2007) An ostracod-conductivity transfer function for Tibetan lakes. Journal of Paleolimnology 38: 509–524. https://doi.org/10.1007/s10933-006-9087-5

Mischke S, Bößneck U, Diekmann B, Herzschuh U, Jin HJ, Kramer A, Wünnemann B, Zhang CJ (2010) Quantitative relationship between water-depth and sub-fossil ostracod assemblages in Lake Donggi Cona, Qinghai Province, China. Journal of Paleolimnology 43: 589–608. https://doi.org/10.1007/s10933-009-9355-2

Namiotko T, Danielopol DL (2004) Review of the *eremita* species-group of the genus *Pseudocandona* Kaufmann (Ostracoda, Crustacea), with the description of a new species. Revista Española de Micropaleontología 36: 109–125.

Namiotko T, Danielopol DL, Meisch C, Gross M, Mori N (2014) Redefinition of the genus *Typhlocypris* Vejdovský, 1882 (Ostracoda, Candonidae). Crustaceana 87: 952–984. https://doi.org/10.1163/15685403-00003338

Okubo I (2004) Nihon tansui san kaimijinko rui ni tsuite. Kabushikigaisha Sanmon Insatsusho, Okayama, 72 pp. [In Japanese]

Peng P, Zhai DY, Smith RJ, Wang QW, Guo Y, Zhu LP (2021) On some modern Ostracoda (Crustacea) from the Tibetan Plateau in SW China, with de-scriptions of three new species. Zootaxa 4942: 501–542. https://doi.org/10.11646/zootaxa.4942.4.2

Sars GO (1895) On some South-African Entomostraca raised from dried mud. Skr Vidensk-Selsk. I Math Naturvidensk Kl 8: 1–56.

Sars GO (1903) Freshwater Entomostraca from China and Sumatra. Archiv for Mathematik og Naturvidenskab 25: 1–44.

Savatenalinton S, Suttajit M (2016) A checklist of Recent non-marine ostracods (Crustacea: Ostracoda) from Thailand, including descriptions of two new species. Zootaxa 4067: 1–34. https://doi.org/10.11646/zootaxa.4067.1.1

Smith RJ, Janz H, Okubo I (2011) Recent Cyprididae and Ilyocyprididae (Crustacea: Ostracoda) from Lake Biwa, Japan, including a summary of the lake's ostracod fauna. Zootaxa 2874: 1–37. https://doi.org/10.11646/zootaxa.2874.1.1

Van der Meeren T, Khand Y, Martens K (2009) On Recent species of *Tonnacypris* Diebel & Pietrzeniuk, 1975 (Crustacea, Ostracoda), with new species descriptions from Mongolia. Zootaxa 2015: 1–41. https://doi.org/10.11646/zootaxa.2015.1.1

Viehberg FA (2002) A new and simple method for qualitative sampling of meiobenthos-communities. Limnologica 32: 350–351. https://doi.org/10.1016/S0075-9511(02)80026-3

Wang SM, Ji L, Yang XD, Xue B, Ma Y, Qin BQ, Dong GB, Pan HX, Hu SY, Xia WL, Shen J, Xiang L, Zhang LR, Zhu YX (1995) Paleolimnology of Hulun Lake. University of Science and Technology of China Press, Hefei, 125 pp. [in Chinese]

Yang LF, Huang BR (1983) Preliminary study on the Ostracoda and their distribution patterns in the surficial deposits of Fuxian Lake, Yunnan Province. Science Bulletin 28: 617–621. [in Chinese]

Yang LF, Fan YQ, Huang BR (1982) Relation between ostracod distribution in surface deposits and water salt of Recent lakes in Xizang Plateau. Haiyang Huzhao Tongbao 1982: 20–28.

Yin Y, Martens K (1997) On a new species of *Fabaeformiscandona* Krstić, 1972 (Crustacea, Ostracoda) from China, with a preliminary checklist of Recent Chinese nonmarine ostracods. Hydrobiologia 357: 117–128. https://doi.org/10.1023/A:1003182720121

Yu N (2014) Non-marine Ostracoda from China. Shanghai: Shanghai Educational Publishing House, Shanghai, 283 pp. [in Chinese]

Yu N, Zhao QH, Li EC, Chen SM, Chen LQ (2009) An undated and annotated checklist of recent nonmarine ostracods from China. Zootaxa 2067: 29–50. https://doi.org/10.11646/zootaxa.2067.1.2

Zhai DY, Xiao JL (2013) On a new species of the genus *Ilyocypris* Brady & Norman, 1889 from Hulun Lake, China. Naturalista Siciliano, Series IV 37: 465–469.

Zhai DY, Zhao WH (2014) On some Recent non-marine ostracods from northern China, with description of a new species. Crustaceana 87: 985–1026. https://doi.org/10.1163/15685403-00003339

Zhai DY, Xiao JL, Fan JW, Zhou L, Wen RL, Pang QQ (2013) Spatial heterogeneity of the population age structure of the ostracode *Limnocythere inopinata* in Hulun Lake, Inner Mongolia and its implications. Hydrobiologia 716: 29–46. https://doi.org/10.1007/s10750-013-1541-6

Zhai DY, Smith RJ, Peng P, Yu N, Ma SX, Li XZ (2017) Cluster analyses of Ostracoda based on dimensions of body structures: Implications for taxonomic classification. Crustaceana 90: 471–502. https://doi.org/10.1163/15685403-00003667

Zhang L, Sun ZC, An ZS, Liu WG, Li XZ (2006) A preliminary distribution analysis on Ostracoda of different water bodies from Qinghai Lake area, NW China. Acta Micropalaeontologica Sinica 23: 425–436. [in Chinese with English abstract]

ZooKeys 1097: 209–216 (2022)
doi: 10.3897/zookeys.1097.82860
https://zookeys.pensoft.net

RESEARCH ARTICLE

A peer-reviewed open-access journal
ZooKeys
Launched to accelerate biodiversity research

A new species of the genus *Separatatus* Chen & Wu (Hymenoptera, Braconidae, Alysiinae) from South Korea

Ju-Hyoeng Sohn[1*], Cornelis van Achterberg[2,3*], Sangjin Kim[1], Jongok Lim[4], Hyojoong Kim[1]

1 *Animal Systematics Lab., Department of Biological Science, Kunsan National University, Gunsan, 54150, Republic of Korea* **2** *State Key Laboratory of Rice Biology and Ministry of Agriculture, Zhejiang University, Hangzhou, 310058, China* **3** *Key Lab of Agricultural Entomology, Institute of Insect Science, Zhejiang University, Hangzhou, 310058, China* **4** *Department of Life and Environmental Sciences, Wonkwang University, Iksan, JB 54538, Republic of Korea*

Corresponding author: Hyojoong Kim (hkim@kunsan.ac.kr)

Academic editor: F. J. Peris Felipo | Received 28 February 2022 | Accepted 6 April 2022 | Published 29 April 2022

http://zoobank.org/09D65569-09A8-48A6-AD90-C5486678865A

Citation: Sohn J-H, van Achterberg C, Kim S, Lim J, Kim H (2022) A new species of the genus *Separatatus* Chen & Wu (Hymenoptera, Braconidae, Alysiinae) from South Korea. ZooKeys 1097: 209–216. https://doi.org/10.3897/zookeys.1097.82860

Abstract

Separatatus megagnathus **sp. nov.** is recorded as new to science from South Korea. Due to this record, the genus *Separatatus* Chen & Wu, 1994 (Braconidae: Alysiinae) is recognized for the first time from South Korea. The genus and species are described and illustrated herein plus an identification key including the Korean new species is provided. In addition, the DNA barcode region of the mitochondrial cytochrome c oxidase subunit I (*COI*) has been analyzed for the new species.

Keywords

COI barcode, cyclostome, koinobiont, natural enemy, parasitoid wasp, systematics, taxonomy

* The authors contributed equally to this paper.

Copyright *Ju-Hyoeng Sohn et al.* This is an open access article distributed under the terms of the Creative Commons Attribution License (CC BY 4.0), which permits unrestricted use, distribution, and reproduction in any medium, provided the original author and source are credited.

Introduction

The subfamily Alysiinae is a relatively large taxon among the family Braconidae, which contains over 2450 valid species and is subdivided into two tribes, Alysiini with 76 genera and Dacnusini with 31 genera (Yu et al. 2016; Peris-Felipo and Belokobylskij 2020). There are 180 species of 21 genera listed in the National Species List of South Korea, South Korea (NIBR 2020). It is known that Alysiini includes mostly koinobiont endoparasitoids of cyclorrhaphous dipteran larvae, which are recognized by using their mandible (usually with 3–4 teeth or lobes) to break open the puparium of the host (Wharton 1977). Some species of Alysiinae are utilized for biological control (Abd-Rabou 2006).

The genus *Separatatus* Chen & Wu, 1994 is a small group of Alysiinae, which includes five Oriental or East Palaearctic species (Yu et al. 2016; Zhu et al. 2017; Zhang et al. 2020). This genus is easily characterized by the rugose second metasomal tergite, robust mandible and metanotum slightly or not protruding dorsally (Zhang et al. 2020). Chen and Wu (1994) created the genus *Separatatus* and described *Separatatus carinatus* Chen & Wu, 1994 as new species from China. *Bobekioides sinicus*, which had been described by Zheng et al. (2013) from China, was transferred to *Separatatus* by Zhu et al. (2017). Zhu et al. (2017) also described a new species, *S. parallelus*, from China. Yao et al. (2018) transferred *Phasmidiasta malaysiae* Fischer, 2006 to *Separatatus*, and added a new species, *S. xuexincheni*, from Thailand. Recently, Zhang et al. (2020) described a new species, *S. yinshani*, from China.

In this study, *Separatatus megagnathus* sp. nov. is recorded as new to science from South Korea. Simultaneously, the genus *Separatatus* Chen & Wu, 1994 (Braconidae: Alysiinae) is recognized for the first time from South Korea. We descried the morphological characters and the barcoding sequences of the *COI* region of this new species. A description, diagnosis and photographs of the diagnostic characters are also provided.

Materials and methods

The holotype was collected with a Malaise trap in South Korea at the DMZ Botanical Garden, Mandae-ri, Haean-myeon, Yanggu-gun, Gangwon-do. Sorting and preparation were done at the Animal Systematics Lab. (**ASL**), Department of Biological Science, Kunsan National University (**KSNU**) at Gunsan, South Korea. Zhu et al. (2017), Yao et al. (2018) and Zhang et al. (2020) were followed for the morphological identification. Morphological characters were observed with a Leica M205C stereo microscope. The Taxapad database (Yu et al. 2016) was used for checking valid species and references. We followed the terminology of Wharton (2002) and van Achterberg (1993). The holotype is deposited in the Insect Museum, Department of Biological Science, KSNU.

A LEICA DMC2900 digital camera and a LEICA M205 C microscope (Leica Geosystems AG, Wetzlar, Germany) were used for photography and several pictures being taken for each height using multifocusing technology. LAS V4.11 (Leica Geosystems AG,

Wetzlar, Germany) and HeliconFocus 7 (Helicon Soft, Kharkiv, Ukraine) software were used for image stacking. After stacking, plates were created using Adobe Photoshop CS6.

Extraction of DNA was done in ASL, KSNU. Whole genomic DNA was extracted from the specimen by using a DNeasy Blood & Tissue kit (QIAGEN Inc., Dusseldorf, Germany) following the manufacturer's protocol. In order to conserve the morphologically complete voucher specimen, DNA extraction was slightly modified from the 'non-destructive method' of Favret (2005) and the 'freezing method' of Yaakop et al. (2009). In the original protocol, the sample was crushed or wounded, and then soaked with 180 µl of buffer ATL + 20 µl of proteinase, following by three hours over incubation at 55 °C. In our slightly modified DNA extraction methods, samples were soaked with 180 µl of buffer ATL + 20 µl of proteinase K without destroying the sample, followed by 10 minutes incubation at 55 °C and then kept in a freezer at -22 °C overnight. After that, the general protocol was used for the remaining steps. The primerset of LCO-1490 (5'-GGTCAACAAATCATAAAGATATTGG-3') and HCO-2198 (5'-TAAACTTCAGGGTGACCAAAAAATCA-3') (Folmer et al. 1994) was used to amplify approximately 658 bp as the partial front region of the *COI*. The polymerase chain reaction (PCR) products were amplified by using AccuPowerH PCR PreMix (BIONEER, Corp., Daejeon) in 20 µl reaction mixtures containing 0.4 µM of each primer, 20 µM of the dNTPs, 20 µM of the $MgCl_2$, and 0.05 µg of the genomic DNA template. PCR amplification was performed using a GS1 thermo-cycler (Gene Technologies, Ltd., Essex, U.K) according to the following procedure: initial denaturation at 95 °C for 5 min, followed by 34 cycles at 94 °C for 35 s; an annealing temperature of 48 °C for 25 s; an extension at 72 °C for 45 s, and a final extension at 72 °C for 5 min. The PCR products were visualized by electrophoresis on a 1.5% agarose gel. A single band was observed, purified using a QIAquick PCR purification kit (QIAGEN, Inc., Milan, Italy), and then sequenced directly using an automated sequencer (ABI Prism 3730 XL DNA Analyzer, ABI, Waltham, MA, USA) at Macrogen Inc. (Seoul, South Korea).

Results and discussion

A total of 620 bp of the COI fragments were sequenced from *Separatatus megagnathus* sp. nov. which was deposited in GenBank (accession number MZ717197). Unfortunately, it could not be used to measure genetic distance between related taxa because there is no sequence of a congeneric species in GenBank. However, the sequence will facilitate the recognition of the new species if other sequences of *Separatatus* are added in future.

Separatatus Chen & Wu, 1994

Separatatus Chen & Wu, 1994: 132. Type species: *Separatatus carinatus* Chen & Wu, 1994.

Diagnosis. Antenna 1.0–1.3 times longer than body; first flagellomere slightly shorter than second (Fig. 1B), face with setae (Fig. 1E), eye slightly oval and glabrous; clypeus

semicircular; labrum long and triangularly shape, mandible with 3–4 teeth or lobes (Fig. 1J), fourth ventral tooth (if present) small; maxillary palp with 6 segments; notauli present on anterior third of mesoscutum; medio-posterior depression distinct, round or longitudinal; scutellar sulcus distinct; fore wing (Fig. 1C) vein 2-SR slightly bent, vein 2-SR slightly shorter than vein 3-SR; vein 2-SR+M not sclerotized; hind wing vein 1-M longer than vein 1r-m; second tergite rugose, longer than first (Fig. 1H); ovipositor sheath slightly shorter than metasoma; tarsal claws slender.

Biology. Unknown.

Distribution. Oriental and Palaearctic region.

Key to species of subgenus *Separatatus*

1 Basal part of pterostigma long and parallel-sided; vein r close to apex of pterostigma; [vein 3-SR of fore wing about 2.9 times longer than vein r; hind femur ca 2.7 times longer than wide]; China (Yunnan, Hainan) .... ***S. parallelus*** **Zhu, van Achterberg & Chen, 2017**

– Basal part of pterostigma comparatively short and elliptical; vein r more removed from apex of pterostigma; [vein 3-SR of fore wing ca 3.0 times longer than vein r, also pterostigma more robust] **2**

2 Mandible hardly emarginated between first and second teeth of mandible (Figs 1J-L); ventral lobe of mandible small (Figs 1J-L); body black or blackish; precoxal sulcus present anteriorly (Fig. 1G); legs partly brown or dark brown (Fig. 1A); [medio-posterior depression of mesoscutum elongate and about half as long as mesoscutum medially; S. Korea] .... ***S. megagnathus*** **Sohn & van Achterberg, sp. nov.**

– Emargination between first and second teeth of mandible distinct; ventral lobe of mandible medium-sized; body reddish brown or yellowish brown; precoxal sulcus absent anteriorly; legs yellow..... **3**

3 Vein r-m of fore wing weakly inclivous; [hind femur of ♀ rather inflated, ca 3.0 times longer than wide]; China (Yunnan) .....***S. carinatus*** **Chen & Wu, 1994**

– Vein r-m of fore wing strongly inclivous **4**

4 Head and fourth antennal segment yellow; hind femur of ♀ ca 3.5 times longer than wide; West Malaysia..... ***S. malaysiae*** **(Fischer, 2006)**

– Head and fourth antennal segment mainly dark brown; hind femur of ♀ ca 2.6 times longer than wide; Thailand..... ***S. xuexincheni*** **Yao, 2018**

Separatatus megagnathus **Sohn & van Achterberg, sp. nov.**
http://zoobank.org/0814AA28-EF2F-4AD8-B33A-5CE461BC36DD
Fig. 1A–L

Type material. ***Holotype***, ♀ (KNA), **South Korea**, DMZ Botanical Garden, Mandae-ri, Haean-myeon, Yanggu-gun, Gangwon-do, 38°15'09.3"N,128°06'40.6"E, 20.VI.–4.VII.2017, Shin & Kim leg. GenBank accession number MZ717197.

Comparative diagnosis. The new species belongs to the subgenus *Separatatus* Chen & Wu (Zhang et al. 2020). It runs in the key by Yao et al. (2018) to *S. malaysiae* because of the less developed areola of the propodeum and distinctly postfurcal vein m-cu of the fore wing. Both species can be separated as follows:

1 Emargination between first and second teeth of mandible absent or nearly so (Fig. 1L); medio-posterior depression of mesoscutum elongate and about half as long as mesoscutum medially (Fig. 1F); ventral (= fourth) lobe of mandible small (Fig. 1L); body black or blackish; precoxal sulcus present anteriorly (Fig. 1G); legs partly brown or dark brown (Fig. 1A); S. Korea..... ..... ***S. megagnathus*** **Sohn & van Achterberg, sp. nov.**

– Incision between first and second teeth of mandible present; medio-posterior depression of mesoscutum round and small; ventral lobe of mandible medium-sized; body reddish brown or yellowish brown; precoxal sulcus absent anteriorly; legs yellow; W. Malaysia..... ***S. malaysiae*** **(Fischer, 2006)**

Description. ♀: length of body in lateral view 2.5 mm, length of antenna 2.6 mm, and length of fore wing 2.8 mm. ***Colour.*** Body entirely dark brown; head in dorsal view entirely black, in anterior view reddish brown, around eye brown, antenna brown, mandible orangish brown and apically dark brown. ***Head.*** Head (Fig. 1D) width 2.2 times median length in dorsal view. Antenna (Fig. 1B) as long as body, 25 segmented. First flagellomere 0.9 times as long as second. Eye slightly oval and glabrous, 1.1 times as long as wide in lateral view. Width of face (Fig. 1E) 2.2 times its height from ventral rim of antennal sockets to upper margin of clypeus; face with long setae and smooth. Eye in dorsal view 1.2 times as long as temple. Ocello-ocular line (OOL) 4.2 times longer than diameter of anterior ocellus; OOL:antero-posterior ocellar line (AOL):postero-ocellar line (POL) = 19:6:8. Vertex smooth and polish with groove. Mandible (Fig. 1J) with four teeth and setae; dorsal tooth large and lobe-shaped, small incision between first and second teeth; ventral (fourth) tooth lobe-shaped, middle of tooth curved down; second tooth relatively narrow and sharp with dark brown tip and separated from first tooth by incision in lateral view (Fig. 1L). Medial length of mandible 1.5 times its maximum width. Labrum 3.2 times longer than wide. Maxillary palp 0.7 times longer than mesosoma. ***Mesosoma.*** Mesosoma (Fig. 1G) 1.8 times longer than wide in dorsal view and 1.4 times its height in lateral view; notauli crenulated, not reaching medio-posterior depression; medio-posterior depression distinctly elongated, half as long as mesoscutum medially; scutellar sulcus with two carinae; in lateral view mesopleuron smooth and shiny, precoxal sulcus (Fig. 1F) distinct but absent posteriorly and with 11 crenulae; metapleuron distinctly rugose and with long setae. Propodeum largely smooth, its median carina medium-sized, connected to irregular transverse carina (Fig. 1F); posterior areola incomplete; in lateral view propodeum curved dorsally, with submedian corner. ***Wings.*** Fore wing (Fig. 1C) 2.3 times longer than wide; pterostigma long and rather broad, 3.8 times longer than wide; base of vein 1-R1 narrow; vein r of fore wing 5.0 times longer than wide, 0.6 times width of pterostigma and arising from its basal 0.6; vein 1-M and vein

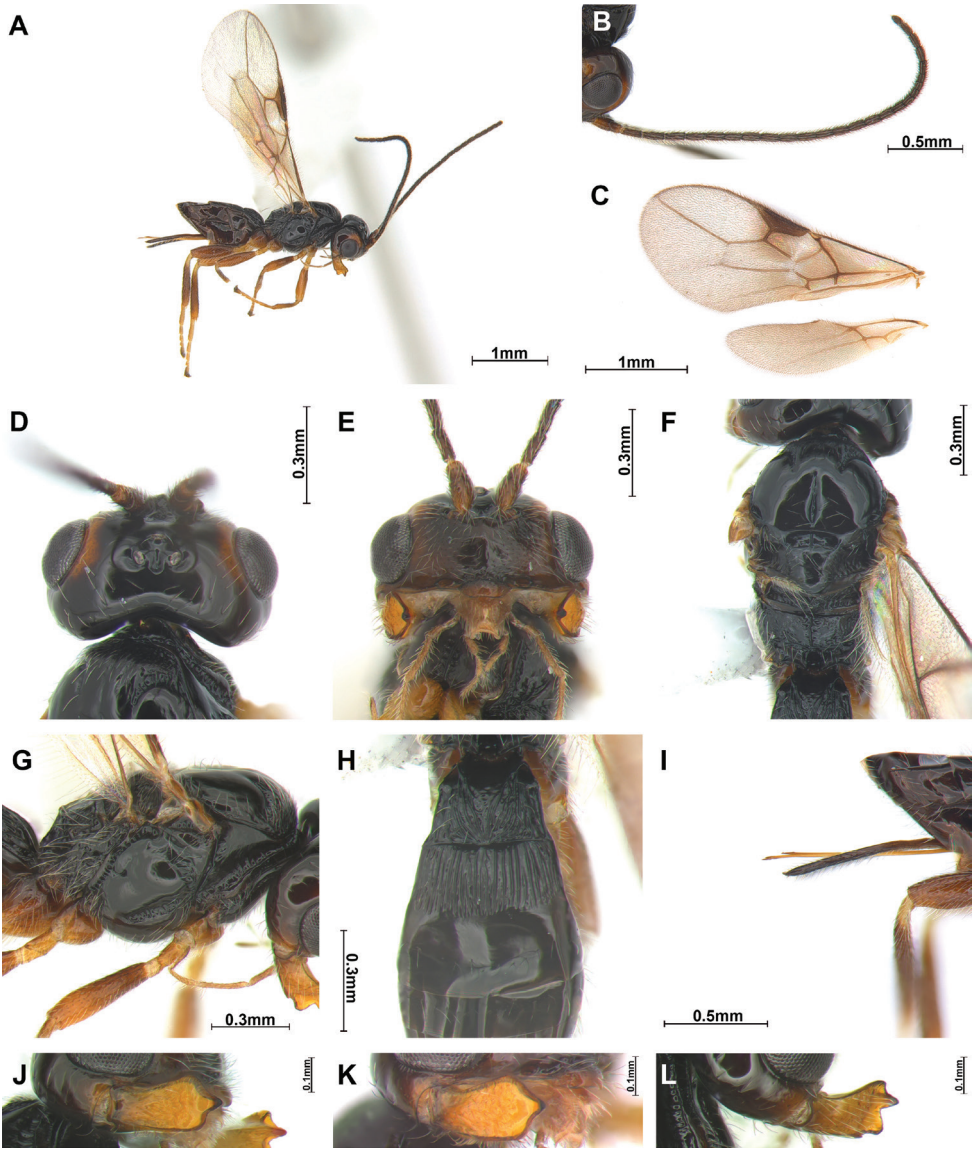

Figure 1. *Separatatus megagnathus* sp. nov., ♀ **A** habitus, lateral view **B** antennae **C** wings **D** head, dorsal view **E** head, front view **F** mesosoma, dorsal view **G** mesosoma, lateral view **H** anterior half of metasoma, dorsal view **I** ovipositor sheath, lateral view **J** mandible, lateral view **K** mandible, antero-lateral view **L** mandible with teeth. Scale bars: 1 mm (**A, C**); 0.5 mm (**B, I**); 0.3 mm (**D–H**); 0.1 mm(**J–L**)

1-SR+M slightly bent; vein 2-SR+M and r-m not sclerotized; vein r-m inclivous; vein 2-SR:vein r:vein 3-SR = 10:3:11; first subdiscal cell of fore wing 2.5 times longer than wide medially; vein m-cu distinctly postfurcal. Hind wing 4.1 times longer than wide; vein M+CU slightly bent; vein M+CU:1-M:1r-m = 11:6:3. ***Legs.*** Hind coxa smooth and 1.1 times longer than trochanter; hind femur 0.8 times as long as hind tibia and

7.1 times longer than wide; hind tibia as long as hind tarsus. ***Metasoma.*** First tergite widened posteriorly, striate and narrow, 0.8 times longer than its apical width; first tergite 0.6 times longer than second. Setose part of ovipositor sheath (Fig. 1I) 0.8 times longer than mesosoma, as long as hind tibia and with long setae. **Male.** Unknown.

Distribution. South Korea.

Etymology. From "megas" (Greek for large) and "gnathos" (Greek for jaw) because of the large mandible.

Acknowledgements

This work was supported by a grant from the National Institute of Biological Resources (NIBR), funded by the Ministry of Environment (MOE) of the Republic of Korea (NIBR202102204). This work was also supported by the Korea National Arboretum (KNA1-1-20). This work was supported by Korea Environment Industry & Technology Institute (KEITI) through Exotic Invasive Species Management Program, funded by Korea Ministry of Environment (MOE)(2018002270005).

References

Abd-Rabou S (2006) Biological control of the leafminer, *Liriomyza trifolii* by introduction, releasing, evaluation of the parasitoids *Diglyphus isaea* and *Dacnusa sibirica* on vegetables crops in greenhouses in Egypt. Archiv für Phytopathologie und Pflanzenschutz 39(6): 439–443. https://doi.org/10.1080/03235400500356079

Chen J-H, Wu Z-S (1994) The Alysiini of China: (Hymenoptera: Braconidae: Alysiinae). China Agricultural Press, Fuzhou, 218 pp. [In Chinese, with summary in English]

Favret C (2005) New non-destructive DNA extraction and specimen clearing technique for aphids (Hemiptera). Proceedings of the Entomological Society of Washington 107: 469–470.

Fischer M (2006) Neue Kieferwespen aus der Sammlung des Biologiezentrums des Oberosterreichischen Landesmuseums in Linz und Mitteilungen uber andere Arten (Hymenoptera, Braconidae, Alysiinae). Linzer Biologische Beitrage 38(1): 605–651.

Folmer O, Black M, Hoeh W, Lutz R, Vrijenhoek R (1994) DNA primers for amplification of mitochondrial cytochrome c oxidase subunit I from diverse metazoan invertebrates. Molecular Marine Biology and Biotechnology 3: 294–299.

NIBR (2020) National List of Species of Korea. National Institute of Biological Resources. http://kbr.go.kr [accessed on 28/12/21].

Peris-Felipo F-J, Belokobylskij S-A (2020) Species of the subgenus *Synaldis* Foerster, 1863 (Hymenoptera: Braconidae: Alysiinae: *Dinotrema* Foerster, 1863) in Papua New Guinea: descriptions of three new species and a key to the Australasian taxa. Insects of Mount Wilhelm, Papua New Guinea - volume 2. Muséum national d'Histoire naturelle Paris: 191–208.

van Achterberg C (1993) Illustrated key to the subfamilies of the Braconidae (Hymenoptera: Ichneumonoidea). Zoologische Verhandelingen Leiden 283: 1–189.

Wharton R-A (1977) New World *Aphaereta* species (Hymenoptera: Braconidae: Alysiinae), with a discussion of terminology used in the tribe Alysiini. Annals of the Entomological Society of America 70(5): 782–803. https://doi.org/10.1093/aesa/70.5.782

Wharton R-A (2002) Revision of the Australian Alysiini (Hymenoptera:Braconidae). Invertebrate Systematics 16(1): 7–105. https://doi.org/10.1071/IT01012

Yaakop S, van Achterberg C, Idris A-B (2009) *Heratemis* Walker (Hymenoptera: Braconidae: Alysiinae: Alysiini): revision and reconstruction of the phylogeny combining molecular data and morphology. Tijdschrift voor Entomologie 152(1): 1–64. https://doi.org/10.1163/22119434-900000268

Yao J-L, van Achterberg C, Sharkey M-J, Chen J-H (2018) *Separatatus* Chen & Wu (Hymenoptera: Braconidae: Alysiinae) newly recorded from Thailand, with description of one new species and one new combination. Zootaxa 4433(1): 187–194. https://doi.org/10.11646/zootaxa.4433.1.12

Yu D-S-K, van Achterberg C, Horstmann K (2016) Taxapad 2016, Ichneumonoidea 2015. Database on flash-drive, Nepean, Ontario, Canada. www.taxapad.com

Zhang R-N, van Achterberg C, Tian X-X, Tan J-L (2020) Review of the Bobekia-group (Braconidae, Alysiinae, Alysiini), with description of a new genus and a new subgenus. ZooKeys 926: 25–51. https://doi.org/10.3897/zookeys.926.47270

Zheng M-L, Chen J-H, Yang J-Q (2013) The discovery of the genus Bobekoides van Achterberg (Hymenoptera, Braconidae) in China, with description of one new species. Dong Wu Fen Lei Xue Bao 38(1): 143–146.

Zhu J-C, van Achterberg C, Chen X-X (2017) An illustrated key to the genera and subgenera of the Alysiini (Hymenoptera, Braconidae, Alysiinae), with three genera new for China. ZooKeys 722: 37–79. https://doi.org/10.3897/zookeys.722.14799